UNIVERSIDADE DO VALE DO TAQUARI

PROGRAMA DE PÓS-GRADUAÇÃO STRICTO SENSU

DOUTORADO EM BIOTECNOLOGIA

ANÁLISE DO POTENCIAL NEUROPROTETOR DE INIBIDORES DE MAPK EM CÉLULAS DE NEUROBLASTOMA SH-SY5Y

Ms. Stephanie Cristine Hepp Rehfeldt

Lajeado, março de 2021

Stephanie Cristine Hepp Rehfeldt

ANÁLISE DO POTENCIAL NEUROPROTETOR DE INIBIDORES DE MAPK EM CÉLULAS DE NEUROBLASTOMA SH-SY5Y

Tese apresentada ao Programa de Pós-graduação Stricto Sensu em Biotecnologia, da Universidade do Vale do Taquari, como parte da exigência para a obtenção do título de Doutora em Biotecnologia, na linha de pesquisa Aspectos Moleculares em Processos Fisiopatológicos.

Orientadora: Profª. Drª. Márcia Inês Goettert

Lajeado, março de 2021

Stephanie Cristine Hepp Rehfeldt

ANÁLISE DO POTENCIAL NEUROPROTETOR DE INIBIDORES DE MAPK EM CÉLULAS DE NEUROBLASTOMA SH-SY5Y

A banca examinadora abaixo aprova a tese apresentada ao Programa de Pós-graduação Stricto Sensu em Biotecnologia, da Universidade do Vale do Taquari, como parte da exigência para a obtenção do título de Doutora em Biotecnologia, na linha de pesquisa Aspectos Moleculares em Processos Fisiopatológicos.

Profª. Drª. Márcia Inês Goettert - Orientadora
Universidade do Vale do Taquari (Univates)

Prof. Dr. Luís Fernando Saraiva Macedo Timmers
Universidade do Vale do Taquari (Univates)

Prof. Dr. Rui Filipe Pinto Pedrosa
Instituto Politécnico de Leiria (IPL)

Profª. Drª. Fernanda Bueno Morrone
Pontifícia Universidade Católica do Rio Grande do Sul (PUCRS)

Lajeado, março de 2021

Aos meus avós.

AGRADECIMENTOS

À Deus por me abençoado e me fortalecido nas horas difíceis.

Aos meus pais, avós, noivo e demais familiares pela compreensão e incentivo. Em especial, agradeço meu avô Klaus Rehfeldt pela tradução no abstract;

À minha orientadora, a Profª. Drª. Márcia Goettert e ao Dr. Stefan Laufer, pela confiança e oportunidade de trabalhar com o FMU200 e a LUT7OG. Em especial, agradeço minha orientadora pela paciência, pelos ensinamentos e por todas as oportunidades que me foram dadas.

Aos colegas de pesquisa e de laboratório pelo auxílio durante as atividades que desenvolvi.

Ao grupo MARE pela oportunidade de colaboração e, em especial, à Joana R. Silva pelo auxílio nos ensaios com a LUT7OG e pelo auxílio nas atividades de laboratório.

À CAPES, pela bolsa de estudos que me permitiu realizar esta tese.

You know I've been around for a while now
Not sure if I have much left to prove
Yeah, I do, haha
I look at me now I'm thinking, "Damn"
How proud of me I am
What I did, it's nothin' to sneeze at
Even if your allergies are bad […]

Higher - Eminem

RESUMO

Os tratamentos atuais para doenças neurodegenerativas (ND) são sintomáticos e não afetam a progressão da doença. Retardar esse avanço continua sendo uma necessidade crucial não atendida para os pacientes e suas famílias. Truncamento e e agregação de proteínas, metabolismo mitocondrial alterado, disfunção sináptica, estresse oxidativo, excitotoxicidade, neuroinflamação e morte celular são marcas de ND conhecidas por ativar a via de proteína quinases ativadas por mitógenos (MAPK), como a quinase N-terminal c-Jun (JNK). Nesse caso, os inibidores de JNK3 podem desempenhar um papel importante na neuroproteção. Assim, no artigo de revisão "*c-Jun N-Terminal Kinase Inhibitors as Potential Leads for New Therapeutics for Alzheimer's Disease*", o papel de JNK na doença de Alzheimer foi destacado e os tratamentos experimentais baseados em inibidores de JNK sintéticos são descritos e discutidos. No entanto, os produtos naturais também se mostraram eficazes no tratamento de ND, conforme discutido no capítulo do livro "*Approaches for the treatment of neurodegenerative diseases related to natural products*". Esta pesquisa, portanto, teve como objetivo avaliar os efeitos neuroprotetor, antiinflamatório e antioxidante de duas moléculas (FMU200 e luteolina-7-O-glucoside (LUT7OG)) nas linhagens celulares SH-SY5Y e RAW264.7. Células SH-SY5Y indiferenciadas e diferenciadas por ácido retinóico (RA) foram pré-tratadas com FMU200 ou LUT7OG e incubadas com 6-hidroxidopamina (6-OHDA) ou peróxido de hidrogênio (H_2O_2). A viabilidade celular e o efeito neuroprotetor foram avaliados com o ensaio MTT. A análise de citometria de fluxo foi realizada para discriminar a apoptose celular. A geração de espécies reativas de oxigênio (ROS) induzida por H_2O_2 ou 6-OHDA e o potencial de membrana mitocondrial ($\Delta\Psi m$) foram avaliados pelos ensaios DCFDA e JC-1, respectivamente. A capacidade antioxidante de LUT7OG foi determinada por ensaios DPPH, FRAP, ORAC e a atividade da caspase-3 e o dano nuclear foram determinados após o tratamento com LUT7OG em células induzidas por 6-OHDA. A fosforilação de JNK foi avaliada por western blot após tratamento com FMU200 em células SH-SY5Y induzidas por H_2O_2. A liberação de TNF-α, IL-6 e IL-10 (efeito antiinflamatório) foi determinada em células RAW264.7 induzidas por LPS por ensaio ELISA. Em células SH-SY5Y indiferenciadas, FMU200 reverteu a neurotoxicidade induzida por 6-OHDA em cerca de 20%, enquanto LUT7OG aumentou a viabilidade celular em 13% após 24h. Em células diferenciadas por RA, o FMU200 reverteu a morte celular em aproximadamente 40% e 90% após 24 e 48h de tratamento, respectivamente, enquanto LUT7OG aumentou a viabilidade celular em aproximadamente 30% e 112% após 24 e 48h, respectivamente. FMU200 reduziu as células apoptóticas precoces e tardias, diminuiu os níveis de ROS, restaurou o $\Delta\Psi m$ e diminuiu a regulação do p-JNK após a exposição ao H_2O_2. LUT7OG mostrou uma alta atividade antioxidante e conferiu um efeito preventivo na despolarização da membrana mitocondrial, diminuiu a atividade da caspase-3 e inibiu a condensação nuclear e fragmentação contra a apoptose induzida por 6-OHDA. Em células RAW264.7 estimuladas por LPS, FMU200 e LUT7OG reduziram os níveis de TNF-α após um tratamento de 3h e aumentaram a IL-10 após 24h. Em resumo, nossos resultados mostram que FMU200 e LUT7OG protegem células de neuroblastoma SH-SY5Y contra apoptose induzida por 6-OHDA e H_2O_2 e protegem células de lesão celular dependente de JNK. Nossos resultados indicam que ambos os compostos podem ser úteis no tratamento de doenças neurodegenerativas.

Palavras-Chave: *c-Jun N-terminal kinase 3* (JNK3); Alvos terapêuticos; Inibidores da quinase; Efeito neuroprotetor; Doenças neurodegenerativas; Apoptose; Estresse oxidativo.

ABSTRACT

Current treatments for neurodegenerative diseases (ND) are symptomatic and do not affect disease progression. Slowing its advancement remains a crucial unmet need for patients and their families. Protein misfolding and aggregation, altered mitochondria metabolism, synaptic dysfunction, oxidative stress, excitotoxicity, neuroinflammation, and cell death are ND hallmarks known to activate the mitogen-activated protein kinases (MAPK) pathway, such as the c-Jun N-terminal kinase (JNK) pathway. In this case, JNK3 inhibitors can play an important role in neuroprotection. As such, in the review article "*c-Jun N-Terminal Kinase Inhibitors as Potential Leads for New Therapeutics for Alzheimer's Disease*" the role of JNK in Alzheimer's Disease was highlighted and experimental treatments based on synthetic JNK inhibitors are described and discussed. However, natural products also have proved to be effective in treating ND, as discussed in the book chapter "*Approaches for the treatment of neurodegenerative diseases related to natural products*". This research, therefore, aims to evaluate the neuroprotective, anti-inflammatory and antioxidant effects of two molecules (FMU200) and luteolin-7-O-glucoside (LUT7OG)) with known JNK3 inhibitory activity in SH-SY5Y and RAW264.7 cell lines. Undifferentiated and retinoic acid (RA)-differentiated SH-SY5Y cells were pre-treated with FMU200 or LUT7OG and incubated with 6-hydroxydopamine (6-OHDA) or hydrogen peroxide (H_2O_2). Cell viability and the neuroprotective effect were assessed with MTT assay. Flow cytometric analysis was performed to discriminate cell apoptosis. H_2O_2 or 6-OHDA-induced reactive oxygen species (ROS) generation and mitochondrial membrane potential ($\Delta\Psi m$) were evaluated by DCFDA and JC-1 assays, respectively. Antioxidant capacity of LUT7OG was determined by DPPH, FRAP, ORAC assays and caspase-3 activity and nuclear damage were determined after LUT7OG treatment in 6-OHDA-induced cells. Phosphorylated JNK was evaluated by western blot after FMU200 treatment in H_2O_2-induced SH-SY5Y cells. Release of TNF-α, IL-6 and IL-10 (anti-inflammatory effect) was determined in LPS-induced RAW264.7 cells by ELISA assay. In undifferentiated SH-SY5Y cells, FMU200 reverted the neurotoxicity induced by 6-OHDA in about 20%, while LUT7OG increased cell viability in 13% after 24h. In RA-differentiated cells, FMU200 reverted cell death in approximately 40% and 90% after 24 and 48h-treatment, respectively while LUT7OG increased cell viability in approximately 30% and 112% after 24 and 48h, respectively. FMU200 reduced both early and late apoptotic cells, decreased ROS levels, restored mitochondrial membrane potential, and downregulated p-JNK after H_2O_2 exposure. LUT7OG showed a high antioxidant activity and conferred a preventive effect in mitochondria membrane depolarization, decreased caspase-3 activity, and inhibited nuclear condensation and fragmentation against 6-OHDA-induced apoptosis. In LPS-stimulated RAW264.7 cells FMU200 and LUT7OG reduced TNF-α levels after a 3h treatment and increased IL-10 after 24h. In summary, our results show that FMU200 and LUT7OG protects neuroblastoma SH-SY5Y cells against 6-OHDA and H_2O_2-induced apoptosis and protect cells from JNK-dependent cell injury. Our findings indicate that both compounds could be useful in the treatment of neurodegenerative disorders.

Keywords: c-Jun N-terminal kinase (JNK); Therapeutic targets; Kinase inhibitors; Neuroprotective effect; Neurodegenerative diseases; Apoptosis; Oxidative stress.

KURZREFERAT

Aktuelle Behandlungen für neurodegenerative Erkrankungen (ND) sind symptomatisch und beeinflussen nicht das Fortschreiten der Krankheit. Die Verlangsamung des Fortschreitens bleibt eine entscheidende, unerfüllte Notwendigkeit für die Patienten und ihre Familien. Proteinfehlfaltung und -aggregation, veränderter Mitochondrienstoffwechsel, synaptische Dysfunktion, oxidativer Stress, Exzitotoxizität, Neuroinflammation und Zelltod sind ND-Kennzeichen, bekannt den Mitogen-aktivierten Proteinkinaseweg (MAPK) aktivieren, wie z. B. der c-Jun N-Terminal Kinase (JNK) Weg. In diesem Fall können die JNK3-Inhibitoren eine wichtige Rolle bei der Neuroprotektion spielen. So wurde im Review-Artikel "*c-Jun N-Terminal Kinase Inhibitors as Potential Leads for New Therapeutics for Alzheimer's Disease*" die Rolle der JNK bei der Alzheimer-Krankheit hervorgehoben und experimentelle Behandlungen auf Basis synthetischer JNK-Inhibitoren beschrieben und diskutiert. Natürliche Produkte haben sich jedoch auch bei der Behandlung von ND als wirksam erwiesen, wie im Kapitel des Buches „*Approaches for the Treatment of Neurodegenerative Diseases Related to Natural Products*" diskutiert wird. Diese Forschung zielte daher darauf ab, die neuroprotektive, entzündungshemmende und antioxidative Wirkung von zwei Molekülen (FMU200 und Luteolin-7-O-Glucosid (LUT7OG)) in den Zelllinien SH-SY5Y und RAW264.7 zu bewerten. Durch Retinsäure (RA) undifferenzierte und differenzierte SH-SY5Y-Zellen wurden mit FMU200 oder LUT7OG vorbehandelt und mit 6-Hydroxydopamin (6-OHDA) oder Wasserstoffperoxid (H_2O_2) inkubiert. Die Zelllebensfähigkeit und die neuroprotektive Wirkung wurden mit dem MTT-Versuch bewertet. Die Analyse der Durchflusszytometrie wurde durchgeführt, um die zelluläre Apoptose zu unterscheiden. Die durch H_2O_2 oder 6-OHDA induzierte Erzeugung von reaktiven Sauerstoffspezies (ROS) und das mitochondriale Membranpotential ($\Delta\Psi m$) wurden im DCFDA- bzw. JC-1-Assays bewertet. Die antioxidative Kapazität von LUT7OG wurde durch DPPH, FRAP, ORAC-Versuche und die Caspase-3-Aktivität und der Kernschäden nach der Behandlung mit LUT7OG in 6-OHDA-induzierten Zellen bestimmt. Die JNK-Phosphorylierung wurde durch western blot nach der Behandlung mit FMU200 in H_2O_2-induzierten SH-SY5Y-Zellen untersucht. Die Freisetzung von TNF-α, IL-6 und IL-10 (entzündungshemmende Wirkung) wurde in LPS-induzierten RAW264.7-Zellen durch ELISA-Versuch bestimmt. In undifferenzierten SH-SY5Y-Zellen kehrte FMU200 die 6-OHDA-induzierte Neurotoxizität um etwa 20% um, während LUT7OG die Zelllebensfähigkeit nach 24H um 13% erhöhte. In den durch RA differenzierten Zellen hatte FMU200 den Zelltod in etwa 40% bzw. 90% nach 24 bzw. 48 h Behandlung zur Folge, während LUT7OG die Zelllebensfähigkeit nach 24 bzw. 48 H um etwa 30% bzw. 112% erhöhte. FMU200 reduzierte sowohl frühe als auch späte apoptotische Zellen, verringerte den ROS-Spiegel, stellte das mitochondriale Membranpotenzial wieder her und senkte p-JNK nach H_2O_2-Exposition. LUT7OG zeigte eine hohe antioxidative Aktivität und verlieh der mitochondrialen Membrandepolarisation eine präventive Wirkung, verringerte Kaspase-3-Aktivität und hemmte die kernnukleare Kondensation und Fragmentierung gegen 6-OHDA-induzierte Apoptose. In LPS-stimulierten RAW264.7-Zellen reduzierten FMU200 und LUT7OG den TNF-α-Spiegel nach einer 3-stündigen Behandlung und erhöhten IL-10 nach 24 h. Zusammenfassend zeigen unsere Ergebnisse, dass FMU200 und LUT7OG die SH-SY5Y Neuroblastomzellen vor 6-OHDA- und H_2O_2-induzierter Apoptose, und Zellen vor JNK-abhängigen Zellverletzungen schützen. Unsere Ergebnisse deuten darauf hin, dass beide

Verbindungen bei der Behandlung neurodegenerativer Erkrankungen nützlich sein können.

Schlüsselwörter: c-jun N-terminale Kinase (JNK)**;** Mitogen-aktivierte Proteinkinase **(**MAPK); Therapeutische Ziele; Kinase-Inhibotoren; Neuroprotektive Wirkung; Apoptose; Oxidativer Stress

LISTA DE FIGURAS

LISTA DE SIGLAS E ABREVIATURAS

5-HT - *5-hydroxytryptamine*

6-OHDA – *6-hydroxydopamine*

aas - *amino acids*

Aβ – *β-amyloid protein*

AICD - *amyloid precursor protein intracellular domain*

ALS - *amyotrophic lateral sclerosis*

APP – *amyloid precursor protein*

ApoE – *alipoprotein E*

ASK – *apoptosis signal-regulating kinase*

ATP – *adenosine triphosphate*

Ach – *acetilcholine*

BACE – *β-site APP clivage enzyme*

BBB – *blood-brain barrier*

BDNF – b*rain-derived neurotrophic factor*

ChAT - c*holine acetyltransferase*

CO_2 – *carbon dioxyde*

CTF – *C-terminal fragment*

DA – *Alzheimer's disease*

DALY - *disability-adjusted life-years*

DCFDA - *2',7'-dichlorofluorescin diacetate*

DCJ – *Creutzfeldt-Jakob's disease*

DH – *Huntington's disease*

DNA – *desoxyrribonucleic acid*

DP – *Parkinson's disease*

DSM – *Diagnosis and Statistic Manual*

DW – *Wilson's disease*

ELISA - *enzyme-linked immunosorbent assay*

ERK – e*xtracelular signal-related kinase*

ETC - *electron transport chain*

FDA – *Food and Drug Administration*

GCK - g*erminal center kinases*

H_2O_2 - *hydrogen peroxyde*

HPK – *homeodomain-Interacting protein kinase*

IBGE – Instituto Brasileiro de Geografia e Estatística

IC_{50} – *inhibitory concentration 50%*

IFNγ - *interferon gamma*

IL-6 – *interleukine-6*

IL-10 – *interleukine-10*

JAK - *janus kinase*

JIP - *JNK-interacting protein*

JNK - *c-Jun N-terminal kinase*

kD – *kiloDalton*

KPI – *kunitz-type protease inhibitor*

LUT7OG – *luteolin-7-O-glucoside*

LPS - *lipopolysaccharide*

MAPK – *mitogen-activated protein kinase*

MAPKK – *mitogen-activated protein kinase kinase*

MAPKKK – *mitogen-activated protein kinase kinase kinase*

MAPKKKK – *mitogen-activated protein kinase kinase kinase kinase*

MCI - *mild cognitive impairment*

MEK – *MAP/ERK kinase*

MHC - m*ajor histocompatibility complex*

MLK – *mixed-lineage kinase*

MOMP - *mitochondrial outer membrane permeabilization*

MPP^+ - *1-methyl-4-phenylpyridinium*

MPTP - *1-methyl-4-phenyl-1,2,3,6-tetrahydropyridine*

mRNA – *messenger RNA*

MTT – *3-(4,5-dimethylthiazol-2-yl)-2,5-diphenyltetrazolium bromide*

NF-kβ – *nuclear factor kappa β*

NO – *nitric oxide*

NFT – *neurofibrillary tangles*

NMDA - *N-methyl-D-aspartate receptor*

PAHO – *Pan-american Health Organization*

PA – *amyloid plaques*

PAK – *p21 activated kinases*

PGE2 - *prostaglandin E_2*

POSH - *plenty of SH3s*

PSEN - *presenilin*

RA – *retinoic acid*

ROS - *reactive oxygen species*

RNA – *ribonucleic acid*

SNC – *central nervous system*

SOCS-3 - *suppressor of cytokine signaling 3*

TACE/ADAM17 – *tumor necrosis fator converting enzyme/α-desintegrin and metalloproteinase 17*

TAK – *transforming growth factor beta-activated kinase*

TLR - *toll-like receptors*

TNF-α – *tumoral necrosis factor α*

UV - *ultraviolet*

VMAT - *vesicular monoamine transporter*

WHO – *World Health Organization*

YLD - *years lived with disability*

YLL - *years of life lost*

SUMÁRIO

Apresentação

Esta Tese de Doutorado está organizada da seguinte forma:

O Capítulo I apresenta uma introdução sobre o trabalho, a identificação do problema da pesquisa, os objetivos do trabalho, a justificativa da pesquisa e o referencial teórico utilizado como base para o projeto.

Os resultados do presente estudo estão apresentados na forma de artigos científicos, nesse sentido, o Capítulo II refere-se a um manuscrito de revisão bibliográfica publicado em 18 de dezembro de 2020 no periódico *International Journal of Molecular Sciences (IJMS).*

O Capítulo III contextualiza o processo de diferenciação da linhagem celular SH-SY5Y por meio do uso de RA.

O Capítulo IV descreve os resultados obtidos com o inibidor de JNK sintético FMU200. O manuscrito foi publicado no periódico *IJMS* em 2 de abril de 2021.

O Capítulo V inclui um manuscrito em preparação, cujos resultados referem-se ao estudo do potencial neuroprotetor do flavonoide LUT7OG.

O Capítulo VI aborda a análise e discussão dos resultados obtidos pela realização da pesquisa e apresenta as considerações finais e atividades futuras, aborda os objetivos alcançados e as considerações realizadas em relação à continuidade da pesquisa.

Por último, a seção de Apêndices e Anexos encontra-se o protocolo de diferenciação de células SH-SY5Y desenvolvido para o presente trabalho, bem como contém um manuscrito publicado também no periódico *IJMS* em 14 de fevereiro de 2021, o qual foi resultado da colaboração com o *Marine and Environmental Sciences Centre* (MARE) do Instituto Politécnico de Leiria (Portugal).

Capítulo I

Introdução;

Objetivos;

Referencial Teórico;

.

1. INTRODUÇÃO

De acordo com os relatórios divulgados pela WHO (*World Health Organization*), pessoas em todo o mundo estão vivendo mais. Em 2050, a população mundial com 60 anos ou mais deve totalizar 2 bilhões, contra 900 milhões em 2015. Hoje, 125 milhões de pessoas têm 80 anos ou mais. Já para a população com 80 anos estima-se que haverão 434 milhões de pessoas nesta faixa etária em todo o mundo, sendo que 80% de todas as pessoas idosas viverão em países de renda baixa e média (AGEING AND HEALTH, [*s. d.*]). No Brasil, de acordo com o censo do IBGE realizado em 2010, a população total do território brasileiro era de pouco mais de 192 milhões de habitantes. Destes, mais de 11 milhões tinham de 60 a 69 anos e aproximadamente 9 milhões, mais de 70 anos.

À medida que as populações estão crescendo e envelhecendo, a prevalência dos principais distúrbios neurológicos incapacitantes aumenta drasticamente (AGEING AND HEALTH, [*s. d.*]; GBD 2016 NEUROLOGY COLLABORATORS, 2019). De fato, no nível biológico, o envelhecimento resulta do impacto do acúmulo de uma ampla variedade de danos moleculares e celulares ao longo do tempo. Isso leva a uma diminuição gradual da capacidade física e mental, um risco crescente de doenças e, por fim, de morte (LÓPEZ-OTÍN *et al.*, 2013; MELZER; PILLING; FERRUCCI, 2020; RUDZIŃSKA *et al.*, 2020). Dentre as doenças associadas ao envelhecimento, destaca-se um tipo específico de demência, a doença de Alzheimer (DA).

No ano de 2016 os distúrbios neurológicos foram a principal causa de DALYs (*disability-adjusted life-years*; a soma dos anos de vida perdidos [YLLs, *years of life lost*] e dos anos vividos com deficiência [YLDs, *years lived with disability*]) (276 milhões) e a segunda principal causa de mortes (9 milhões). Identificou-se que, em quase 30 anos (1990 à 2016) o número absoluto de mortes aumentou em 39%, enquanto que o número de DALYs cresceu em 15%. Dados globais (195 países) indicaram que os quatro maiores contribuintes de DALYs neurológicos foram acidente vascular cerebral (42,2%), enxaqueca (16,3%), Alzheimer e outras demências (10,4 %) e meningite (7,9%) (GBD 2016 DEMENTIA COLLABORATORS, 2019; GBD 2016 NEUROLOGY COLLABORATORS, 2019). Isso sugere que os governos enfrentarão uma demanda crescente por tratamento, reabilitação e serviços de apoio para distúrbios neurológicos. Além disso, a escassez de riscos

modificáveis estabelecidos para a maior parte das doenças neurológicas demonstra que novos conhecimentos são necessários para desenvolver estratégias eficazes de prevenção e tratamento.

Já se passaram 114 anos desde o primeiro diagnóstico oficial de DA e um progresso considerável foi feito, mas alguns aspectos complexos permanecem obscuros. A DA é uma doença multifatorial, pois parece resultar de aspectos genéticos, epigenéticos, interatômicos e ambientais interagindo de maneiras diferentes, resultando em fenótipos altamente heterogêneos. Além disso, apesar da grande prevalência, até o momento não existe um tratamento que promova a cura da doença. De fato, nenhum dos fármacos disponíveis atualmente para o tratamento da DA é capaz de diminuir ou interromper a destruição neuronal e apesar de que 244 novos fármacos foram testados entre 2002 e 2012, apenas um conseguiu avançar até a fase final – mas ainda aguarda por aprovação do FDA (ALZHEIMER'S ASSOCIATION, 2019; DRUG SAFETY AND AVAILABILITY | FDA).

O alto índice de falha sugere que moléculas que possuam alvos terapêuticos diferentes deveriam ser exploradas (ALZHEIMER'S ASSOCIATION, 2019; FERRI *et al.*, 2005; SCHNEIDER, Lon S *et al.*, 2015; SERRANO-POZO *et al.*, 2011). Nesse sentido, o alvo terapêutico de um fármaco pode ser, por exemplo, uma proteína cuja disfunção está relacionada a um processo patológico. Contudo, somente a identificação de alvos terapêuticos e o desenvolvimento de moléculas que interajam com tais alvos não é suficiente, uma vez que a determinação da toxicidade é essencial para identificar os efeitos adversos tanto durante o processo de validação e otimização das moléculas quanto após a aprovação e comercialização. Nesse sentido, por meio do uso de ferramentas biotecnológicas como estudos *in vitro* para determinar a citotoxicidade de novas moléculas, é possível identificar precocemente drogas candidatas que sejam inadequadas para o uso humano ou animal, permitindo economizar recursos financeiros. Já o uso de modelos experimentais *in vitro* de doenças (a partir de neurotoxinas, por exemplo) permite, até certo ponto, determinar alguns dos efeitos terapêuticos que ela possui. Além disso, a partir de resultados obtidos de ensaios *in vitro*, é possível determinar se aquela molécula candidata deverá ser modificada para atingir o ideal efeito *in vitro*, além avaliar a especificidade da molécula e identificar interações indesejáveis com proteínas "*off-target*".

1.1 Tema

Inibição de proteínas da via JNK3/p38 e doenças neurodegenerativas.

1.2 Problema

As moléculas FMU200 e luteolina-7-o-glicosídeo (LUT7OG) possuem potencial de inibir a apoptose em células de neuroblastoma (SH-SY5Y) via JNK3/ p38 em modelo *in vitro* de DA?

1.3 Objetivos

1.3.1 Objetivo Geral

Identificar e investigar o potencial farmacológico de drogas candidatas frente ao processo de neurodegeneração na DA em modelo celular *in vitro*.

1.3.2 Objetivos Específicos

- Determinar a viabilidade de células de neuroblastoma SH-SY5Y e macrófagos RAW264.7 submetidas ao tratamento de inibidores de JNK3/p38;
- Desenvolver e validar um protocolo de diferenciação de células SH-SY5Y por meio de RA;
- Desenvolver e validar um modelo *in vitro* de neurodegeneração por meio de 6-OHDA com células diferenciadas;
- Analisar e Identificar o efeito neuroprotetor dos compostos em células de neuroblastoma SH-SY5Y diferenciadas e não diferenciadas quando expostas à 6-OHDA;
- Estudar dos mecanismos de morte celular em células de neuroblastoma SH-5YSY submetidas ao tratamento de inibidores de JNK3/p38 expostas a H_2O_2 por citometria de fluxo;
- Analisar o $\Delta\Psi m$ em células de neuroblastoma SH-5YSY submetidas ao tratamento de inibidores de JNK3/p38 expostas a H_2O_2 por meio de citometria de fluxo e espectrofotometria de fluorescência por leitor de microplacas;
- Avaliar a produção de ROS em células de neuroblastoma SH-5YSY submetidas ao tratamento de inibidores de JNK3/p38 expostas a H_2O_2 por método espectroanalítico de fluorescência;

- Analisar o potencial anti-inflamatório dos inibidores de JNK3/p38 em cultura de macrófagos RAW 264.7 através da dosagem de citocinas inflamatórias TNF-α, IL-6 e IL-10;

- Identificar novos alvos e propor o mecanismo de ação dos compostos testados por meio da análise da expressão protéica de marcadores moleculares JNK, p-JNK e β-actina;

1.4 Justificativa

Apesar de ser uma doença conhecida há mais de cem anos, o tratamento atual parece ser mais paliativo ao restringir-se ao manejo dos sintomas ao retardar temporariamente o comprometimento cognitivo (BURKE *et al.*, 2014; CUMMINGS *et al.*, 2017; DEY *et al.*, 2017; FRIEDLANDER, 2003; JOVICIC *et al.*, 2015; TARAGANO *et al.*, 1997). De acordo com a *Food and Drug Administration* (FDA) e a *Alzheimer's Association*, existem cinco medicamentos aprovados para o tratamento da DA: Donepezila, galantamina, memantina, rivastigmina, além de uma associação entre memantina e donepezila (DRUG SAFETY AND AVAILABILITY | FDA, [*s. d.*]) [29]. Durante 20 anos, a tacrina foi um sexto medicamento disponível para o mesmo fim, mas seu uso está proibido desde 2013 devido à elevada hepatotoxicidade (TACRINE - DRUGBANK, [*s. d.*]). Isso significa que, de modo genérico, os sintomas da DA são passíveis de manejo, mas nenhum medicamento é capaz de retardar a progressão da doença nem impedir a morte das células neuronais, o que torna a DA incurável e fatal em todos os casos.

Há ainda inúmeros pontos que permanecem incertos tanto em relação a fisiopatologia quanto ao tratamento da DA e isso resulta em um impacto no desenvolvimento de novas drogas. Apesar de cerca de 200 medicamentos estarem em fase 2 de análise, esses mostram um efeito clínico limitado e há controvérsia quanto à sua eficácia terapêutica. Além disso, nenhuma nova droga foi aprovada desde 2003 (BURKE *et al.*, 2014; SCHNEIDER, Lon S *et al.*, 2015). Nesse sentido, existem muitos alvos de fármaco potenciais e, até agora, não há alvos validados, exceto talvez para o sistema colinérgico (DEY *et al.*, 2017; REVETT *et al.*, 2013; SCHNEIDER, Lon S *et al.*, 2015).

De acordo com a clássica hipótese da via amiloidogênica, as alterações encontradas na DA são caracterizadas por acumulações extracelulares de placas

amiloides (PA), formadas de proteína β-amilóide (Aβ) e emaranhados neurofibrilares intracelulares (NFTs) compostos por proteínas τ hiperfosforiladas. Por conseguinte, a neurodegeneração na DA ocorre devido a um processamento anormal de proteínas precursoras de amiloides (APP) através da atividade da enzima de clivagem de APP do β-site 1 (BACE1) e presenilina 1 (PS1). Todos esses processos levam à produção de oligômeros Aβ tóxicos que se acumulam e levam a disfunção sináptica e perturbação da atividade de proteínas quinases, resultando em perda neuronal e demência (BURKE *et al.*, 2014; BU; RAO; WANG, 2016; CRAFT *et al.*, 2017; DAVIES; MALONEY, 1976; DRACHMAN; LEAVITT, 1974; KEREN-SHAUL *et al.*, 2017; MAEZAWA *et al.*, 2011; MAYEUX, 2006; MCKEEVER *et al.*, 2017). Contudo, embora a presença de Aβ seja necessária para um diagnóstico definitivo de DA, os agregados não são suficientes para causar declínio cognitivo (PILLAI *et al.*, 2020; REVETT *et al.*, 2013). Nesse caso, a disfunção sináptica, o estresse oxidativo e a excitotoxicidade, que induzem a ativação das vias de proteínas quinase ativadas por mitógenos (MAPK), como a via JNK (c-Jun N-terminal kinase), também são necessárias para provocar a perda progressiva de neurônios e sinapses, atrofia cerebral e aumento dos ventrículos cerebrais (POOLER; NOBLE; HANGER, 2014; ROSKOSKI, 2015; SAVAGE *et al.*, 2002; SERRANO-POZO *et al.*, 2013; TAKASHIMA, 2016; YARZA *et al.*, 2015). Ou seja, a toxicidade decorrente dos eventos moleculares em resposta ao acúmulo de PA e NTF, induz a ativação da via JNK/p38, podendo levar à morte neuronal contribuindo para o dano neurológico e aparecimento dos sintomas clássicos da DA (BOGOYEVITCH *et al.*, 2010; CHANG; KARIN, 2001; CLARKE *et al.*, 2012; COFFEY, 2014; HAEUSGEN *et al.*, 2009; JOVICIC *et al.*, 2015; OKAZAWA; ESTUS, 2002; RAMAN; CHEN; COBB, 2007; YOON *et al.*, 2012).

Ou seja, considerando que inúmeras drogas candidatas que objetivavam impactar de alguma forma a via amiloidogênica foram reprovadas em ensaios clínicos de fases II e III (LIU, *et al.*, 2019), e sabendo-se do envolvimento de JNK na propagação de sinais pró-apoptóticos nas vias extrínseca e intrínseca (GALEOTTI; GHELARDINI, 2012; KONDOH; NISHIDA, 2007; TOURNIER *et al.*, 2000), a inibição de JNK3 vem sendo explorada como um possível alvo terapêutico (HEPP REHFELDT *et al.*, 2020).

2. REFERENCIAL TEÓRICO

2.1 Aspectos neuropsiquiátricos de transtornos demenciais: Doença de Alzheimer (DA)

Em 1906, o Dr. Alois Alzheimer descreveu, pela primeira vez, uma doença incomum do córtex cerebral. Segundo o neurologista alemão, a paciente sofria de perda de memória, desorientação no tempo e no espaço, alucinações e disfunção da linguagem. Após a morte precoce da paciente, aos 55 anos de idade, o médico realizou um exame *post-mortem* no cérebro da paciente e notou que havia um afinamento no córtex cerebral, além da presença de placas e emaranhados dentro e fora dos neurônios (ALZHEIMER, 1907; SMALL; CAPPAI, 2006).

Hoje, a "doença incomum" é conhecida como DA e é responsável por aproximadamente 60 a 70% dos casos de demência de início tardio. De acordo com a 5ª edição do Manual Diagnóstico e Estatístico de Transtornos Mentais (DSM-V, p. 591), a demência caracteriza-se por uma síndrome com prejuízo de memória e de, pelo menos, uma outra capacidade cognitiva incapacitante, representando um declínio nos níveis de funcionamento intelectual e que não esteja presente exclusivamente durante um *delirium*. Entretanto, o termo demência é uma definição genérica para uma síndrome que acomete indivíduos em estágios finais da vida e que possui uma variedade de etiologias. Ou seja, a demência pode apresentar outros fatores etiológicos como no caso das demências do sistema lenticulo-estriatal que incluem as doenças de Huntinton (DH), Parkinson (DP), Wilson (DW), entre outras, bem como demências vasculares, demência hidrocefálica ou doença de Creutzfeldt-Jakob (DCJ), por exemplo.

Os pesquisadores acreditam que a prevalência geral de DA em indivíduos com mais de 60 anos de idade é de 40,19% em todo o mundo (GBD 2016 DEMENTIA COLLABORATORS, 2019). Há cinco anos, o relatório anual World Alzheimer Report de 2015 apontava que o percentual de indivíduos com mais de 60 anos com diagnóstico de DA correspondia a 12,2% da população mundial na época. O mesmo relatório projeta um aumento desse percentual para 16,3% em 2030 e 21,2% em 2050, prevendo que o número de casos quase dobraria a cada 20 anos (ALZHEIMER'S ASSOCIATION, 2017, 2019).

Clinicamente, a DA é dividida em DA 'de início tardio' ou 'esporádica' (LOAD) - que é a forma mais comum de DA - e DA 'de início precoce' ou 'familiar' (EOAD), que é responsável por 1-5% de todos os casos de DA e é causada por mutações hereditárias dominantes em genes como *APP, PSEN1, PSEN2* e *APOE* (CUYVERS; SLEEGERS, 2016). Um diagnóstico definitivo de DA somente é possível por meio de autópsia, onde são identificadas alterações histopatológicas. Por outro lado, é possível deduzir um diagnóstico possível, provável ou ainda improvável de acordo com alguns critérios específicos (MCKHANN, *et al.*, 1984; MCKHANN, *et al.*, 2011). Sendo assim sintomas como prejuízo da aprendizagem de informações novas, lembrança deficiente de material remoto, nomeação e compreensão auditiva prejudicadas, deterioração das capacidades construtivas e visuo-espaciais, cálculo, abstração e julgamento deficientes podem indicar uma possível DA. Além disso, o paciente geralmente tende a demonstrar pouca ou nenhuma preocupação com as falhas cognitivas que apresenta. Ainda, é possível identificar a presença de alterações na personalidade, apatia, alterações do humor, ansiedade, irritabilidade, desinibição, distúrbios da atividade psicomotora, delírios, alucinações e alterações comportamentais abrangendo distúrbios do sono e distúrbios do apetite, comportamento sexual alterado, entre outros (DSM-V, p. 611-614; BRAAK; BRAAK, 1997).

Como uma doença neurodegenerativa progressiva, alguns sinais e sintomas como apraxia podem estar presentes em estágios iniciais da doença, enquanto que a agnosia, um sintoma facilmente associado a DA, inclusive por leigos, torna-se presente em estágios finais. De forma semelhante, a fluência verbal, habilidade de repetição e de leitura em voz alta são mantidas até os estágios finais da DA, assim como as funções motora e sensorial. Com o decorrer dos anos, já na fase final da doença, o paciente apresenta quase que uma total extinção da função intelectual, bem como uma perda progressiva da locomoção e coordenação motora, disfagia e incontinência. Devido a isso, é comum que pneumonias por aspiração, infecções do trato urinário, septicemias, em decorrência de úlceras de decúbito infectadas ou outras doenças independentes, relacionadas à idade como doenças cardiovasculares ou câncer, levem o paciente a óbito. Isso significa que o curso da doença é inexoravelmente progressivo e que, em geral, os pacientes sobrevivem

uma década do diagnóstico até a morte (DUTHIE; CHEW; SOIZA, 2011; HAAKSMA *et al.*, 2017; MCCORMICK *et al.*, 1994).

2.1.1 Características etiológicas, anatomofisiopatológicas e moleculares da DA

Apesar da etiologia da DA ainda não estar totalmente compreendida, autores apontam que tanto fatores genéticos quanto ambientais podem contribuir para a patogênese e progressão da doença (GOLDMAN *et al.*, 2011; REVETT *et al.*, 2013; SERRANO-POZO *et al.*, 2013; WILLIAMSON; GOLDMAN; MARDER, 2009). Do ponto de vista genético, estudos de ligação indicam que um pequeno grupo de indivíduos com DA familiar possuem um padrão de herança autossômico dominante envolvendo majoritariamente três genes: *APP* (*amyloid beta precursor protein*), *PSEN1* (*presenilin 1*) e *PSEN2* (*presenilin 2*). Autores identificaram que alterações genéticas no gene APP levam ao aumento da capacidade de clivagem proteolítica da Aβ (*β-amyloid protein*). Entretanto, a maioria dos casos ainda parece estar ligada a mutações pontuais nos genes da família *PSEN*, especialmente *PSEN1, 2* e *3* (CROSS-DISORDER GROUP OF THE PSYCHIATRIC GENOMICS CONSORTIUM *et al.*, 2013; GOLDMAN *et al.*, 2011; IMBIMBO; LOMBARD; POMARA, 2005; REVETT *et al.*, 2013).

Ainda, outro gene amplamente associado a DA é o *APOE* (*alipoprotein E*). Em 1993, foi possível estabelecer uma relação entre a APOE e a DA na qual identificou-se não apenas uma maior presença do alelo ε4 do gene *APOE* em pacientes classificados como possíveis ou prováveis DA, em comparação com indivíduos controle (SAUNDERS *et al.*, 1993), mas também que o risco conferido pela presença deste alelo aumenta de forma “dose-dependente”, ou seja, o risco de desenvolver DA aumenta de 20% a 90%, e a média de idade de início da doença diminui de 84 para 68 anos, com a presença de dois alelos ε4 (CORDER *et al.*, 1993).

Embora esses achados sejam críticos na compreensão da patogênese biológica da DA, mutações genéticas são responsáveis por apenas 30 a 50% dos casos de DA de início precoce, o que, por sua vez, apenas representa entre 6 e 8% de todos os casos de DA (YANG; SONG; QING, 2017). Ou seja, a falta de ligação genética conclusiva, na maioria dos casos de DA, não só destaca a possível

existência de fatores de risco genéticos não identificados, mas também a importância dos fatores ambientais no desenvolvimento da patologia da doença.

Nesse sentido, apesar de recentes evidências identificarem novos fatores ambientais como possíveis contribuintes para a DA (ACCORRONI *et al.*, 2017; BENEDICTUS *et al.*, 2017; CRAFT *et al.*, 2017), certos fenômenos e modificações moleculares parecem ter suas consequências e influências diretas sobre a patogênese da DA melhor compreendidas até agora. Existem várias hipóteses descritivas sobre as causas da DA, incluindo a hipótese amilóide, hipótese de propagação de τ, hipótese colinérgica, hipótese mitocondrial, hipótese inflamatória e outras. A hipótese mais conhecida é a amiloidogênica, uma vez que descreve algumas características clássicas da DA (CASTELLO; SORIANO, 2014). Dentre elas, o depósito de placas amilóides (PA) e os emaranhados neurofibrilares (NFTs), duas características neuropatológicas comuns na DA. Outros autores defendem ainda que há um declínio importante de sinapses, o que explicaria melhor a relação entre as alterações cerebrais e o declínio cognitivo (CASTELLO; SORIANO, 2014; IMBIMBO; LOMBARD; POMARA, 2005; MOHANDAS; RAJMOHAN; RAGHUNATH, 2009; REVETT *et al.*, 2013; SERRANO-POZO *et al.*, 2016; SWERDLOW, 2007; YANG; SONG; QING, 2017).

As PA são agregados compostos por acúmulo de proteínas Aβ que, ao serem secretadas no espaço extracelular, conferem uma importante toxicidade nos neurônios circundantes. Por sua vez, a Aβ é formada a partir de proteína precursora β-amilóide (APP), por meio de duas clivagens subsequentes realizadas pelas secretases. Nesse sentido, esse acúmulo de Aβ ocorre basicamente devido a duas possíveis situações: produção elevada de APP (em consequência de expressão gênica aumentada) ou eliminação ineficiente de Aβ no cérebro (CASTELLO; SORIANO, 2014; IMBIMBO; LOMBARD; POMARA, 2005; MOHANDAS; RAJMOHAN; RAGHUNATH, 2009; POOLER; NOBLE; HANGER, 2014; REVETT *et al.*, 2013; SAUNDERS *et al.*, 1993; SERRANO-POZO *et al.*, 2016; SWERDLOW, 2007; YANG; SONG; QING, 2017).

O gene APP está localizado no cromossomo 21 e seu mRNA (RNA mensageiro) pode sofrer splicing alternativo nos éxons 7 e 8, e produzir três isoformas principais, denominadas APP 695, APP 751 e APP 770. A isoforma de 695 aminoácidos é predominantemente encontrada nos neurônios, e as isoformas de

751 e 770 aminoácidos são preferencialmente expressas de forma sistêmica, sendo que, no córtex cerebral humano, a proporção das diferentes isoformas de mRNA de APP é aproximadamente APP 770:APP 751:APP 695 = 1:10:20, embora existam diferenças regionais. Constitucionalmente, a isoforma APP 751 contém um domínio adicional, denominado KPI (*Kunitz-type protease inhibitor*) em comparação a APP 695. Já a isoforma APP 770, por sua vez, além de conter o domínio KPI também contém outro domínio composto por 19 aminoácidos chamado OX2. Finalmente, o domínio Aβ, presente em todas as isoformas, localiza-se parcialmente no meio extracelular (ectodomínio) e no espaço transmembranar. Esse domínio pode ainda apresentar de 40 a 43 resíduos de aminoácidos, sendo que a isoforma associada à doença de Aβ é Aβ42 e representa 5-10% da quantidade total de Aβ que é produzida (COFFEY, 2014; GOLDMAN *et al.*, 2011; IMBIMBO; LOMBARD; POMARA, 2005; KANUNGO, 2017; MOHANDAS; RAJMOHAN; RAGHUNATH, 2009; POOLER; NOBLE; HANGER, 2014; SAUNDERS *et al.*, 1993) (Figura 1).

Figura 1. Representação esquemática das três principais isoformas da APP e seus principais domínios

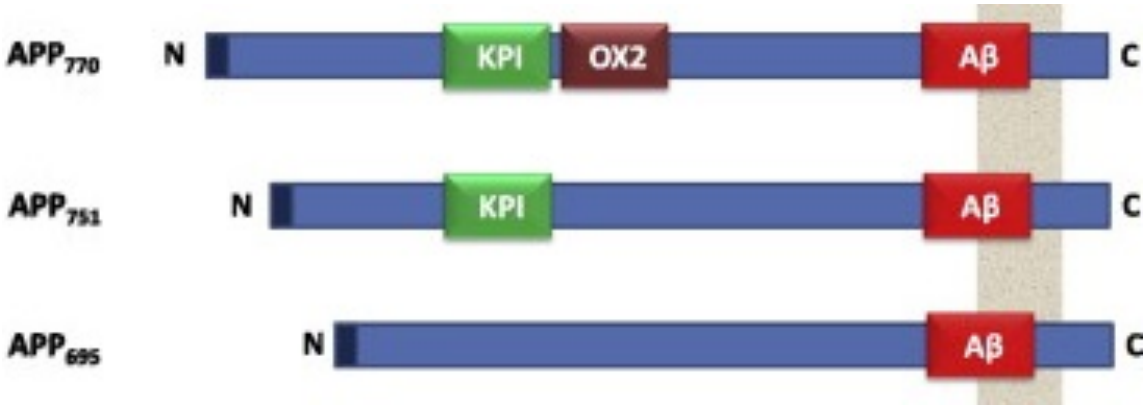

Fonte: adaptado de Gabibov et al. (2013).

Fisiologicamente, a APP é processada proteoliticamente, sofrendo uma clivagem nos sítios de α ou β-secretases, para liberar grandes ectodomínios no meio extracelular, designados sAPPα ou sAPPβ, respectivamente. Ao ser clivada pela β-secretase BACE1 (*β-site amyloid precursor protein cleaving enzyme 1*) na porção N-terminal, inicia-se o processamento amiloidogênico (ou via amiloidogênica) na qual ocorre a liberação da sAPPβ, além de um fragmento C-terminal (CTF) de 99 resíduos de aminoácidos, denominado C99. Esse fragmento C99, por sua vez, sofre uma segunda clivagem no sítio γ por γ-secretase, liberando um domínio intracelular

AICD e pequenos fragmentos de Aβ contendo entre 39 e 43 resíduos de aminoácidos. As formas mais comuns desse peptídeo geralmente contêm 40 e 42 aminoácidos, sendo designadas portanto, Aβ40 e Aβ42, respectivamente. Embora Aβ42 represente apenas de 5 a 10% da quantidade de Aβ total produzida, é a principal componente proteico das PA. Por outro lado, uma rota alternativa envolve o processamento não amiloidogênico de moléculas de APP que envolve a clivagem no sítio α, localizado dentro da região Aβ. Essa clivagem inicial é realizada por outro membro da família de enzimas secretases, a TACE/ADAM17 (*tumor necrosis factor converting enzyme/α disintegrin and metalloproteinase 17*), resultando na liberação de sAPPα, além de um CTF de 83 aminoácidos (C83). De forma semelhante, ocorre uma segunda clivagem de C83 por uma γ-secretase, o que resulta em uma proteína Aβ truncada e não tóxica na porção N-terminal, a chamada p3 (COFFEY, 2014; GOLDMAN *et al.*, 2011; IMBIMBO; LOMBARD; POMARA, 2005; KANUNGO, 2017; MOHANDAS; RAJMOHAN; RAGHUNATH, 2009; POOLER; NOBLE; HANGER, 2014; SAUNDERS *et al.*, 1993; SWERDLOW, 2007; WILLIAMSON; GOLDMAN; MARDER, 2009) (Figura 2):

Figura 2. Representação das vias amiloidogênica e não-amiloidogênica

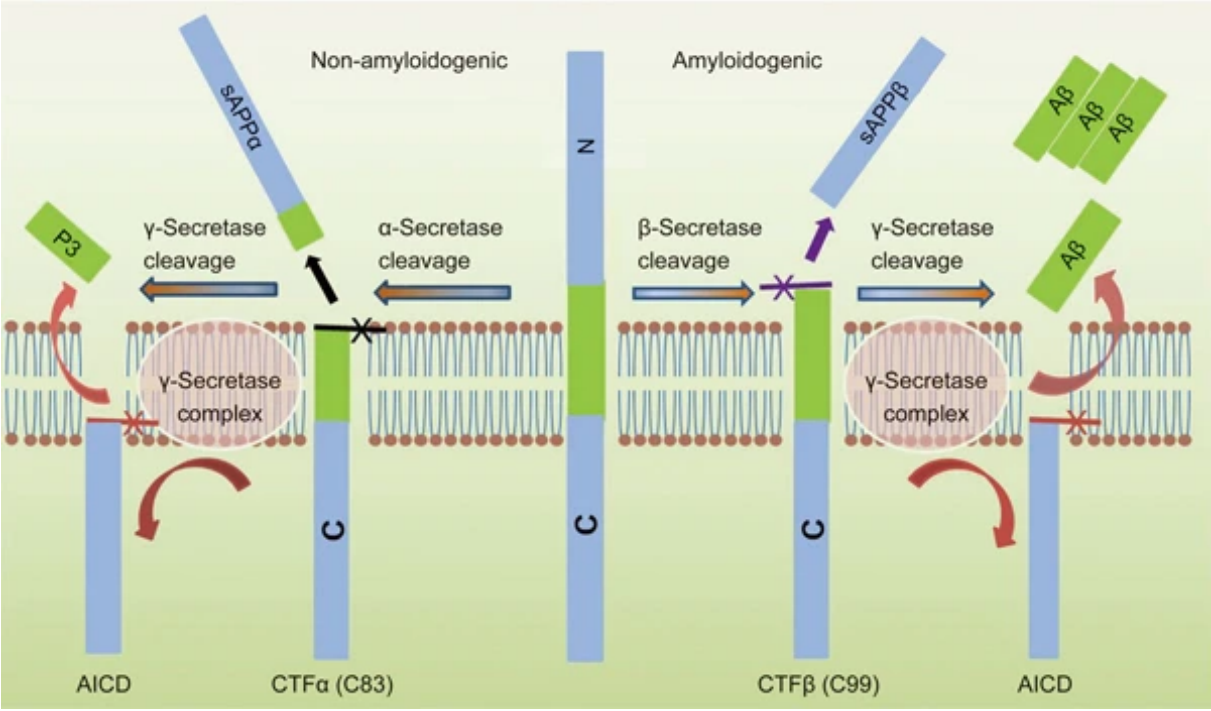

Fonte: Adaptado de CHEN *et al.,* (2017).

Nesse sentido, a manifestação clínica da DA é, portanto, associada a altos níveis de agregados Aβ amplamente distribuídos por todo o cérebro. Além disso, a Aβ demonstrou promover a agregação τ, sugerindo que a agregação de proteínas representa um iniciador e/ou promotor da doença. Como resultado, um alto nível de produção de Aβ está diretamente relacionado a outros eventos críticos, como formação de emaranhados, morte neuronal, perda ou disfunção sináptica. Além disso, Aβ também é relatado como responsável por conferir excitotoxicidade e ativar vias de sinalização relacionadas ao estresse (CASTELLO; SORIANO, 2014; LIU, *et al.*, 2015; SAVAGE *et al.*, 2002; SCHULZ *et al.*, 2014; TAKAHASHI; NAGAO; GOURAS, 2017; TAKASHIMA, 2016).

Assim, um conjunto de proteínas quinases pertencentes a família da MAPK (*mitogen-activated protein kinase*), denominadas JNK (*c-Jun N-terminal kinases*) e p38, ganhou notoriedade ao ser apontado como mediador central do dano excitotóxico no SNC adulto (ZEKE *et al.*, 2016) e, desde então vem sendo explorado como um possível alvo terapêutico.

2.2 Proteínas quinases ativadas por mitógenos: JNK/p38

A grande família das proteínas quinases ativadas por mitógenos (MAPK) pode ser considerada como a principal propagadora de sinais extracelulares da membrana plasmática para o núcleo. Dentre elas, as três subfamílias mais conhecidas são as ERK (*extracellular signal-regulated kinase*), JNK e p38. Enquanto que a via ERK é ativada majoritariamente em resposta a um estímulo mitótico, as vias JNK e p38 são ativadas por estressores celulares (Figura 3) (KANUNGO, 2017; MITTAL *et al.*, 2014).

Figura 3. Rota de sinalização das MAPK

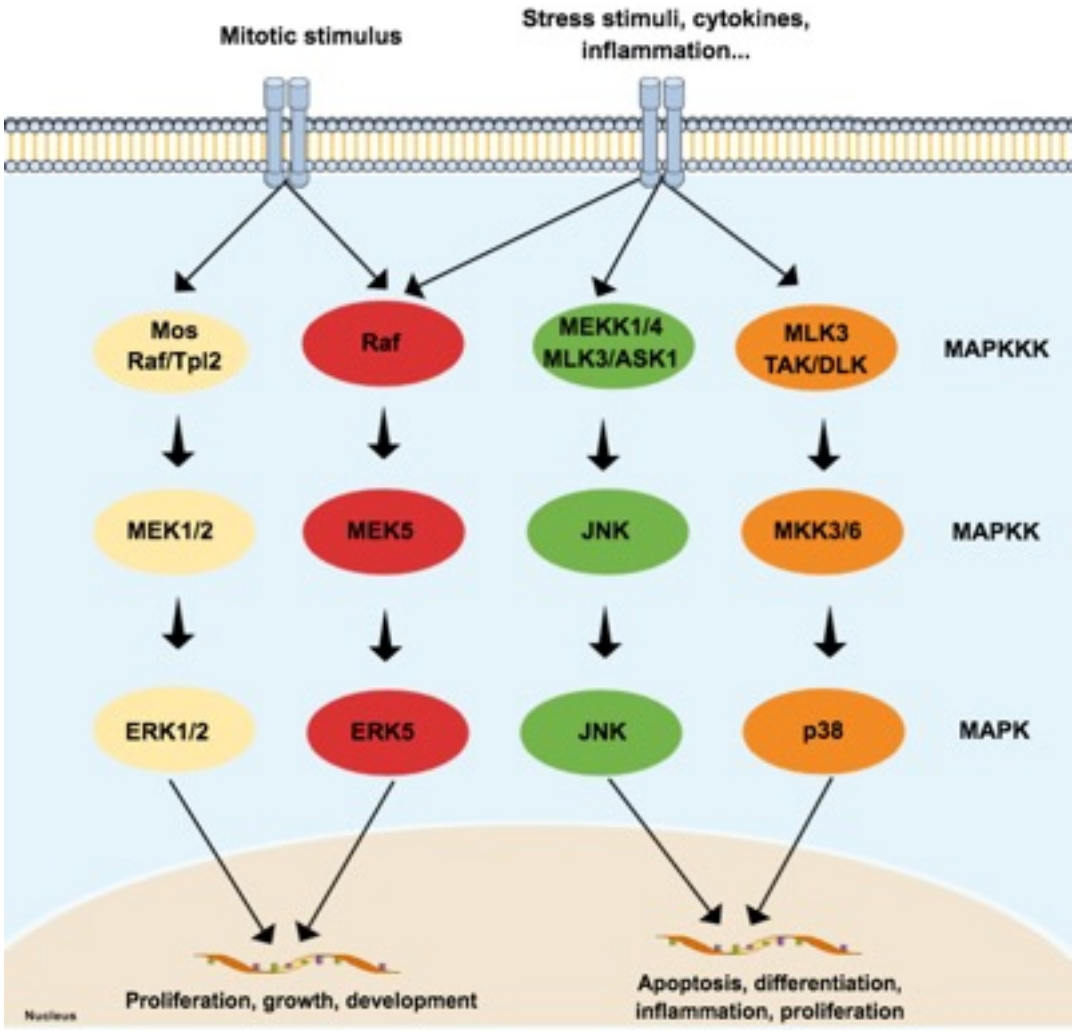

Fonte: Rehfeldt *et al.* (2020).

Constituindo o início da cascata de sinalização extrínseca das MAPK, as MAPKKK (*Mitogen-Activated Protein Kinase Kinase Kinases*) podem ser moduladas por interações entre proteínas ou por modificações covalentes. Podem ser ativadas, de acordo com o estímulo percebido por GTPases como Ras (Raf) ou GTPases da família Rho (MLK3 ativada por Cdc42 e MEKK1 ativada por RhoA), ubiquitinação do receptor de IL-1 para sinalização de TAK1, auto-ubiquitinação de MEKK1 ou, ainda, fosforiladas por uma MAPKKKK como PAK, GCK e HPK, envolvidas no controle de interação de MAPKKK com outras proteínas. Essa diversidade na regulação de MAPKKK permite a ativação de MAPK em resposta a um grande número de estímulos (KHEIRI *et al.*, 2018; KHOLODENKO; BIRTWISTLE, 2009; KIM; CHOI, 2010; RAMAN; CHEN; COBB, 2007; SHUAIB *et al.*, 2016; YUE; LÓPEZ, 2020).

Uma vez que a célula identifica um desses estímulos, é iniciado uma via de sinalização apoptótica podendo esta ser extrínseca, iniciada por TNF, TRAIL, Aβ, 6-OHDA (*6-hydroxydopamine*), UV (radiação ultra-violeta), por exemplo, ou intrínseca, mediada por eventos mitocondriais, como a liberação do citocromo C e ativação de caspases. Entretanto, embora as vias das MAPK possuam diversas interligações que, por vezes dificultam a separação das vias, JNK e p38 particularmente destacam-se das demais MAPKs uma vez que podem ativar sinais pró-apoptóticos por duas formas distintas: 1) via extrínseca, na qual há uma ativação de fatores de transcrição específicos, como c-Jun, ATF-2 ou p53 que aumentarão a expressão de genes pró-apoptóticos; 2) via intrínseca por modulação da atividade de proteínas mitocondriais pró e anti-apoptoticas (COFFEY, 2014; KANUNGO, 2017; MITTAL *et al.*, 2014; YUE; LÓPEZ, 2020).

De uma forma geral, a ativação da JNK que ocorre via MAPKK (via extrínseca) é uma das vias mais complexas, uma vez que envolve o recrutamento de um grande número de MAPKKK. Ou seja, MAPKKK, como MEKKs (*MAP/ERK Kinase-Kinases*), ASKs (*Apoptosis Signal-regulating Kinases*) e MLKs (*Mixed-Lineage Kinases*) são capazes de ativar MAPKKs como MKK4 e MKK7 levando à apoptose. Entretanto, para a ativação da JNK, ainda é necessária uma interação entre proteínas scaffold JIP 1-3 e o complexo “HPK1-MLK1-MKK4/7-JNK” que confere uma modificação estrutural nesse complexo para a correta fosforilação de JNK. Além de JIP 1-3, outras proteínas como POSH também são fundamentais para ancoragem ao complexo, uma vez que parecem facilitar a interação entre GTP-Rac1 e as proteínas subsequentes conforme pode ser observado na Figura 4 abaixo (AHMED *et al.*, 2020; HEPP REHFELDT *et al.*, 2020; HERLAAR; BROWN, 1999; SILVERS; BACHELOR; BOWDEN, 2003; WHITMARSH, 2006; YUE; LÓPEZ, 2020).

Figura 4. Rota de sinalização da JNK

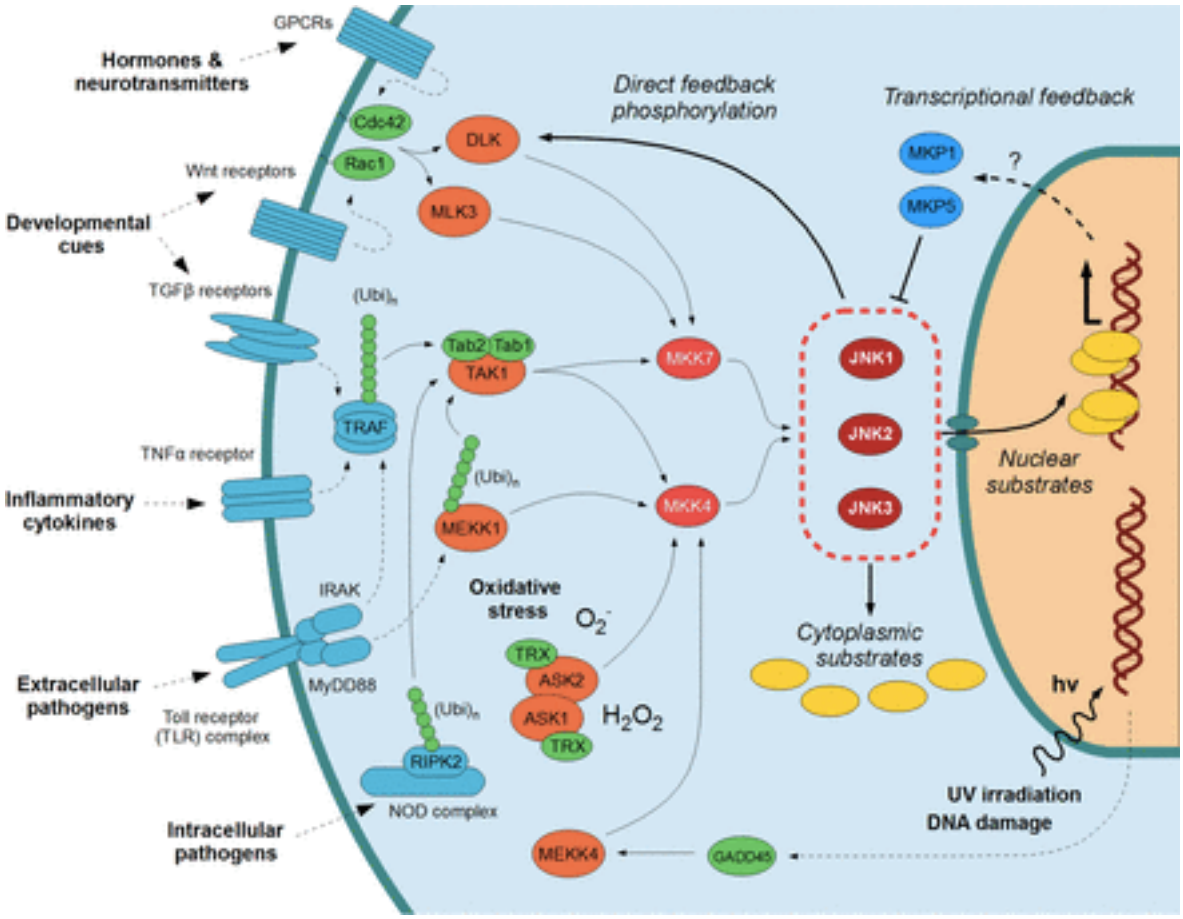

Fonte: Zeke *et al.* (2016).

Após a dissociação do complexo, a JNK ativada é translocada para o núcleo celular, onde irá fosforilar c-Jun que, por sua vez, é capaz de interagir com JunB, JunD, c-Fos e ATF, constituindo assim o fator de transcrição AP-1 que modulará sinais intracelulares e, finalmente, ativará caspases, culminando em um estímulo apoptótico (AKHTER *et al.*, 2015; BOGOYEVITCH *et al.*, 2004; GOURMAUD *et al.*, 2015; HANAWA *et al.*, 2008; SCHROETER *et al.*, 2003; YARZA *et al.*, 2015). Por outro lado, a partir da via intrínseca JNK é capaz de fosforilar e ativar diretamente proteínas relacionadas com a apoptose, como BAX e BMF, também levando a ativação das caspases. Por outro lado, JNK também é responsável por fosforilar e inibir as proteínas anti-apoptóticas DP5-HRK, Bcl-2 e Bcl-xL, intensificando o estímulo apoptótico (SAVAGE *et al.*, 2002; YARZA *et al.*, 2015). Além disso, um dos eventos mitocondriais cruciais que iniciam a apoptose é a liberação do citocromo C para a o citoplasma e embora o mecanismo preciso pelo qual a JNK medeia a liberação do citocromo C não seja totalmente compreendido, JNK mostrou ser

criticamente necessário para a liberação do citocromo C das mitocôndrias durante a apoptose induzida por UV, uma vez que em modelos knockout JNK1$^{-/-}$ não foi possível identificar a liberação do citocromo C em resposta à radiação UV (TOURNIER *et al.*, 2000).

Por outro lado, em resposta a estímulos apropriados como citocinas, os resíduos de treonina e tirosina da p38 podem ser fosforilados por três MKKs. A MKK6 pode fosforilar os quatro membros da família p38, enquanto o MKK3 ativa p38α, p38γ e p38δ, mas não p38β. Tanto MKK3 quanto MKK6 são altamente específicos para p38 MAPKs. Além disso, p38a também pode ser foforilado por MKK4 (ativador da via JNK) (HENSLEY *et al.*, 1999; MUNOZ; AMMIT, 2010; ZARUBIN; HAN, 2005; ZHU, X *et al.*, 2000). Dessa forma, a ativação da também p38a pode ocorrer por duas vias distintas: a) via MKK4, regulada por Rac/cdc42 e; b) via MKK3/MKK6, que pode ser ativada por TNF-α. A partir da ativação da p38, um grande número de proteínas citosólicas podem ser fosforiladas, incluindo a proteína τ e proteínas da família Bcl-2. Além disso, várias quinases ativadas pela via p38 MAPK estão envolvidas no controle da expressão gênica, uma vez que MSK 1 e 2 podem fosforilar e ativar fatores de transcrição tais como CREB, ATF1, NF-κβ, p65 e STAT (Figura 5) (CLARKE *et al.*, 2012; CUADRADO; NEBREDA, 2010; DHANASEKARAN; JOHNSON, 2007; HERLAAR; BROWN, 1999; RAMAN; CHEN; COBB, 2007).

Figura 5. Rota de sinalização de p38

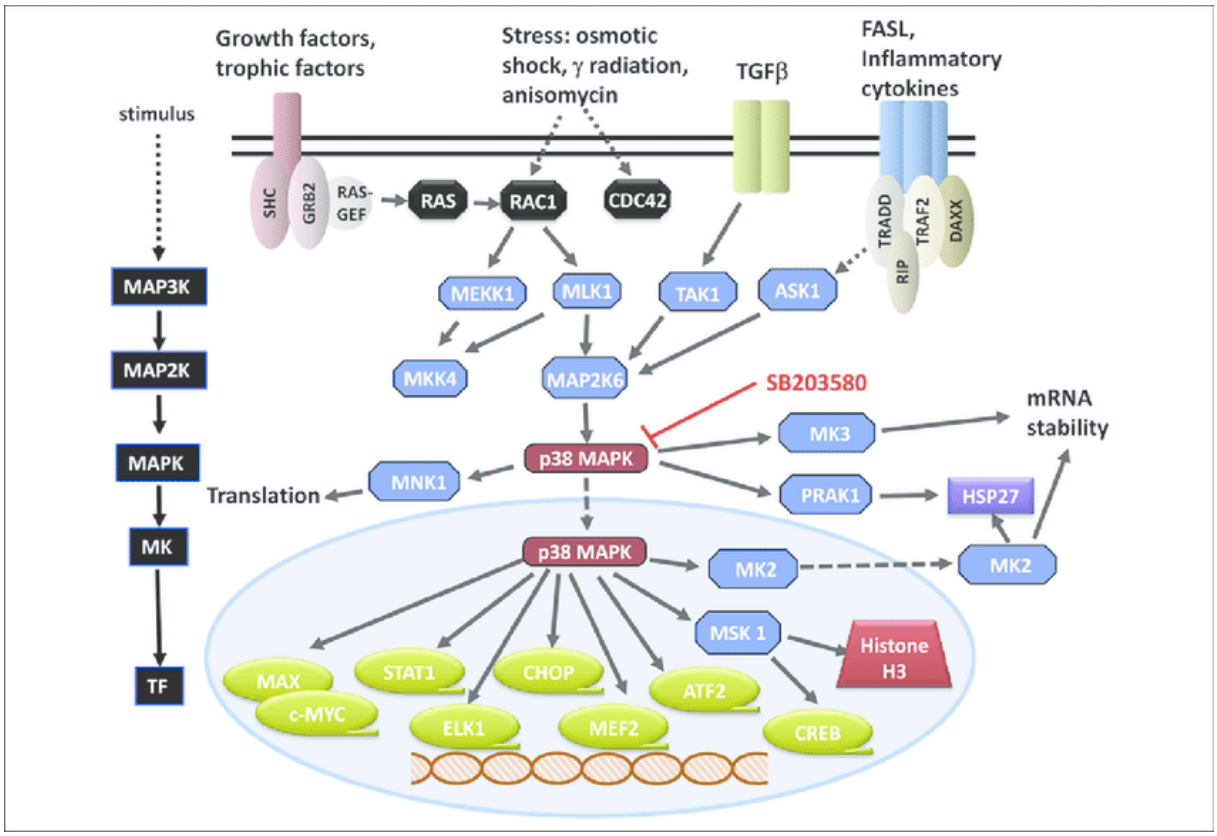

Fonte:.Young (2013).

2.2.1 JNK3

O genoma humano contém três genes relacionados a JNK: *JNK1* (ou *Mitogen-activated protein kinase 8* [*MAPK 8*]), *JNK2* (ou *Mitogen-activated protein kinase 9* [*MAPK 9*]), e *JNK3* (ou *Mitogen-activated protein kinase 10* [*MAPK 10*]) e, em geral, codificam proteínas com aproximadamente 400 aas, contendo um domínio canônico de fosforilação Ser/Thr. Foram identificados 10 isoformas de JNK, sendo que quatro delas são resultado de splicing alternativo de *JNK1* e o restante consiste em variações de *JNK2* e *JNK3*, o que provoca diferenças na afinidade com os fatores de transcrição nucleares ATF2 (CREB2), ELK1 e Jun (Figura 6) (KANDEL; DUDAI; MAYFORD, 2014; MCKEEVER *et al.*, 2017; MITTAL *et al.*, 2014; OKAZAWA; ESTUS, 2002; ZHOU, *et al.*, 2015; ZHOU, *et al.*, 2016).

Figura 6. Diferenças estruturais entre as proteínas JNK 1, 2 e 3 e suas respectivas isoformas

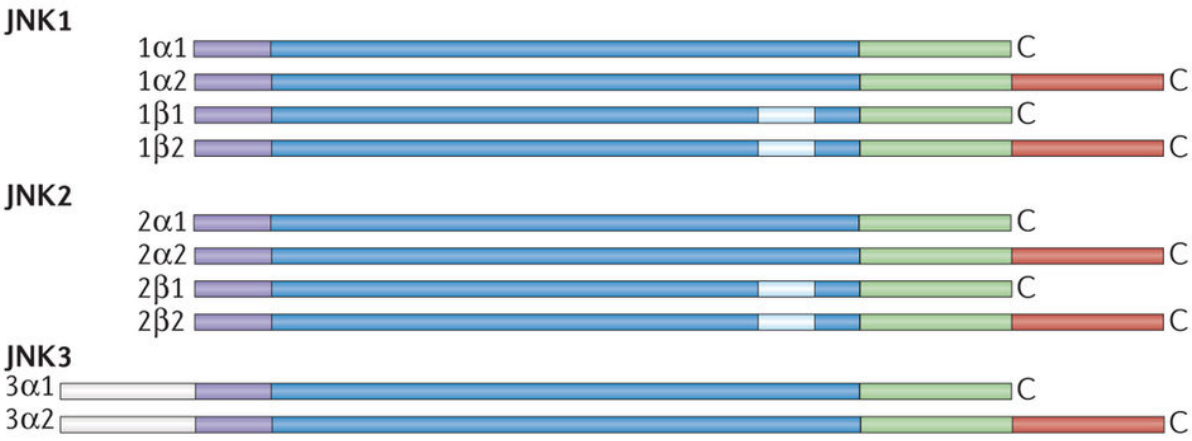

Fonte: adaptado de Coffey (2014).

Tanto o gene *JNK1* quanto o *JNK2* são expressos em todos os tecidos do corpo humano, enquanto que o *JNK3* se restringe quase que exclusivamente ao SNC. Entretanto, de uma forma geral, animais knockout para os genes *JNK* apresentam variados níveis de defeitos a nível de SNC (Figura 7):

Figura 7. Padrão de expressão de *JNK 1, 2 e 3* na região telencefálica e cerebelar

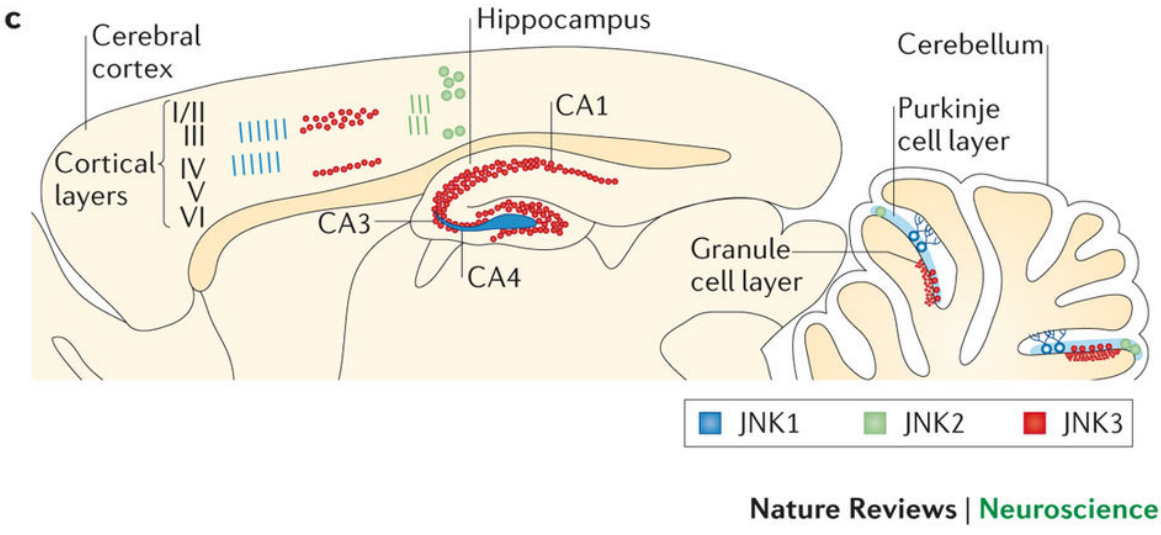

Fonte: adaptado de Coffey (2014).

Uma vez identificada a especificidade de expressão de *JNK3* no SNC, estudos objetivaram elucidar a participação da via da JNK em processos

fisiopatológicos. Nesse sentido, foi demonstrada uma maior expressão de *JNK* fosforilada em cérebros de pacientes com DA *post-mortem*, além da presença de Aβ (KILLICK *et al.*, 2014; ZHU, *et al.*, 2001; ZHU, *et al.*, 2001). Posteriormente outros estudos identificaram que *JNK3*, mais especificamente, é altamente expressa e ativada no tecido cerebral e líquido cefalorraquidiano em pacientes com DA, além de estar estatisticamente correlacionada com o nível de declínio cognitivo (GOURMAUD *et al.*, 2015; TAKAHASHI; NAGAO; GOURAS, 2017).

De fato, em 2012, um estudo demonstrou que a ativação de JNK3 é essencial para a fisiopatologia da DA por manter um feedback positivo de produção de Aβ42. Ou seja, a Aβ42 ativa AMPK, inibindo a rota mTOR, levando ao estresse oxidativo que, por sua vez, ativa JNK3. Uma vez ativada, a pJNK3 promove o processamento de APP ao fosforilar a proteína na posição T668P, o que induz a internalização de APP, facilitando sua clivagem/fosforilação diretamente, favorecendo a produção de Aβ42, dando novamente início ao ciclo. A partir desse estudo, foi demonstrado que JNK3 é a principal quinase promotora de fosforilação de APP em T668, uma vez que camundongos knockout *JNK3*$^{-/-}$ demonstraram redução dramática nos níveis de Aβ42, bem como número maior de células neuronais e melhor função cognitiva (YOON *et al.*, 2012). Posteriormente, outros estudos reforçaram essa hipótese ao demonstrar que os peptídeos Aβ são capazes de induzir a ativação de JNK, além de aumentar os níveis de JNK após o tratamento *in vitro* com Aβ em culturas celulares como C57BL/6 de ratos e em células de neuroblastoma SH-SY5Y (Figura 8) (YARZA *et al.*, 2015).

Figura 8. Rotas envolvendo JNK e a fisiopatologia da DA

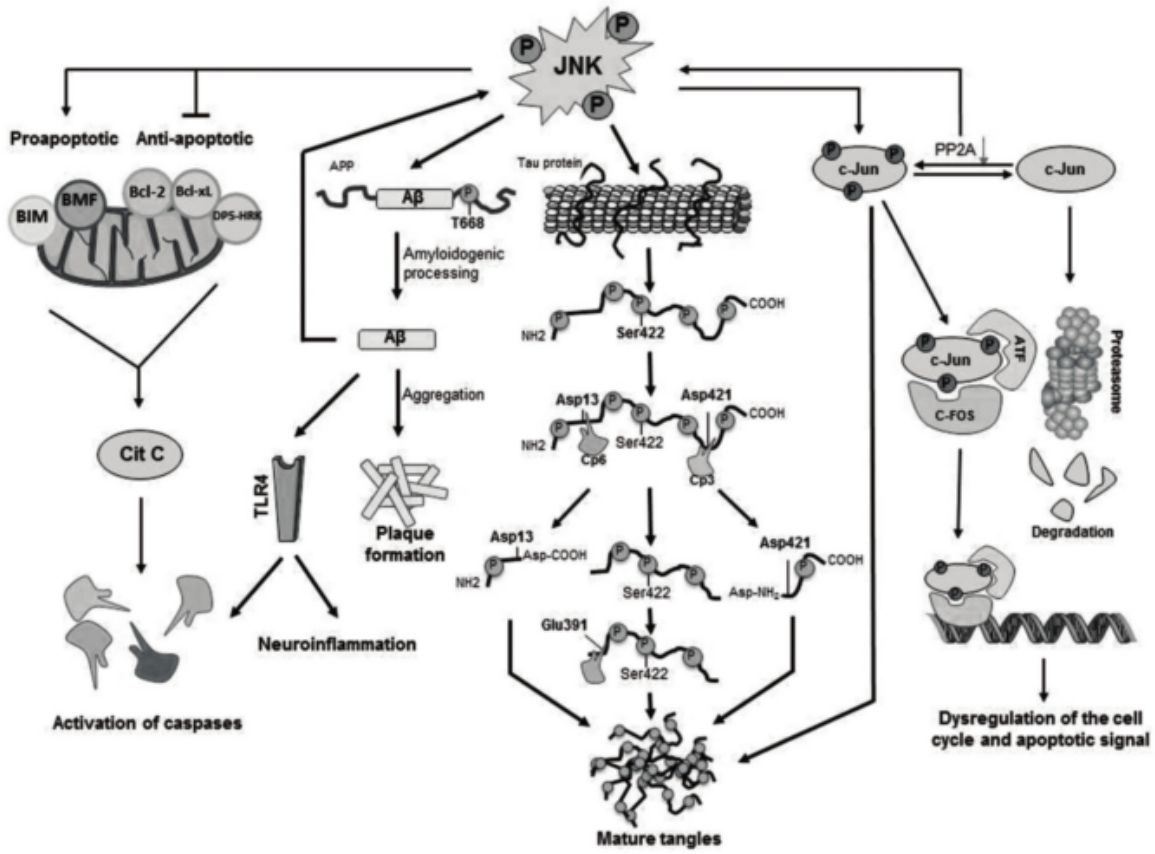

Fonte: Yarza *et al.* (2016).

2.2.2 p38

A p38 é um polipeptídeo de 38 kDa que pode ser encontrado em 4 isoformas (α, β, γ, δ) e é fortemente ativado por estresses ambientais e citocinas inflamatórias. As quatro MAPKs p38 são codificados por diferentes genes e possuem diferentes padrões de expressão tecidual, sendo que a *p38α* é expressa em níveis significativos na maioria dos tipos de células, enquanto que as outras parecem ser expressas de maneira mais específica como por exemplo a expressão de *p38β* no cérebro, *p38γ* no músculo esquelético e *p38δ* nas glândulas endócrinas (CLARKE *et al.*, 2012; CUADRADO; NEBREDA, 2010; DHANASEKARAN *et al.,* 2007; HERLAAR; BROWN, 1999; LIU *et al.*, 2015; RAMAN; CHEN; COBB, 2007; ZHU *et al.*, 2001).

A micróglia compreende células imunocompetentes e fagocíticas residentes que representam entre 10% e 20% de todas as células do SNC (KEREN-SHAUL *et al.*, 2017; MAEZAWA *et al.,* 2011; MAPHIS *et al.,* 2015). Sabe-se que essas células

atuam como sensores de danos neuronais e são responsáveis pela reparação de tecidos e de regeneração neural. No contexto da DA, ao receber algum estímulo estressor, como a deposição de Aβ, a micróglia é ativada na tentativa de minimizar os danos tóxicos dos oligômeros, resultando em neuroinflamação (MAPHIS *et al.,* 2015). Uma vez ativada, a microglia produz diversos mediadores inflamatórios, como IL-1β, IL-6, TNFα, PGE2, NO, BDNF, os quais, conforme supracitado, possuem a capacidade de ativar a via p38. De fato, estudos indicam que a microglia ativada pode contribuir para a patologia da DA através da produção de IL-1, ativação do p38-MAPK neuronal e alterações sinápticas e do citoesqueleto (MAEZAWA *et al.,* 2011; MAPHIS *et al.*, 2015) hiperfosforilação de τ, favorecimento para a agregação de NTFs (CASTELLO; SORIANO, 2014; KANUNGO, 2017; LI *et al.,* 2003; POOLER; NOBLE; HANGER, 2014; REVETT *et al.,* 2013), entre outros, (Figura 9), o que confirma sua participação da DA e, assim, torna-se um alvo terapêutico importante.

Figura 9. Papel da p38 na fisiopatologia da DA

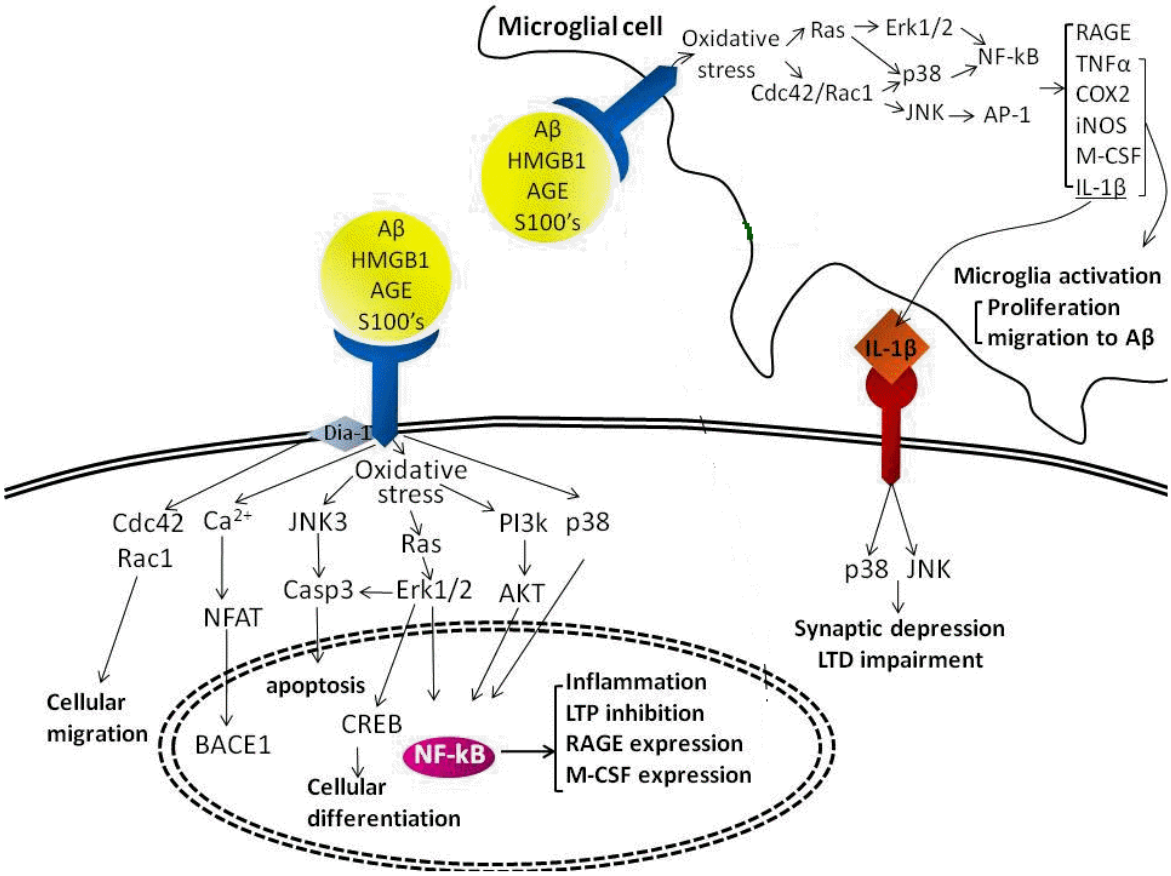

Fonte: Han et al. 2012

2.3 Propostas terapêuticas embasadas em compostos sintéticos

Em 1974, Drachman e Leavitt sugeriram que a memória estava relacionada ao sistema colinérgico e dependia da idade (DRACHMAN; LEAVITT, 1974), uma noção que ainda hoje é considerada válida. Ao mesmo tempo, dois grupos britânicos demonstraram, independentemente, que a patologia da DA estava associada a uma perda grave de neurônios colinérgicos centrais, mais precisamente, a gravidade da demência foi correlacionada com a extensão da perda colinérgica no núcleo basal de Meynert (BOWEN *et al.*, 1976; DAVIES; MALONEY, 1976). A hipótese colinérgica levou ao desenvolvimento de fármacos durante os anos 80 e 90, e continua a fornecer uma base para os atuais esforços de desenvolvimento, com moduladores de receptores nicotínicos neuronais e outras moléculas que possuem efeitos sobre a função colinérgica como agonistas muscarínicos e nicotínicos, agonistas parciais e moduladores alostéricos de receptor de 5-hidroxitriptamina (5-HT) (BURKE *et al.*, 2014; DRACHMAN; LEAVITT, 1974; FUSTER-MATANZO *et al.*, 2013; SCHNEIDER, *et al.*, 2015). Ou seja, embora outros alvos terapêuticos sejam investigados, o desenvolvimento de drogas tem sido mais influenciado pela hipótese colinérgica e pela hipótese da cascata amiloide, principalmente essa última. De fato, a hipótese de cascata amilóide dominou o desenvolvimento de drogas nas últimas duas décadas e apresenta diversos alvos, entre elas a inibição de ativação de proteínas quinases (SCHNEIDER, *et al.*, 2015).

Apesar de que a atividade normal da rota JNK é essencial para o neurodesenvolvimento e regeneração neuronal, uma ativação excessiva desta rota é capaz de induzir apoptose em neurônios. Assim, técnicas que permitem a inibição específica de JNK têm sido desenvolvidas e apontadas como agentes neuroprotetores, podendo ser utilizados no tratamento não apenas na DA, mas também de outras patologias externas ao SNC (CHILMONCZYK *et al.*, 2017; CLARKE *et al.*, 2012; COFFEY, 2014; HAEUSGEN *et al.*, 2009; MULLER *et al.*, 2007).

A partir disso, compostos químicos foram sintetizados com diferentes proteínas-alvo mas que culminassem no mesmo efeito final: inibição de JNK. Nesse sentido, dentre essas diferentes “classes” de inibidores, pode-se citar os inibidores competitivos de ATP, dentre os quais encontra-se o composto amplamente explorado

SP600125 (Anthra[1,9-cd]pyrazol-6-(2H)-one). Modelos *in vivo* e *in vitro* de DA demonstraram que SP600125 previne a morte de neurônios induzida pela produção de βAPP. Além disso, outros estudos demonstraram que injeções intracerebroventriculares de SP600125 melhoraram aspectos neurológicos relacionados à DA em modelos animais. Entretanto, tal composto oferece uma especificidade limitada, uma vez que, além de inibir JNK, inferfere em outras quinases como MKK4 e MKK7, além de proteínas não relacionadas a via da JNK, como SGK, S6K1 (p70 ribosomal protein S6 kinase), AMPK, CDK2, CK1d e DYRK1A. Além do grupo que compreende a SP600125, ainda existem a classe de inibidores de MLK que, por down-regulation, modulam a sinalização de JNK e, portanto, conferem atividades antiapoptóticas e neuroprotetoras. Em culturas celulares primárias, compostos como K252a e CEP1347 inibiram a morte neuronal induzida por Aβ, sendo que, esse último, inclusive, chegou a fase de estudos clínicos. Entretanto, não apresentou um desempenho suficientemente satisfatório para prosseguir para os testes seguintes (BOGOYEVITCH *et al.*, 2010; CHOI, *et al.*, 1999; GALEOTTI; GHELARDINI, 2012; HEPP REHFELDT *et al.*, 2020; LEHMENSIEK *et al.*, 2006; PRAUSE *et al.*, 2016; TAN *et al.*, 2006).

2.3.1 Piridinilimidazois tetra-substituídos: FMU200

Os imidazois tetra-substituídos são conhecidos como inibidores duplos de JNK3 e p38 (DAVIS *et al.*, 2011; DUONG; LEE; AHN, 2020; MUTH *et al.*, 2017; ROSKOSKI, 2016; WU *et al.*, 2020). Nesse sentido, compostos derivados foram preparados e avaliados em um ensaio para quantificar sua capacidade de inibir ambas as quinases JNK3 e p38a (MUTH *et al.*, 2017). A partir da identificação da faixa nanomolar, foi possível identificar os valores de IC50 para as moléculas. Dentre várias identificadas, o FMU200 (***compound 7***, Figura 10, (MUTH *et al.*, 2017)) apresentou excelentes solubilidade e estabilidade metabólica podendo servir como ferramentas úteis para estudos pré-clínicos.

Figura 10. Estrutura do composto FMU200

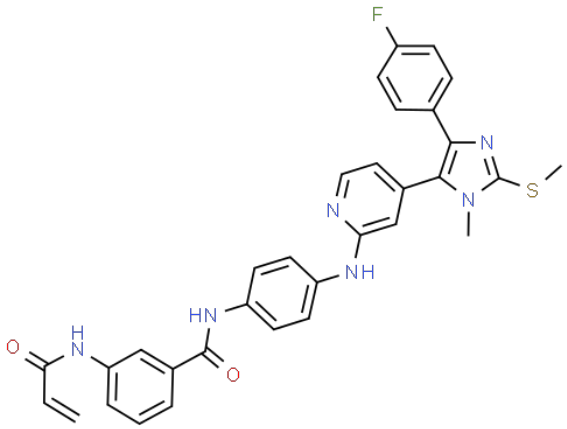

Fonte: Adaptado de MUTH *et al.,* (2017)

2.4 Propostas terapêuticas embasadas em compostos derivados naturais

Conforme explorado nos tópicos acima, inúmeras moléculas sintéticas apresentam características terapêuticas interessantes. Entretanto, uma ampla gama de compostos naturais vem sendo investigada, por demonstrar efeitos benéficos no tratamento de doenças (GRIMMIG *et al.*, 2017; NEWMAN; CRAGG, 2016; SILVA *et al.*, 2019, 2021, 2018). Dentre esses compostos, destaca-se a classe dos polifenóis, os quais compreendem metabólitos secundários de origem vegetal, envolvidos na defesa de plantas contra agentes patogênicos e danos causados por radiação UV (TREUTTER, 2005).

Os compostos naturais contendo polifenóis são amplamente reconhecidos por desempenhar efeitos em múltiplos pontos críticos da fisiopatologia de doenças neurodegenerativas, incluindo efeitos antioxidantes, propriedades de neutralização de radicais livres, modulação de sinalização celular, comprimento de telômero e das proteínas de sirtuína (BU; RAO; WANG, 2016; JAYASENA *et al.*, 2013). Ainda, mais especificamente relacionada à DA, compostos fenólicos possuem atividade anti-amiloidogênica ao inibir a formação de fibrilas Aβ e desestabilizar fibrilas Aβ pré-formadas por ligação direta a Aβ monomérico ou agregados maduros. Ou seja, os compostos que convertem fibrilas Aβ maduras em agregados menores ou não tóxicos e evitam a regeneração de intermediários de agregação tóxicos (Figura 11) (ALBARRACIN *et al.*, 2012; ATANASOV; WALTENBERGER; PFERSCHY-WENZIG,

2016; BAKHTIARI *et al.*, 2017; BU; RAO; WANG, 2016; CHEN, *et al.*, 2016; FERNÁNDEZ-PACHÓN *et al.*, 2009; GUZZI *et al.*, 2017; JAYASENA *et al.*, 2013; KERIMI; WILLIAMSON, 2018; WILLIAMS; SPENCER, 2012).

Figura 11. Proposta de mecanismo de ação anti-amiloidogênica dos flavonoides

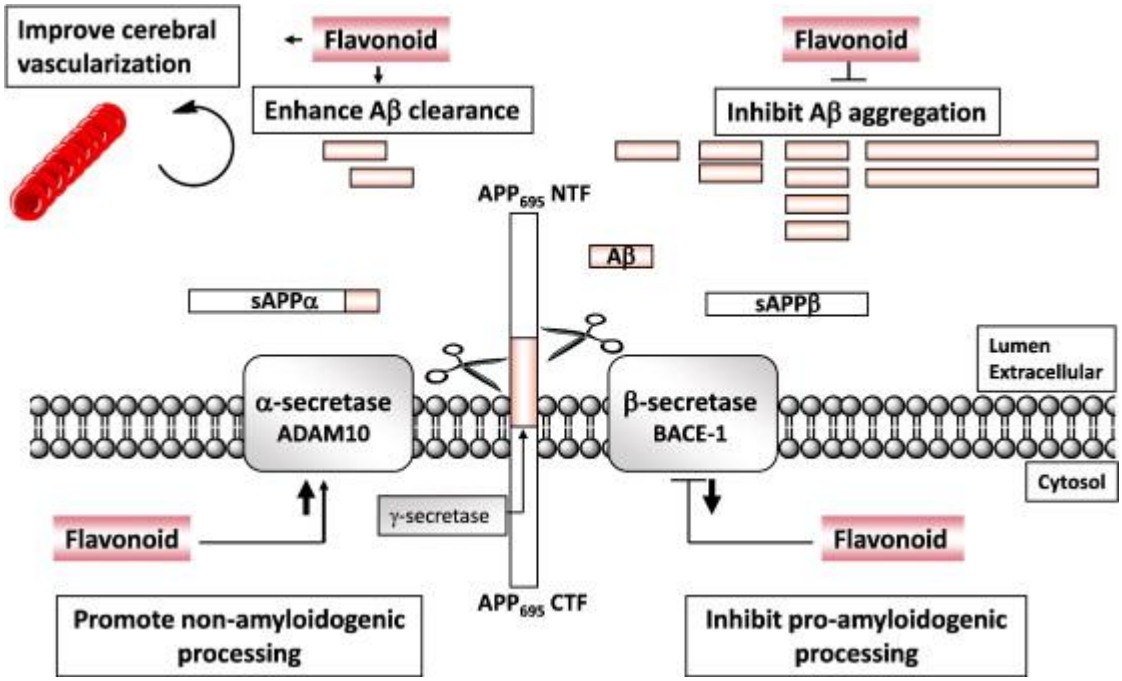

Fonte: Williams e Spencer, 2012.

Além disso, os mecanismos moleculares envolvidos no efeito de neuroproteção também podem estar envolvidos na regulação da expressão de genes apoptóticos. De fato, os resultados de um estudo realizado com células de neuroblastoma SH-SY5Y demonstraram que o composto polifenólico encontrado no chá verde diminuiu a expressão dos genes pró-apoptóticos Bax, Bad, inibidor do ciclo celular Gadd45, Fas e TRAIL. No entanto, a expressão de Bcl-2 e Bcl- x não foi afetada (LEVITES *et al.*, 2002).

2.4.1 Luteolina e luteolina-7-o-glicosídeo (LUT7OG)

Quimicamente, os polifenóis incluem uma grande variedade de biomoléculas que contém vários grupos hidroxil, em um ou mais anéis aromáticos. Esse grupo de moléculas, em especial os flavonoides, desempenham diversos efeitos benéficos para a saúde. De fato, ervas contendo flavonoides vêm sendo utilizadas desde o início da antiga medicina tradicional chinesa (IAKOVLEVA *et al.*, 2015). Com mais de

8000 fitoquímicos distintos, os flavonoides podem ser divididos ainda em sub-classes, de acordo com suas estruturas químicas em chalconas, flavonas, flavonóis, flavanonas, flavanóis, antocianinas, isoflavonas, entre outros (CROFT, 1998; HEIM; TAGLIAFERRO; BOBILYA, 2002; SHASHANK; ABHAY, 2013; TREUTTER, 2005).

Pertencente à classe das flavonas, a luteolina, tem sido alvo de estudos acerca de moléculas naturais com potencial terapêutico. A luteolina é um dos flavonoides mais comuns presentes em plantas comestíveis e seus potenciais benefícios no SNC incluem diminuição da inflamação e do dano axonal ao prevenir a migração de monócitos através da barreira hematoencefálica (BBB) (BAKHTIARI *et al.*, 2017; HEIM; TAGLIAFERRO; BOBILYA, 2002; RASOOL *et al.*, 2014). Estudos pré-clínicos mostraram que essas flavonas possuem uma variedade de atividades farmacológicas, incluindo anti-inflamatória, antioxidante, anti-proliferativa anti-angiogênica e anti-metastática. Além disso, a luteolina suprimiu a produção de citocinas pró-inflamatórias em macrófagos bloqueando as vias de sinalização de NF-kβ e ativador proteína 1 (AP1) e inibiu a produção de óxido nítrico e eicosanóides pró-inflamatório. A Luteolina também diminuiu a liberação de TNF e superóxido em indizido por lipopolissacarídeo (LPS) em culturas de células microgliais e reduziu a produção de IL-6 induzida por LPS na microglia cerebral *in vivo* (DIRSCHERL *et al.*, 2010; KANG *et al.*, 2004; KERIMI; WILLIAMSON, 2018; RAMASSAMY, 2006).

Entretanto, em geral, essas flavonas são encontrados naturalmente hidroxilados, metoxilados e/ou glicosilados. O açúcar ligado geralmente é glicose ou ramnose. O número de açúcar é geralmente um, mas pode ser dois ou três e existem várias posições de substituições no polifenol. A glicosilação influencia as propriedades químicas, físicas e biológicas dos flavonoides e na sua absorção pelo intestino delgado. Por exemplo, se os compostos fenólicos contêm uma molécula de açúcar, como glicose, galactose, serão absorvidos através do intestino delgado pela enzima citosólica β-glicosidase/lactase e florizina hidroxilase. A absorção também está relacionada à especificidade dos transportadores (CHOI, *et al.*, 2014; RAMASSAMY, 2006). Nesse sentido, a forma glicosilada da luteolina, a luteolina-7-o-glicosídeo (LUT7OG) está representada na Figura 12, a seguir.

Figura 12. Estrutura química da LUT7OG

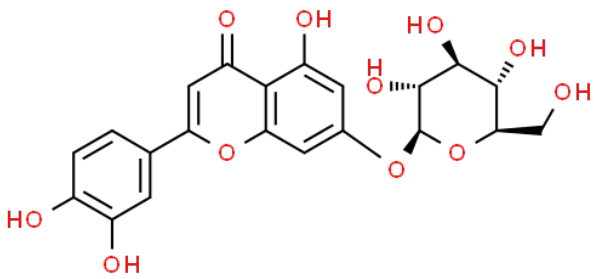

Fonte: PubChem (2021).

Contudo, apesar de alguns estudos terem avaliado os efeitos da LUT7OG *in vitro*, o número de estudos que avaliou a molécula isolada ou moléculas sintéticas mimetizas ainda é muito limitado e os resultados apresentados são divergentes (IAKOVLEVA *et al.*, 2015; KIM; CHIN; CHO, 2017), reforçando a necessidade de mais estudos explorando as capacidades farmacológicas em sua totalidade. Além disso, de acordo com estudos prévios (GOETTERT *et al*., 2010), a LUT7OG foi capaz de interagir e inibir JNK3 *in vitro*, conforme demonstrado na Figura 13 abaixo e, portanto trata-se de uma molécula cujo potencial ainda não foi explorado em sua totalidade.

Figura 13. Interação entre LUT7OG e o sítio ativo de JNK3

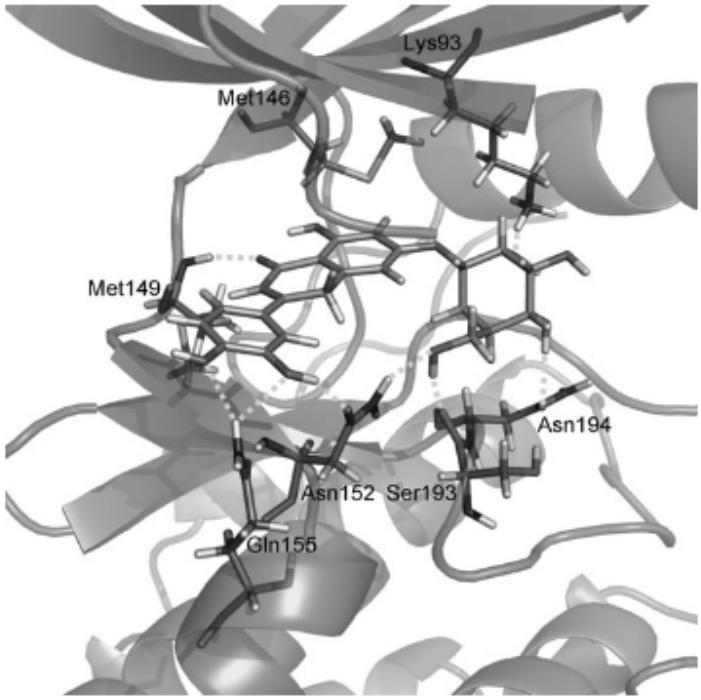

Fonte: Goettert *et al.* 2010.

Capítulo II

Artigo de revisão:

"c-Jun N-Terminal Kinase Inhibitors as Potential Leads for New Therapeutics for Alzheimer's Disease"

Publicado em 2020 no periódico *International Journal of Molecular Sciences*
(Fator de Impacto: 4,556)

International Journal of
Molecular Sciences

MDPI

Review

c-Jun N-Terminal Kinase Inhibitors as Potential Leads for New Therapeutics for Alzheimer's Diseases

Stephanie Cristine Hepp Rehfeldt [1], Fernanda Majolo [1,2], Márcia Inês Goettert [1,*] and Stefan Laufer [3,*]

1 Graduate Program in Biotechnology, University of Vale do Taquari (Univates), Lajeado CEP 95914-014, Rio Grande do Sul, Brazil; rehfeldt.stephanie@gmail.com (S.C.H.R.); nandamajolo@gmail.com (F.M.)
2 Brain Institute of Rio Grande do Sul (BraIns), Pontifical Catholic University of Rio Grande do Sul (PUCRS), Porto Alegre CEP 90619-900, Rio Grande do Sul, Brazil
3 Department of Pharmaceutical/Medicinal Chemistry, Institute of Pharmaceutical Sciences, Faculty of Sciences, University of Tuebingen, D-72076 Tuebingen, Germany
* Correspondence: marcia.goettert@univates.br (M.I.G.); stefan.laufer@uni-tuebingen.de (S.L.); Tel.: +55-5137147000 (ext. 5445) (M.I.G.)

Received: 17 November 2020; Accepted: 12 December 2020; Published: 18 December 2020

Abstract: Alzheimer's Disease (AD) is becoming more prevalent as the population lives longer. For individuals over 60 years of age, the prevalence of AD is estimated at 40.19% across the world. Regarding the cognitive decline caused by the disease, mitogen-activated protein kinases (MAPK) pathways such as the c-Jun N-terminal kinase (JNK) pathway are involved in the progressive loss of neurons and synapses, brain atrophy, and augmentation of the brain ventricles, being activated by synaptic dysfunction, oxidative stress, and excitotoxicity. Nowadays, AD symptoms are manageable, but the disease itself remains incurable, thus the inhibition of JNK3 has been explored as a possible therapeutic target, considering that JNK is best known for its involvement in propagating pro-apoptotic signals. This review aims to present biological aspects of JNK, focusing on JNK3 and how it relates to AD. It was also explored the recent development of inhibitors that could be used in AD treatment since several drugs/compounds in phase III clinical trials failed. General aspects of the MAPK family, therapeutic targets, and experimental treatment in models are described and discussed throughout this review.

Keywords: c-Jun N-terminal kinase (JNK); brain diseases; therapeutic targets; kinase inhibitors

1. Introduction

In 1906, Dr. Alois Alzheimer described for the first time an unusual disease of the cerebral cortex. According to the German neurologist, the patient whose brain he examined was a woman who had been suffering from memory loss, disorientation in time and space, hallucinations, and language dysfunction. She eventually died at 55 years of age. During a post-mortem examination of the patient's brain, he noted that the cortex was thinner than average, and he also observed the presence of abnormalities such as plaques and tangles in and outside the brain cells [1,2]. Today, the 'unusual disease' is known as Alzheimer's Disease (AD), and, as the population lives longer, diseases such as AD are becoming more prevalent. Researchers believe the overall prevalence of AD in individuals over 60 years of age is 40.19% across the world [3]. Five years ago, the annual World Alzheimer Report of 2015 pointed out that the percentage of individuals over 60 years old diagnosed with AD corresponded to 12.2% of the world population at that time. The same report projected an increase in that percentage to 16.3% in 2030 and 21.2% in 2050, anticipating that the number of cases would almost double every 20 years [4,5].

It has been 114 years since the first official AD diagnosis and considerable progress has been made, but some complex aspects remain unclear. AD is a multifactorial disease as it appears to be a result from genomic, epigenetic, interatomic, and environmental aspects interacting in different ways, resulting in highly heterogeneous phenotypes. Clinically, AD is divided into 'late-onset' or 'sporadic' AD (LOAD)—which is the most common form of AD—and 'early-onset' or 'familiar' AD (EOAD), which accounts for 1-5% of all AD cases and is caused by dominantly inherited mutations in genes including *APP*, *PSEN1*, *PSEN2*, and *APOE* [6]. Genetic evidence indicates that heritability to LOAD is 58-79%, while for EOAD is thought to be over 90%. Recently, over 50 *loci* were identified and linked to LOAD reinforcing the role of multiple pathways and cellular events, such as immunity, endocytosis, cholesterol transport, ubiquitination, amyloid-β, and τ (tau) processing [7].

There are several descriptive hypotheses regarding the causes of AD including the amyloid hypothesis, τ propagation hypothesis, cholinergic hypothesis, mitochondrial hypothesis, inflammatory hypothesis, and others. The most well-known hypothesis is the amyloidogenic one since it describes some classical AD hallmarks [8]. One of these hallmarks is originated from abnormal processing of amyloid precursor protein (APP), a single-pass transmembrane protein that is normally present in neurons and cleaved by several secretases. In AD, APP follows the amyloidogenic pathway where it is cleaved by β-site APP-cleaving enzyme 1 (BACE1) to originate amyloidogenic C-terminal derivatives (sAPPβ) [9], which are cleaved by γ-secretase, generating APP intercellular domain (AICD) and β-amyloid peptides (Aβ), including Aβ42. These toxic oligomers can accumulate in neurites and disrupt the synaptic function. It is believed that disconnected terminals create neurites around Aβ42 deposits, originating the neuritic plaques (NP) [10]. A second common finding in AD are intracellular neurofibrillary tangles (NFTs) composed of poorly soluble hyperphosphorylated τ protein. τ protein is a microtubule-associated protein normally synthesized by neuronal cell bodies and transported to axons, where it interacts with tubulin to assure microtubule stability. If there are perturbations in the cytoskeleton, it can compromise both the function and viability of the neurons. Even after cell death, it is still possible to observe the extracellular NFTs left behind [11,12]. It was believed that NP and NFTs acted independently, but recent evidence points to a complex relationship where they act synergistically towards neurodegeneration [13]. High levels of Aβ aggregates and NFTs distributed mainly throughout the hippocampus lead to critical events. Those molecular and morphological abnormalities are the hallmarks of brain injury observed in dementia and are likely to develop over a period of at least decades before the symptomatic phase. A study found significantly higher levels of total τ (T-τ) in cerebrospinal fluid 34 years before the symptomatic onset of AD, while changes in cognitive aspects were detected 10 to 15 years prior to the symptomatic phase [14]. In addition, the distinct pattern of plasma levels of τ phosphorylated at Thr217 could discriminate AD from other neurodegenerative diseases and are therefore gaining attention as a potential biomarker for AD [15–17].

While Aβ is a necessary feature to diagnose AD in a patient, aggregates are not sufficient to cause cognitive decline [18,19]. In this case, synaptic dysfunction, oxidative stress, and excitotoxicity, which induces the activation of mitogen-activated protein kinases (MAPK) pathways such as the JNK (c-Jun N-terminal kinase) pathway, are also necessary to provoke progressive loss of neurons and synapses, brain atrophy, and augmentation of brain ventricles [20–25]. Considering that JNK is best known for its involvement in propagating pro-apoptotic signals via extrinsic and intrinsic pathways [26–28], the inhibition of JNK3 has been explored as a possible therapeutic target. Nowadays, AD symptoms are manageable, but the disease itself remains incurable. According to the U.S. Food and Drug Administration (FDA) and the Alzheimer's Association, no drug available today for AD is able to slow down the progression of the disease nor stop the neuron cells from dying, which makes AD fatal in all cases. On the other hand, there are five FDA-approved drugs to manage AD nowadays: Donepezil, galantamine, memantine, rivastigmine, and an association of memantine and donepezil [29]. Tacrine used to be a sixth drug available for the same purpose, but it was discontinued in 2013, after having gained approval 20 years earlier, because of increased hepatotoxicity [30]. When considering the failure of several drugs/compounds in phase III clinical trials that focused primarily on the amyloid

hypothesis [31], it becomes clearer that new targets should be explored. This review presents the role of JNK3 in AD pathogenesis and explores the recent development of inhibitors that could be used in AD treatment. In this sense, we first describe the general aspects of the MAPK family. Next, we discuss the biological aspects of JNK, focusing on JNK3 and how it relates to AD. Subsequently, we explore therapeutic targets and experimental treatment in models.

2. General Aspects of Mitogen-Activated Protein Kinases (MAPKs) Family

Kinases are considered the largest protein family in the human proteome, and approximately 2% of eukaryotic genes encode kinase superfamily members [32]. These enzymes catalyze the transference of the γ-phosphate from ATP to serine, threonine, or tyrosine amino acid residues of a downstream protein substrate, creating a communication cascade that is fundamental to eukaryotic cells. Over 500 kinases were identified in humans. The so-called 'human kinome' is divided into typical kinases and atypical kinases. The 478 typical kinases possess a well-defined architecture that is similar across all members, while the 40 atypical kinases (the 'dark kinome') are poorly understood [33]. Most typical kinases are dually phosphorylated at serine and threonine residues and, as a result, are called Ser/Thr kinases. Kinases are clustered according to similarities at the kinase domain, which results in different kinase groups/families. According to evolutionary conservation data, the CMGC kinase group is an ancient group made up by nine highly conserved families found in most eukaryotes [34]. This group was named after the initials of some of its key members: cyclin-dependent kinase (CDK), MAPK, glycogen synthase kinase (GSK), and CDK-like kinases (CLK).

The MAPK family is considered the main propagator of extracellular signals from the cell membrane to the nucleus as they catalyze the transfer of the γ-phosphate from ATP to serine or threonine residues of various substrates [35], including transcription factors, which regulate the expression of specific sets of genes, and thus mediate a specific response according to the stimulus received by cells [36–39]. Among the MAPK family, fourteen members share both structures and biochemical properties. Depending on those characteristics, each member is grouped in one of the seven different MAPK subfamilies. The extracellular signal-regulated kinases 1/2 (ERK1/2), ERK5, JNK, and p38 subfamilies can be activated by dual phosphorylation of threonine and tyrosine residues (known as 'tripeptide motif' or 'Thr-X-Tyr motif') at the activation loop site (also called 'A-loop') and activate the pathway by propagating the phosphorylation in downstream kinases. Those four subfamilies follow a classical three-tiered signaling pathway that is highly conserved in eukaryotic organisms, where each phosphorylation of a MAPK is carried out by specific upstream kinases. Usually, MAPKKK (MAP3K) receives a variety of inputs and transmits them to downstream kinases MAPKK (MAP2K), which activates MAPK (Figure 1) [40–42]. On the other hand, ERK3/4, ERK7/8, and NLK (nemo-like kinase) compose the 'atypical' MAPK subfamilies that do not follow the same dual-phosphorylation and three-tiered module pattern. However, since the focus of this paper is on 'typical' MAPK—specifically in JNK—the 'atypical' MAPK will not be reviewed in detail and will be referred to as appropriate. A detailed review of their dynamics can be checked elsewhere [40,41].

MAP3K activates more than one MAP2K, and MAP2K can phosphorylate more than one MAPK. The cross-talking is important to signal integration and coordination but may also represent an obstacle in therapy since it is likely to be involved in drug resistance in cancer, for example [43]. Although the MAPK pathways have several interconnections that sometimes hinder the separation of these pathways, the JNK and p38 pathways are both activated by cellular stressors, such as cytokines for example, and are frequently associated with cellular death and inflammation [36,39,44]. On the other hand, both JNK and p38 can mediate anti-apoptotic events as well and do not always work 'as a team', since recent evidence suggests negative regulation of p38 over JNK in some cellular contexts [45].

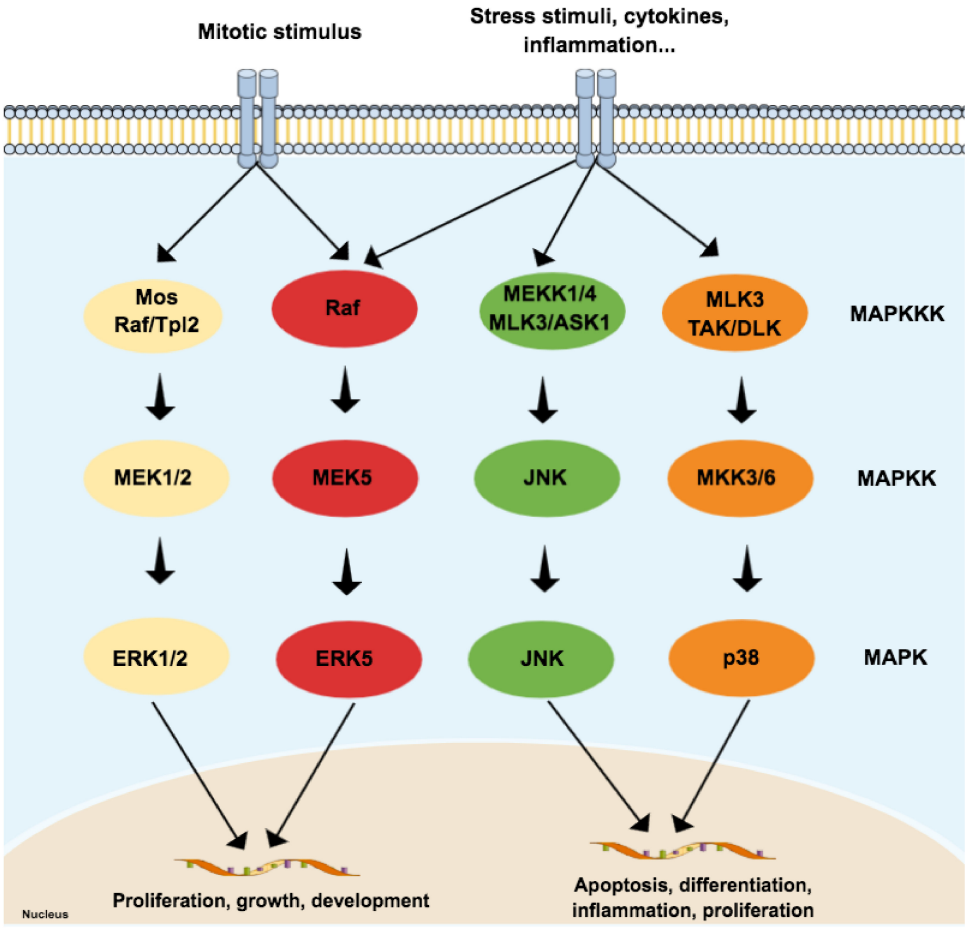

Figure 1. Schematic representation of the typical mitogen-activated protein kinases (MAPK) pathway, composed of three levels (three-tier module) and four subfamilies: extracellular signal-regulated kinases (ERK) 1/2, p38, c-Jun N-terminal kinase (JNK), and ERK5. Each subfamily regulates different phenotypes. While the canonical ERK subfamily (ERK1/2) responds to mitotic stimuli and controls cellular differentiation and proliferation, JNK and p38 are activated by stressor stimuli and are involved in apoptosis. Since the ERK5 subfamily responds to both mitotic and stressor stimuli, being associated with cell survival, it is presented in a special subfamily.

2.1. JNK3 (and p38), Apoptosis and AD: The Perfect Storm

2.1.1. JNK Participates in Both Intrinsic and Extrinsic Pathways of Apoptosis

JNK is a MAPK activated by pro-inflammatory cytokines or exposure to environmental stress and is best known for its role in programed cell death [46]. The term 'apoptosis' was suggested in 1972, and it describes a regulated cell death process that requires a complex molecular program of self-destruction where cells retain plasma integrity and some level of metabolic activity until the outcome [47]. Apoptotic processes are divided into extrinsic and intrinsic pathways, and a detailed review of this topic is available elsewhere [47,48]. Here we will discuss general aspects that involve the role of JNK in apoptosis, as illustrated in Figure 2.

The intrinsic pathway is activated by extracellular or intracellular perturbations usually found in AD, such as oxidative stress and microtubular alterations caused by NTFs [12,49]. This pathway is controlled by members of the Bcl-2 family, which is divided into three groups known as pro-apoptotic pore-formers (Bax, Bak, and Bok), pro-apoptotic BH3-only proteins (Bad, Bid, Bik, Bmf, Hrk, Noxa, Puma, etc), and anti-apoptotic proteins (Bcl-2, Bcl-XL, Bcl-W, Mcl-1, Bfl-1) [50]. The Bcl-2 family is under the control of JNK and p38 [45], and a significant part of them can transit between cytosol

and organelles. In response to a deleterious stimulus, the JNK-mediated phosphorylation of 14-3-3 protein at the Ser184/186 site induces the translocation of pro-apoptotic proteins (Bax and Bad) from the cytoplasm to the mitochondria. However, it was reported that JNK can directly phosphorylate Bad at Ser128, Bim at Ser65, and Bid at Thr59, inducing the pro-apoptotic activity, and inhibiting anti-apoptotic proteins, since Bad, Bim, and Bmf inhibit Bcl-2 antiapoptotic effect [48,49,51]. JNK also phosphorylates Bcl-2 and Mcl-1, blocking their anti-apoptotic activity. This pathway is also known as the 'mitochondrial pathway' since the relocation of pro-apoptotic proteins causes mitochondrial outer membrane permeabilization (MOMP), allowing the cytosolic release of pro-apoptogenic factors that normally reside in the mitochondrial intermembrane space, such as cytochrome c and Smac/DIABLO. Cytochrome c then associates with Apaf-1, pro-caspase 9 (CASP9), (and possibly other proteins) to form an apoptosome, which activates CASP9. When activated, CASP9 catalyzes the proteolytic activation of CASP3 and CASP7 (known as 'executioner caspases'), which handle cell demolition during intrinsic and extrinsic apoptosis pathways. In this sense, both pathways can induce caspase activation that causes the morphological and biochemical features commonly seen during apoptosis, including DNA fragmentation and phosphatidylserine exposure [52]. However, both the pathways usually operate independently, since Bid, a pro-apoptotic Bcl-2 family member, can be cleaved by CASP8, promoting cytochrome c release [49].

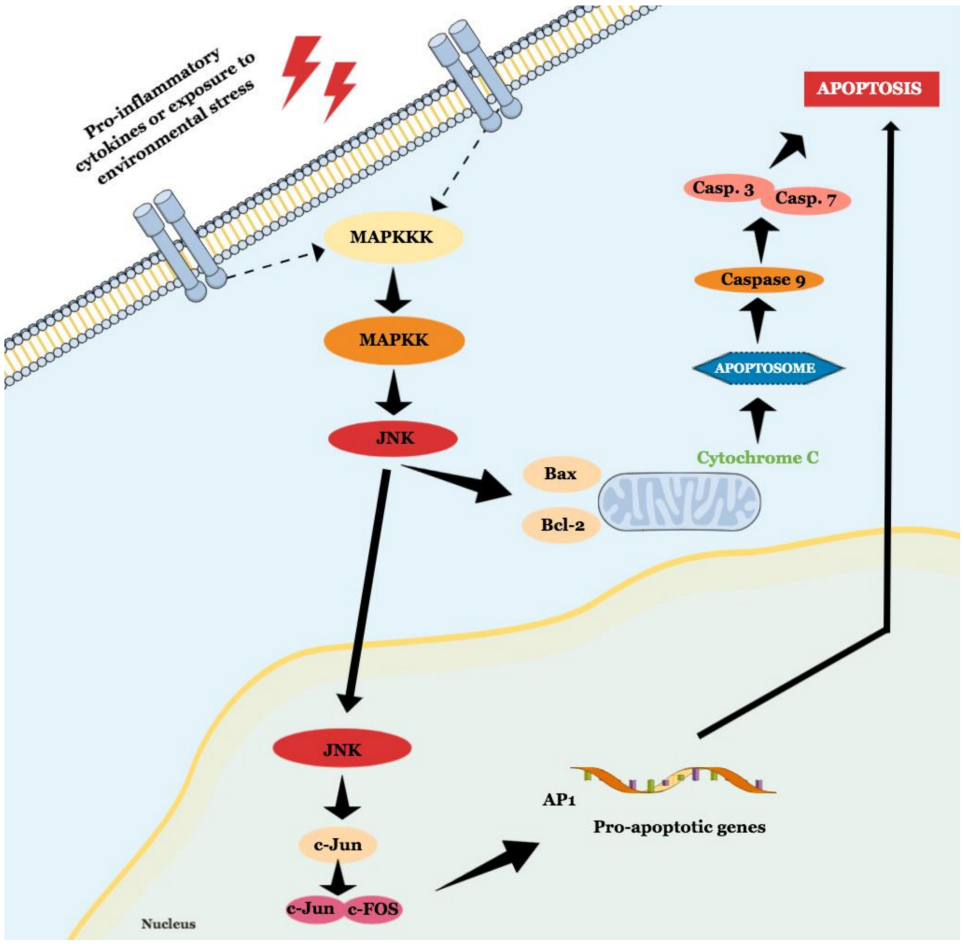

Figure 2. Schematic representation of JNK role in intrinsic and extrinsic apoptosis.

The extrinsic pathway initiates when perturbations on the extracellular environment are detected by cell-surface death receptors (or 'dependence receptors') and therefore is also known as 'death-receptor pathway'. Death receptors include Fas (known as CD95 or APO-1), tumor necrosis factor receptor (TNFR), TNF-related apoptosis-inducing ligand (TRAIL), and others [53]. The dual role of Fas in both

apoptotic and anti-apoptotic signaling is under debate. In animal models, repetitive and coordinated activation of Fas improved spatial memory and increased adult neurogenesis in the hippocampus, indicating that Fas could be involved in neuroprotection rather than neurodegeneration in mild cognitive impairment (MCI) [53–56]. However, depending on the cellular context, these receptors activate CASP8 and propagate the apoptotic signal by direct cleavage of CASP3 and Bid, converging to the mitochondrial pathway. On the other hand, the extrinsic pathway can be activated according to the stimulus perceived by MAP3K, such as transforming growth factor-β-activated kinase 1 (TAK1), mammalian MAP/ERK kinase kinase 1 (MEKK1), MEKK4, apoptosis signal-regulating kinase 1 (ASK1), and mixed-lineage kinase (MLK), by GTPases like Ras (Raf) or GTPases of the Rho family (Cdc42-mediated MLK3 activation and RhoA-mediated MEKK1 activation) or, further, phosphorylated by a MAP4K, such as p21-activated kinase (PAK), germinal center kinase (GCK), and homeodomain-interacting protein kinase (HPK), involved in the control of MAP3K interaction with other proteins. This diversity in MAP3K regulation allows the activation of MAPK in response to many stimuli and one of the most complex pathways since it involves the recruitment of a large number of MAP3K [23,26,44,57–65]. MAP3Ks activate the most important MAP2K substrates in the JNK pathway, such as MKK4 and MKK7. Next, JNK is dually phosphorylated on the Thr-X-Tyr motif on Thr-221 by MKK7 and Tyr-223 by MKK4, preferentially. However, for JNK activation, an interaction between scaffold proteins JNK-interacting protein (JIP) 1-3 and the 'ASK1-MKK4/7-JNK' complex still provides a structural modification in this complex for the correct phosphorylation of JNK, which results in Bid cleavage. Besides JIP 1-3, other proteins such as POSH (plenty of SH3s) are also critical for complex anchoring since they appear to facilitate an interaction between GTP-Rac1 and subsequent proteins [23,26,44,59,61,66–71]. Then, JNK phosphorylates transcription factors, which induces the expression of pro-apoptotic proteins and decreases the expression of anti-apoptotic proteins. The major JNK target is the transcription factor AP-1, which is a complex formed by members of Jun, Fos, ATF, and MAF protein families. JNK phosphorylates ATF2 at the NH_2-terminal activation domain on Thr69 and Thr71 residues, increasing ATF2 transcriptional activity. JNK phosphorylates the δ-domain on the NH_2-terminal region of c-Jun on Ser63 and Ser73, which increases c-Jun transcriptional activity. JunD is a poor substrate, while JunB binds to JNK (2-fold less when compared to c-Jun) but is not a substrate. The δ-domain in the NH_2-terminal region (present in c-Jun) is required for the phosphorylation but poorly conserved within the other two members (JunD and JunB) of the Jun family of transcription factors. Deletion of the δ-domain domain blocks the phosphorylation by JNK, indicating it could be a potential target. Besides the fact that the combination of the components of AP-1 might vary, each isoform displays differences in binding affinity to the JNK substrates [23,39,63,69,72,73]. While binding of JNK2β1 and JNK2β2 to ATF2 is 2-fold greater than the binding to c-Jun, binding of JNK2α1 and JNK2α2 to c-Jun is 2-fold greater than ATF2 [74]. Another substrate for JNK is p53, another protein responsible for increasing the expression of pro-apoptotic proteins in stress-induced cell death. To induce this death signal, JNK phosphorylates p53 at Thr81, allowing p53 to form a dimer with p73. This p53-p73 complex induces the expression of pro-apoptotic genes such as *puma* and *bax*. On the other hand, p53 can trigger the MOMP as well in a transcription-independent manner by activating pro-apoptotic Bcl-2 proteins (Bax or Bak) or by inactivating anti-apoptotic Bcl-2 proteins (Bcl-2 and Bcl-X1). Other transcription factors were reported as JNK substrates and could also induce apoptosis in different stress situations, indicating that JNK pathway activation is context-specific and cell type-specific [45].

2.1.2. JNK Isoforms: Are They All the Same Thing?

The human genome contains three genes known as *JNK1* (*MAPK8*), *JNK2* (*MAPK9*), and *JNK3* (*MAPK10*), which encode several JNK isoforms via alternative splicing of mRNA. In 1994, JNK1 isoform was isolated from a fetal brain cDNA library [45], while a second isoform, JNK2, was isolated from HeLa [75] and Jurkat [76] cDNA libraries. In 1996, while screening adult brain cDNA libraries, a group confirmed the two previously identified isoforms and found eight new sequences that corresponded to novel JNK isoforms [74]. For both JNK1 and JNK2, four isoforms were identified for each enzyme, a

total of eight isoforms. These alternative sequences show differences in COOH-termini and protein kinases subdomains IX and X. For JNK3, two isoforms with different COOH-termini but the same IX and X subdomains were identified as well. The major difference between JNK3 and the other JNK is an extended NH_2-terminal region fused in-frame to the conserved methionine residue that serves as the NH_2-terminus of the other JNK. The isoforms are listed in the following table (Table 1):

Table 1. c-Jun N-terminal kinase (JNK) isoforms described by Gupta et al. (1996).

JNK1	JNK2	JNK3 [2]
1α1	2α1	3α1
1α2 [1]	2α2 [1]	3α2 [1]
1β1	2β1	
1β2	2β2	

[1] Canonical isoform of each JNK. [2] A third JNK3 isoform was later described by another research group [77] but is not listed in the present table. This third isoform lacks the first 38 amino acids. Furthermore, according to UniProt database, another 68 potential JNK3 isoforms were mapped in silico [78]. The three JNK3 isoforms are 81.68% identical between each other, while JNK3α1 and JNK3α2 are 89.87% identical.

The expression of multiple JNK isoforms is fundamental to generate tissue-specific responses to the activation of JNK. Although all three isoforms and their upstream activators are indispensable to neurodevelopment; several human tissues express both the JNK1 and JNK2, while JNK3 expression is limited to a specific subset of neurons in the nervous system. Somehow JNK3 appears to be associated with multiple neuropsychiatric conditions, such as epileptic encephalopathy [79] and anxiety induced by hepatic encephalopathy [80]. It was reported in the literature that JNK3 knockout in mice (*JNK3*$^{-/-}$) leads to significant SNC-associated defects and embryonic death [81]. A weak expression was found in other tissues in both pathological and physiological conditions [82].

2.1.3. Brain Regions Normally Affected in AD Are the Same Regions Where JNK3 Expression Was Identified. Is It a Coincidence?

One of the first pieces of evidence that fed the hypothesis associating JNK3 and AD was described 15 years ago [83] when it was demonstrated that the expression of JNK3 is co-located with ALZ-50 antigen in brains in AD hippocampal sections. This co-occurrence indicates the presence of both JNK3 expression and abnormally phosphorylated τ protein, which is a precursor for the formation of NTF [11,12,84]. At that time, researchers showed for the first time the presence of JNK3 in specific tissues. Northern blot assay performed using mRNA from heart, placenta, lung, liver, skeletal muscle, kidney, pancreas, and testis identified a weak hybridization in kidney and testis tissues, while other tissues showed no hybridization. In addition, analysis of JNK3 mRNA by both Northern blot and in situ hybridization in post-mortem brain samples of neurotypical individuals ranging from 35 to 56 years old found JNK3 expression in a particular subset of pyramidal neurons in CA1, CA4, and subiculum regions of the hippocampus and layers III and V of Brodmann's areas 4, 10, and 17 of the neocortex. JNK3 was also identified in the cerebellum, striatum, and brain stem, and a weak signal was detected in the spinal cord as well. There was no expression of JNK3 found in white matter that lacks neuronal cell bodies [83].

The clinical presentation of AD indicates that neuronal death and dysfunction affect specific brain regions that are critical to memory functioning, learning, and cognitive performance [84]. As discussed on the previous topics, a perturbation in these brain networks occurs because of different aspects including cytoskeletal abnormalities in neurons due to NFT and NP, the presence of Aβ plaques in regions responsible for receiving inputs from other regions causing synaptic interruption, reductions of neurotransmitters, loss of neurons, and local glial inflammatory reactions usually associated with plaques. Those regions include the basal forebrain, cholinergic system, hippocampus, entorhinal cortex, limbic cortex, and neocortex, and different researchers demonstrated that AD patients showed an anatomic alteration in their brains via MRI such as hippocampal atrophy, with subsequent temporal atrophy and ventricular expansion [85]. Those relationships suggest some possible correlations of the

architectonic distribution of neurodegenerative damage and brain circuits involved in the control of certain social and emotional behaviors and are summarized in Table A1.

By mapping 39 cortical areas of 11 brain samples from AD patients, one study revealed that higher levels of NFT were found in the limbic penallocortex (area 28), subiculum and CA1 zones of the hippocampus (area 51), basal nucleus of the amygdala (areas 11, 12, and 24), anterior insula (areas 38 and 35), non-primary association cortex (areas 32, 46, 40, and 39), posterior parahippocampal cortex (areas 37 and 36), primary sensory association cortex (areas 7, 18, 19, 22, 21, and 20), agranular cortex (areas 44, 45, 8, 6, and 4), and primary sensory cortex (areas 41 and 42). The distribution of NFT appeared to be more selective to limbic and temporal lobes than frontal, parietal, or occipital lobes, while there were more neuritic plaques (NP) in temporal and occipital lobes [84]. Still, when considering atrophy in well-defined brain structures and AD symptoms, areas with higher expression of JNK3 are also in evidence. Research found regions of decreased gray matter volume associated with neuropsychiatric behaviors in patients with mild AD. Delusion symptoms were associated with decreased gray matter density in the left frontal lobe (medial frontal gyrus/area II and inferior frontal gyrus/area 45), in the right frontoparietal cortex (inferior frontal gyrus/area 45 and inferior parietal lobule/area 40) and the left claustrum. Apathy, which is often seen in early AD and may be present even before noticeable memory deficits, was associated with gray matter density loss in the anterior cingulate (area 24) and frontal cortex bilaterally (inferior frontal gyrus/area 47, middle frontal gyrus/area 9, superior frontal gyrus/area 10) the head of the left caudate nucleus and in bilateral putamen (nucleus lentiform), and agitation was associated with decreased gray matter values in the left insula (area 13), and the anterior cingulate cortex bilaterally (area 24). Those findings suggest that AD symptoms are associated with neurodegeneration in specific neural networks supporting personal memory, reality monitoring, processing of reward, interoceptive sensations, and subjective emotional experience [86].

The expression profile of JNK3 suggests it is expressed by cells in specific brain regions commonly affected in AD patients. More recently, studies have emphasized the role of JNK3 in neurodegenerative diseases like AD. In this sense, studies on post-mortem brain samples have shown a greater expression of phosphorylated JNK3 in AD patients besides the presence of Aβ [87–89]. Further studies have identified that JNK3 is highly expressed and activated in brain tissue and cerebrospinal fluid in patients with AD, besides being statistically correlated with the level of cognitive decline [90,91]. In fact, in 2012, one study showed that the activation of JNK3 is essential for the pathophysiology of AD by maintaining positive feedback on Aβ42 production [92]. The Aβ42 activates AMPK, inhibiting the mTOR route, leading to oxidative stress, which activates JNK3. Once activated, JNK3 promotes the processing of APP by phosphorylating the protein at position T668P, which induces the internalization of APP, facilitating its cleavage/phosphorylation directly, favoring the production of Aβ42, restarting the cycle. From this study, JNK3 was shown to be the main kinase promoter of APP phosphorylation in T668, since *JNK3*$^{-/-}$ knockout mice showed a dramatic reduction in Aβ42 levels, and higher numbers of neuronal cells, and better cognitive function.

At the epigenetic level, unique patterns of methylation in CpG and CpH sites of enhancers were observed, suggesting that epigenetic control of these enhancers is involved in AD and neuronal dysfunction. Even though the CpH methylation decreases with age, it was accelerated in AD. In samples of the prefrontal cortex of individuals diagnosed with AD, JNK3 (*MAPK10*) showed enhancer hypomethylation [93]. This finding, therefore, corroborates with other researchers that found overexpression of JNK3 in specific brain areas and reinforces the role of JNK3 in inducing some AD hallmarks. In the middle temporal gyrus, it was found that JNK3 (*MAPK10*), Bcl-2 family members (Bid, BAK1), and multiple caspases (CASP8, CASP3, CASP7) for example, were also hypomethylated in patients with AD, suggesting an upregulation of apoptotic pathways in AD neurons [94]. Human-induced pluripotent stem cell-derived neurons carrying isogenic apoE3/3 transplanted to apoE4/4 knock-in mouse hippocampus showed dysregulation of many pathways involved in cell stress, such as apoptosis. It was revealed that JNK3 (*MAPK10*) was the gene implicated in the largest number of dysregulated pathways [95].

The overall importance of JNK signaling in brain development results from the multitude of basal functions such as regulating region-specific neuronal death or migration and neuronal polarity, neuronal regeneration, learning, and memory, for example [44]. On the other hand, JNKs are expressed in microglia, astrocytes, and oligodendrocytes as well as in neurons [96,97], and despite having different roles, microglia and neurons 'communicate' often, and one way to do so is via JNK signaling axis [98] showing its fundamental role in both pathological events such as neuroinflammation and physiological processes like regeneration.

2.1.4. JNK and p38 Working Together towards Chaos

Despite glial cells having been reported to induce deregulation in mitochondria and endoplasmic reticulum dysfunction resulting in bioenergetic and Ca^{2+} homeostasis disruption [99], neuroinflammation is critical for AD since it appears to modulate the disease progression [100,101]. The integration of the immune system and the central nervous system was recently reviewed [102]. In AD, the neuroinflammation relies on innate immune responses mediated by microglia [103]. The microglia, a subtype of neuroglial cells, comprise resident immunocompetent and phagocytic cells originated from yolk sac-derived erythro-myeloid progenitors that gain CNS-surveilling properties during early fetal development, and are not replaced by circulating bone marrow-derived cells throughout their lifespan [104,105], and represent 8%-20% of all CNS cells [106–108]. On the other hand, they share some phenotypic traits and innate immunological functions with peripheral macrophages since they express major histocompatibility complex (MHC) antigens, and T and B cell markers, but differ from other tissue macrophages due to their tight regulation by the CNS microenvironment [109]. Among other functions, the key role of the microglia consists of the regulation of inflammation, synaptic connectivity, programed cell death, wiring and circuitry formation, phagocytosis of cell debris, and synaptic pruning and sculpting of postnatal neural circuits [110]. Research identified a correlation of specific expression patterns in microglia from the brain cortex and AD risk variations, indicating that neuroinflammation may have a more important role in AD than in other neuropsychiatric diseases [99]. It was revealed that inflammatory pathways are also linked to rapid cognitive decline in the mild cognitive impairment stage of AD [18]. Thus, a link between some AD hallmarks and neuroinflammation continues to grow stronger. It was reported that microglia from animals carrying the ε4 allele of the *apoE* gene are deficient in clearing Aβ aggregates [95]. Despite the major function of apoE being associated with cholesterol transportation, it is usually related to increasing Aβ clearance by promoting migration and activating phagocytosis in microglia, and mutations are associated with EOAD [103]. However, it was suggested that Presenilin1 also modulates Aβ clearance [111].

In the pre-clinical stages of AD, the microglia play a protective role by phagocyting and depredating toxic Aβ aggregates. On the other hand, as the disease progresses, the Aβ clearance by microglia appears to decrease due to overstimulation [100,101,108,112]. In other words, after some point, microglia cells appear to gradually lose their phagocytic phenotype. In vivo AD models corroborate this hypothesis, since it was found that microglia decrease the expression of their Aβ-binding receptors and Aβ-degrading enzymes while maintaining the ability to produce pro-inflammatory cytokines [113]. For a time, it was believed that the microglia under physiological conditions (so-called 'resting microglia') could switch into a reactive morphology, being called 'activated microglia' through activation of macrophage polarization in which it could acquire an M1 or an M2 phenotype. The M1 phenotype is associated with pro-inflammatory induction, similar to activated peripheral macrophages and Th cells, while the M2 phenotype is associated with an anti-inflammatory state [110,114]. Recently, this categorization has been under discussion because it is difficult to fully characterize the 'pro-inflammatory' phenotype of microglia in neurological diseases, and the classification appears to be too restrictive, which hinders research progress [115]. For further information about the role of microglia in neurodegenerative diseases, please check the following references [116,117].

Despite the controversy, it is widely accepted that in the past two decades, neuroinflammation has been considered an important component of the disease pathogenesis. As mentioned above, microglia may contribute to neurodegeneration effects since it reacts to Aβ, for example. One mechanism of Aβ clearance in the brain is the uptake and degradation of those aggregates by the microglia-mediated by Toll-like receptors (TLRs) TLR2 and TLR4, for example. After a stimulus, the microglia produce several inflammatory mediators, such as IL-1β, IL-6, TNF-α, prostaglandin E2 (PGE2), nitric oxide (NO), brain-derived neurotrophic factor (BDNF), which can activate the JNK pathway. The major contribution of JNK to neuroinflammation is via its transcription factor, AP-1, which regulates pro-inflammatory genes such as *COX2*, *NOS2*, *TNF-α*, *CCL2*, and *VCAM-1* [74]. The CCL2 level in cerebrospinal fluid (CSF) is comparable to the hippocampal volume in predicting a rapid cognitive decline in MCI, a preclinical phase of AD [18]. ATF2, another JNK substrate, is also associated with pro-inflammatory genes. The activation of JNK contributes to AD pathophysiology through pro-apoptotic and pro-inflammatory effects.

On the other hand, studies indicate that microglia may contribute to the pathology of AD through the production of IL-1, activation of neuronal p38-MAPK, and synaptic and cytoskeletal alterations [107,108], which manages the aggregation of NTFs [8,19,22,36,118], which confirms their participation in AD, and thus become an important therapeutic target. p38 is a 38 kD polypeptide MAPK found in 4 isoforms (α, β, γ, δ) and it is strongly activated by environmental stresses and inflammatory cytokines [119,120]. Similar to JNK, phosphorylated p38 was found especially in the CA2 and the subiculum, but at the CA1 in the hippocampus as well [121], and near NP and NTF in *post-mortem* brains of AD patients [35,122,123]. In response to Aβ, NTF, or oxidative stress, also a common feature in AD brains, JNK and p38 induce NF-kβ, synaptic excitotoxicity, and neuroinflammation [123–127]. Corroborating these findings, it was demonstrated that NJK14047 (selective p38α/β inhibitor) reduced NOS, COX-2, TNF-α, and IL-1β in vitro, decreased microglia activation in vivo [128], and improved cognitive functions in an AD mouse model [129]. This could be explained by the fact that p38α expression stimulates BACE1 and, therefore, the Aβ generation, but also induces dysfunctional autophagy in neurons [129]. Evidence suggests that patients with neurodegenerative diseases such as AD might also benefit from p38 MAPK inhibitors [130]. Besides, p38 might modulate (at some point) psychiatric symptoms observed in AD such as depression [131]. The prevalence of major depression in demented patients is 32% [132], in AD patients is over 20% [131], while the lifetime prevalence of depression is 10.8% [133]. Evidence showed that IL-1β and TNF-α increased the serotonin transporter (SERT) activity (and therefore decreased synaptic availability of serotonin) via p38 activation in vitro and in vivo [134,135]. LPS-treated mice showed increased SERT activity and depressive-like behavior, but when the animals were treated with SB203580, increased serotonin uptake and depressive symptoms were no longer observed [135].

Other studies showed that neuronal deletion of p38α had neither impact on the hippocampal and cortical development nor on learning and memory skills, motor coordination, and muscle function. On the other hand, the animals showed increased anxiety behavior and higher levels of JNK activation on the CA1, CA3, and dentate gyrus. Inhibition of JNK using SP600125 or D-JNKi, however, decreased JNK activation in vitro and ex-vivo and reverted the anxiety-like behavior induced by deletion of p38α in vivo. This suggests that the specific activation of the p38α isoform is necessary to control behavioral states related to anxiety through JNK inhibition in CNS since other isoforms did not decrease JNK levels in both in vivo and in vitro models [136]. It opens an interesting discussion because the selective inhibition of p38 could induce anxiety symptoms principally needs to be taken into account when dealing with elderly individuals.

2.1.5. JNK Structure

Similar to other kinases, JNK presents 11 subdomains (I-XI) in a conserved arrangement of two lobes, the C-terminal lobe and the N-terminal lobe that are connected through a catalytic site (the ATP-binding site) and signature sequences that contribute to proper stabilization [137,138].

In the N-lobe, at the subdomain I, between the β1 and β2-strands there is a glycine-rich sequence Gly-X-Gly-X-X-Gly-X-X (also called 'G-loop', residues Gly71 to Val78) that comprises the ATP-binding site and is followed by a valine residue at the β2-strand that makes a hydrophobic contact with the adenine of ATP. The subdomain II contains Lys43 at the β3-strand that forms a salt bridge with a glutamate residue from subdomain III. So, the third subdomain is composed of a αC-helix and contains Glu111 that interacts with Lys43 (subdomain II) in the active conformation, as the salt bridge couples with ATP. Subdomain IV contains a β4-strand, which contributes to the structure of the N-lobe, while subdomain V contains a hydrophobic β5-strand in the N-lobe and an αD-helix in the C-lobe. The sequence between β5-strand and αD-helix links the N-lobe and the C-lobe. At the subdomain V, there is a gatekeeper residue (Met146) that is positioned deep inside the ATP-binding pocket and is between two hydrophobic regions [139]. This residue takes part in the protein conformation structure and determines the size of the binding pocket. The subdomain VIa contains the αE-helix that parallels the αF-helix from subdomain IX. In the C-lobe, the subdomain VIb influences catalytic reactions as it contains the catalytic loop ('C-loop') with a conserved HDR motif (His187-Arg188-Asp189). Asp189 forms a hydrogen bond with Tyr223 and is the catalytic base that accepts the hydrogen removed from the hydroxyl group being phosphorylated. Subdomain VII contains the activation segment, which starts with a DFG motif (Asp207-Phe208-Gly209). This motif is particularly important to activate the protein. When Phe208 is inside the hydrophobic pocket created by residues from the C lobe and N lobe, the conformation is called 'DFG-in'. On the other hand, if Phe208 is outside the hydrophobic pocket (called 'DFG-out' conformation) the enzyme is inactivated as Asp207 can no longer properly orient Mg^{2+} to the active site, and as a result, the transference of phosphate from ATP to the substrate is disrupted [140]. Subdomain VIII contains the threonine and tyrosine residues whose phosphorylation activates JNK (called 'TYP motif', Thr221-Pro222-Tyr223), the 'APE motif' (Ala231-Pro232-Glu233), and the p+1 loop (Arg227-Arg230), which is between TYP and APE motifs. The region between the DFG motif (subdomain VII) and APE motif (subdomain VIII) is referred to as the activation loop (A-loop, Ser217-Thr226). Once Thr221 and Tyr223 are phosphorylated, the protein changes its conformation so that the activation loop is oriented to render the active site cleft accessible; DFG and HDR motifs are properly positioned for catalysis and the p+1 loop can interact with the substrate. Subdomain IX contains mostly the hydrophobic αF-helix and aspartate, while subdomains X and XI contain α-helices involved in binding substrate proteins [42,141,142]. The so-called D-recruiting site (DRS) is also important to properly coordinating the binding structure and comprises the docking groove (residues 145 to 169), the ED site (residues 196 to 204), and a common docking motif (D-motif) (residues 359 to 372). Figure 3 illustrates a two-dimensional view of JNK3 structure and important regions linked to either JNK signaling or JNK conformation.

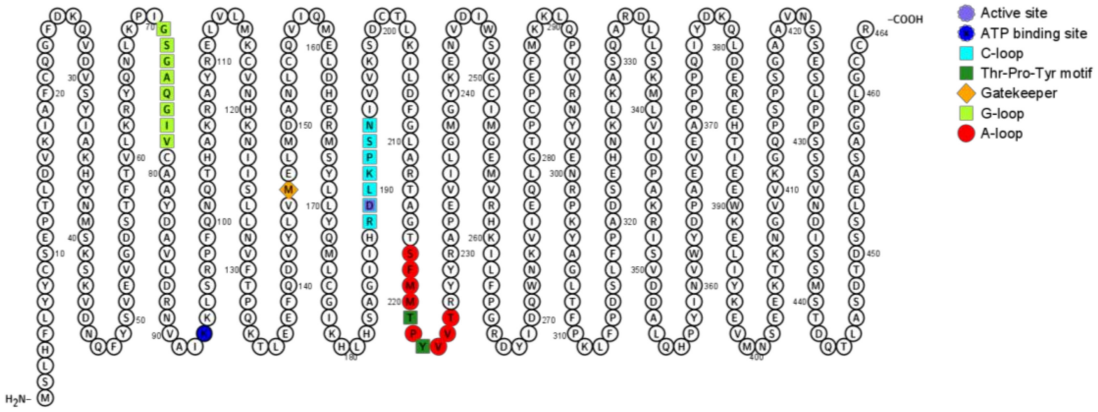

Figure 3. Two-dimensional structure of JNK3. Key structure elements are colored as shown in legend. Figure generated with Protter.

organic compounds do not cross the blood–brain barrier (BBB), which is fundamental when dealing with drugs supposed to act at the SNC. This is a crucial issue and must be taken into account in this case.

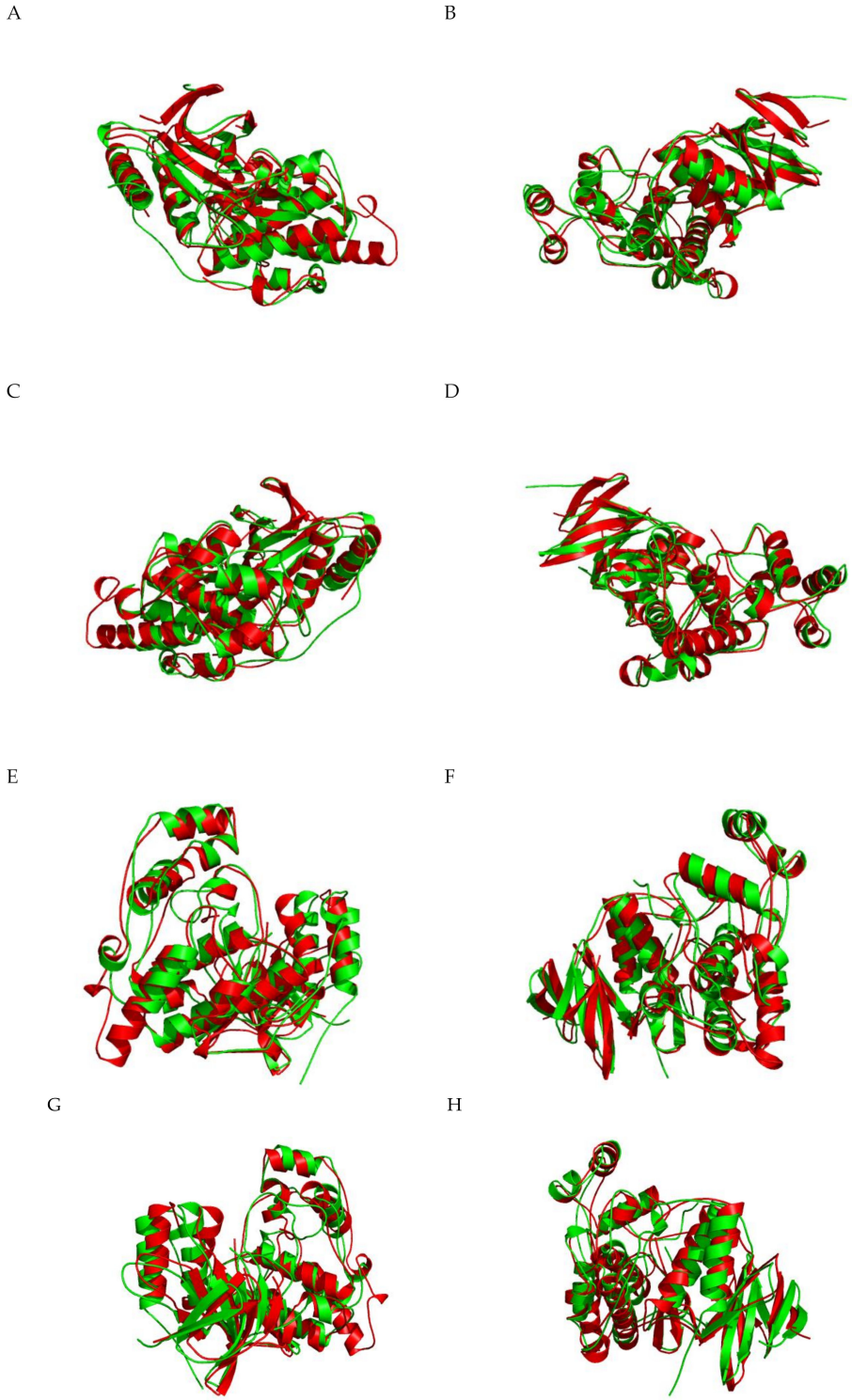

Figure 4. (**A**–**D**) Structural superposition of JNK3 (PDB code: 3OY1, chain A, represented in red) and ERK1 (PDB code: 2ZOQ, chain A, represented in green); (**E**–**H**) Structural superposition of JNK3 (PDB code: 3OY1, chain A, represented in red) and p38α (PDB code: 1A9U, chain A, represented in green). Figure generated by iPBA.

As previously mentioned, the CMGC kinase group shares many similarities within their kinase domain, especially at the catalytic subunit, which catalyzes the transfer of the γ-phosphate from ATP to serine or threonine residues of protein substrates [35]. These identical or very similar domains make it a challenging task to develop selective inhibitors. Potential kinase inhibitors may fail in clinical trials because they bind to multiple targets due to structural similarity. In this case, a deeper understanding of the kinase target of each drug is required to develop successful treatment strategies, although some off-target effects are beneficial once drug repurposing is particularly interesting [143].

Regarding structure, the homologous region of JNK3 (Phe48-Glu397) is similar to other MAPK (45% identical in amino acid sequence to ERK2 and 51% identical to p38). However, some segments, such as the A-loop region, show a high structure variance between JNK, p38, and ERK. In JNK3, the activation loop is 10 amino acids long, so the A-loop of JNK3 is four residues shorter than ERK and two residues longer than p38. Additionally, the residue between two phosphorylation sites at the Thr-X-Tyr motif is proline in JNK3 (Thr221-Pro222-Tyr223), and therefore, for JNK, the Thr-X-Tyr motif is also called TPY motif. For p38, glycine is present, whereas in ERK it is glutamate. ERK and p38 lack a 12 amino acid sequence at the C-terminal domain that is present in all JNK isoforms' (residues 283-328). These variations cause changes in the protein structure and impact the drug specificity. Figure 4 (A–D) shows the superposition of JNK3 (represented in red) and ERK1 (represented in green), while Figure 4 (E–H) presents a superposition of JNK3 (red) and p38 (green).

On the other hand, JNK has three isoforms and several studies already pointed out that it is particularly challenging to design highly selective JNK3 inhibitors because it shares 77% amino acid sequence identity with JNK2 and 75% identity with JNK1 as well. The sequence identity at the ATP binding pocket is 98% identical between all three JNK isoforms. The ATP binding region has been explored as a potential target, but since this is a highly conserved region, drugs targeting the ATP binding pocket lack specificity. On the other hand, the hydrophobic region is an interesting 'place' to explore JNK selectiveness but is 'protected' by a gatekeeping amino acid residue. The open conformation of the gatekeeper Met146 also contributes to selectivity.

The presence of a leucine residue (Leu144) within the binding pocket could explain the selectiveness of JNK2/JNK3 isoforms over JNK1, which presents an isoleucine residue (Ile106) in the same position. The presence of Leu144 provides the proper accommodation of the naphthalene ring into the selectivity binding pocket, which is not possible in other MAPKs. Another study confirmed this finding when it suggested that Leu144 located within the hydrophobic pocket of JNK3 was responsible for the selectivity [144]. On the other hand, the selectivity of JNK3 over JNK2 is explained by the presence of isoleucine and methionine residues (Ile92 and Met115) in the JNK3 isoform, while the JNK2 isoform presents valine and leucine residues in the same position (Val54 and Leu77). A recent study suggested that hydrophobic interactions with other amino acids, such as valine and glycine, are also necessary to confer a selective inhibition of JNK3 [144].

Crystallographic structures solved by X-ray of the JNK3 protein are useful for understanding the interaction between ligand and target. The three-dimensional structure of JNK3 bound to an inhibitor with in vitro CNS-like pharmacokinetic properties is shown in Figure 5A. A more detailed interaction between the ligand and JNK3 amino acids is represented in Figure 5B. Experimental studies determined that the molecule 5-[2-(cyclohexylamine)pyridin-4-yl]-4-naphthalene-2-yl-2-(tetrahydro-2H-pyran-4-yl)-2,4-dihydro-3H-1,2,4-triazol-3-one (referred to as 589) preferably inhibits JNK3 (IC50 = 0.016 μM) and JNK2 (IC50 = 0.097 μM) over JNK1 [145].

Despite the ligand appearing to be highly selective to JNK2/3, the ligand molecule was designed to possibly treat AD, and therefore, it must show high biological activity and low toxicity. Authors demonstrated that early ADMET (absorption, distribution, metabolism, excretion, and toxicity) profiling in drug discovery drastically decreases the fraction of pharmacokinetics-related failure in clinical trials [146,147]. In this case, in silico methods can predict the ADMET profiling from a molecular structure, saving time and resources. Another important aspect is that approximately 98% of small

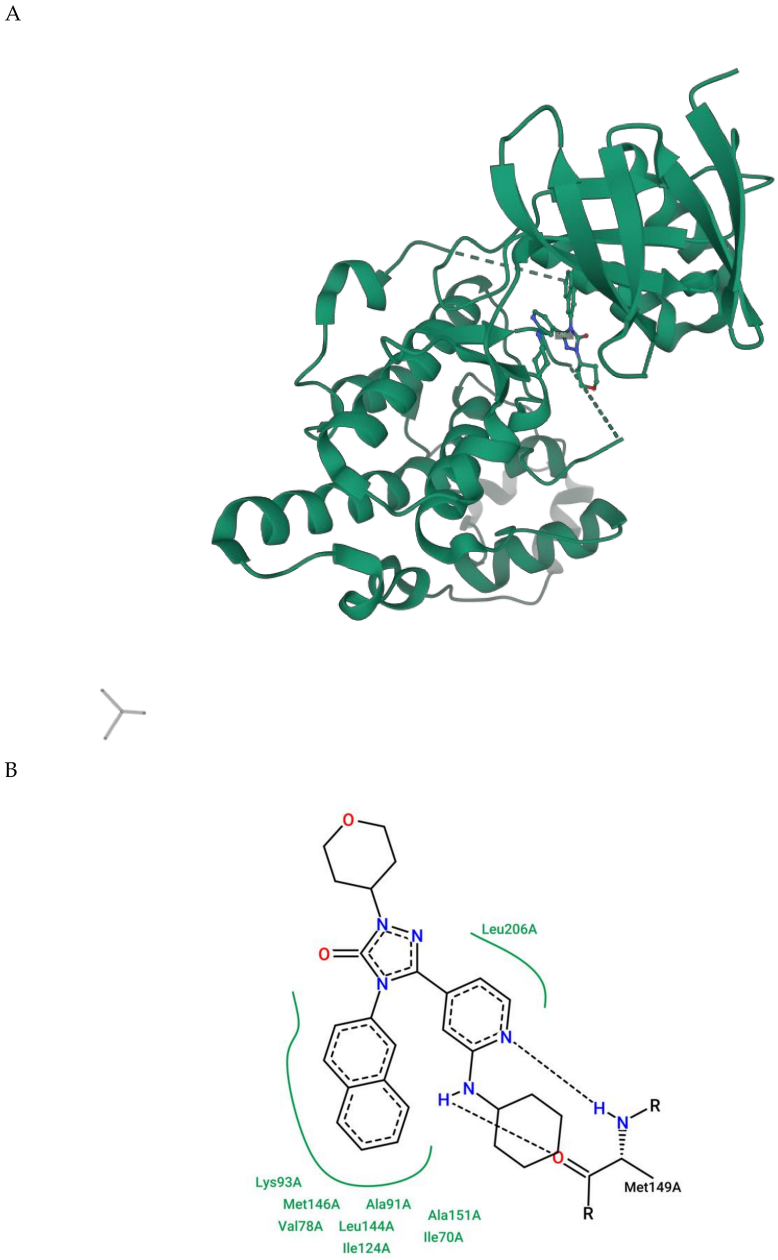

Figure 5. (**A**) Overview of the three-dimensional structure of the JNK3 interacting with its ligand (PDB code: 3OY1); (**B**) 2D protein-ligand interaction plot for 3OY1, emphasizing the interactions between the ligand and the residue Met149. The hydrogen bond (at atom level) is shown in dashed lines. Amino acids that do not interact with the ligand via hydrogen bond are shown in green. Water molecules are not shown. Plot automatically generated by ProteinsPlus using the PoseView tool based on the 2Ddraw library.

3. Therapeutic Proposal

In 1974, Drachman and Leavitt suggested that memory was related to the cholinergic system and depended on age [148], a notion that is still considered valid today. At the same time, two British groups independently demonstrated that the pathology of AD was associated with a severe loss of central cholinergic neurons, more precisely, the severity of dementia was correlated with the extent of cholinergic loss in the basal nucleus of Meynert [149,150]. The cholinergic hypothesis led to the development of drugs during the 1980s and 1990s and continues to provide a basis for current development efforts with modulators of neuronal nicotinic receptors and other molecules that have

effects on cholinergic function such as muscarinic and nicotinic agonists, partial agonists, and allosteric modulators of 5-hydroxytryptamine (5-HT) receptor [148,151–153]. So, although other therapeutic targets are being investigated, the cholinergic hypothesis and the amyloid cascade hypothesis have influenced drug development more profoundly, especially by the latter. The amyloid cascade hypothesis has dominated drug development in the past two decades and presents several targets, including inhibition of protein kinase activation [152]. In fact, among the different hypotheses for AD, like amyloid hypothesis, neurotransmitter hypothesis, tau propagation, mitochondrial cascade, neurovascular, exercise, inflammatory, and virus, the first cited was the most strongly tested one in clinical trials until 2019 (22.3%), followed by the neurotransmitter hypothesis, with 19.0% of trials [31].

Despite having been a known disease for over a hundred years, the current treatment of AD seems to be more palliative by restricting itself to the management of symptoms by temporarily delaying cognitive impairment [4,49–54]. However, there are still many points that remain uncertain concerning the pathophysiology and the treatment of AD, impacting the development of new drugs. There are currently four drugs approved by the FDA and used clinically, totaling five therapies, the fifth being a combination of two drugs. Clinical treatments are mainly divided into two categories: Acetylcholinesterase inhibitors (AChEIs), represented by donepezil, and N-methyl-D-aspartic acid (NMDA) receptor antagonist, represented by memantine [93]. Unfortunately, only the symptoms are treated because the drugs are regulators of neurotransmitters with no significant effect on the progression of AD. Therefore, it is necessary to seek alternative strategies to treat AD given the limited progress of therapy in phase III clinical trials and the fact that no new drugs have been approved since 2003 [49,55]. About 200 drugs are in phase II of analysis, albeit they show a limited clinical effect, and there is a controversy regarding their therapeutic efficacy. There are many potential drug targets, and so far, there are no validated targets, except perhaps for the cholinergic system [53,55,56]. The 'normal' JNK pathway is essential for neurodevelopment and neuronal regeneration, albeit excessive activation of this route can induce apoptosis in neurons. Thus, techniques that allow specific inhibition of JNK have been developed and identified as neuroprotective agents, which can not only treat AD but also other pathologies external to the CNS [44,61,81,154–156]. Evidence shows that JNKs can be therapeutic targets in several conditions [157], including Parkinson's disease [158] and AD [159], obesity and insulin resistance [160,161], rheumatoid arthritis [162], asthma [163–165], vascular disease, and atherosclerosis [166]. Given its performance in various biological and pathological processes, different approaches are used to pharmacologically block JNK activity.

In the human body, there are hundreds of kinases, and several of them are somehow involved in different conditions, including AD, and therefore, they constitute an interesting molecular target [167]. The first small molecule kinase inhibitor, Imatinib (Gleevec, Novartis), was FDA-approved in 2001 to treat leukemia. As of June 2020, there are now 61 FDA-approved kinase inhibitors and a simple search for the term 'kinase inhibitor' on the ClinicalTrials.gov website revealed 6464 trials, reinforcing its relevance. Most kinase inhibitors comprehend the ATP-competitive inhibitor types. Within this group, type I inhibitors bind to the active DGF-in conformation of the kinase, while type II inhibitors bind to the inactive conformation of the kinase (DFG-out) in a such way that the A-loop blocks the substrate from binding to the enzyme [140,168–171]. These compounds have a heterocyclic ring that mimics the interaction of the purine ring of the ATP and occupies the adenine binding region of the ATP-binding pocket, while other parts of the molecule occupy adjacent hydrophobic regions [168]. Compared to type I, type II inhibitors have more selectivity as there is higher heterogeneity among inactive conformation states but less affinity to active kinases [172,173]. Aminopyrazoles, aminopyridines, aminopyrimidines, indazoles, pyridine carboxamides, benzothien-2-ylamides, and benzothiazol-2-yl acetonitriles are some small molecules already reported as ATP-competitor JNK inhibitors [157,174].

One of the first molecules to be explored was SP600125 (PubChem ID 8515), a pan-JNK inhibitor with IC50 values for JNK1, JNK2, and JNK3 of 40, 40, and 90 nM, respectively. In vivo and in vitro models of AD demonstrated that SP600125 prevents neuronal death induced by βAPP production. Besides, other studies showed that intracerebroventricular injections of SP600125 improved AD-related

neurological aspects in animal models. However, such a compound offers limited specificity. SP600125 helped in understanding the role of JNK in many physiological and pathological conditions, and despite still being broadly used in research, the lack of specificity confers variable degrees of responses and toxicity profiles. Along with all three JNK isoforms, it inhibits upstream kinases of the JNK pathway such as MKK4 and MKK7 but also interferes with the signaling of proteins not directly related to the classical JNK pathway, such as SGK, S6K1 (p70 ribosomal protein S6 kinase), AMPK, CDK2, CK1d, and DYRK1A, a total of at least 13 other kinases [175] [176]. Tanzisertib (Celgene) (PubChem ID 11597537) is a pan-JNK inhibitor developed based on the SP600125 structure with reported inhibition of JNK3 activity (PBD ID 3TTI) [177]. This molecule, also known as CC-930, was the first orally active molecule discovered and was being investigated in phase II clinical trials for treating idiopathic pulmonary fibrosis (NCT01203943) and discoid lupus erythematosus (NCT01466725). Trials were discontinued in 2012 due to increased hepatotoxicity [178,179]. Bentamapimod (also known as AS602801 or PGL5001, PubChem ID 10195250) is another orally active pan-JNK inhibitor (PregLem SA). This ATP-competitive molecule with an IC50 of 80 nM, 90 nM, and 230 nM for JNK1, JNK2, and JNK3, respectively, demonstrated a sufficient safety and toxicity profile in phase I and II clinical trials for inflammatory endometriosis (NCT01630252) [180,181]. In combination with enzalutamide, treatment with Bentamapimod showed antineoplasic activity in a prostate cancer model in vitro [182]. CC-401 (PubChem ID 10430360), developed by Celgene, is a pan-JNK inhibitor derivate from SP600125 with an inhibition constant (Ki) ranging from 25 to 50 nM with 40-fold selectivity for JNK than other kinases. The compound entered a phase I clinical trial (NCT00126893) to determine the optimal dosing for individuals with high-risk myeloid leukemia, but the trial was discontinued [183,184]. However, type I and type II inhibitors bind to the same ATP-binding site, which is a highly conserved domain within the MAPK family [33]. In this case, the design of a specific kinase inhibitor capable of blocking a single kinase by either type I or type II mechanisms of action is a considerable challenge. Since lack of specificity is a disadvantage, non-ATP-competitive inhibitors are thought to be more selective than ATP-competitive inhibitors. While type III inhibitors bind to catalytic sites close to the ATP-binding site, type IV binds to a catalytic site distant from the ATP-pocket. Similarly, in primary cell cultures, compounds such as K252a and CEP1347 inhibited Aβ-induced neuronal death, the latter even reaching the stage of clinical studies. However, it did not perform satisfactorily enough to proceed to the following tests [23,27,36,61,66–68,70,90,92,156,185–192]

Type IV kinase inhibitors do not target allosteric regions outside the ATP-binding site or the catalytic site. Instead, they inhibit the enzymatic activity by either blocking the access to upstream activators or by preventing the phosphorylation of some downstream substrates while preserving the biological function of other important substrates. They target allosteric sites at the C-lobe, N-lobe, or allosteric pockets at the kinase domain superficies [193]. Type IV JNK inhibitors disrupt the interaction between JIP-1 and β-arrestin-2 with JNK, which is essential for the function and regulation of JNK signaling, providing critical tools for manipulating the 'signalosome' and the cellular response to different stimuli [183]. In this sense, blocking JIP1-JNK could be an alternative to treat neurological diseases because even though knockout of JIP-1 did not affect APP transport or Aβ production [194], it interacts with the APP intracellular domain [195]. Still, JIP-1 inhibition prevented apoptosis in sympathetic neurons [196], and transgenic mice with less JIP-1-mediated JNK activation showed enhanced long-term synaptic plasticity, which is linked to learning and memory skills [197]. In this sense, brimapitide (also known as XG-102, AM-111, or D-JNKI1, PubChem ID 315661186) (Auris Medical AG/Xigen SA) is a cell-permeable peptide and comprises 20 amino acids of the JNK-binding domain JIP-1/IB1 (JBD_{20}) conjugated to a carrier peptide derived from HIV-TAT_{48-51} [176] and is a very strong and selective inhibitor in JNKs, and differs from all common chemical inhibitors, inhibiting JNK1, JNK2, and JNK3 with Ki values of 3.3 M, 430 nM and 540nM [183]. In this sense, it is a peptide that inhibits the JNK-JIP interaction (type IV JNK inhibitor) with a reported anti-apoptotic effect in cochlear neurons [198] that was also evaluated in labyrinthitis [199] and acute inflammatory bowel disease in vivo models [200]. The efficacy of intratympanic administration of this agent in the treatment of

severe idiopathic sudden sensorineural hearing loss underwent phase II (NCT00802425) and III clinical trials (EudraCT 2013-002077-21/NCT02561091 and NCT02809118) revealing promising results [201,202]. Phase I (NCT01570205) aimed to determine the safety, tolerability, and pharmacokinetics of a single intravenous infusion to treat inflammatory conditions, while the clinical efficacy of a subconjunctival injection with a sterile ophthalmic solution containing brimapitide for treatment of ocular inflammation and pain associated with cataract surgery underwent a clinical trial of phase III (NCT02508337 and NCT02235272), revealing a similar anti-inflammatory effect when compared with dexamethasone eye drops [203,204]. Figure 6 shows the mechanism of action of JNK inhibitors under clinical trials.

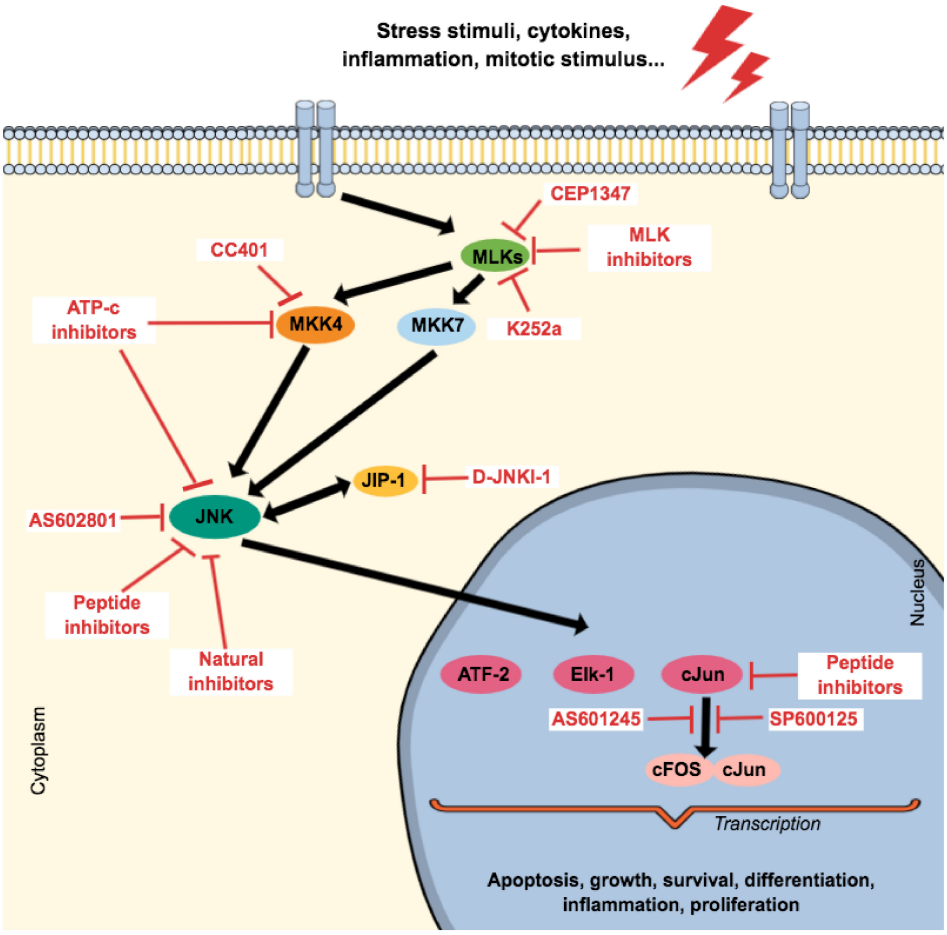

Figure 6. Schematic representation of the mechanism of action of JNK inhibitors.

The protective action in diseases of the nervous system has been tested in several experimental models, having the ability to interfere in AD, more specifically with phosphorylation of APP in cortical neurons [183,205,206]. In this sense, it may be a promising drug since it is currently under clinical trials (phase III) but has also shown improved cognitive function, reduced cell death, and pro-inflammatory markers after six months of treatment in an in vivo model of AD [207]. On the other hand, kinase inhibitors that target sites outside the ATP-binding site show low affinity and a dissociation constant (K_D) in the micro or millimolar range, and this case, the half-life is too rapid (ranging in a microsecond time scale). Additionally, β-arrestin-2, an important scaffolding protein from the JNK3 cascade in the CNS, represents the possibility of developing a specific inhibitor of JNK3 to combat neurodegenerative disorders. Considering that JNK3 is highly expressed in CNS, it is important to note that although β-arrestin-2 can bind to all JNK isoforms through the common binding motif linked to the N terminal of JNK3; it leads to its specific activation without affecting JNK1 and 2 activity. β-arrestin can also contribute to the regulation of synaptic receptors since they are important adapters that link receptors

to the clathrin-dependent pathway of internalization [183,208,209]. In addition, type V combines an ATP-competitive ligand to a secondary binding ligand. In this multi-target profile, type V inhibitors have higher potency and selectivity [210]. Molecules that form an irreversible covalent bond with the catalytic site are known as type VI inhibitors [193,211,212]. There are no types III, V, and VI JNK inhibitors under clinical trials. Figure 7 shows the main JNK3 small molecules explored so far with a promising future as therapeutic proposals for AD.

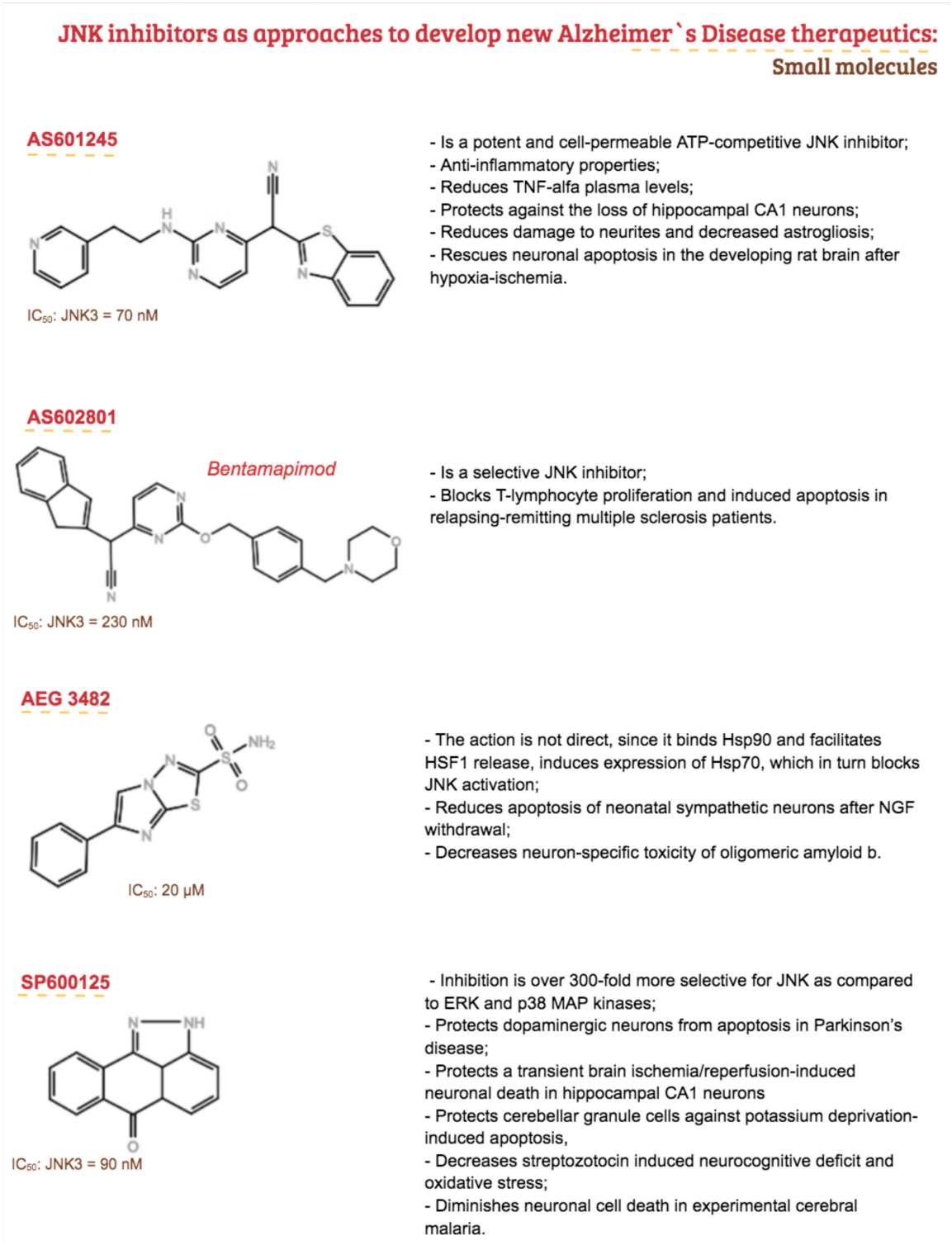

Figure 7. *Cont.*

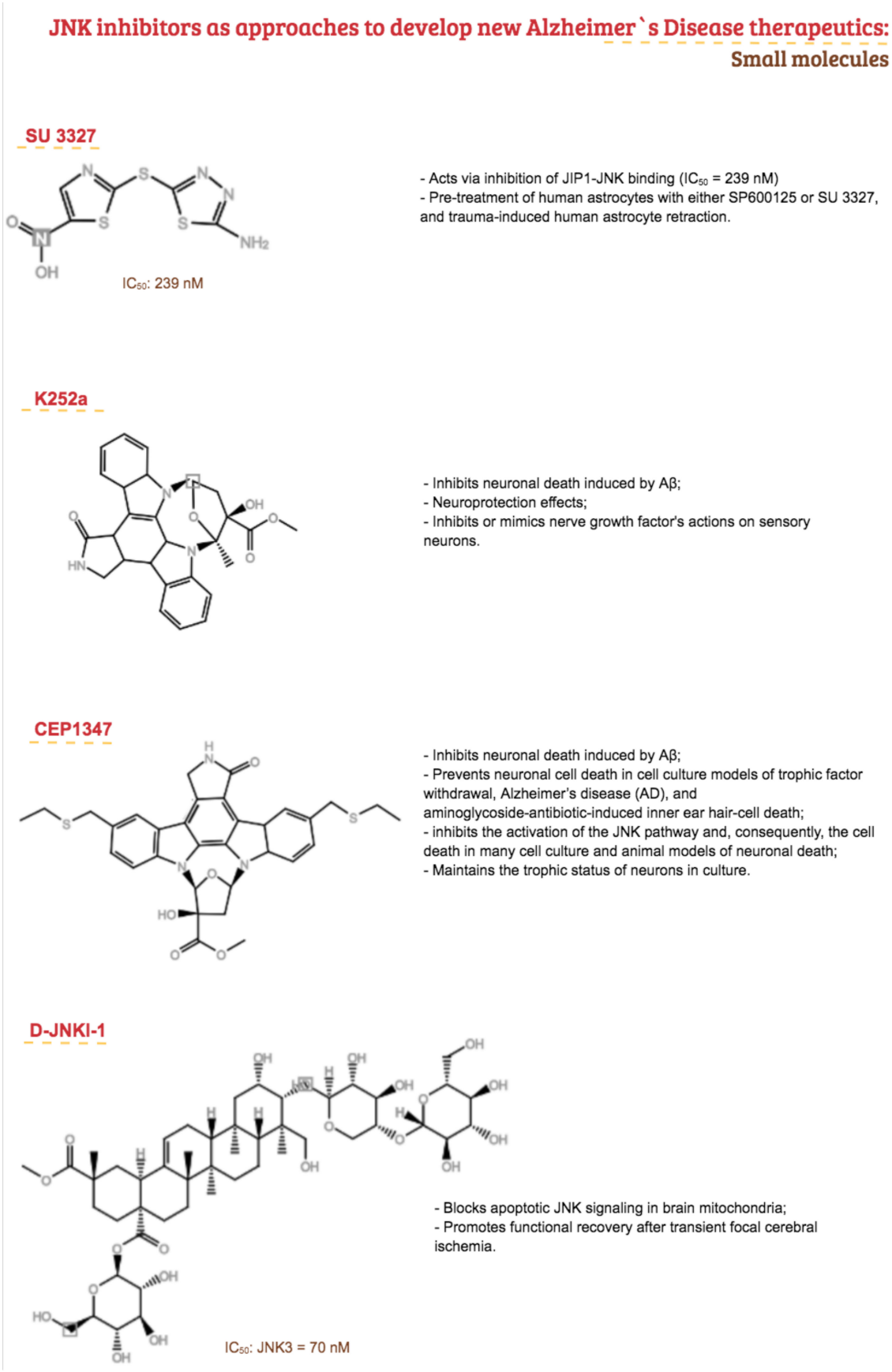

Figure 7. Summary of small molecules of JNK inhibitors used in neurological models that could be used as approaches to develop new Alzheimer's disease (AD) therapeutics [157,185–192,213–217].

4. Conclusions and Perspectives

The heterogeneity of AD, the lack of extensive knowledge about the pathophysiology of AD, and the restricted therapeutic approaches open opportunities for candidate drugs to treat AD in a more effective manner. The high failure rate of the aforementioned test drugs may be because of failing to explore the correct targets.

In this context, JNK3/p38 inhibitors represent an interesting therapeutic alternative since results from post-mortem immunohistochemical studies revealed a significant increase in pJNK and pp38 in the frontal cortex of the brains of patients with AD compared to the brains of control subjects, for example. Already, p38 activates microglia in response to neurotoxic molecules and increases the production of pro-inflammatory cytokines, but shreds of evidence suggest that JNK and p38 are important to AD's pathophysiology, and the selective p38 inhibitors might not be suitable, especially for elderly and/or anxious individuals. On the other hand, there are some examples of JNK inhibitors tested in vitro and with good results. Despite some molecules being considered not suitable for human use, these inhibitors proved useful in elucidating the role of JNK signaling in neurodegeneration. The key challenge is to improve research in this field and develop orally active molecules that can cross the BBB without generating major side effects.

Author Contributions: S.C.H.R. and F.M. drafted the manuscript and wrote the article. M.I.G. participated in its design and coordination and helped to draft the manuscript. S.C.H.R., F.M., M.I.G. and S.L. read and approved the final manuscript. All authors have read and agreed to the published version of the manuscript.

Funding: This study was funded in part by the Coordenação de Aperfeiçoamento de Pessoal de Nível Superior—Brasil (CAPES)—Finance Code 001 and Conselho Nacional de Pesquisa (CNPq) Grant number 420381/2018-0.

Acknowledgments: The authors thank Kristine Schmidt for proof-reading (language) of the manuscript.

Conflicts of Interest: The authors declare no conflict of interest. The funders had no role in the design of the study; in the collection, analyses, or interpretation of data; in the writing of the manuscript, or in the decision to publish the results

Appendix A

Table A1. Summary of brain areas and systems commonly affected in AD patients and the major consequences according to Arnold et al. (1991), Firth et al. (2019), and Bruen et al. (2008).

Affected Area/System	Major Consequence
Entorhinal cortex Hippocampus Medial temporal cortex	Memory impairments
Neocortex	Deficits in higher cognitive functions, such as language, calculation, problem-solving, and judgement
Basal forebrain cholinergic system	Contributes to memory and attention deficits
Limbic cortex Amygdala Thalamus Monoaminergic system	Behavioral and emotional disturbances

References

1. Small, D.H.; Cappai, R. Alois Alzheimer and Alzheimer's disease: A centennial perspective. *J. Neurochem.* **2006**, *99*, 708–710. [CrossRef] [PubMed]
2. Alzheimer, A. Über eine eigenartige Erkrankung der Hirnrinde. *Allgemeine Zeitschrift fur Psychiatrie und Psychisch-gerichttliche Medizin* **1907**, *64*, 146–148.

3. Nichols, E.; Szoeke, C.E.I.; Vollset, S.E.; Abbasi, N.; Abd-Allah, F.; Abdela, J.; Aichour, M.T.E.; Akinyemi, R.O.; Alahdab, F.; Asgedom, S.W.; et al. Global, regional, and national burden of Alzheimer's disease and other dementias, 1990–2016: A systematic analysis for the Global Burden of Disease Study 2016. *Lancet Neurol.* **2019**, *18*, 88–106. [CrossRef]
4. Alzheimer's Association. Alzheimer's disease facts and figures. *Alzheimer's Dementia* **2017**, *13*, 325–373. [CrossRef]
5. Alzheimer's Association. Alzheimer's Disease Facts and Figures. *Alzheimer's Dementia* **2019**, *15*, 321–387. [CrossRef]
6. Cuyvers, E.; Sleegers, K. Genetic variations underlying Alzheimer's disease: Evidence from genome-wide association studies and beyond. *Lancet Neurol.* **2016**, *15*, 857–868. [CrossRef]
7. Sims, R.; Hill, M.; Williams, J. The multiplex model of the genetics of Alzheimer's disease. *Nat. Neurosci.* **2020**, *23*, 311–322. [CrossRef]
8. Castello, M.A.; Soriano, S. On the origin of Alzheimer's disease. Trials and tribulations of the amyloid hypothesis. *Ageing Res. Rev.* **2014**, *13*, 10–12. [CrossRef]
9. Vassar, R. BACE1: The β-secreiase enzyme in Alzheimer's disease. *J. Mol. Neurosci.* **2004**, *23*, 105–113. [CrossRef]
10. Ashton, N.J.; Schöll, M.; Heurling, K.; Gkanatsiou, E.; Portelius, E.; Höglund, K.; Brinkmalm, G.; Hye, A.; Blennow, K.; Zetterberg, H. Update on biomarkers for amyloid pathology in Alzheimer's disease. *Biomark. Med.* **2018**, *12*, 799–812. [CrossRef]
11. Braak, E.V.A.; Considerations, A. Staging of Alzheimer's Disease-Related Neurofibrillary Changes. *Neurobiol. Aging* **1995**, *16*, 271–278. [CrossRef]
12. Iqbal, K.; Zaidi, T.; Wen, G.Y.; Grundke-Iqbal, I.; Merz, P.A.; Shaikh, S.S.; Wisniewski, H.M.; Alafuzoff, I.; Winblad, B. Defective brain microtubule assembly in alzheimer's disease. *Lancet* **1986**, *328*, 421–426. [CrossRef]
13. Busche, M.A.; Hyman, B.T. Synergy between amyloid-β and tau in Alzheimer's disease. *Nat. Neurosci.* **2020**, 1–11. [CrossRef]
14. Zetterberg, H.; Schott, J.M. Biomarkers for Alzheimer's disease beyond amyloid and tau. *Nat. Med.* **2019**, *25*, 201–203. [CrossRef]
15. Janelidze, S.; Stomrud, E.; Smith, R.; Palmqvist, S.; Mattsson, N.; Airey, D.C.; Proctor, N.K.; Chai, X.; Shcherbinin, S.; Sims, J.R.; et al. Cerebrospinal fluid p-tau217 performs better than p-tau181 as a biomarker of Alzheimer's disease. *Nat. Commun.* **2020**, *11*, 1–12. [CrossRef]
16. Palmqvist, S.; Janelidze, S.; Quiroz, Y.T.; Zetterberg, H.; Lopera, F.; Stomrud, E.; Su, Y.; Chen, Y.; Serrano, G.E.; Leuzy, A.; et al. Discriminative Accuracy of Plasma Phospho-tau217 for Alzheimer Disease vs. Other Neurodegenerative Disorders. *JAMA* **2020**. [CrossRef]
17. Fyfe, I. Tau species has potential for Alzheimer disease blood test. *Nat. Rev. Neurol.* **2020**, *16*, 521. [CrossRef]
18. Pillai, J.A.; Bena, J.; Bebek, G.; Bekris, L.M.; Bonner-Jackson, A.; Kou, L.; Pai, A.; Sørensen, L.; Neilsen, M.; Rao, S.M.; et al. Inflammatory pathway analytes predicting rapid cognitive decline in MCI stage of Alzheimer's disease. *Ann. Clin. Transl. Neurol.* **2020**, *7*, 1225–1239. [CrossRef]
19. Revett, T.J.; Baker, G.B.; Jhamandas, J.; Kar, S. Glutamate system, amyloid? peptides and tau protein: Functional interrelationships and relevance to Alzheimer disease pathology. *J. Psychiatry Neurosci.* **2013**, *38*, 6–23. [CrossRef]
20. Roskoski, R., Jr. A historical overview of protein kinases and their targeted small molecule inhibitors. *Pharmacol. Res.* **2015**, *100*, 1–23. [CrossRef]
21. Serrano-Pozo, A.; Qian, J.; Monsell, S.E.; Frosch, M.P.; Betensky, R.A.; Hyman, B.T. Examination of the Clinicopathologic Continuum of Alzheimer Disease in the Autopsy Cohort of the National Alzheimer Coordinating Center. *J. Neuropathol. Exp. Neurol.* **2013**, *72*, 1182–1192. [CrossRef] [PubMed]
22. Pooler, A.M.; Noble, W.; Hanger, D.P. A role for tau at the synapse in Alzheimer's disease pathogenesis. *Neuropharmacology* **2014**, *76 Pt A*, 1–8. [CrossRef] [PubMed]
23. Yarza, R.; Vela, S.; Solas, M.; Ramirez, M.J. c-Jun N-terminal Kinase (JNK) Signaling as a Therapeutic Target for Alzheimer's Disease. *Front. Pharmacol.* **2016**, *6*, 1–12. [CrossRef] [PubMed]
24. Takashima, A. Mechanism of neurodegeneration through tau and therapy for Alzheimer's disease. *J. Sport Health Sci.* **2016**, *5*, 391–392. [CrossRef]

25. Savage, M.J.; Lin, Y.; Ciallella, J.R.; Flood, D.G.; Scott, R.W. Activation of c-Jun N-Terminal Kinase and p38 in an Alzheimer's Disease Model Is Associated with Amyloid Deposition. *J. Neurosci.* **2002**, *22*, 3376–3385. [CrossRef]
26. Kondoh, K.; Nishida, E. Regulation of MAP kinases by MAP kinase phosphatases. *Biochim. Biophys. Acta Mol. Cell Res.* **2007**, *1773*, 1227–1237. [CrossRef]
27. Galeotti, N.; Ghelardini, C. Regionally selective activation and differential regulation of ERK, JNK and p38 MAP kinase signalling pathway by protein kinase C in mood modulation. *Int. J. Neuropsychopharm.* **2017**, 781–793. [CrossRef]
28. Tournier, C.; Hess, P.; Yang, D.D.; Xu, J.; Turner, T.K.; Nimnual, A.; Bar-sagi, D.; Jones, S.N.; Flavell, R.A.; Davis, R.J.; et al. Requirement of JNK for stress-induced activation of the cytochrome c-mediated death pathway. *Science* **2000**, *288*, 870–874. [CrossRef]
29. FDA. Drug Safety and Availability. Available online: https://www.fda.gov/drugs/drug-safety-and-availability (accessed on 8 July 2020).
30. Tacrine—DrugBank. Available online: https://www.drugbank.ca/drugs/DB00382 (accessed on 8 July 2020).
31. Liu, P.-P.; Xie, Y.; Meng, X.-Y.; Kang, J.-S. History and progress of hypotheses and clinical trials for Alzheimer's disease. *Signal Transduct. Target. Ther.* **2019**, *4*, 1–22. [CrossRef]
32. Parang, K.; Till, J.H.; Ablooglu, A.J.; Kohanski, R.A.; Hubbard, S.R.; Cole, P.A. Mechanism-based design of a protein kinase inhibitor. *Nat. Struct. Biol.* **2001**, *8*, 37–41. [CrossRef]
33. Modi, V.; Dunbrack, R.L. A Structurally-Validated Multiple Sequence Alignment of 497 Human Protein Kinase Domains. *Sci. Rep.* **2019**, *9*, 19790. [CrossRef] [PubMed]
34. Manning, G. The Protein Kinase Complement of the Human Genome. *Science* **2002**, *298*, 1912–1934. [CrossRef] [PubMed]
35. Pei, J.J.; Braak, E.; Braak, H.; Grundke-Iqbal, I.; Iqbal, K.; Winblad, B.; Cowburn, R.F. Localization of active forms of C-jun kinase (JNK) and p38 kinase in Alzheimer's disease brains at different stages of neurofibrillary degeneration. *J. Alzheimer's Dis.* **2001**, *3*, 41–48. [CrossRef] [PubMed]
36. Kanungo, J. DNA-PK and P38 MAPK: A Kinase Collusion in Alzheimer's Disease? *Brain Disord. Ther.* **2017**. [CrossRef]
37. Borroto-Escuela, D.O.; Tarakanov, A.O.; Guidolin, D.; Ciruela, F.; Agnati, L.F.; Fuxe, K. Moonlighting characteristics of G protein-coupled receptors: Focus on receptor heteromers and relevance for neurodegeneration. *IUBMB Life* **2011**, *63*, 463–472. [CrossRef]
38. Shi, Z.; Han, Y.; Han, X.; Zhang, K.; Chang, Y.; Hu, Z.; Qi, H. Journal of the Neurological Sciences Upstream regulators and downstream effectors of NF-κ B in Alzheimer ' s disease. *J. Neurol. Sci.* **2016**, *366*, 127–134. [CrossRef]
39. Mittal, M.; Siddiqui, M.R.; Tran, K.; Reddy, S.P.; Malik, A.B. Reactive oxygen species in inflammation and tissue injury. *Antioxid. Redox Signal.* **2014**, *20*, 1126–1167. [CrossRef]
40. Shuaib, A.; Hartwell, A.; Kiss-Toth, E.; Holcombe, M. Multi-compartmentalisation in the MAPK signalling pathway contributes to the emergence of oscillatory behaviour and to ultrasensitivity. *PLoS ONE* **2016**, *11*. [CrossRef]
41. Tian, T.; Harding, A. How MAP kinase modules function as robust, yet adaptable, circuits. *Cell Cycle* **2014**, *13*, 2379–2390. [CrossRef]
42. Mishra, P.; Günther, S. New insights into the structural dynamics of the kinase JNK3. *Sci. Rep.* **2018**, *8*, 9435. [CrossRef]
43. Rudalska, R.; Dauch, D.; Longerich, T.; McJunkin, K.; Wuestefeld, T.; Kang, T.-W.; Hohmeyer, A.; Pesic, M.; Leibold, J.; von Thun, A.; et al. In vivo RNAi screening identifies a mechanism of sorafenib resistance in liver cancer. *Nat. Med.* **2014**, *20*, 1138–1146. [CrossRef] [PubMed]
44. Coffey, E.T. Nuclear and cytosolic JNK signalling in neurons. *Nat. Rev. Neurosci.* **2014**, *15*, 285–299. [CrossRef]
45. Yue, J.; López, J.M. Understanding MAPK signaling pathways in apoptosis. *Int. J. Mol. Sci.* **2020**, *21*, 2346. [CrossRef] [PubMed]
46. Davis, R.J. Signal Transduction by the JNK Group of MAP Kinases. *Cell* **2000**, *103*, 239–252. [CrossRef]
47. Kerr, J.F.R.; Wyllie, A.H.; Currie, A.R. Apoptosis: A basic biological phenomenon with wide-ranging implications in tissue kinetics. *Br. J. Cancer* **1972**, *26*, 239–257. [CrossRef]
48. Hengartner, M.O. The biochemistry of apoptosis. *Nature* **2000**, *407*, 770–776. [CrossRef]

49. Li, H.; Zhu, H.; Xu, C.J.; Yuan, J. Cleavage of BID by caspase 8 mediates the mitochondrial damage in the Fas pathway of apoptosis. *Cell* **1998**, *94*, 491–501. [CrossRef]
50. Kale, J.; Osterlund, E.J.; Andrews, D.W. BCL-2 family proteins: Changing partners in the dance towards death. *Cell Death Differ.* **2018**, *25*, 65–80. [CrossRef]
51. Schroeter, H.; Boyd, C.S.; Ahmed, R.; Spencer, J.P.E.; Duncan, R.F.; Rice-Evans, C.; Cadenas, E. c-Jun N-terminal kinase (JNK)-mediated modulation of brain mitochondria function: New target proteins for JNK signalling in mitochondrion-dependent apoptosis. *Biochem. J.* **2003**, *372*, 359–369. [CrossRef]
52. Galluzzi, L.; Vitale, I.; Aaronson, S.A.; Abrams, J.M.; Adam, D.; Agostinis, P.; Alnemri, E.S.; Altucci, L.; Amelio, I.; Andrews, D.W.; et al. Molecular mechanisms of cell death: Recommendations of the Nomenclature Committee on Cell Death 2018. *Cell Death Differ.* **2018**, *25*, 486–541. [CrossRef]
53. Wajant, H. The Fas Signaling Pathway: More Than a Paradigm. *Science* **2002**, *296*, 1635–1636. [CrossRef] [PubMed]
54. Kim, S.; Kim, N.; Lee, J.; Kim, S.; Hong, J.; Son, S.; Do Heo, W. Dynamic Fas signaling network regulates neural stem cell proliferation and memory enhancement. *Sci. Adv.* **2020**, *6*, eaaz9691. [CrossRef] [PubMed]
55. Stavitsky, K.; Brickman, A.M.; Scarmeas, N.; Torgan, R.L.; Tang, M.-X.; Albert, M.; Brandt, J.; Blacker, D.; Stern, Y. The progression of cognition, psychiatric symptoms, and functional abilities in dementia with Lewy bodies and Alzheimer disease. *Arch. Neurol.* **2006**, *63*, 1450–1456. [CrossRef] [PubMed]
56. Reich, A.; Spering, C.; Schulz, J.B. Death receptor Fas (CD95) signaling in the central nervous system: Tuning neuroplasticity? *Trends Neurosci.* **2008**, *31*, 478–486. [CrossRef] [PubMed]
57. Schulz, E.; Wenzel, P.; Münzel, T.; Daiber, A. Mitochondrial redox signaling: Interaction of mitochondrial reactive oxygen species with other sources of oxidative stress. *Antioxid. Redox Signal.* **2014**, *20*, 308–324. [CrossRef]
58. Kandel, E.R. The molecular biology of memory: cAMP, PKA, CRE, CREB-1, CREB-2, and CPEB. *Mol. Brain.* **2012**, *5*, 1–12. [CrossRef]
59. Raman, M.; Chen, W.; Cobb, M.H. Differential regulation and properties of MAPKs. *Oncogene* **2007**, 3100–3112. [CrossRef]
60. Dhanasekaran, D.N.; Johnson, G.L. MAPKs: Function, regulation, role in cancer and therapeutic targeting. *Oncogene* **2007**, 3097–3099. [CrossRef] [PubMed]
61. Kim, E.K.; Choi, E. Biochimica et Biophysica Acta Pathological roles of MAPK signaling pathways in human diseases. *BBA Mol. Basis Dis.* **2010**, *1802*, 396–405. [CrossRef]
62. Ardito, F.; Giuliani, M.; Perrone, D.; Troiano, G.; Muzio, L.L.O. The crucial role of protein phosphorylation in cell signaling and its use as targeted therapy (Review). *Int. J. Mol. Med.* **2017**, 271–280. [CrossRef]
63. Kandel, E.R.; Dudai, Y.; Mayford, M.R. Review The Molecular and Systems Biology of Memory. *Cell* **2014**, *157*, 163–186. [CrossRef] [PubMed]
64. Cohen, P.; Alessi, D.R. Kinase Drug Discovery—What's Next in the Field? *ASC Chem. Biol.* **2014**, *8*, 96–104. [CrossRef] [PubMed]
65. Chang, L.; Karin, M. Mammalian MAP kinase signalling cascades. *Nature* **2001**, *410*, 37–40. [CrossRef]
66. Misheva, M.; Bogoyevitch, M.A. JNK Signaling: Regulation and Functions Based on Complex Protein-Protein Partnerships. *Microbiol. Mol. Biol. Rev.* **2016**, *80*, 793–835. [CrossRef]
67. Yasuda, J.U.N.; Whitmarsh, A.J.; Cavanagh, J.; Sharma, M.; Davis, R.J. The JIP Group of Mitogen-Activated Protein Kinase Scaffold Proteins. *Mol. Cell. Biol.* **1999**, *19*, 7245–7254. [CrossRef]
68. Whitmarsh, A.J. The JIP family of MAPK scaffold proteins. *Biochem. Soc. Trans.* **2006**, *34*, 828–832. [CrossRef]
69. Okazawa, H.; Estus, S. The JNK/c-Jun cascade and Alzheimer's disease. *Am. J. Alzheimer's Dis. Other Dement.* **2002**, *17*, 79–88. [CrossRef]
70. Xu, Z.; Kukekov, N.V.; Greene, L.A. POSH acts as a scaffold for a multiprotein complex that mediates JNK activation in apoptosis. *EMBO J.* **2003**, *22*, 252–261. [CrossRef]
71. Zhang, F.; Yu, J.; Yang, T.; Xu, D.; Chi, Z.; Xia, Y.; Xu, Z. A Novel c-Jun N-terminal Kinase (JNK) Signaling Complex Involved in Neuronal Migration during Brain Development. *J. Biol. Chem.* **2016**, *291*, 11466–11475. [CrossRef]
72. Zhou, X.; Li, Y.; Shi, X.; Ma, C. An overview on therapeutics attenuating amyloid β level in Alzheimer's disease: Targeting neurotransmission, inflammation, oxidative stress and enhanced cholesterol levels. *Am. J. Transl. Res.* **2016**, *8*, 246–269.

73. Kim, S.; Chin, Y.; Cho, J. Protection of Cultured Cortical Neurons by Luteolin against Oxidative Damage through Inhibition of Apoptosis and Induction of Heme. *Biol. Pharm. Bull.* **2017**, *40*, 256–265. [CrossRef] [PubMed]
74. Gupta, S.; Barrett, T.; Whitmarsh, A.J.; Cavanagh, J.; Sluss, H.K.; Dérijard, B.; Davis, R.J. Selective interaction of JNK protein kinase isoforms with transcription factors. *EMBO J.* **1996**, *15*, 2760–2770. [CrossRef] [PubMed]
75. Sluss, H.K.; Barrett, T.; Dérijard, B.; Davis, R.J. Signal transduction by tumor necrosis factor mediated by JNK protein kinases. *Mol. Cell. Biol.* **1994**, *14*, 8376–8384. [CrossRef] [PubMed]
76. Kallunki, T.; Su, B.; Tsigelny, I.; Sluss, H.K.; Derijard, B.; Moore, G.; Davis, R.; Karin, M. JNK2 Contains a Specificity-Determining Region Responsible for Efficient c-Jun Binding and Phosphorylation. *Genes Dev.* **1994**, *8*, 2996–3007. [CrossRef]
77. Ota, T.; Suzuki, Y.; Nishikawa, T.; Otsuki, T.; Sugiyama, T.; Irie, R.; Wakamatsu, A.; Hayashi, K.; Sato, H.; Nagai, K.; et al. Complete sequencing and characterization of 21,243 full-length human cDNAs. *Nat. Genet.* **2004**, *36*, 40–45. [CrossRef] [PubMed]
78. Saito, T.; Sadoshima, J. Searching and navigating UniProt databases. *Curr. Protoc. Bioinform.* **2016**, *116*, 1477–1490. [CrossRef]
79. Shoichet, S.A.; Laurence, A.E.; Ae, D.; Hagens, O.; Waetzig, V.; Corinna, A.E.; Ae, M.; Herdegen, T.; Schweiger, S.; Bernard, A.E.; et al. Original investigation Truncation of the CNS-expressed JNK3 in a patient with a severe developmental epileptic encephalopathy. *Hum. Genet.* **2006**. [CrossRef]
80. Ahmadi, S.; Khaledi, S. Anxiety in rats with bile duct ligation is associated with activation of JNK3 mitogen-activated protein kinase in the hippocampus. *Metab. Brain Dis.* **2020**. [CrossRef]
81. Haeusgen, W.; Boehm, R.; Zhao, Y.; Herdegen, T.; Waetzig, V. Neuroscience forefront review specific activities of individual c-Jun N-terminal. *NSC* **2009**, *161*, 951–959. [CrossRef]
82. Nakano, R.; Nakayama, T.; Sugiya, H. Biological Properties of JNK3 and Its Function in Neurons, Astrocytes, Pancreatic β-Cells and Cardiovascular Cells. *Cells* **2020**, *9*, 1802. [CrossRef]
83. Mohit, A.A.; Martin, J.H.; Miller, C.A. p493F12 Kinase: A Novel MAP Kinase Expressed in a Subset of Neurons in the Human Nervous System. *Neuron* **1995**, *14*, 67–78. [CrossRef]
84. Arnold, S.E.; Hyman, B.T.; Flory, J.; Damasio, A.R.; Van Hoesen, G.W. The topographical and neuroanatomical distribution of neurofibrillary tangles and neuritic plaques in the cerebral cortex of patients with alzheimer's disease. *Cereb. Cortex* **1991**, *1*, 103–116. [CrossRef] [PubMed]
85. Firth, N.C.; Primativo, S.; Marinescu, R.-V.; Shakespeare, T.J.; Suarez-Gonzalez, A.; Lehmann, M.; Carton, A.; Ocal, D.; Pavisic, I.; Paterson, R.W.; et al. Longitudinal neuroanatomical and cognitive progression of posterior cortical atrophy. *Brain* **2019**. [CrossRef] [PubMed]
86. Bruen, P.D.; Mcgeown, W.J.; Shanks, M.F.; Venneri, A. Neuroanatomical correlates of neuropsychiatric symptoms in Alzheimer's disease. *Brain* **2008**. [CrossRef] [PubMed]
87. Killick, R.; Ribe, E.M.; Malik, B.; Hooper, C.; Fernandes, C.; Dobson, R.; Nolan, P.M.; Lourdusamy, A.; Furney, S.; Lin, K.; et al. Clusterin regulates b-amyloid toxicity via Dickkopf-1-driven induction of the wnt-PCP-JNK pathway. *Mol. Psychiatry* **2014**, 88–98. [CrossRef]
88. Neurochemistry, J.O.F. *Cell Biology and Physiology Division*; CSIR-Indian Institute of Chemical Biology: Kolkata, India, 2015; pp. 1091–1103. [CrossRef]
89. Zhu, X.; Castellani, R.J.; Takeda, A.; Nunomura, A.; Atwood, C.S.; Perry, G.; Smith, M.A. Differential activation of neuronal ERK, JNK/SAPK and p38 in Alzheimer disease: The 'two hit' hypothesis. *Mech. Ageing Dev.* **2001**, *123*, 39–46. [CrossRef]
90. Gourmaud, S.; Paquet, C.; Dumurgier, J.; Pace, C.; Bouras, C.; Gray, F.; Laplanche, J.; Meurs, E.F.; Mouton-liger, F.; Hugon, J. Increased levels of cerebrospinal fluid JNK3 associated with amyloid pathology: Links to cognitive decline. *J. Psychiatry Neurosci. JPN* **2015**, *40*, 151–161. [CrossRef] [PubMed]
91. Takahashi, R.H.; Nagao, T.; Gouras, G.K. Plaque formation and the intraneuronal accumulation of b-amyloid in Alzheimer's disease. *Pathol. Int.* **2017**, 185–193. [CrossRef]
92. Yoon, S.O.; Park, D.J.; Ryu, J.C.; Ozer, H.G.; Tep, C.; Shin, Y.J.; Lim, T.H.; Pastorino, L.; Kunwar, A.J.; Walton, J.C.; et al. Article JNK3 Perpetuates Metabolic Stress Induced by A b Peptides. *Neuron* **2012**, *75*, 824–837. [CrossRef] [PubMed]
93. Aupperle, P.M. Navigating patients and caregivers through the course of Alzheimer's disease. *J. Clin. Psychiatry* **2006**, *67*, 8–14.

94. Brokaw, D.; Piras, I.; Mastroeni, D.; Weisenberger, D.; Nolz, J.; Delvaux, E.; Serrano, G.; Beach, T.; Huentelman, M.; Coleman, P. Cell Death and Survival Pathways in Alzheimer's Disease: An Integrative Hypothesis Testing Approach Utilizing-Omic Datasets. *Neurobiol. Aging* **2020**, *95*, 15–25. [CrossRef] [PubMed]
95. Najm, R.; Zalocusky, K.A.; Zilberter, M.; Yoon, S.Y.; Hao, Y.; Koutsodendris, N.; Nelson, M.; Rao, A.; Taubes, A.; Jones, E.A.; et al. In Vivo Chimeric Alzheimer's Disease Modeling of Apolipoprotein E4 Toxicity in Human Neurons. *Cell Rep.* **2020**, *32*, 107962. [CrossRef] [PubMed]
96. Waetzig, V.; Czeloth, K.; Hidding, U.; Mielke, K.; Kanzow, M.; Brecht, S.; Goetz, M.; Lucius, R.; Herdegen, T.; Hanisch, U.R. c-Jun N-terminal kinases (JNKs) mediate pro-inflammatory actions of microglia. *GLIA* **2005**, *50*, 235–246. [CrossRef] [PubMed]
97. Hidding, U.; Mielke, K.; Waetzig, V.; Brecht, S.; Hanisch, U.; Behrens, A.; Wagner, E.; Herdegen, T. The c-Jun N-terminal kinases in cerebral microglia: Immunological functions in the brain. *Biochem. Pharmacol.* **2002**, *64*, 781–788. [CrossRef]
98. Christensen, D.P.; Ejlerskov, P.; Rasmussen, I.; Vilhardt, F. Reciprocal signals between microglia and neurons regulate α-synuclein secretion by exophagy through a neuronal cJUN-N-terminal kinase-signaling axis. *J. Neuroinflamm.* **2016**, *13*. [CrossRef] [PubMed]
99. Agarwal, D.; Sandor, C.; Volpato, V.; Caffrey, T.M.; Monzón-Sandoval, J.; Bowden, R.; Alegre-Abarrategui, J.; Wade-Martins, R.; Webber, C. A single-cell atlas of the human substantia nigra reveals cell-specific pathways associated with neurological disorders. *Nat. Commun.* **2020**, *11*, 4183. [CrossRef]
100. Fan, Z.; Brooks, D.J.; Okello, A.; Edison, P. An early and late peak in microglial activation in Alzheimer's disease trajectory. *Brain* **2017**, *140*, 792–803. [CrossRef]
101. Hamelin, L.; Lagarde, J.; Dorothée, G.; Leroy, C.; Labit, M.; Comley, R.A.; De Souza, L.C.; Corne, H.; Dauphinot, L.; Bertoux, M.; et al. Early and protective microglial activation in Alzheimer's disease: A prospective study using 18F-DPA-714 PET imaging. *Brain* **2016**, *139*, 1252–1264. [CrossRef]
102. Schiller, M.; Ben-Shaanan, T.L.; Rolls, A. Neuronal regulation of immunity: Why, how and where? *Nat. Rev. Immunol.* **2020**. [CrossRef]
103. Shi, Y.; Holtzman, D.M. Interplay between innate immunity and Alzheimer disease: APOE and TREM2 in the spotlight. *Nat. Rev. Immunol.* **2018**, *18*, 759–772. [CrossRef]
104. Kracht, L.; Borggrewe, M.; Eskandar, S.; Brouwer, N.; de Sousa, L.S.M.C.; Laman, J.D.; Scherjon, S.A.; Prins, J.R.; Kooistra, S.M.; Eggen, B.J.L. Human fetal microglia acquire homeostatic immune-sensing properties early in development. *Science* **2020**, *369*, 530–537. [CrossRef] [PubMed]
105. Perdiguero, E.G.; Klapproth, K.; Schulz, C.; Busch, K.; Azzoni, E.; Crozet, L.; Garner, H.; Trouillet, C.; De Bruijn, M.F.; Geissmann, F.; et al. Tissue-resident macrophages originate from yolk-sac-derived erythro-myeloid progenitors. *Nature* **2015**, *518*, 547–551. [CrossRef] [PubMed]
106. Keren-shaul, H.; Spinrad, A.; Weiner, A.; Colonna, M.; Schwartz, M.; Amit, I.; Keren-shaul, H.; Spinrad, A.; Weiner, A.; Matcovitch-natan, O.; et al. Article A Unique Microglia Type Associated with Restricting Development of Alzheimer's Disease. *Cell* **2017**, *169*, 1276–1290.e17. [CrossRef]
107. Maezawa, I.; Zimin, P.I.; Wulff, H.; Jin, L.W. Amyloid-? protein oligomer at low nanomolar concentrations activates microglia and induces microglial neurotoxicity. *J. Biol. Chem.* **2011**, *286*, 3693–3706. [CrossRef] [PubMed]
108. Maphis, N.; Xu, G.; Kokiko-Cochran, O.N.; Jiang, S.; Cardona, A.; Ransohoff, R.M.; Lamb, B.T.; Bhaskar, K. Reactive microglia drive tau pathology and contribute to the spreading of pathological tau in the brain. *Brain* **2015**, *138*, 1738–1755. [CrossRef] [PubMed]
109. Heneka, M.T.; Carson, M.J.; El Khoury, J. Neuroinflammation in Alzheimer's disease. *Lancet Neurol.* **2015**, *14*, 388–405. [CrossRef]
110. Subhramanyam, C.S.; Wang, C.; Hu, Q.; Dheen, S.T. Microglia-mediated neuroinflammation in neurodegenerative diseases. *Semin. Cell Dev. Biol.* **2019**, *94*, 112–120. [CrossRef]
111. Ledo, J.H.; Liebmann, T.; Zhang, R.; Chang, J.C.; Azevedo, E.P.; Wong, E.; Silva, H.M.; Troyanskaya, O.G.; Bustos, V.; Greengard, P. Presenilin 1 phosphorylation regulates amyloid-β degradation by microglia. *Mol. Psychiatry* **2020**, 1–16. [CrossRef]
112. Harry, G.J. Microglia during development and aging. *Pharmacol. Ther.* **2013**, *139*, 313–326. [CrossRef]
113. Hickman, S.E.; Allison, E.K.; El Khoury, J. Microglial dysfunction and defective β-amyloid clearance pathways in aging alzheimer's disease mice. *J. Neurosci.* **2008**, *28*, 8354–8360. [CrossRef]

114. Tang, Y.; Le, W. Differential Roles of M1 and M2 Microglia in Neurodegenerative Diseases. *Mol. Neurobiol.* **2016**, *53*, 1181–1194. [CrossRef] [PubMed]
115. Ransohoff, R.M. A polarizing question: Do M1 and M2 microglia exist. *Nat. Neurosci.* **2016**, *19*, 987–991. [CrossRef] [PubMed]
116. Lue, L.F.; Beach, T.G. Walker Alzheimer's Disease Research Using Human Microglia. *Cells* **2019**, *8*, 838. [CrossRef] [PubMed]
117. Rodríguez-Gómez, J.A.; Kavanagh, E.; Engskog-Vlachos, P.; Engskog, M.K.R.; Herrera, A.J.; Espinosa-Oliva, A.M.; Joseph, B.; Hajji, N.; Venero, J.L.; Burguillos, M.A. Microglia: Agents of the CNS Pro-Inflammatory Response. *Cells* **2020**, *9*, 1717. [CrossRef] [PubMed]
118. Li, Y.; Liu, L.; Barger, S.W.; Griffin, W.S. Interleukin-1 mediates pathological effects of microglia on tau phosphorylation and on synaptophysin synthesis in cortical neurons through a p38-MAPK pathway. *J. Neurosci.* **2003**, *23*, 1605–1611. [CrossRef]
119. Zarubin, T.; Han, J. Activation and signaling of the p38 MAP kinase pathway. *Cell Res.* **2005**, *15*, 11–18. [CrossRef]
120. Enslen, H.; Brancho, D.M.; Davis, R.J. Molecular determinants that mediate selective activation of p38 MAP kinase isoforms. *EMBO J.* **2000**, *19*, 1301–1311. [CrossRef]
121. Sun, A.; Liu, M.; Nguyen, X.V.; Bing, G. p38 MAP kinase is activated at early stages in Alzheimer's disease brain. *Exp. Neurol.* **2003**, *183*, 394–405. [CrossRef]
122. Hensley, K.; Floyd, R.A.; Zheng, N.Y.; Nael, R.; Robinson, K.A.; Nguyen, X.; Pye, Q.N.; Stewart, C.A.; Geddes, J.; Markesbery, W.R.; et al. p38 Kinase is activated in the Alzheimer's disease brain. *J. Neurochem.* **1999**, *72*, 2053–2058. [CrossRef]
123. Zhu, X.; Rottkamp, C.A.; Boux, H.; Takeda, A.; Perry, G.; Smith, M.A. Activation of p38 kinase links tau phosphorylation, oxidative stress, and cell cycle-related events in Alzheimer disease. *J. Neuropathol. Exp. Neurol.* **2000**, *59*, 880–888. [CrossRef]
124. Ugbode, C.; Fort-Aznar, L.; Evans, G.; Chawla, S.; Sweeney, S. JNK Signalling Mediates Context-Dependent Responses to Reactive Oxygen Species in Neurons. *SSRN Electron. J.* **2019**. [CrossRef]
125. Kheiri, G.; Dolatshahi, M.; Rahmani, F.; Rezaei, N. Role of p38/MAPKs in Alzheimer's disease: Implications for amyloid beta toxicity targeted therapy. *Rev. Neurosci.* **2019**, *30*, 9–30. [CrossRef] [PubMed]
126. Chen, R.W.; Qin, Z.H.; Ren, M.; Kanai, H.; Chalecka-Franaszek, E.; Leeds, P.; Chuang, D.M. Regulation of c-Jun N-terminal kinase, p38 kinase and AP-1 DNA binding in cultured brain neurons: Roles in glutamate excitotoxicity and lithium neuroprotection. *J. Neurochem.* **2003**, *84*, 566–575. [CrossRef] [PubMed]
127. Yang, X.; Zhang, H.; Wu, J.; Yin, L.; Yan, L.-J.; Zhang, C. Humanin Attenuates NMDA-Induced Excitotoxicity by Inhibiting ROS-dependent JNK/p38 MAPK Pathway. *Int. J. Mol. Sci.* **2018**, *19*, 2982. [CrossRef]
128. Gee, M.S.; Kim, S.W.; Kim, N.; Lee, S.J.; Oh, M.S.; Jin, H.K.; Bae, J.S.; Inn, K.S.; Kim, N.J.; Lee, J.K. A Novel and Selective p38 Mitogen-Activated Protein Kinase Inhibitor Attenuates LPS-Induced Neuroinflammation in BV2 Microglia and a Mouse Model. *Neurochem. Res.* **2018**, *43*, 2362–2371. [CrossRef]
129. Gee, M.S.; Son, S.H.; Jeon, S.H.; Do, J.; Kim, N.; Ju, Y.J.; Lee, S.J.; Chung, E.K.; Inn, K.S.; Kim, N.J.; et al. A selective p38α/β MAPK inhibitor alleviates neuropathology and cognitive impairment, and modulates microglia function in 5XFAD mouse. *Alzheimer's Res. Ther.* **2020**, *12*. [CrossRef]
130. Munoz, L.; Ammit, A.J. Targeting p38 MAPK pathway for the treatment of Alzheimer's disease. *Neuropharmacol.* **2010**, *58*, 561–568. [CrossRef]
131. Dafsari, F.S.; Jessen, F. Depression—An underrecognized target for prevention of dementia in Alzheimer's disease. *Transl. Psychiatry* **2020**, *10*, 1–13. [CrossRef]
132. Snowden, M.B.; Atkins, D.C.; Steinman, L.E.; Bell, J.F.; Bryant, L.L.; Copeland, C.; Fitzpatrick, A.L. Longitudinal association of dementia and depression. *Am. J. Geriatr. Psychiatry* **2015**, *23*, 897–905. [CrossRef]
133. Lim, G.Y.; Tam, W.W.; Lu, Y.; Ho, C.S.; Zhang, M.W.; Ho, R.C. Prevalence of Depression in the Community from 30 Countries between 1994 and 2014. *Sci. Rep.* **2018**, *8*, 1–10. [CrossRef]
134. Zhu, C.B.; Blakely, R.D.; Hewlett, W.A. The proinflammatory cytokines interleukin-1beta and tumor necrosis factor-alpha activate serotonin transporters. *Neuropsychopharmacology* **2006**, *31*, 2121–2131. [CrossRef] [PubMed]
135. Zhu, C.B.; Lindler, K.M.; Owens, A.W.; Daws, L.C.; Blakely, R.D.; Hewlett, W.A. Interleukin-1 receptor activation by systemic lipopolysaccharide induces behavioral despair linked to MAPK regulation of CNS serotonin transporters. *Neuropsychopharmacology* **2010**, *35*, 2510–2520. [CrossRef] [PubMed]

136. Stefanoska, K.; Bertz, J.; Volkerling, A.M.; van der Hoven, J.; Ittner, L.M.; Ittner, A. Neuronal MAP kinase p38α inhibits c-Jun N-terminal kinase to modulate anxiety-related behaviour. *Sci. Rep.* **2018**, *8*, 1–12. [CrossRef] [PubMed]
137. Hanks, S.; Quinn, A.; Hunter, T. The protein kinase family: Conserved features and deduced phylogeny of the catalytic domains. *Science* **1988**, *241*, 42–52. [CrossRef] [PubMed]
138. McClendon, C.L.; Kornev, A.P.; Gilson, M.K.; Taylor, S.S. Dynamic architecture of a protein kinase. *Proc. Natl. Acad. Sci. USA* **2014**, *111*, E4623–E4631. [CrossRef] [PubMed]
139. Zuccotto, F.; Ardini, E.; Casale, E.; Angiolini, M. Through the "Gatekeeper Door": Exploiting the Active Kinase Conformation. *J. Med. Chem.* **2010**, *53*, 2681–2694. [CrossRef] [PubMed]
140. Treiber, D.K.; Shah, N.P. Ins and Outs of Kinase DFG Motifs. *Chem. Biol.* **2013**, *20*, 745–746. [CrossRef] [PubMed]
141. Xie, X.; Gu, Y.; Fox, T.; Coll, J.T.; Fleming, M.A.; Markland, W.; Caron, P.R.; Wilson, K.P.; Su, M.S. Crystal structure of JNK3: A kinase implicated in neuronal apoptosis. *Structure* **1998**, *6*, 983–991. [CrossRef]
142. Scapin, G.; Patel, S.B.; Lisnock, J.M.; Becker, J.W.; LoGrasso, P.V. The structure of JNK3 in complex with small molecule inhibitors: Structural basis for potency and selectivity. *Chem. Biol.* **2003**, *10*, 705–712. [CrossRef]
143. Macalino, S.J.Y.; Gosu, V.; Hong, S.; Choi, S. Role of computer-aided drug design in modern drug discovery. *Arch. Pharm. Res.* **2015**, *38*, 1686–1701. [CrossRef]
144. Park, H.J.; Iqbal, S.; Hernandez, P.; Mora, R.; Zheng, K.; Feng, Y.; LoGrasso, P. Structural basis and biological consequences for JNK2/3 isoform selective aminopyrazoles. *Sci. Rep.* **2015**, *5*, 8047. [CrossRef] [PubMed]
145. Probst, G.D.; Bowers, S.; Sealy, J.M.; Truong, A.P.; Hom, R.K.; Galemmo, R.A.; Konradi, A.W.; Sham, H.L.; Quincy, D.A.; Pan, H.; et al. Highly selective c-Jun N-terminal kinase (JNK) 2 and 3 inhibitors with in vitro CNS-like pharmacokinetic properties prevent neurodegeneration. *Bioorganic Med. Chem. Lett.* **2011**, *21*, 315–319. [CrossRef] [PubMed]
146. Hay, M.; Thomas, D.W.; Craighead, J.L.; Economides, C.; Rosenthal, J. Clinical development success rates for investigational drugs. *Nat. Biotechnol.* **2014**, *32*, 40–51. [CrossRef] [PubMed]
147. Daina, A.; Michielin, O.; Zoete, V. SwissTargetPrediction: Updated data and new features for efficient prediction of protein targets of small molecules. *Nucleic Acids Res.* **2019**, *47*, 357–364. [CrossRef]
148. Drachman, D.A.; Leavitt, J. Human memory and the cholinergic system. A relationship to aging? *Arch. Neurol.* **1974**, *30*, 113–121. [CrossRef]
149. Bowen, D.M.; Smith, C.B.; White, P.; Davison, A.N. Neurotransmitter-related enzymes and indices of hypoxia in senile dementia and other abiotrophies. *Brain* **1976**, *99*, 459–496. [CrossRef]
150. Davies, P.; Maloney, A.J.F. Selective Loss of Central Cholinergic Neurons in Alzheimer'S Disease. *Lancet* **1976**, *308*, 1403. [CrossRef]
151. Burke, J.F.; Langa, K.M.; Hayward, R.A.; Albin, R.L. Modeling test and treatment strategies for presymptomatic alzheimer disease. *PLoS ONE* **2014**, *9*, 1–20. [CrossRef]
152. Schneider, L.S.; Mangialasche, F.; Andreasen, N.; Feldman, H.; Giacobini, E.; Jones, R.; Mantua, V.; Mecocci, P.; Pani, L. Disease: An Appraisal From 1984 To 2014. *J. Intern. Med.* **2014**, *275*, 251–283. [CrossRef]
153. Fuster-Matanzo, A.; Llorens-Martin, M.; Hernandez, F.; Avila, J. Role of neuroinflammation in adult neurogenesis and Alzheimer disease: Therapeutic approaches. *Mediat. Inflamm.* **2013**, *2013*, 260925. [CrossRef]
154. Muller, F.L.; Lustgarten, M.S.; Jang, Y.; Richardson, A.; Van Remmen, H. Trends in oxidative aging theories. *Free Radic. Biol. Med.* **2007**, *43*, 477–503. [CrossRef]
155. Chilmonczyk, Z.; Bojarski, A.J.; Pilc, A.; Sylte, I. Pharmacological Reports Serotonin transporter and receptor ligands with antidepressant activity as neuroprotective and proapoptotic agents. *Pharmacol. Rep.* **2017**, *69*, 469–478. [CrossRef] [PubMed]
156. Clarke, M.; Pentz, R.; Bobyn, J.; Hayley, S. Stressor-Like Effects of c-Jun N-Terminal Kinase (JNK) Inhibition. *PLoS ONE* **2012**, *7*. [CrossRef]
157. Cicenas, J. JNK inhibitors: Is there a future? *MAP Kinase* **2015**, *4*. [CrossRef]
158. Hunot, S.; Vila, M.; Teismann, P.; Davis, R.J.; Hirsch, E.C.; Przedborski, S.; Rakic, P.; Flavell, R.A. JNK-mediated induction of cyclooxygenase 2 is required for neurodegeneration in a mouse model of Parkinson's disease. *Proc. Natl. Acad. Sci. USA* **2004**, *101*, 665–670. [CrossRef] [PubMed]

159. Mehan, S.; Meena, H.; Sharma, D.; Sankhla, R. JNK: A stress-activated protein kinase therapeutic strategies and involvement in Alzheimer's and various neurodegenerative abnormalities. *J. Mol. Neurosci.* **2011**, *43*, 376–390. [CrossRef]
160. Hirosumi, J.; Tuncman, G.; Chang, L.; Görgün, C.Z.; Uysal, K.T.; Maeda, K.; Karin, M.; Hotamisligil, G.S. A central, role for JNK in obesity and insulin resistance. *Nature* **2002**, *420*, 333–336. [CrossRef]
161. Sabio, G.; Kennedy, N.J.; Cavanagh-Kyros, J.; Jung, D.Y.; Ko, H.J.; Ong, H.; Barrett, T.; Kim, J.K.; Davis, R.J. Role of Muscle c-Jun NH2-Terminal Kinase 1 in Obesity-Induced Insulin Resistance. *Mol. Cell. Biol.* **2010**, *30*, 106–115. [CrossRef]
162. Han, Z.; Chang, L.; Yamanishi, Y.; Karin, M.; Firestein, G.S. Joint damage and inflammation in c-Jun N-terminal kinase 2 knockout mice with passive murine collagen-induced arthritis. *Arthritis Rheum.* **2002**, *46*, 818–823. [CrossRef]
163. Pelaia, G.; Cuda, G.; Vatrella, A.; Gallelli, L.; Caraglia, M.; Marra, M.; Abbruzzese, A.; Caputi, M.; Maselli, R.; Costanzo, F.S.; et al. Mitogen-activated protein kinases and asthma. *J. Cell. Physiol.* **2005**, *202*, 642–653. [CrossRef]
164. Blease, K.; Lewis, A.; Raymon, H.K. Emerging treatments for asthma. *Expert Opin. Emerg. Drugs* **2003**, *8*, 71–81. [CrossRef] [PubMed]
165. Chialda, L.; Zhang, M.; Brune, K.; Pahl, A. Inhibitors of mitogen-activated protein kinases differentially regulate costimulated T cell cytokine production and mouse airway eosinophilia. *Respir. Res.* **2005**, *6*, 36. [CrossRef]
166. Osto, E.; Matter, C.M.; Kouroedov, A.; Malinski, T.; Bachschmid, M.; Camici, G.G.; Kilic, U.; Stallmach, T.; Boren, J.; Iliceto, S.; et al. c-Jun N-Terminal kinase 2 deficiency protects against hypercholesterolemia-induced endothelial dysfunction and oxidative stress. *Circulation* **2008**, *118*, 2073–2080. [CrossRef] [PubMed]
167. Noble, M.E.M.; Endicott, J.A.; Johnson, L.N. Protein Kinase Inhibitors: Insights into Drug Design from Structure. *Science* **2004**, *303*, 1800–1805. [CrossRef] [PubMed]
168. Comess, K.M.; Sun, C.; Abad-Zapatero, C.; Goedken, E.R.; Gum, R.J.; Borhani, D.W.; Argiriadi, M.; Groebe, D.R.; Jia, Y.; Clampit, J.E.; et al. Discovery and Characterization of Non-ATP Site Inhibitors of the Mitogen Activated Protein (MAP) Kinases. *ACS Chem. Biol.* **2011**, *6*, 234–244. [CrossRef] [PubMed]
169. Liu, Y.; Gray, N.S. Rational design of inhibitors that bind to inactive kinase conformations. *Nat. Chem. Biol.* **2006**, *2*, 358–364. [CrossRef] [PubMed]
170. Roskoski, R. Classification of small molecule protein kinase inhibitors based upon the structures of their drug-enzyme complexes. *Pharmacol. Res.* **2016**, *103*, 26–48. [CrossRef]
171. Huang, D.; Zhou, T.; Lafleur, K.; Nevado, C.; Caflisch, A. Kinase selectivity potential for inhibitors targeting the ATP binding site: A network analysis. *Bioinformatics* **2010**, *26*, 198–204. [CrossRef]
172. Kufareva, I.; Abagyan, R. Type-II Kinase Inhibitor Docking, Screening, and Profiling Using Modified Structures of Active Kinase States. *J. Med. Chem.* **2008**, *51*, 7921–7932. [CrossRef]
173. Zhao, Z.; Wu, H.; Wang, L.; Liu, Y.; Knapp, S.; Liu, Q.; Gray, N.S. Exploration of Type II Binding Mode: A Privileged Approach for Kinase Inhibitor Focused Drug Discovery? *ACS Chem. Biol.* **2014**, *9*, 1230–1241. [CrossRef]
174. LoGrasso, P.; Kamenecka, T. Inhibitors of c-jun-N-Terminal Kinase (JNK). *Mini-Rev. Med. Chem.* **2008**, *8*, 755–766. [CrossRef] [PubMed]
175. Bain, J.; Plater, L.; Elliott, M.; Shpiro, N.; Hastie, C.J.; McLauchlan, H.; Klevernic, I.; Arthur, J.S.C.; Alessi, D.R.; Cohen, P. The selectivity of protein kinase inhibitors: A further update. *Biochem. J.* **2007**, *408*, 297–315. [CrossRef] [PubMed]
176. Bonny, C.; Oberson, A.; Negri, S.; Sauser, C.; Schorderet, D.F. Cell-Permeable Peptide Inhibitors of JNK: Novel Blockers of -Cell Death. *Diabetes* **2001**, *50*, 77–82. [CrossRef] [PubMed]
177. Krenitsky, V.P.; Nadolny, L.; Delgado, M.; Ayala, L.; Clareen, S.S.; Hilgraf, R.; Albers, R.; Hegde, S.; D'Sidocky, N.; Sapienza, J.; et al. Discovery of CC-930, an orally active anti-fibrotic JNK inhibitor. *Bioorg. Med. Chem. Lett.* **2012**, *22*, 1433–1438. [CrossRef]
178. Atsriku, C.; Hoffmann, M.; Ye, Y.; Kumar, G.; Surapaneni, S. Metabolism and disposition of a potent and selective JNK inhibitor [14C]tanzisertib following oral administration to rats, dogs and humans. *Xenobiotica* **2015**, *45*, 428–441. [CrossRef]
179. van der Velden, J.L.J.; Ye, Y.; Nolin, J.D.; Hoffman, S.M.; Chapman, D.G.; Lahue, K.G.; Abdalla, S.; Chen, P.; Liu, Y.; Bennett, B.; et al. JNK inhibition reduces lung remodeling and pulmonary fibrotic systemic markers. *Clin. Transl. Med.* **2016**, *5*, 36. [CrossRef]

180. Hussein, M.; Chai, D.C.; Kyama, C.M.; Mwenda, J.M.; Palmer, S.S.; Gotteland, J.-P.; D'Hooghe, T.M. c-Jun NH2-terminal kinase inhibitor bentamapimod reduces induced endometriosis in baboons: An assessor-blind placebo-controlled randomized study. *Fertil. Steril.* **2016**, *105*, 815–824.e5. [CrossRef]
181. Palmer, S.S.; Altan, M.; Denis, D.; Tos, E.G.; Gotteland, J.-P.; Osteen, K.G.; Bruner-Tran, K.L.; Nataraja, S.G. Bentamapimod (JNK Inhibitor AS602801) Induces Regression of Endometriotic Lesions in Animal Models. *Reprod. Sci.* **2016**, *23*, 11–23. [CrossRef]
182. Li, Z.; Sun, C.; Tao, S.; Osunkoya, A.O.; Arnold, R.S.; Petros, J.A.; Zu, X.; Moreno, C.S. The JNK inhibitor AS602801 Synergizes with Enzalutamide to Kill Prostate Cancer Cells In Vitro and In Vivo and Inhibit Androgen Receptor Expression. *Transl. Oncol.* **2020**, *13*, 100751. [CrossRef]
183. Antoniou, X.; Falconi, M.; Di Marino, D.; Borsello, T. JNK3 as a therapeutic target for neurodegenerative diseases. *J. Alzheimer's Dis.* **2011**, *24*, 633–642. [CrossRef]
184. Bogoyevitch, M.A.; Boehm, I.; Oakley, A.; Ketterman, A.J.; Barr, R.K. Targeting the JNK MAPK cascade for inhibition: Basic science and therapeutic potential. *Biochim. Biophys. Acta Proteins Proteom.* **2004**, *1697*, 89–101. [CrossRef] [PubMed]
185. Colombo, A.; Repici, M.; Pesaresi, M.; Santambrogio, S.; Forloni, G.; Borsello, T. The TAT-JNK inhibitor peptide interferes with beta amyloid protein stability. *Cell Death Differ.* **2007**, *14*, 1845–1848. [CrossRef] [PubMed]
186. Colombo, A.; Bastone, A.; Ploia, C.; Sclip, A.; Salmona, M.; Forloni, G.; Borsello, T. JNK regulates APP cleavage and degradation in a model of Alzheimer's disease. *Neurobiol. Dis.* **2009**, *33*, 518–525. [CrossRef]
187. Gourmaud, S.; Thomas, P.; Thomasseau, S.; Tible, M.; Abadie, C.; Paquet, C.; Hugon, J. Brimapitide Reduced Neuronal Stress Markers and Cognitive Deficits in 5XFAD Transgenic Mice. *J. Alzheimer's Dis.* **2018**, *63*, 665–674. [CrossRef] [PubMed]
188. Guo, C.; Whitmarsh, A.J. The β-arrestin-2 scaffold protein promotes c-Jun N-terminal kinase-3 activation by binding to its nonconserved N terminus. *J. Biol. Chem.* **2008**, *283*, 15903–15911. [CrossRef]
189. Shenoy, S.K.; Lefkowitz, R.J. Seven-transmembrane receptor signaling through beta-arrestin. *Sci. Signal.* **2005**, *2005*, cm10. [CrossRef]
190. Gower, C.M.; Chang, M.E.K.; Maly, D.J. Bivalent inhibitors of protein kinases. *Crit. Rev. Biochem. Mol. Biol.* **2014**, *49*, 102–115. [CrossRef]
191. Muth, F.; El-gokha, A.; Ansideri, F.; Eitel, M.; Doering, E.; Sievers, A.; Lange, A.; Boeckler, F.M.; Lämmerhofer, M.; Koch, P.; et al. Tri- and Tetra-substituted Pyridinylimidazoles as Covalent Inhibitors of c-Jun N-Terminal Kinase 3 Tri- and Tetra-substituted Pyridinylimidazoles as Covalent Inhibitors of c-Jun N-Terminal Kinase 3. *J. Med. Chem.* **2016**, *60*, 594–607. [CrossRef]
192. Zhang, T.; Inesta-Vaquera, F.; Niepel, M.; Zhang, J.; Ficarro, S.B.; Machleidt, T.; Xie, T.; Marto, J.A.; Kim, N.; Sim, T.; et al. Discovery of Potent and Selective Covalent Inhibitors of JNK. *Chem. Biol.* **2012**, *19*, 140–154. [CrossRef]
193. Guan, Q.; Pei, D.; Liu, X.; Wang, X.; Xu, T.; Zhang, G. Neuroprotection against ischemic brain injury by SP600125 via suppressing the extrinsic and intrinsic pathways of apoptosis. *Brain Res.* **2006**, *92*. [CrossRef]
194. Bogoyevitch, M.A.; Ngoei, K.R.W.; Zhao, T.T.; Yeap, Y.Y.C.; Ng, D.C.H. Biochimica et Biophysica Acta c-Jun N-terminal kinase (JNK) signaling: Recent advances and challenges. *BBA Proteins Proteom.* **2010**, *1804*, 463–475. [CrossRef]
195. Guan, Q.; Pei, D.; Zhang, Q.; Hao, Z. The neuroprotective action of SP600125, a new inhibitor of JNK, on transient brain ischemia/reperfusion-induced neuronal death in rat hippocampal CA1 via nuclear and non-nuclear pathways. *Brain Res.* **2005**, *1035*, 51–59. [CrossRef] [PubMed]
196. Wang, W.; Shi, L.; Xie, Y.; Ma, C.; Li, W.; Su, X.; Huang, S.; Chen, R.; Zhu, Z.; Mao, Z.; et al. SP600125, a new JNK inhibitor, protects dopaminergic neurons in the MPTP model of Parkinson's disease. *Neurosci. Res.* **2004**, *48*, 195–202. [CrossRef] [PubMed]
197. Mu, F.; Haas, E.; Schwenzer, R.; Schubert, G.; Grell, M.; Smith, C.; Scheurich, P.; Wajant, H. TRAIL/Apo2L Activates c-Jun NH_2-terminal Kinase (JNK) via Caspase-dependent and Caspase-independent Pathways. *J. Biol. Chem.* **1998**, *273*, 33091–33098.
198. Prause, M.; Adrian, L.; Ibarra, A.; Hyldgaard, M.; Billestrup, N.; Mandrup-poulsen, T.; Størling, J. Molecular and Cellular Endocrinology TRAF2 mediates JNK and STAT3 activation in response to IL-1 b and IFN g and facilitates apoptotic death of insulin-producing b-cells. *Mol. Cell. Endocrinol.* **2016**, *420*, 24–36. [CrossRef] [PubMed]

199. Tan, Y.; Dourdin, N.; Wu, C.; Veyra, T.; De Elce, J.S.; Greer, P.A. Ubiquitous Calpains Promote Caspase-12 and JNK Activation during Endoplasmic Reticulum Stress-induced Apoptosis. *J. Biol. Chem.* **2006**, *281*, 16016–16024. [CrossRef]
200. Choi, W.; Yoon, S.; Oh, T.H.; Choi, E.; Malley, K.L.O. Two Distinct Mechanisms Are Involved in 6-Hydroxydopamine- and MPP-Induced Dopaminergic Neuronal Cell Death: Role of Caspases, ROS, and JNK. *J. Neurosci. Res.* **1999**, *94*, 86–94. [CrossRef]
201. Martinez, R.; Defnet, A.; Shapiro, P. Avoiding or Co-Opting ATP Inhibition: Overview of Type III, IV, V, and VI Kinase Inhibitors. In *Next Generation Kinase Inhibitors*; Springer International Publishing: Berlin/Heidelberg, Germany, 2020; pp. 29–59.
202. Vagnoni, A.; Glennon, E.B.C.; Perkinton, M.S.; Gray, E.H.; Noble, W.; Miller, C.C.J. Loss of c-Jun N-terminal kinase-interacting protein-1 does not affect axonal transport of the amyloid precursor protein or Aβ production. *Hum. Mol. Genet.* **2013**, *22*, 4646–4652. [CrossRef]
203. Matsuda, S.; Yasukawa, T.; Homma, Y.; Ito, Y.; Niikura, T.; Hiraki, T.; Hirai, S.; Ohno, S.; Kita, Y.; Kawasumi, M.; et al. c-Jun N-terminal kinase (JNK)-interacting protein-1b/islet-brain-1 scaffolds Alzheimer's amyloid precursor protein with JNK. *J. Neurosci.* **2001**, *21*, 6597–6607. [CrossRef]
204. Harding, T.C.; Xue, L.; Bienemann, A.; Haywood, D.; Dickens, M.; Tolkovsky, A.M.; Uney, J.B. Inhibition of JNK by Overexpression of the JNK Binding Domain of JIP-1 Prevents Apoptosis in Sympathetic Neurons. *J. Biol. Chem.* **2001**, *276*, 4531–4534. [CrossRef]
205. Morel, C.; Sherrin, T.; Kennedy, N.J.; Forest, K.H.; Barutcu, S.A.; Robles, M.; Carpenter-Hyland, E.; Alfulaij, N.; Standen, C.L.; Nichols, R.A.; et al. JIP1-mediated JNK activation negatively regulates synaptic plasticity and spatial memory. *J. Neurosci.* **2018**, *38*, 3708–3728. [CrossRef] [PubMed]
206. Omotehara, Y.; Hakuba, N.; Hato, N.; Okada, M.; Gyo, K. Protection against ischemic cochlear damage by intratympanic administration of AM-111. *Otol. Neurotol.* **2011**, *32*, 1422–1427. [CrossRef] [PubMed]
207. Barkdull, G.C.; Hondarrague, Y.; Meyer, T.; Harris, J.P.; Keithley, E.M. AM-111 reduces hearing loss in a guinea pig model of acute labyrinthitis. *Laryngoscope* **2007**, *117*, 2174–2182. [CrossRef] [PubMed]
208. Reinecke, K.; Eminel, S.; Dierck, F.; Roessner, W.; Kersting, S.; Chromik, A.M.; Gavrilova, O.; Laukevicience, A.; Leuschner, I.; Waetzig, V.; et al. The JNK inhibitor XG-102 protects against TNBS-induced colitis. *PLoS ONE* **2012**, *7*, e30985. [CrossRef] [PubMed]
209. Suckfuell, M.; Lisowska, G.; Domka, W.; Kabacinska, A.; Morawski, K.; Bodlaj, R.; Klimak, P.; Kostrica, R.; Meyer, T. Efficacy and safety of AM-111 in the treatment of acute sensorineural hearing loss: A double-blind, randomized, placebo-controlled phase II study. *Otol. Neurotol.* **2014**, *35*, 1317–1326. [CrossRef] [PubMed]
210. Staecker, H.; Jokovic, G.; Karpishchenko, S.; Kienle-Gogolok, A.; Krzyzaniak, A.; Lin, C.-D.; Navratil, P.; Tzvetkov, V.; Wright, N.; Meyer, T. Efficacy and Safety of AM-111 in the Treatment of Acute Unilateral Sudden Deafness—A Double-blind, Randomized, Placebo-controlled Phase 3 Study. *Otol. Neurotol.* **2019**, *40*, 584–594. [CrossRef]
211. Beydoun, T.; Deloche, C.; Perino, J.; Kirwan, B.-A.; Combette, J.-M.; Behar-Cohen, F. Subconjunctival Injection of XG-102, a JNK Inhibitor Peptide, in Patients with Intraocular Inflammation: A Safety and Tolerability Study. *J. Ocul. Pharmacol. Ther.* **2015**, *31*, 93–99. [CrossRef]
212. Chiquet, C.; Aptel, F.; Creuzot-Garcher, C.; Berrod, J.-P.; Kodjikian, L.; Massin, P.; Deloche, C.; Perino, J.; Kirwan, B.-A.; de Brouwer, S.; et al. Postoperative Ocular Inflammation: A Single Subconjunctival Injection of XG-102 Compared to Dexamethasone Drops in a Randomized Trial. *Am. J. Ophthalmol.* **2017**, *174*, 76–84. [CrossRef]
213. Zhao, Y.; Spigolon, G.; Bonny, C.; Culman, J.; Vercelli, A.; Herdegen, T. The JNK inhibitor D-JNKI-1 blocks apoptotic JNK signaling in brain mitochondria. *Mol. Cell Neurosci.* **2012**, *49*, 300–310. [CrossRef]
214. Esneault, E.; Castagne, V.; Moser, P.; Bonny, C.; Bernaudin, M. D-JNKi, a peptide inhibitor of c-Jun N-terminal kinase, promotes functional recovery after transient focal cerebral ischemia in rats. *Neuroscience* **2008**, *152*, 308–320. [CrossRef]
215. Wang, L.H.; Besirli, C.G.; Johnson, E.M., Jr. Mixed-lineage kinases: A target for the prevention of neurodegeneration. *Annu. Rev. Pharmacol. Toxicol.* **2004**, *44*, 451–474. [CrossRef] [PubMed]
216. Ylikoski, J.; Xing-Qun, L.; Virkkala, J.; Pirvola, U. Blockade of c-Jun N-terminal kinase pathway attenuates gentamicin-induced cochlear and vestibular hair cell death. *Heart Res.* **2002**, *163*, 71–81. [CrossRef]

217. Buck, H.; Winter, J. K252a modulates the expression of nerve growth factor-dependent capsaicin sensitivity and substance P levels in cultured adult rat dorsal root ganglion neurones. *J. Neurochem.* **1996**, *67*, 345–351. [CrossRef] [PubMed]

Capítulo III

Diferenciação celular em células de neuroblastoma SH-SY5Y.

Diferenciação celular

A linhagem celular de neuroblastoma humano SH-SY5Y é um modelo experimental *in vitro* amplamente utilizado. São caracterizadas morfologicamente por corpos celulares semelhantes a neuroblastos, não polarizados, com poucos processos truncados. As células tendem a crescer em aglomerados e podem formar aglomerados celulares à medida que as células parecem crescer umas sobre as outras (Figura 14).

Figura 14. Células SH-SY5Y não diferenciadas.

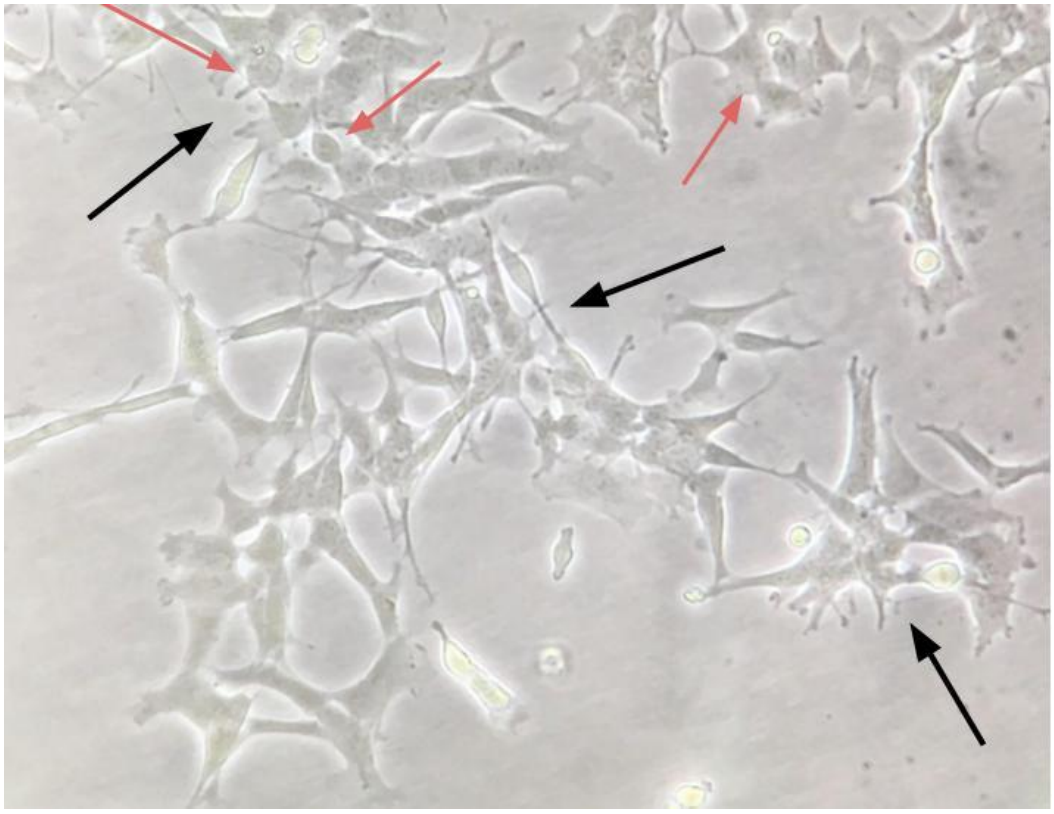

As células tendem a crescer em aglomerados (seta preta) e podem formar grupos de células arredondadas umas sobre as outras (seta vermelha). Fonte: da autora (2021).

As células SH-SY5Y não diferenciadas proliferam continuamente, expressam marcadores neuronais imaturos e não possuem marcadores neuronais maduros (PÅHLMAN et al., 1984). As células indiferenciadas são consideradas as que mais assemelham-se aos neurônios catecolaminérgicos imaturos (LOPES, et al., 2010; XIE; HU; LI, 2010). Apesar das células SH-SY5Y diferenciadas e não-diferenciadas terem sido usadas em modelos experimentais, autores sugerem que as células devem ser diferenciadas, uma vez que as células indiferenciadas são provenientes de um tumor metastático e continuamente sofrem divisão, tornando difícil prever o

efeito de agentes protetores contra neurotoxinas (XIE; HU; LI, 2010). De fato, diferenças nos perfis de expressão gênica, capacidade antioxidante, síntese de neurotransmissores e outros aspectos fenotípicos foram observados entre células diferenciadas e indiferenciadas (KORECKA et al., 2013; KRISHNA et al., 2014; LUCHTMAN; SONG, 2010). Nesse sentido, células SH-SY5Y podem ser "direcionadas" para uma variedade de fenótipos neuronais maduros (colinérgicos, adrenérgicos ou dopaminérgicos), conforme as condições de cultivo (XIE; HU; LI, 2010). Um dos métodos mais comumente implementados e melhor caracterizados para indução de diferenciação em células SH-SY5Y é através da adição de RA ao meio de cultura celular. O RA é um derivado da vitamina A conhecido por inibir a proliferação celular e induzir a diferenciação celular (MELINO et al., 1997).

Normalmente, o RA é administrado a uma concentração de 10 μM por um mínimo de 3-5 dias em meio sem soro ou com baixo teor de soro para induzir a diferenciação (CHEUNG et al., 2009; SHIPLEY; MANGOLD; SZPARA, 2016; XIE; HU; LI, 2010), embora variações nas concentrações de cada componente também tenham sido relatadas. Nesse sentido, diferentemente das células não diferenciadas, as células SH-SY5Y diferenciadas tornam-se morfologicamente mais semelhantes aos neurônios primários com processos longos distribuídos aleatoriamente (neuritos). A diferenciação de células SH-SY5Y também induz uma diminuição na taxa de proliferação (PÅHLMAN et al., 1984) (Figura 15).

Figura 15. Células SH-SY5Y diferenciadas.

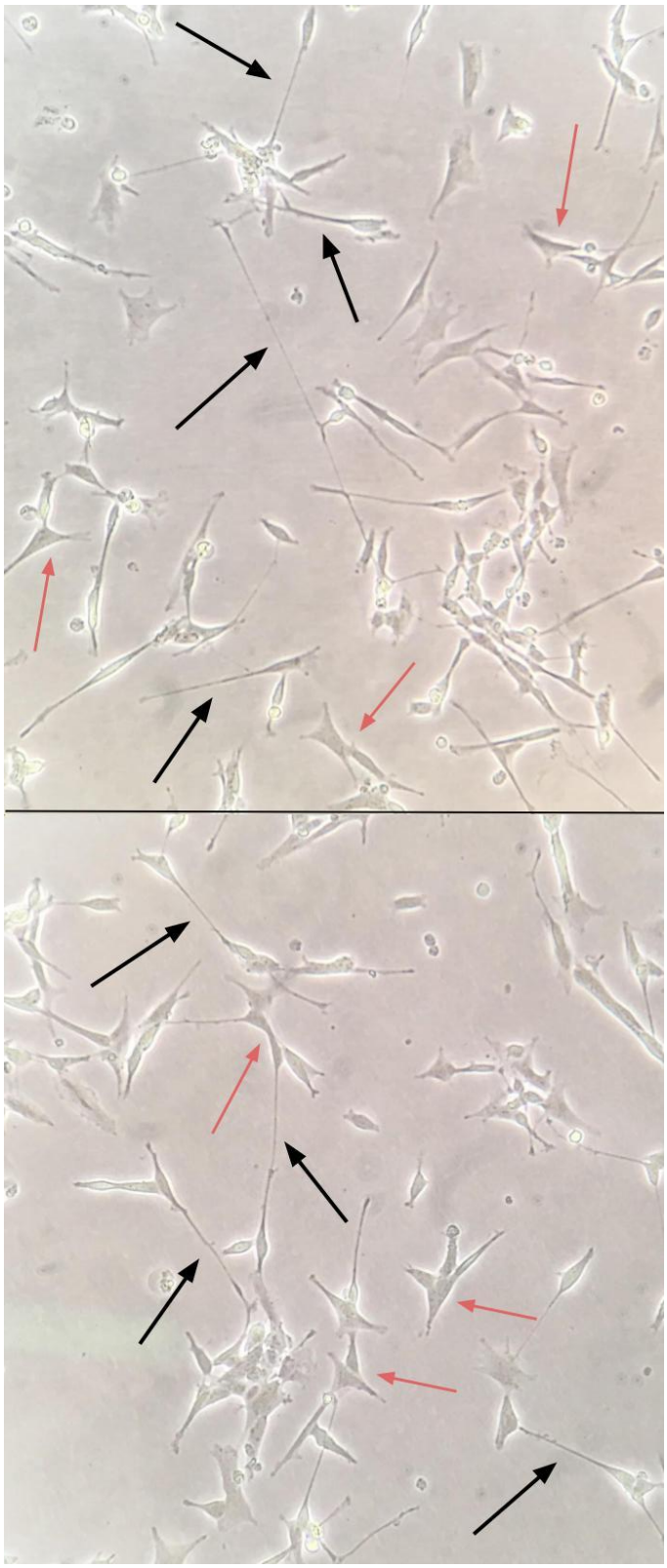

As células não se agrupam e têm um corpo celular com formato mais piramidal (seta vermelha). Neuritos começam a se estender (seta preta). Fonte: da autora (2021).

O método de diferenciação selecionado para experimentos *in vitro* deve ser determinado pelo fenótipo desejado após a diferenciação. Em resposta ao tratamento com RA, as células SH-SY5Y diferenciam-se principalmente em um fenótipo de neurônio colinérgico, conforme evidenciado pela expressão aumentada da atividade da colina-acetiltransferase (ChAT) e do transportador vesicular de monamina (VMAT) (LOPES, *et al.*, 2010; PRESGRAVES *et al.*, 2004). Após a diferenciação, observou-se um aumento na expressão de genes envolvidos com a defesa antioxidante (CHEUNG *et al.*, 2009; DE BITTENCOURT PASQUALI *et al.*, 2016; KUNZLER *et al.*, 2017; SCHNEIDER, *et al.*, 2011), além de um aumento na fosforilação oxidativa (FORSTER *et al.*, 2016). Este perfil modificado de expressão gênica reflete diretamente na capacidade das células de se recuperarem do estresse oxidativo causado pela 6-OHDA (CHEUNG *et al.*, 2009).

6-OHDA é uma toxina catecolaminérgica amplamente utilizada como modelo experimental *in vitro* da doença de Parkinson. É formada a partir da dopamina na presença de Fe^{2+} e H_2O_2 e seu principal mecanismo de neurotoxicidade depende de dois eventos principais. O primeiro depende da auto-oxidação de 6-OHDA, no qual o dano celular é resultado de ROS derivadas de 6-OHDA. De fato, 6-OHDA é rapidamente oxidada por oxigênio molecular para formar H_2O_2, ânions superóxido ($O2^{\bullet -}$) e radicais hidroxila (OH^-) (COHEN; HEIKKILA, 1974). Portanto, nos ensaios usamos a 6-OHDA como indutor de apoptose, adicionamos 0,2% de ácido ascórbico à reação para evitar a rápida auto-oxidação da 6-OHDA. Foi relatado que a presença de ácido ascórbico (AA) diminuiu o consumo de O_2 e a quantidade de H_2O_2, indicando que o AA reduziu a taxa de auto-oxidação de 6-OHDA (SOTO-OTERO *et al.*, 2000). Inclusive, é provável que um efeito semelhante ocorra *in vivo* uma vez que os antioxidantes disponíveis no tecido cerebral podem ser suficientes para prevenir a rápida oxidação de 6-OHDA. Isso fornece suporte para a teoria de que a toxicidade de 6-OHDA ocorre por um mecanismo secundário e alternativo no qual 6-OHDA promove a inibição dos complexos mitocondriais I e IV (GLINKA, Y; GASSEN; YOUDIM, 1997).

Para confirmar esta maior resistência, um controle positivo de doxorrubicina (10 μM) foi incluído. O mecanismo de ação da doxorrubicina é através do bloqueio específico da atividade da enzima topoisomerase II, que está envolvida na replicação do DNA durante a mitose e não interfere no estresse oxidativo e, portanto,

não afeta o dano causado pela 6-OHDA. A doxorrubicina é um antineoplásico da classe das antraciclinas amplamente utilizada para o tratamento de vários tumores sólidos. Ao intercalar-se com o DNA induz a quebra da dupla fita e, portanto, a morte celular. Além disso, pode inibir a enzima topoisomerase II (CHEN, X; JI; CHEN, 2002; FORNARI *et al.*, 1994).

O protocolo de diferenciação das células SH-SY5Y por meio de RA (APÊNDICE 1) mostrou-se eficaz na obtenção de células diferenciadas e fenotipicamente mais semelhantes a células neuronais maduras. Já o modelo *in vitro* de doença neurodegenerativa com células SH-SY5Y diferenciadas induzidas por 6-OHDA desenvolvido no presente estudo contribuiu adequadamente para a execução dos ensaios *in vitro* e para estudos na busca de potenciais moléculas potencias para o tratamento de doenças neurodegenerativas.

Capítulo IV

Artigo científico:

"A Highly Selective In Vitro JNK3 Inhibitor, FMU200, Restores Mitochondrial Membrane Potential and Reduces Oxidative Stress and Apoptosis in SH-SY5Y Cells"

Publicado em 2021 no periódico *International Journal of Molecular Sciences*
(Fator de Impacto: 4,556)

International Journal of
Molecular Sciences

MDPI

Article

A Highly Selective In Vitro JNK3 Inhibitor, FMU200, Restores Mitochondrial Membrane Potential and Reduces Oxidative Stress and Apoptosis in SH-SY5Y Cells

Stephanie Cristine Hepp Rehfeldt [1], Stefan Laufer [2,3,*] and Márcia Inês Goettert [1,*]

[1] Graduate Program in Biotechnology, University of Vale do Taquari (Univates), Lajeado, RS 95914-014, Brazil; srehfeldt@universo.univates.br
[2] Department of Pharmaceutical and Medicinal Chemistry, Institute of Pharmacy, Eberhard Karls Universität Tübingen, D-72076 Tübingen, Germany
[3] Tübingen Center for Academic Drug Discovery (TüCAD2), D-72076 Tübingen, Germany
* Correspondence: stefan.laufer@uni-tuebingen.de (S.L.); marcia.goettert@univates.br (M.I.G.); Tel.: +55-(51)3714-7000 (ext. 5445) (M.I.G.)

Abstract: Current treatments for neurodegenerative diseases (ND) are symptomatic and do not affect disease progression. Slowing this progression remains a crucial unmet need for patients and their families. c-Jun N-terminal kinase 3 (JNK3) are related to several ND hallmarks including apoptosis, oxidative stress, excitotoxicity, mitochondrial dysfunction, and neuroinflammation. JNK inhibitors can play an important role in addressing neuroprotection. This research aims to evaluate the neuroprotective, anti-inflammatory, and antioxidant effects of a synthetic compound (FMU200) with known JNK3 inhibitory activity in SH-SY5Y and RAW264.7 cell lines. SH-SY5Y cells were pretreated with FMU200 and cell damage was induced by 6-hydroxydopamine (6-OHDA) or hydrogen peroxide (H_2O_2). Cell viability and neuroprotective effect were assessed with an MTT assay. Flow cytometric analysis was performed to evaluate cell apoptosis. The H_2O_2-induced reactive oxygen species (ROS) generation and mitochondrial membrane potential ($\Delta\Psi m$) were evaluated by DCFDA and JC-1 assays, respectively. The anti-inflammatory effect was determined in LPS-induced RAW264.7 cells by ELISA assay. In undifferentiated SH-SY5Y cells, FMU200 decreased neurotoxicity induced by 6-OHDA in approximately 20%. In RA-differentiated cells, FMU200 diminished cell death in approximately 40% and 90% after 24 and 48 h treatment, respectively. FMU200 reduced both early and late apoptotic cells, decreased ROS levels, restored mitochondrial membrane potential, and downregulated JNK phosphorylation after H_2O_2 exposure. In LPS-stimulated RAW264.7 cells, FMU200 reduced TNF-α levels after a 3 h treatment. FMU200 protects neuroblastoma SH-SY5Y cells against 6-OHDA- and H_2O_2-induced apoptosis, which may result from suppressing the JNK pathways. Our findings show that FMU200 can be a useful candidate for the treatment of neurodegenerative disorders.

Keywords: 6-hydroxydopamine; hydrogen peroxide; apoptosis; mitochondrial membrane potential; neurodegenerative diseases; oxidative stress

Citation: Rehfeldt, S.C.H.; Laufer, S.; Goettert, M.I. A Highly Selective In Vitro JNK3 Inhibitor, FMU200, Restores Mitochondrial Membrane Potential and Reduces Oxidative Stress and Apoptosis in SH-SY5Y Cells. *Int. J. Mol. Sci.* **2021**, *22*, 3701. https://doi.org/10.3390/ijms22073701

Academic Editor: Kohji Fukunaga

Received: 9 March 2021
Accepted: 30 March 2021
Published: 2 April 2021

1. Introduction

In neurodegenerative disorders (ND), such as Alzheimer's disease (AD), it is common that neurons start degenerating during a prolonged preclinical period, where individuals are by definition asymptomatic and cognitively normal [1]. In recent years, researchers have put more effort into understanding neurodegenerative diseases and investing in patient management based on molecular approaches with potential disease-specific and/or disease-modifying treatments specifically targeting neuroprotection. Neuroprotection can be characterized as a substantial and lasting slowdown in the disease's progression associated with a delay in neuronal degeneration [2]. While a few drugs can improve the patient's quality of life, there is neither a cure nor a disease-modifying drug for treating

AD and the disease inevitably progresses, making AD fatal in all cases. According to the U.S. Food and Drug Administration (FDA) and the Alzheimer's Association, there are only five FDA-approved drugs to manage AD nowadays: donepezil, galantamine, memantine, rivastigmine, and a combination of memantine and donepezil [3] (Figure 1). The limited number of drugs and the failure of several drugs/compounds in phase III clinical trials (focused primarily on the amyloid hypothesis) [4] indicates that new targets should be explored.

In this sense, it is known that cell perturbations provoked by β-amyloid peptides (Aβ), neurofibrillary tangles, and oxidative stress, for example, can culminate in the activation of mitogen-activated protein kinase (MAPK) pathways, such as the JNK (c-Jun N-terminal kinase) pathway, best known for its involvement in propagating pro-apoptotic signals via extrinsic and intrinsic pathways [5,6]. Studies on post-mortem brain samples have shown a greater expression of phosphorylated JNK3 in AD patients in addition to the presence of (Aβ) [7], while further studies have identified JNK3 to be highly expressed and activated in brain tissue and cerebrospinal fluid in patients with AD, in addition to being statistically correlated with the level of cognitive decline [8,9].

On the other hand, mitochondria are considered the major source of reactive oxygen species (ROS) in the cell and the accumulation of ROS-associated damage in DNA, proteins, and lipids, and may cause progressive cell dysfunctions and, in consequence, apoptosis. For this reason, authors have recognized mitochondria as a critical organelle for various pathological conditions and aging. It was also shown that mitochondrial JNK signaling can impact mitochondrial physiology [10] likewise, and the culmination of oxidative stress in the mitochondria is the dissipation of mitochondrial membrane potential (MMP) and subsequent release of cytochrome c [11,12]. Therefore, the inhibition of JNK3 has been explored as a possible therapeutic target.

Kinase inhibitors are not a novel type of treatment [13,14]. This issue has been widely discussed over the last two decades and a review conducted by Koch et al. in 2015 [15] acknowledged the need for JNK isoform-specific inhibitors. The authors gave a detailed description of the available inhibitors' chemical characteristics, but also pointed out the complexity of developing new drugs. Since then, some inhibitors cited in the paper have advanced to clinical trials or showed promising results in recent animal model studies. However, other compounds did not advance as much, especially due to a lack of specificity. Recently, the role of JNK3 in Alzheimer's disease was reviewed [16]. The authors also pointed to JNK3 inhibitors explored so far with a promising future as therapeutic proposals for AD.

Although JNK3 is present in specific tissues such as the brain, heart, placenta, lung, liver, skeletal muscle, kidney, pancreas, and testis, over 500 kinases were identified in humans [17]. The structure of many MAPKs is very similar. JNK3 shares 77% and 75% amino acid sequence identity with JNK2 and JNK1, respectively. The sequence identity at the ATP-binding pocket is 98% identical between all three JNK isoforms [18]. The selectivity of JNK3 inhibitors is often pointed out to be problematic. Even though many JNK3 inhibitors are cited in the literature, most of them display very weak JNK3 selectivity and/or cannot properly inhibit the phosphorylation of JNK3 substrates [15,16,19]. In this sense, cysteine-directed covalent inhibitors possess an ability to control kinase selectivity using both non-covalent and covalent recognition of the kinase and the ability to exhibit prolonged pharmacodynamics [20]. FMU200 is a tetrasubstituted imidazole that forms a covalent bond with JNK3 described by Muth et al., 2016. This compound binds to the Cys-154 of JNK3 and shows a picomolar inhibitory effect for JNK3 and a 120-fold preference compared to the IC50 value of p38α, for example (IC50 JNK3: 0.3 nM). Within the JNK group, at 0.1 μM, FMU200 inhibits JNK1 activity by 16%, JNK2 by 73%, and JNK3 by 80%; at 0.5 μM FMU200, the residual activity of JNK1, JNK2, and JNK3 are 16%, 5% and, 4%, respectively [21]. Based on this molecule's interesting inhibitory profile, this study aimed to explore the neuroprotective, anti-inflammatory and antioxidant potential of FMU200 in an in vitro model of neurodegenerative disease.

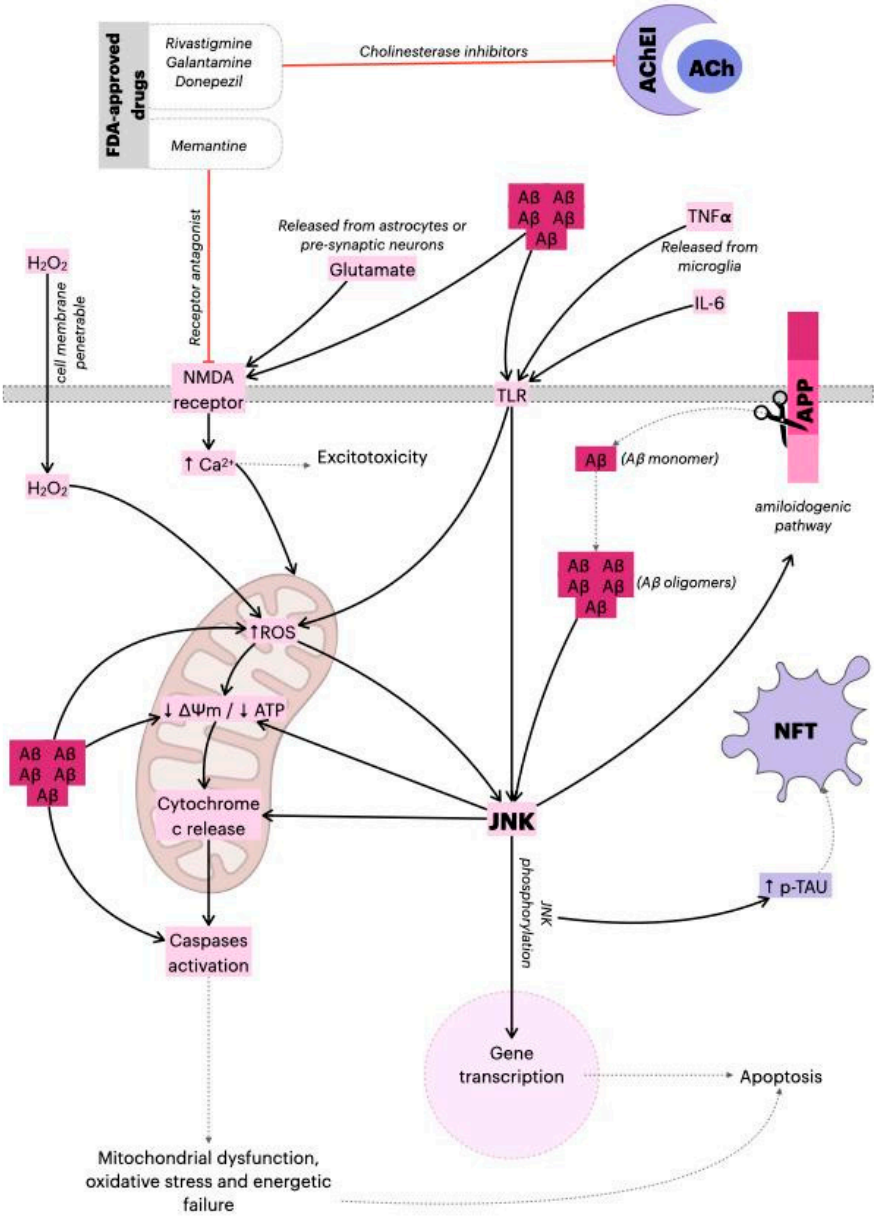

Figure 1. Mechanism of action of FDA-approved drugs and the role of JNK in AD. The Aβ monomers are generated by amyloid precursor protein (APP) cleavage, and subsequently released from neurons. The monomers sequentially assemble into Aβ oligomer aggregates, and ultimately into amyloid plaques. The Aβ oligomers can alter mitochondria function and induce ROS production, dissipation of ΔΨm, caspase-3 activation, and ATP reduction. Additionally, Aβ oligomers activate the JNK pathway, thereby aggravating synaptic dysfunction. As a result, phosphorylated JNK induces dissipation of ΔΨm, cytochrome c release, and the activation of transcription factors such as AP-1 or c-Jun, which leads to apoptosis. However, JNK directly phosphorylates Tau and induces the amyloidogenic pathway, contributing to the formation of neurofibrillary tangles (NFTs) and amyloid plaques, respectively, causing the gradual loss of cholinergic neurons in Alzheimer's disease (AD). The main pharmacological actions of donepezil, galantamine and memantine (acetylcholinesterase/cholinesterase inhibitors (AChEI)) are believed to occur as the result of acetylcholinesterase activity inhibition. By blocking breakdown of ACh, the cholinergic transmission is enhanced, and the symptoms of AD are relieved. Additionally, in response to Aβ aggregation, microglia release pro-inflammatory cytokines (TNF-α, IL-6) that activate astrocytes and induce apoptotic signals in neurons via TLR-JNK activation. The excessive activation of the NMDA receptor by glutamate results in excitotoxicity and Ca^{2+}-dependent cell death. Memantine (N-methyl-D-aspartic acid (NMDA) receptor antagonist) inhibits calcium influx into cells that is normally caused by chronic NMDA receptor activation by glutamate. This leads to the improvement of Alzheimer's dementia symptoms, demonstrated by increased cognition and other beneficial central nervous system effects [22–24]. ↓: represents decrease; ↑ represents increase.

2. Results

2.1. The Cytotoxic and Neuroprotective Effect of FMU200 in Undifferentiated and RA-Differentiated SH-SY5Y Cells

The pharmacological inhibition of the MAPK pathway is a common research method used to understand mechanisms of cellular functions and fundamental processes [25,26]. A number of pharmacological inhibitors have been developed to block MAPKs either directly or indirectly, by targeting upstream regulators. In this case, we included an p38 inhibitor (SB203580) [27] and a JNK inhibitor, SP600125 [28] in our analysis. According to previous studies, SP600125 (10 μM) was considered cytotoxic in different cell lines such as four different leukemia cell lines (U937, K562, HL60, and THP-1) [29], NphA2 cells [30], while SB203580 and SP600125 at 20 μM did not alter cell viability neither in MCF7 cells [31] nor in JEG-3 cells [32]. However, it is known that distinct cell lines respond differently to cytotoxic compounds. Among 1353 compounds tested in 13 different cell types, SH-SY5Y was classified as the second most sensitive cell line to compound-induced toxicity. Overall, SH-SY5Y cells were more sensitive to compound-induced toxicity than SK-N-SH cells, the parental cell line of the SH-SY5Y cells [33]. Since there are conflicting results whether SP600125 and SB203580 are cytotoxic or not, and due to the highly heterogeneous cellular response to both SP600125 and SB203580, we started our concentration screening with a 10 μM concentration for all three compounds (FMU200, SP600125, and SB203580).

In this case, the first set of analyses examined the impact of FMU200, SP600125 and SB203580 on cell viability. The results, as shown in Figure 2A, indicate that in SH-SY5Y cells, FMU200 at 10 μM reduced cell viability by 24.33% ($p < 0.05$). At 1 μM, FMU200 reduced cell viability by only 14.75% ($p > 0.05$). SB230580 at 10 μM reduced cell viability by 35.5% ($p < 0.001$), while SP600125 at 10μM reduced viability by 34.3% ($p < 0.001$). Since all three compounds (FMU200, SP600125, and SB203580) showed statistically significant cytotoxicity to SH-SY5Y cells at 10 μM, we did not use this concentration in further assays.

6-OHDA is a highly reactive and oxidizable molecule being rapidly and non-enzymatically oxidized by molecular oxygen to form hydrogen peroxide (H_2O_2). However, the presence of ascorbic acid (AA) decreased O_2 consumption and H_2O_2 amount indicating that AA reduced the autoxidation rate of 6-OHDA [34]. Therefore, 6-OHDA was stabilized with 0.02% AA before being added to cells.

Undifferentiated and RA-differentiated SH-SY5Y neuroblastoma cells were pretreated with 1 and 0.1 μM of FMU200 for 1 h prior to 6-OHDA exposure and incubated for 24 or 48 h. Cell viability was examined with an MTT assay. For undifferentiated cells, 6-OHDA reduced cell viability by 81.65% (after 24 h) and by 68.42% (after 48 h) when compared to control ($p < 0.001$). Similarly, when compared to control, treatment with FMU200 at both concentrations also decreased cell viability. However, if compared to the 6-OHDA group, after 24 h, FMU200 at 1 μM and 0.1 μM increased cell viability by 18.29% ($p < 0.001$) and 18.9% ($p < 0.001$), respectively (Figure 2B). After 48 h treatment, FMU200 at 1 μM and 0.1 μM increased cell viability by 17.86% and 5.92%, respectively (Figure 2C).

For RA-differentiated cells, the cells were incubated with 10 μM RA for 10 days to induce neuronal differentiation before exposure to FMU200 and 6-OHDA. After 24 h, 6-OHDA decreased cell viability by 23.84% when compared to control ($p < 0.001$). Treatment with FMU200 at 1 μM and 0.1 μM did not show any significant difference when compared to control. On the other hand, FMU200 at 1 μM increased cell viability by 37.87%, while FMU200 at 0.1 μM increased cell viability by 32.83% (when compared to 6-OHDA, $p < 0.001$) (Figure 2D). After 48 h, 6-OHDA decreased cell viability by 36.54% ($p < 0.05$) when compared to control. When compared to 6-OHDA, treatment with FMU200 at 1 μM increased cell viability by 91.04% ($p < 0.001$), while FMU200 at 0.1 μM increased cell viability by 82.54% ($p < 0.001$) (Figure 2E).

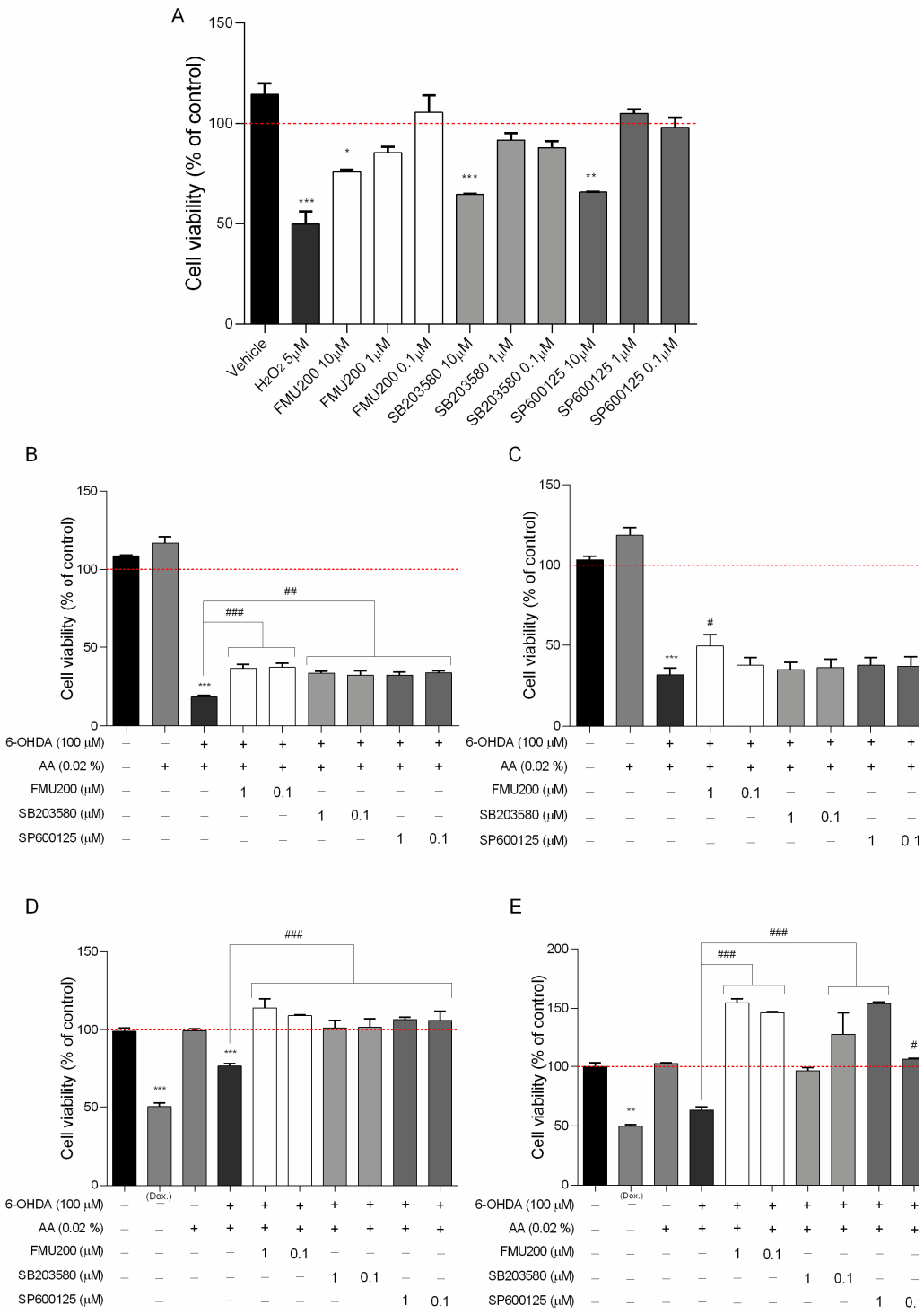

Figure 2. (**A**) Cytotoxicity induced by FMU200 on SH-SY5Y cell viability after a 24 h incubation period in SH-SY5Y cells (% of control); the neuroprotective effect of FMU200 against 6-OHDA (stabilized with 0.02% of ascorbic acid) induced neurotoxicity in undifferentiated SH-SY5Y cells and RA-differentiated SH-SY5Y cells. SH-SY5Y cells were pretreated with different concentrations of FMU200 for 1 h, prior to 6-OHDA exposure. Undifferentiated cells were incubated for (**B**) 24 h and (**C**) 48 h. Cells were differentiated in 10-μM retinoic acid (RA) and the effect was also evaluated in RA-differentiated cells after (**D**) 24 h and (**E**) 48 h. The results are the mean ± SEM of at least three experiments in triplicates. Statistical calculations were performed by ANOVA via the Tukey post hoc test. Statistical significance values were *** $p < 0.001$; ** $p < 0.01$; * $p < 0.05$ (vs. control); ### $p < 0.001$; ## $p < 0.01$; # $p < 0.05$ (vs. 6-OHDA). Negative control (untreated cells) was considered to be 100% viable and is represented by the red dashed line. Doxorubicin was used as positive control; DMSO 0.1% was used as vehicle.

2.2. Response to H_2O_2: Apoptosis, ROS Production and MMP

Apoptosis is an important event in neurodegeneration and flow cytometry-based apoptosis assays have proved to be especially useful as they offer an individual cell-based method of analysis. In this case, to further characterize H_2O_2-induced cell death, we performed flow cytometric analysis of SH-SY5Y cells using annexinV-PE and 7-AAD, which has been used to determine early apoptosis and necrosis/late apoptosis. Figure 3 shows the percentage of early apoptosis (FL2 positive/FL3 negative) and necrosis/late apoptosis (FL2 positive/FL3 positive) was increased in SH-SY5Y cells challenged with 10 μM of H_2O_2. Cells pretreated with FMU200 at 1 μM and 0.1 μM showed fewer annexinV-PE-positive/7-AAD-positive cells and fewer annexinV-PE-positive/7-AAD-negative cells.

Reactive oxygen species (ROS) are involved in both physiological and pathological processes and mitochondria are widely accepted as the major site for ROS formation. The mitochondrial membrane potential (ΔΨm) reflects the functional metabolic status of mitochondria. Mitochondrial dysfunction with a loss of mitochondrial membrane potential (MMP) is also a critical event in neuronal degeneration. JC-1 dye can selectively enter mitochondria and reversibly change color from red to green as the membrane potential decreases. In flow cytometric analysis of JC-1 fluorescence, healthy cells with high mitochondrial ΔΨm, JC-1 spontaneously forms complexes known as J-aggregates with intense red fluorescence. On the other hand, in apoptotic or unhealthy cells with low ΔΨm, JC-1 remains in the monomeric form, which shows only green fluorescence (Figure 4A).

However, since SH-SY5Y cells are required to be in suspension, we also determined the ΔΨm and ROS production with fluorescence microplate reader since trypsinization may induce oxidative stress [35,36]. In this case, in order to determine if the inhibitor FMU200 had an impact on JNK-mediated physiological responses, such as loss of MMP and ROS generation induced by H_2O_2, cells were treated as previously described and incubated with JC-1 dye to monitor the MMP. The samples were analyzed by detecting the red fluorescence and green fluorescence ratio. Exposure of SH-SY5Y cells to H_2O_2 decreased the ratio of red fluorescence/green fluorescence by 40.57% compared with control ($p < 0.001$). However, co-treatment with FMU200 at 1 μM and 0.1 μM increased MMP by 52.79% and 22.08%, respectively ($p < 0.001$) (Figure 4B).

The 2′-7′-Dichlorodihydrofluorescein diacetate (DCFH-DA) is one of the most widely used techniques for directly measuring the redox state of a cell. In order to determine if FMU200 could protect cells against oxidative stress caused by H_2O_2, cellular ROS formation was quantified by the DCFDA assay. Cells were pretreated with FMU200 at 1 μM and 0.1 μM prior to H_2O_2 exposure (6 h). Treatment with H_2O_2 increased ROS production by 108.9% when compared to control. However, after treatment with FMU200 at 1 μM, ROS production was decreased by 51.08%, while FMU200 at 0.1 μM decreased ROS production by 38.73%. There was no significant difference between FMU200 (1 μM), NAC (5 mM), and the control group, indicating a possible antioxidant effect of FMU200 (Figure 4C).

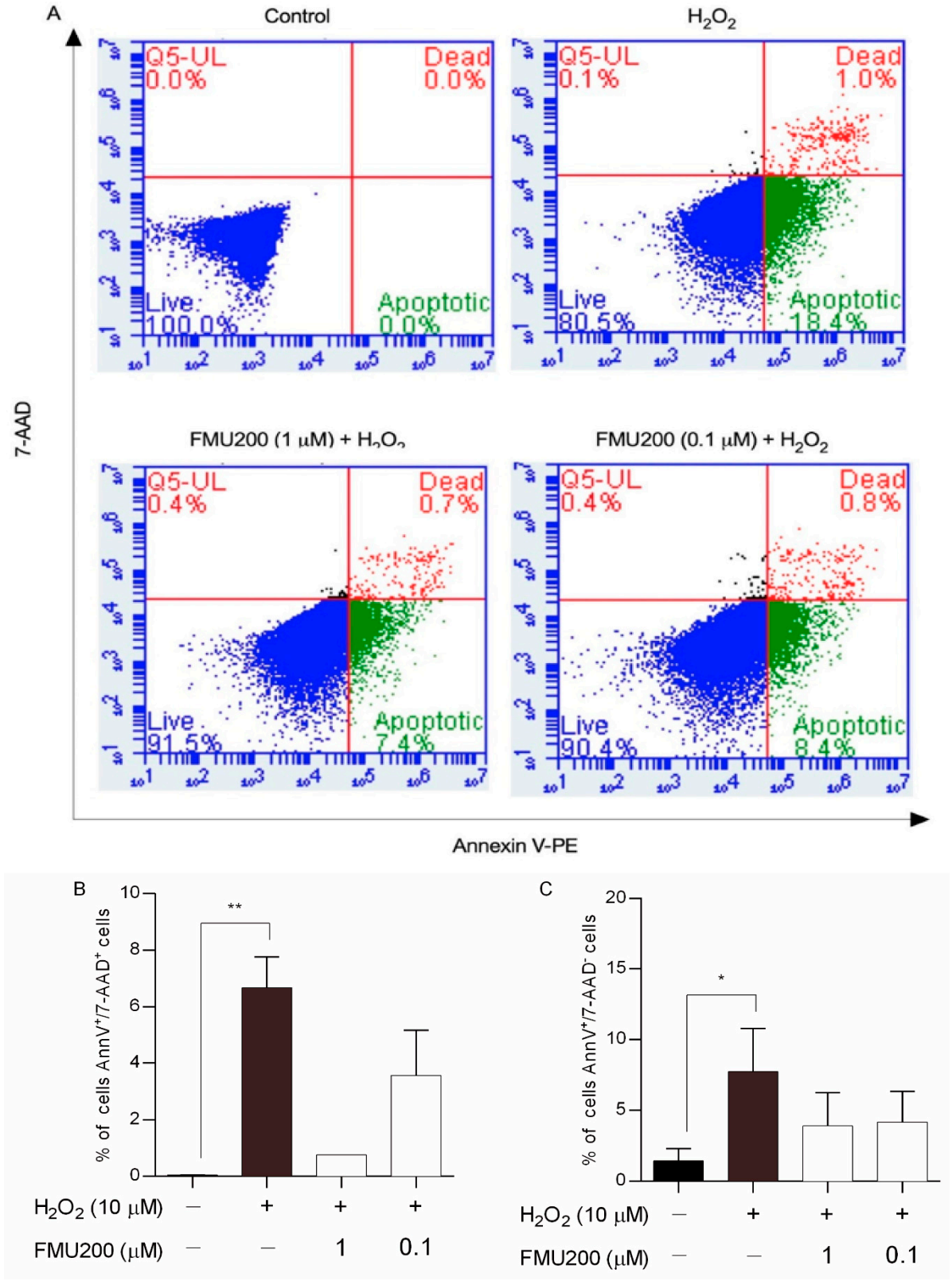

Figure 3. Effects of co-treatment with H_2O_2 and FMU200 after 6 h. (**A**) FL-2 (Annexin V-PE) vs. FL-3 (7-AAD) dot plots for untreated cells (control), cells treated with 10 μM H_2O_2 only, cells pretreated with 1 μM FMU200, and cells pretreated with 0.1 μM FMU200 for 1 h before H_2O_2 exposure; (**B**) percentage of dead cells (cells stained with both 7-AAD and Annexin V-PE); (**C**) percentage of early apoptotic cells (cells stained with Annexin V-PE only). The data are expressed as the means of three independent experiments together with the standard error of the mean (mean ± SEM). Statistical calculations were performed by ANOVA via the Tukey post hoc test. Statistical significance values were ** $p < 0.01$; * $p < 0.05$ (vs. control).

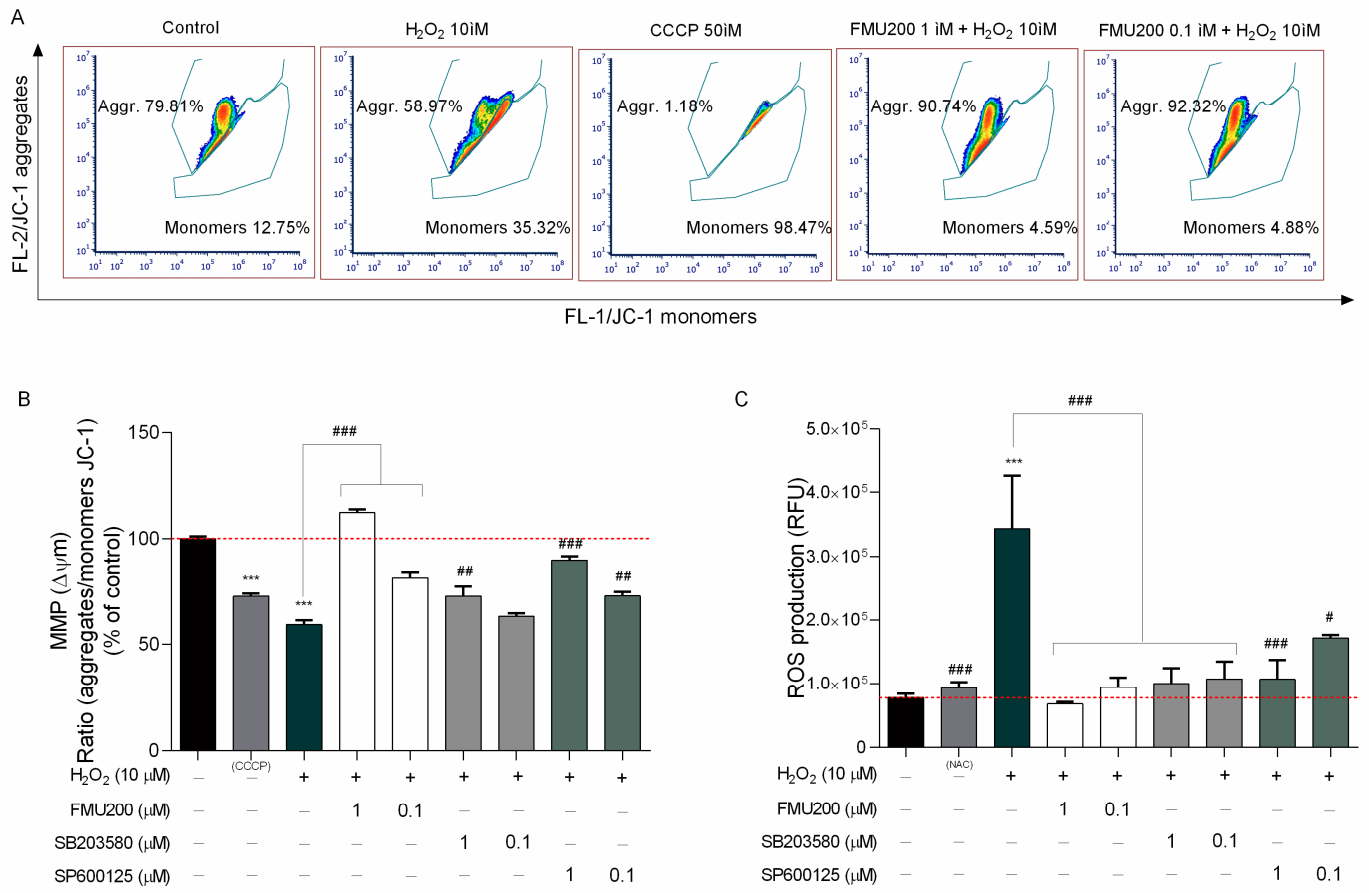

Figure 4. (**A**) Representative flow cytometric analysis showing that FMU200 inhibited H_2O_2-induced ΔΨm depolarization monitored by JC-1 dye; (**B**) changes of mitochondria stained with JC-1 were also detected using a fluorescence microplate reader. The ratio of red fluorescence to green fluorescence of the control was defined as 100%; (**C**) intracellular ROS levels were measured by DCF-DA staining in SH-SY5Y cells after H_2O_2-induced damage. Data are expressed as relative fluorescence unit (RFU) per cell. The data are expressed as the means of three independent experiments together with the standard error of the mean (mean ± SEM). Statistical calculations were performed by ANOVA via the Tukey post hoc test. Statistical significance values were *** $p < 0.001$ (vs. control); ### $p < 0.001$; ## $p < 0.01$; # $p < 0.05$ (vs. H_2O_2).

2.3. JNK Inhibition by FMU200

The IC_{50} value for JNK3 of FMU200 was previously determined by ELISA assay [21,37]. The authors performed a screening among 410 kinases to investigate the selectivity profile of FMU200 among the kinome and revealed that, in addition to JNK, only three other kinases were inhibited by FMU200 (CK1δ, MAPKAPK2, and TIE2), and the covalent bond to Cys154 of JNK3 was confirmed by liquid chromatography−mass spectrometry (LC−MS). The relevance of covalent binding to Cys154 was previously reported with another potent JNK3 inhibitor (JNK-IN-7) [20]. However, additional virtual simulations suggest that FMU200 may form hydrogen bonds to residues Met149, Asn152, and Gln155, as shown in Figure S1. It was reported that indenoquinoxaline-derived JNK inhibitors, such as IQ-3, were H-bonded mainly with Asn152, Gln155, or Met149 residues of JNK3 indicating that these residues play an important role in enzyme binding activity and selectivity. In this case, it was demonstrated that at 0.1 μM, FMU200 inhibits JNK2 by 73% and JNK3 by 80%, while at 0.5 μM, the residual activity of JNK2 and JNK3 are 5% and 4%, respectively [21]. The representative data acquired via Western blot of JNK inhibition are shown in Figure 5A. Our results indicate that a pretreatment (1 h) with FMU200 (at 1 μM or 0.1 μM) followed a 24 h treatment with H_2O_2 decreased the phosphorylated JNK (p-JNK) to total JNK (p-JNK/JNK)

ratio by 60.75% and 29.49%, respectively ($p < 0.001$) (Figure 5B), and downregulated p-JNK expression by 54.12% and 37.5%, respectively ($p < 0.001$) if compared to cells treated with H_2O_2-only (Figure 5C), confirming the inhibitory activity of FMU200.

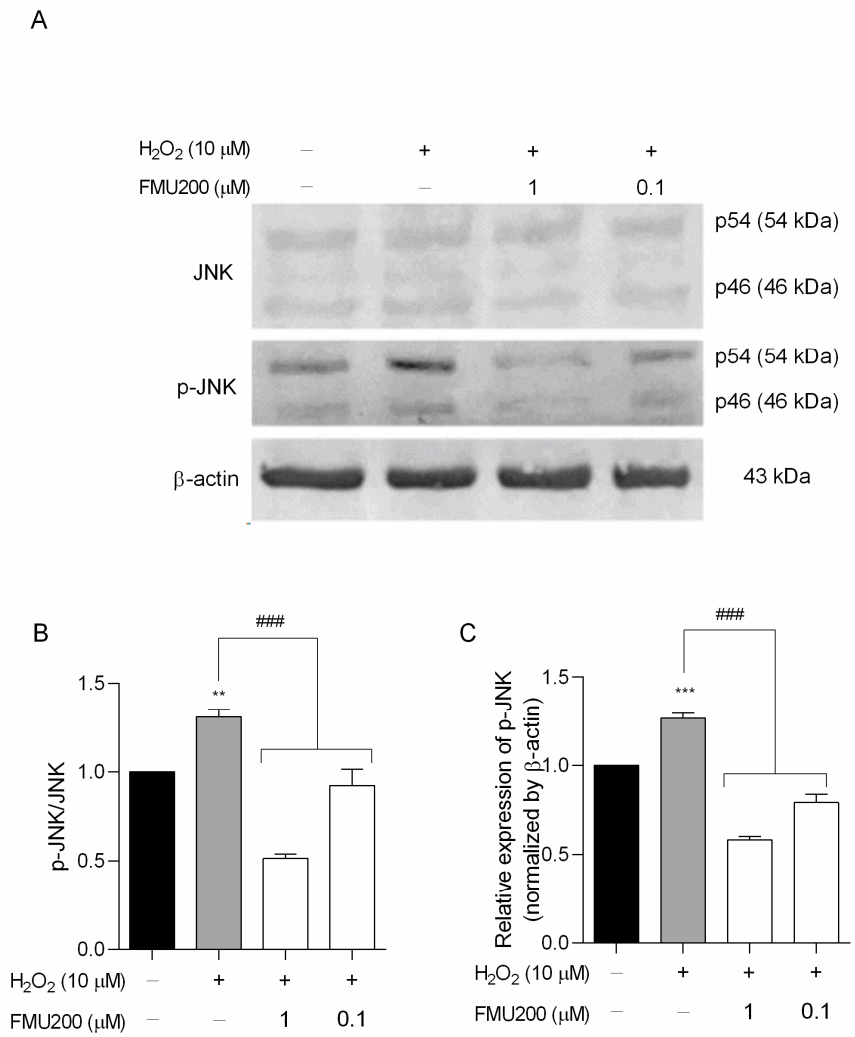

Figure 5. FMU200 inhibited JNK phosphorylation in SH-SY5Y H_2O_2-stimulated cells. (**A**) Representative Western blots of total and phosphorylated JNK (p-JNK) showing both JNK isoforms (p46 and p54) and β-actin; (**B**) densitometry ratios of p-JNK to total JNK; (**C**) densitometry for p-JNK protein levels normalized to β-actin. *** $p < 0.001$; ** $p < 0.01$ (vs. control); ### $p < 0.001$ (vs. H_2O_2).

2.4. Anti-Inflammatory Effect

As presented in Figure 2A, FMU200 showed moderate cytotoxicity at 10 μM in SH-SY5Y cells. As a result, we determined the cytotoxic effect in RAW264.7 cells at lower concentrations (Figure 6A). No significant reduction in cell viability was found compared with control.

After determining the effects of FMU200 on cell viability ROS production and mitochondrial function, we evaluated proinflammatory cytokines, such as IL-6 and TNF-α, which are thought to be involved in mediating neuroinflammation and inducing neuronal death in various neurodegenerative diseases [38,39]. Additionally, JNK and ROS are also associated with pro-inflammatory events [40].

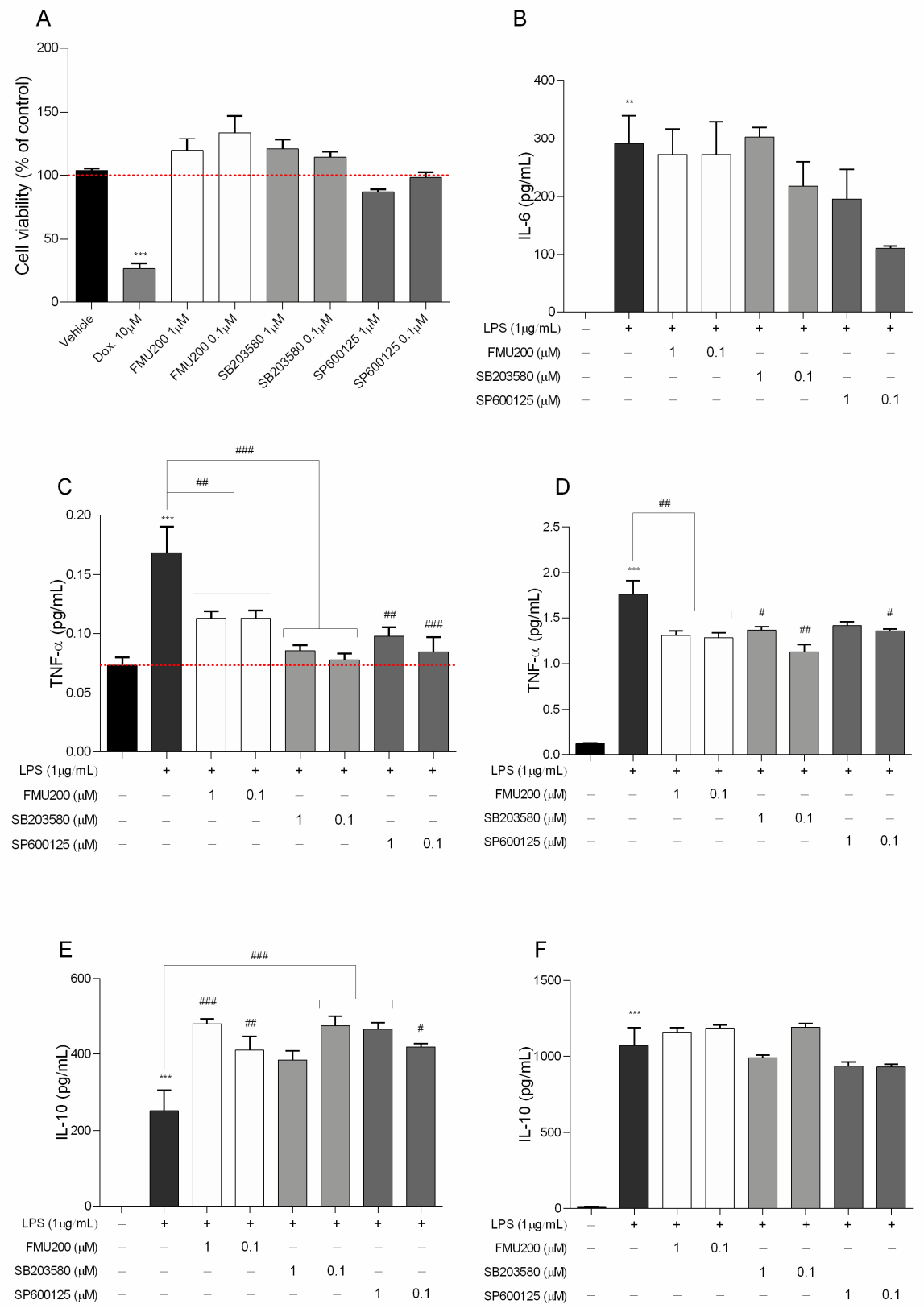

Figure 6. (**A**) Cytotoxicity induced by FMU200 on RAW264.7 cell viability after a 24 h incubation period; negative control (untreated cells) was considered to be 100% viable and is represented by the red dashed line. Doxorubicin was used as positive control; DMSO 0.1% was used as vehicle; (**B**) IL-6 was determined after 12 h of treatment; (**C**) TNF levels after 3 h and (**D**) after 24 h of treatment. IL-10 was evaluated (**E**) after 24 h; and after (**F**) 48 h of treatment. Mean ± SEM of at least three experiments. *** $p < 0.001$; ** $p < 0.01$ (vs. control); ### $p < 0.001$; ## $p < 0.01$; # $p < 0.05$ (vs. LPS or doxorubicin).

In the present study, an inflammatory model was successfully established using LPS-stimulated RAW264.7 cells, and therefore, we investigated the effect of FMU200 on the levels of IL-10, IL-6, and TNF-α in LPS-stimulated RAW264.7 cells. TNF-α is the earliest endogenous mediator of an inflammatory reaction, and IL-6 is a major pro-inflammatory cytokine that plays an important role in the acute-phase response of inflammation [41]. Both cytokines can be used as markers of neuroinflammation [42]. To detect its effect over pro-inflammatory cytokines, we pretreated RAW264.7 cells with FMU200 for 1 h, and then exposed these cells to LPS (1 μg/mL) for different time period. IL-6, a pro-inflammatory cytokine was determined after 12 h of co-treatment with LPS and FMU200 at different concentrations. It was revealed that FMU200 did not influence IL-6 levels (Figure 6B). The results demonstrated that after 3 h of LPS stimulation of RAW264.7 cells, treatment with FMU200 at 1 μM and 0.1 μM reduced TNF-α levels by 32.73% and 33%, respectively (Figure 6C). After 24 h, FMU200 at 1 μM and 0.1 μM decreased TNF-α levels by 25.56% and 27.05%, respectively (Figure 6D). Additionally, we evaluated levels of IL-10, an anti-inflammatory cytokine. Since the secretion of IL-10 is delayed and always follows that of proinflammatory factors with a latency period [43], we collected the supernatant after 24 and 48 h. After 24 h, FMU200 at 1 μM and 0.1 μM increases IL-10 levels (91.37%, $p < 0.01$ and 63.05%) (Figure 6E), but after 48 h, FMU200 at 1 μM and 0.1 μM appears to promote a discrete increase (8.89 and 11.32%, respectively) (Figure 6F), but not statistically significant.

3. Discussion

The human neuroblastoma cell line SH-SY5Y is widely used as an in vitro experimental model of ND. The undifferentiated SH-SY5Y cells proliferate continuously, express immature neuronal markers, and lack mature neuronal markers [44]. Undifferentiated cells are considered the ones that most resemble immature catecholaminergic neurons [45,46]. Here, we tested whether pretreatment with FMU200 could protect cells against 6-OHDA-induced apoptosis. 6-OHDA is a catecholamine analog that can be formed from dopamine in the presence of Fe^{2+} and H_2O_2. It is a substrate for monoamine oxidase (MAO), and competes with dopamine for dopamine β-hydroxylase and COMT reactions, involved in norepinephrine biosynthesis and dopamine degradation, respectively. However, the more cytosolic dopamine, 6-OHDA is more likely to occur, especially if dopamine metabolism is affected by MAO or COMT inhibitors, drugs used in Parkinson's disease treatment [47].

The main mechanism of neurotoxicity of 6-OHDA relies on two major events. The first one relies on the autoxidation of 6-OHDA where the cell damage is a result of 6-OHDA-derived ROS. Indeed, it is known that 6-OHDA is a highly reactive and oxidizable catecholamine analog that is rapidly and non-enzymatically oxidized by molecular oxygen to form hydrogen peroxide (H_2O_2), superoxide anions (O_2^-), and hydroxyl radicals (OH^-) [48]. In all assays, we used 6-OHDA as an apoptosis inducer, and, additionally, we added 0.02% of ascorbic acid to the mixture to avoid rapid 6-OHDA autoxidation [34]. Additionally, it is likely that this effect occurs in vivo since the antioxidants available might be sufficient to prevent rapid oxidation of 6-OHDA, supporting a secondary and alternative route 6-OHDA toxicity: the inhibition of brain mitochondrial complexes I and IV [47].

Several studies indicated that 6-OHDA is a potent inhibitor of complex I and IV in the brain's mitochondria [47,49,50], inhibiting the mitochondrial respiratory chain complexes mediated by non-radical interactions. Glinka et al. reported that mitochondrial complex I inhibition induced by 6-OHDA is not prevented by antioxidants, and cell death (and therefore neurodegeneration) is caused by ATP depletion [47,51]. It is known that complex I is the main entry point of electrons into the respiratory chain and its inhibition results in the blockade of most of the oxidative metabolic reactions within mitochondria [52], providing support for the theory. Deficiency in complex I of the ETC has been described in PD [53,54] and AD patients [55,56], while decreased complex IV activity and ATP production [57,58] were reported in animal models of AD. In other words, in neurons, one of the 6-OHDA effects is complex I and IV inhibition, causing ATP levels to decrease, facilitating apoptosis. In mice hepatocytes, acetaminophen decreased ATP levels (similarly to

6-OHDA in neurons), while pretreatment with SP600125 prevented a decline in ATP levels, suggesting that JNK translocates to mitochondria and inhibits mitochondrial bioenergetics (at least in part) by triggering mitochondrial permeability transition [59,60]. A similar effect was observed in isolated brain mitochondria, where JNK directly induced mitochondrial permeability transition [61]. Here, we report that FMU200 reduced 6-OHDA-induced cell death in undifferentiated SH-SY5Y cells after 24 and 48 h treatments. Although our results cannot confirm or discard the possibility, it is reasonable to think that FMU200 (like SP600125 treatment in hepatocytes) could prevent a decrease in ATP levels, contributing to the decreased cell death we observed in our MTT assays. We suggest further analysis in order to confirm (or not) the effect of FMU200 over ATP levels.

However, SH-SY5Y cells can be "oriented" to a variety of mature neuronal phenotypes (cholinergic, adrenergic, or dopaminergic), depending on the culture conditions [45]. One of the most commonly implemented and best-characterized methods for inducing differentiation in SH-SY5Y cells is through the addition of retinoic acid (RA) to the cell culture medium. RA is a derivative of vitamin A known to inhibit cell proliferation and induce cell differentiation [62]. Normally, RA is administered at a concentration of 10 μM for a minimum of 3–5 days in a serum-free or low-serum medium to induce differentiation [45,63,64], although small variations in the media are reported. In this sense, other than non-differentiated cells, differentiated SH-SY5Y cells become morphologically more similar to primary neurons with long processes randomly distributed (neurites). Differentiation of SH-SY5Y cells also induces a decrease in the rate of proliferation [44]. The differentiation method selected for in vitro experiments must be determined by the desired phenotype after differentiation. In response to RA treatment, SH-SY5Y cells differentiate mainly into a cholinergic neuron phenotype, as evidenced by the increased expression of choline acetyltransferase (ChAT) and vesicular monoamine transporter (VMAT) activity [46,65]. After differentiation, cells begin to upregulate genes involved in antioxidant defense. This modified gene expression profile directly reflects the cells' ability to recover from the oxidative stress caused by 6-OHDA [63]. To confirm this greater resistance, a second positive control with doxorubicin (10 μM) was included. When interleaved with the DNA, doxorubicin induces the breaking of the double-strand and, therefore, cell death. In addition, it can inhibit the enzyme topoisomerase II [66,67]. According to our results, FMU200 promoted a neuroprotective effect in RA-differentiated cells after 24 h, but the most prominent effect was observed after 48 h.

After confirming the neuroprotective effect of FMU200 in both undifferentiated and RA-differentiated SH-SY5Y cells, we aimed to understand the mechanism of action of FMU200 and the nature of the effects of FMU200 over different events related to JNK signaling and ROS production that usually precedes apoptosis. It is important to note that in subsequent tests (intracellular levels of ROS and the potential of mitochondrial membrane ($\Delta\Psi m$)), we used undifferentiated SH-SY5Y cells stimulated by H_2O_2. We opted for using undifferentiated cells as our experimental model because the differentiation process promotes a series of modifications that could mask or interfere with our results. RA treatment has been shown to promote the survival of SH-SY5Y cells by activating the phosphatidylinositol 3-kinase/Akt signaling pathway and by positive regulation of the anti-apoptotic Bcl-2 protein [68,69]. In addition, some studies show that RA-differentiated cells are less vulnerable than undifferentiated cells to common agents used to induce cell death including 6-OHDA, 1-methyl-4-phenyl-1,2,3, 6-tetrahydropyridine (MPTP), or its metabolite, ion 1-methyl-4-phenyl-pyridinium (MPP^+) than undifferentiated cells [63]. Additionally, we evaluated the effect of FMU200 over H_2O_2-induced cell injury in the following assays because (a) H_2O_2 is the most stable ROS, (b) it transits through cell membranes easily, (c) one of the subproducts of 6-OHDA degradation is H_2O_2 [34,47,48], (d) in N18 cells, the damage to cell structure and function induced by 6-OHDA and H_2O_2 was similar [70], (e) H_2O_2 acts as both extracellular and intracellular messenger [71–73] and; (f) the JNK pathway plays a pivotal role in cell death of several cell types and the activation of JNK3 appears to be essential for the pathophysiology of many neurodegenerative diseases, and H_2O_2 is

widely used as general oxidative stress in vitro model of neurodegenerative diseases [74]. In this case, previous evidence suggested that FMU200, a tetrasubstituted imidazole, forms a covalent bond with JNK3, inhibiting its phosphorylation and downstream activation. Our Western blot analysis is consistent with Muth et al., 2016, indicating a downregulation in p-JNK. In this case, our study supports evidence from previous observations that pointed to a decrease in JNK3 activity. JNK is widely associated with cell death and participates in both extrinsic and intrinsic pathways. In the intrinsic pathway, JNK phosphorylates transcription factors inducing the expression of pro-apoptotic proteins and decreases the expression of anti-apoptotic proteins. The major JNK target is the transcription factor AP-1, which is a complex formed by members of Jun, Fos, ATF, and MAF protein families. JNK phosphorylates ATF2 at the NH_2-terminal activation domain on Thr69 and Thr71 residues, increasing ATF2 transcriptional activity. However, JNK mediates apoptosis not only through its effects on gene transcription but also through transcriptional-independent mechanisms involved in the intrinsic pathway of cell death. The activation of JNK can simultaneously change the mitochondrial membrane potential (MMP) and the release of cytochrome c, which induces apoptosis via the intrinsic pathway. Since the JNK pathway and ATF2 transcriptional activity can be activated by ROS, it was hypothesized if FMU200 had any effect on ROS production.

Cells constantly generate reactive oxygen species (ROS) during aerobic metabolism. Due to the brain's high metabolic rate, it consumes almost 25% of the body's total intake of glucose and 20% of the total oxygen uptake during ATP production. During this process, ROS are also generated as a result of the activity of the electron transport chain (ETC) during oxidative phosphorylation and, as a result, the brain tissue is particularly susceptible to oxidative stress [73,75]. Several events have been associated with neurodegeneration such as synaptic dysfunction, excitotoxicity, and oxidative stress. Indeed, because of its high metabolic rate combined with a limited capacity of cellular regeneration, the brain is particularly sensitive to oxidative damage. The damage caused by reactive oxygen species in specific brain regions was associated with AD, mild cognitive impairment (MCI), Parkinson's disease (PD), and amyotrophic lateral sclerosis (ALS) [76–80]. In other words, there is evidence linking ROS and the pathophysiology of several neurodegenerative diseases. However, randomized trials evaluated the effects of antioxidants in AD patients, providing conflicting results [81,82]. Higher levels of ROS activate cell death processes [71] and, in this case, antioxidant therapy appears to be insufficient to promote significant improvements, supporting the need for exploring novel targets.

ROS and JNK are highly interconnected, and previous studies reported that treatment with a JNK3 inhibitor (compound 9l or SR-3562) had shown potent inhibition of ROS generation following JNK activation in HeLa cells [10] and INS-1 cells [83]. Here, we demonstrated that FMU200 (at 1 and 0.1 µM) was also able to decrease ROS production, corroborating with studies previously published that evaluated other JNK inhibitors. In addition, SR-3562, like FMU200, prevented ROS formation in a similar way to NAC, a generic antioxidant [10]. In this case, it appears that JNK activation (by H_2O_2) induces ROS generation, while the inhibition of JNK by FMU200 decreases ROS production. To provide further support to our results, the radical-trapping antioxidant properties of FMU200 should be evaluated.

Any increase in mitochondrial ROS production depends on the metabolic state of this organelle and a correlation between mitochondrial membrane potential ($\Delta\Psi m$) and reactive oxygen species (ROS) production [60,84,85] has been demonstrated. In mitochondrial disorders, decreased $\Delta\Psi m$ and activity of the respiratory chain are observed with a simultaneous increase in ROS production [86,87]. Additionally, $\Delta\Psi m$ depolarization is generally correlated to neuronal death [54,88]. Mitochondrial depolarization induced by JNK was evaluated in Huh7 and HepG2 cells [89]. Heslop and colleagues demonstrated that mitochondrial dysfunction is mediated by JNK activation, while the JNK inhibition by JNK inhibitor VIII and SP600125 prevented mitochondrial dysfunction and blocked JNK translocation to the mitochondria. By preventing the JNK translocation to the outer

mitochondrial membrane, a decrease in ROS production [90] was observed. In human melanoma cells, JNK activation was necessary for ΔΨm change and cell apoptosis [91] and treatment with SP600125 prevented both the loss of ΔΨm and the increase in apoptosis by inhibiting JNK activation in different cell types [92–95]. One possible explanation for these findings is that JNK plays a significant role in apoptosis via the intrinsic pathway (also known as the 'mitochondrial pathway'), which is activated by extracellular or intracellular perturbations usually found in AD, such as oxidative stress. In response to a deleterious stimulus (such as ROS), JNK phosphorylates 14-3-3 protein and induces the translocation of pro-apoptotic proteins (Bax and Bad) from the cytoplasm to the mitochondria, the major source of ROS in cells. However, it was reported that JNK can directly phosphorylate Bad, Bim, and Bid inducing their pro-apoptotic activity while inhibiting anti-apoptotic proteins. Once translocated to the mitochondria, JNK increases ROS formation in 80%, especially by complex I [10]. In the present study, FMU200 attenuated H_2O_2-induced production of intracellular ROS and inhibited H_2O_2-induced depolarization of ΔΨm, which are important molecular markers for reflecting the mitochondria oxidative stress status. These results connect the JNK pathway directly with mitochondrial-dependent apoptosis, suggesting that mitochondria are an important target organelle of FMU200 and may be essential for its neuroprotective action (Figure 7).

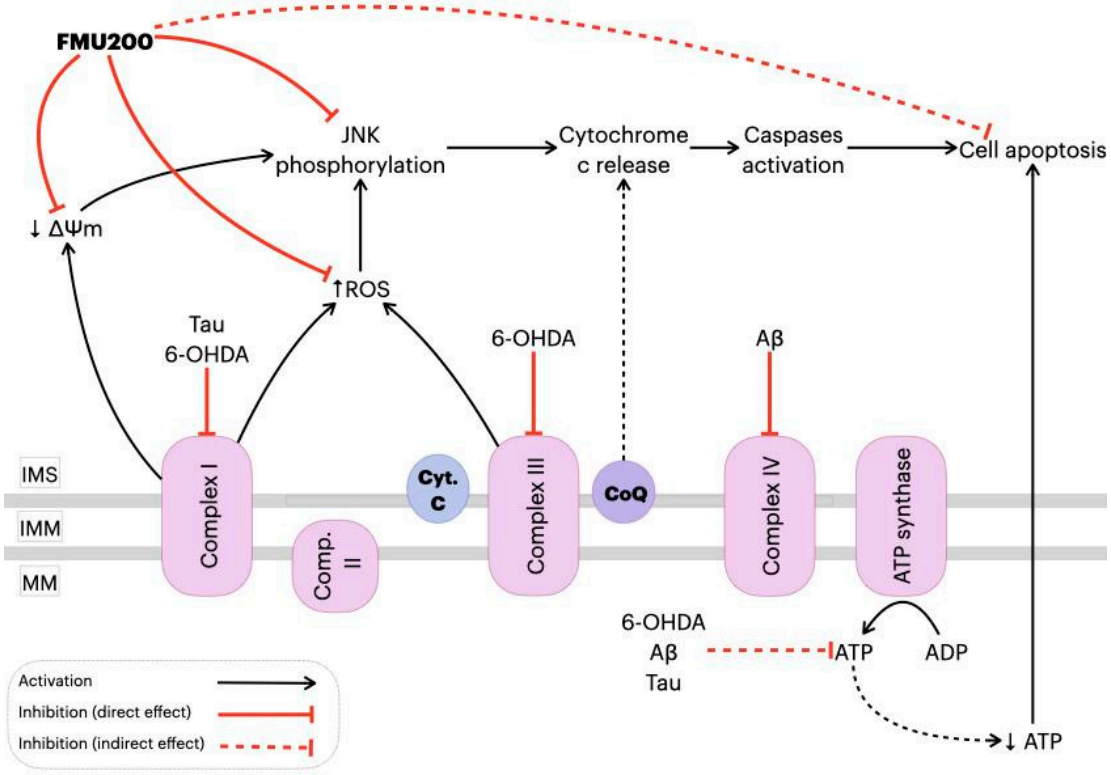

Figure 7. Proposed mechanism of action of FMU200 in mitochondria. Decrease in complex I activity induced by hyperphosphorylated Tau or 6-OHDA causes an ΔΨm depolarization and, consequently, JNK pathway activation [89,96,97]. In addition to complex I inhibition, 6-OHDA also inhibits complex III [47], while Aβ is reported to inhibit the complex IV [97]. A defective oxidative phosphorylation results in excessive ROS production, which activates the JNK pathway. Additionally, dysfunction of mitochondrial complexes also results in decreased ATP production, which directly leads to apoptosis. However, FMU200 was able to reduce ROS production, prevent ΔΨm depolarization and JNK phosphorylation, demonstrating a protective effect over common AD and PD-related mitochondrial perturbations. ↓: represents decrease; ↑ represents increase. Inner mitochondrial space (IMS); inner mitochondrial membrane (IMM); mitochondrial matrix (MM); cytochrome c (Cyt. C); coenzymeQ (CoQ).

Despite its major contribution to the pathophysiology of neurodegenerative diseases through pro-apoptotic signals, JNK can also promote pro-inflammatory effects [98]. In AD, for example, neuroinflammation relies on an innate immune response mediated by microglia [99]. After a stimulus, the microglia produce several inflammatory mediators, such as IL-1β, IL-6, TNF-α, prostaglandin E2 (PGE2), nitric oxide (NO), brain-derived neurotrophic factor (BDNF), which can activate the JNK pathway. The major contribution of JNK to neuroinflammation is via its transcription factor, AP-1, which regulates proinflammatory genes such as *COX2*, *NOS2*, *TNF-α*, *CCL2*, and *VCAM-1* [100], and evidence suggests that ROS production induced by TNF-α is JNK-dependent [101,102]. In this case, we identified that FMU200 decreased TNF-α release in RAW264.7 cells after a 3 h treatment, but there was a smaller reduction in TNF-α after 24 h. In general, authors report a decrease in proinflammatory cytokines along with an increase in anti-inflammatory cytokines in LPS-induced RAW264.7 cells treated with SP600125 [103–106]. The cytotoxicity of different concentrations of LPS was evaluated in RAW264.7 cells by Tong et al. According to their results, LPS at a maximum concentration of 1.25 μg/mL was not cytotoxic, (which provides support for the LPS concentration we used) and cytokine release (TNF-α and IL-6) was dose-dependent to LPS concentration. In this case, it should be mentioned that in our study cells were pretreated with LPS at higher concentrations compared to other studies (1 μg/mL vs. 0.5 μg/mL [103,106] vs. 0.1 μg/mL [104,105]. Furthermore, in these studies, LPS-stimulated RAW264.7 cells were exposed to concentrations of SP600125 of 10 μM [103,106] and 20 μM [104]. Since data from our initial screening with SH-SY5Y (Figure 2A) indicated increased cytotoxicity of SP60125 at 10 μM, we cannot perform a direct comparison. It is important to bear in mind the possible bias in these conflicting responses. On the other hand, other previous work reported that RAW264.7 cells treated with SP600125 reduced c-Jun activation but did not impact IL-1β, IL-6, and TNF-α at mRNA and protein levels [107].

In addition to TNF-α, IL-6 levels were also evaluated. Apparently, FMU200 has no impact over IL-6. Although IL-6 is understood as a pro-inflammatory interleukin, it is a pleiotropic cytokine with a multitude of functions [108]. The authors showed that the cytokine signaling suppressor 3 (SOCS-3) is a key regulator for the pro-inflammatory action of IL-6 and anti-inflammatory of IL-10, and, in the absence of SOCS-3, IL-6 induces an anti-inflammatory response [109]. In fact, a higher amount of SOCS-3 mRNA was found in post-mortem analysis of AD patients [110]. Furthermore, a 20 year cohort observed a correlation of cognitive impairment and higher or increasing levels of IL-6 over the years [111]. On the other hand, the hypothesis that IL-6 attenuates the neurotoxic effects of NMDA on cholinergic neurons has been discussed for almost 30 years [112–115]. Excessive stimulation caused by glutamate in NMDA receptors causes a phenomenon known as "excitotoxicity" and induces cell death through JNK activation [116,117]. It is noteworthy that meanwhile, one of the drugs used for treating AD is an NMDA receptor antagonist [118] and that treatment with JNK inhibitors such as D-JNKI1, SP600125 or TAT-JNK-III protects against glutamate excitotoxicity and cell death in vivo and in vitro [119–121]. In addition, chronic exposure to exogenous IL-6 prevented neuronal death and an increase in NMDA-induced caspase-3 activity. Both AG490 (JAK2 inhibitor) and PD98059 (ERK inhibitor) blocked the protection of IL-6 against a decrease in neuronal vitality induced by NMDA and increased activation of caspase-3 [122,123]. Still, recently, it was demonstrated that the inhibition of IL-6 could contribute to the worsening of depressive disorders [124] which are more prevalent in the elderly population and, even more so, in the elderly population with some neurodegenerative disease [125–127]. In this sense, it can be inferred that the neuroprotective effect of IL-6 depends on the concentration of IL-6 and the degree of neuronal damage. It is hypothesized that total blockage of the IL-6 production is not beneficial in the treatment of neurodegenerative diseases. In this case, an IL-6 modulation through JNK inhibition is preferable. Such a modulatory effect could be achieved through treatment with FMU200, since treatment with SR3306, a selective inhibitor of JNK2/3, reduced the

expression of SOCS-3 in in vivo models [128]. The fact that in the present study IL-6 levels were not affected by FMU200 can therefore be understood as an ambiguous result.

Levels of a second interleukin were also evaluated. IL-10 is known to inhibit secretion of pro-inflammatory cytokines (IL-1α, IL-1β, IL-6, TNF-α) induced by LPS or IFN-γ [129,130]. In the present study, pretreatment with FMU200 (1 and 0.1 μM) increased levels of IL-10 after 24 h compared to the group treated with LPS only, while after 48 h no effect on IL-10 levels was observed. RAW264.7 cells stimulated with 1 μg/mL LPS (the same concentration we used), SP600125 at 2 μM apparently had a minimal effect over IL-10 [131]. Despite IL-10 being known to inhibit pro-inflammatory cytokines, an increase in *IL10* expression in several animal models of AD provoked a decrease in Aβ phagocytosis by microglia and exacerbated Aβ deposits, leading to cognitive impairment. On the other hand, blocking *IL-10* promotes a reduction in IL-10/STAT3 signaling, and seems to increase microglial phagocytic activity [132,133]. It is important to emphasize that higher IL-10 levels were found in patients with AD [134–137].

Neurons, microglial cells and macrophages, for example, are also known to express TLR receptors (especially TLR2, 4 and 9) and these receptors are overexpressed in patients with Alzheimer's or Parkinson's diseases, and in various experimental models of these diseases [138]. In addition, there is a consensus that the activation of TLR receptors triggers the JNK pathway. Despite the deleterious effects of TLR receptor activation, it is known that IL-10 synthesis depends, in part, on TLR activation. It has been shown that TLR stimulation leads to MAPK activation, which then modulates IL-10 production. On the other hand, the inhibition of ERK, p38 or JNK in LPS-stimulated macrophages led to a significant reduction in IL-10 [138–144]. In addition, transcription factors activated by JNK such as ATF-1, MAF, NF-kβ (p65), JUN, CREB, have been described to regulate IL-10 expression [145]. Such observations could partially explain the results we observed after 48 h, since FMU200, as a JNK inhibitor, may be negatively modulating IL-10 expression. Finally, it is evident that there is a complexity in the regulation of cytokines through positive and negative feedback cycles and that strict control is essential to achieve a balance between an effective immune response and immunopathology. Collectively, these results suggest that the rebalancing of innate cerebral immunity and the promotion of "beneficial neuroinflammation" may be more effective than a generalized anti-inflammatory therapy for AD. Although the classification of cytokines as "pro" or "anti-inflammatory" is widely adopted in the literature and interesting from a didactic point of view, it is a reductionist characterization and should be avoided since the beneficial or harmful actions of IL-10 and IL-6 depend on a broader context.

Despite the promising potential of FMU200, there are two major limitations in this study that could be addressed in future research. First, the primary focus of our study was to unravel the effect of FMU200 over JNK3-related apoptosis in in vitro models of neurodegenerative diseases and, therefore, the mechanisms underlying the anti-inflammatory effect of FMU200 were not totally explored. Thus, the evaluation of inflammatory mediators such as iNOS and COX-2, as well as, growth factors (i.e., neurotrophins), transcription factors (i.e., Nrf2), and cell receptors (i.e., TLR4) would be of extreme value to fully elucidate the anti-inflammatory mechanisms of FMU200, especially based on co-culturing systems with neuron and microglia-derived cells, for example. Second, although FMU200 is highly selective to JNK3, some of the reported effects might also be due to the inhibition of off-target kinases. The clinical implications of this study are unclear at this point, but based on our observations, we highly suggest further analysis with FMU200 in order to fully elucidate its mechanism of action and further explore its beneficial effects.

4. Materials and Methods

4.1. Cell Lines and Reagents

Dulbecco's modified Eagle medium (DMEM) (D5523), F12 (N6760), heat-inactivated fetal bovine serum (FBS) (F4135), 6-hydroxydopamine hydrobromide (6-OHDA) (162957), 3-[4,5-dimethylthiazol-2]-2,5 diphenyltetrazolium bromide (MTT) (M5655), penicillin (P3032),

streptomycin (S9137), LPS (from *Escherichia coli*, O111:B4, L2630), trypsin-EDTA (T4049), 2′,7′-Dichlorofluorescin diacetate (DCFDA) (D6883), Protease Inhibitor Cocktail (P8340), and 3-3′-diaminobenzidine (DAB) (D8001) were purchased from Sigma-Aldrich™ (St. Louis, MO, USA). DMEM (1200-058) used to culture RAW264.7 cell line and enzyme-linked immunosorbent assay (ELISA) kits for TNF-α, IL-6, and IL-10 were obtained from Gibco®, Invitrogen Life Science Technologies (Grand Island, NY, USA). All-trans-retinoic acid (ATRA) (SC200898) and the primary antibodies for total JNK (D-2), phospho-JNK (Thr183/Tyr185) (G-7), and β-actin (C-4) were purchased from Santa Cruz Biotechnology, (Dallas, TX, USA). Spectrophotometer-based analyses were performed using SpectraMax® i3 (Molecular Devices, San Jose, CA, USA). 5,5,6,6-tetrachloro-1,1,3,3-tetraethylbenzimidazolylcarbocyanine iodide (JC-1) staining is from Molecular Probes (Eugene, OR, USA). PE Annexin V Apoptosis Detection Kit I was purchased from BD Biosciences (USA). Secondary antibodies for anti-mouse IgG, HRP-linked, (7076) and anti-rabbit IgG, HRP-linked (7074) were bought from Cell Signaling Technology (Danvers, MA, USA). SH-SY5Y (ATCC© CRL-2266™) and RAW264.7 cell line (ATCC© TIB-71™) was acquired from American Type Culture Collection (ATCC). FMU200 and the MAPK inhibitors (SP600125 and SB203580) were synthesized by research of Prof. Dr. Stefan Laufer with a high purity grade (≥95%).

4.2. Cell Culture Methods

4.2.1. SH-SY5Y Cell Line

Undifferentiated human SH-SY5Y neuroblastoma cells were cultured in DMEM mixed with F12 (1:1) and supplemented with 10% (*v*/*v*) FBS and 1% streptomycin/penicillin under controlled conditions in a 95% humidified atmosphere, at 37 °C and 5% CO_2. The culture medium was replaced every two days until the cells reached confluence 4–5 days after the initial seeding. For subculture, SH-SY5Y cells were dissociated with trypsin-EDTA (0.25%), split into a 1:3 ratio. Cells were grown to 80% confluence before treatment. Culture conditions were performed according to ATCC recommendations.

4.2.2. SH-SY5Y Differentiation Protocol

To differentiate the SH-SY5Y cells, we adapted a previously described protocol and exposed cells to 10 μM of ATRA for 10 days [45].

4.2.3. RAW264.7 Cell Line

RAW264.7 cells were cultured in DMEM supplemented with 10% (*v*/*v*) of FBS and 1% of streptomycin/penicillin. The medium was replaced every 2 to 3 days. Subculturing was carried out with a cell scraper at a 1:4 split ratio. All procedures were made following ATCC recommendations.

4.3. Determination of Cell Viability and Neuroprotection Potential by MTT Assay

4.3.1. MTT Assay and Cytotoxicity of FMU200

Cell viability was assessed using the colorimetric MTT assay. SH-SY5Y (differentiated and undifferentiated) and RAW264.7 cells were seeded in 96-well dishes and left overnight in the incubator for proper attachment. Cells were exposed to different concentrations (10–0.1 μM) of FMU200 for 24 or 48 h. At the end of the incubation period, MTT reagent was applied to each well at a final concentration of 5 mg/mL and the plate was placed in a humidified incubator at 37 °C with 5% of CO_2 for a further 3 h period. Formazan salts were dissolved in DMSO and the colorimetric determination of the reduction of MTT was determined at 570 nm wavelength using the spectrophotometer SpectraMax® i3. Control cells treated with maintenance media were considered to be 100% viable.

4.3.2. Neuroprotection Potential

To investigate the neuroprotective potential of the compound, SH-SY5Y (differentiated and undifferentiated) cells were seeded at a density of 2×10^4 per well in a 96-well dish and left in the incubator overnight. Next, the medium was replaced with different concentrations (1 or 0.1 µM) of FMU200 for 30 min before adding 100 µM of 6-OHDA stabilized with 0.02% of ascorbic acid to avoid auto-oxidation of 6-OHDA. After 24 or 48 h, the treatment was removed, and MTT (5 mg/mL) was added for 3 h. Following the MTT removal, DMSO was used to dissolve the formazan salts and the OD was evaluated at 570 nm using a spectrophotometer (SpectraMax®).

4.4. Apoptosis Assay by Flow Cytometry

PE Annexin V versus 7-aminoactinomycin D (7-AAD) staining was performed and analyzed by flow cytometry. Briefly, cells were plated into 6-well culture dishes (3×10^5 cells/well) and left overnight for attachment. The next day, cells were pretreated for 1 h with different concentrations of FMU200. Following the 1 h pretreatment, apoptosis was induced with H_2O_2 for an additional 5 h. After 6 h of incubation, cells were harvested, washed with cold PBS 1X, and suspended in 1× binding buffer at a concentration of 1×10^6 cells/mL. Then, 100µL of the cell suspension were added to a tube, treated with 5 µL of PE Annexin V and 5 µL of 7-AAD, and incubated for 15 min at room temperature in the dark, according to the manufacturer's instructions. The fluorescence was immediately determined by a flow cytometer (Accuri C6, BD Biosciences, San Jose, CA, USA) using FL-2 and FL-3 filters.

4.5. Mitochondrial Membrane Potential (MMP) Assay

Cells were seeded in 96-well plates and left in the incubator overnight. Next, SH-SY5Y cells were treated with H_2O_2 (100 µM) for 6 h, in the absence or presence of FMU200 (0.1 or 1 µM). After the appropriate period of exposure, cells were washed with PBS 1X and incubated with JC-1 at 37 °C for 30 min. Then, the reagent was gently removed, and cells were washed with PBS 1X. 100 µL/well of PBS 1X was added and the fluorescence was measured at 540/570 nm (red fluorescence) and 485/535 nm (green fluorescence) using a fluorescence microplate reader SpectraMax® i3. Mitochondrial membrane potential was estimated by measuring the fluorescence of free JC-1 monomers (green) and JC-1 aggregates in mitochondria (red) and the results were expressed as the ratio of the aggregates/monomers of JC-1 in the percentage of control. Mitochondrial depolarization was indicated by a decrease in the polymer/monomer fluorescence intensity ratio. We included carbonyl cyanide *m*-chlorophenyl hydrazone (CCCP) as a positive control.

4.6. ROS Production

ROS production was measured by fluorogenic dye H_2-DCFDA, which is oxidized by intracellular ROS. Cells seeded in 96-well plates were treated with FMU200 at different concentrations (0.1 or 1 µM) and 10 µM H_2O_2 for 6 h. Following treatment, cells were washed with PBS (1X) and incubated with carboxyH2DCFDA for 1 h at 37 °C. Next, the fluorescent compound was detected by a fluorescence microplate reader with excitation and emission of 495 and 529 nm, respectively.

4.7. Western Blot

SH-SY5Y cells were pretreated (1 h) with FMU200 at 0.1 or 1 µM before H_2O_2 exposure (24 h). Cells were washed with PBS and then harvested with radioimmunoprecipitation assay buffer (RIPA) [150 mM NaCl, 50 mM Tris-HCl, 0.5% NP-40, 0.1% sodium dodecyl sulfate (SDS), 1 mM EDTA, pH 7.4] supplemented with protease inhibitors and phosphatase inhibitors (NaF and Na_3VO_4). Cells were incubated with lysis buffer at 4 °C for 30 min while rocking gently. Cells were scraped from the culture surface and transferred to a microcentrifuge tube. The cell lysate was centrifuged at 14,000× *g* for 15 min to remove cellular debris. Protein concentrations of total cell lysates were measured by Lowry assay [146]. For

Western blot analysis, proteins were resolved by SDS-PAGE, and transferred to nitrocellulose membranes. Membranes were incubated with TBST buffer (1X TBS, 0.1% Tween-20 with 5% *w/v* non-fat dry milk [NFM] or 5% bovine serum albumin [BSA], pH 7.4) for 2 h. For phospho-Western blots, membranes were blocked with TBST buffer containing 5% BSA (BSA/TBST buffer) rather than non-fat milk (NFM/TBST buffer). The membranes were incubated with primary antibodies specific for total JNK, phospho-JNK (Thr183/Tyr185), or β-actin at dilutions of 1:300 in BSA/TBST or NFM/TBST buffer. Membranes were washed three times for 5 min in 1X TBST. Membranes were incubated with secondary antibodies in the BSA/TBST or NFM/TBST buffer at 1:3000 for HRP-conjugated antibody (anti-mouse IgG, HRP-linked) and the reaction was revealed with DAB [147]. Densitometry analysis was performed with the ImageJ gel analysis plug-in as described elsewhere [148].

4.8. Cytokine Determination in RAW264.7 Cell Line

The evaluation of the anti-inflammatory potential of FMU200 was performed as previously described [149]. In summary, RAW264.7 cells were seeded at a density of 5×10^5 cells/well in a 24-well plate. After adherence time, cells were pretreated with FMU200 for 1 h before LPS (1 µg/mL) was added. The supernatant was collected at different times. To evaluate TNF-α release, samples of supernatant were collected after 3 and 24 h of treatment. For IL-6 analysis, samples were collected after 12 h of treatment. For IL-10, samples were analyzed after 24 and 48 h of treatment. All samples were frozen at −80 °C until the analysis. The ELISA assay was performed according to the manufacturer's instructions. The absorbances were measured at 450 and 570 nm using a spectrophotometer (SpectraMax® i3). Values of 570 nm were subtracted from those of 450 nm to remove background interference. TNF-α, IL-6 and IL-10 standard curves were used to quantify the release from each cytokine.

4.9. Statistical Analysis

The statistical analysis was performed on GraphPad Prism 6.0 software using ANOVA. The results are expressed in mean ± standard error of the mean (SEM). A $p < 0.05$ was considered statistically significant.

5. Conclusions

The present study supports our hypothesis that the neuroprotective effects of FMU200 were mediated by mitochondrial protection, a reduction in oxidative stress conditions, inflammation, apoptosis, and inhibition of the JNK pathway as proposed in Figure 8. It is possible that the inhibition of JNK by FMU200 prevents apoptotic death by downregulating p-JNK but also decreasing mitochondrial disruption, as shown in Figure 7. In conclusion, considering the role of JNK3 in ND's, the limited number of pharmacologic therapies in AD, the use of kinase inhibitors in treating other diseases, and the results of our report, FMU200 demonstrated to be a promising molecule and should be considered in further and more complex researches.

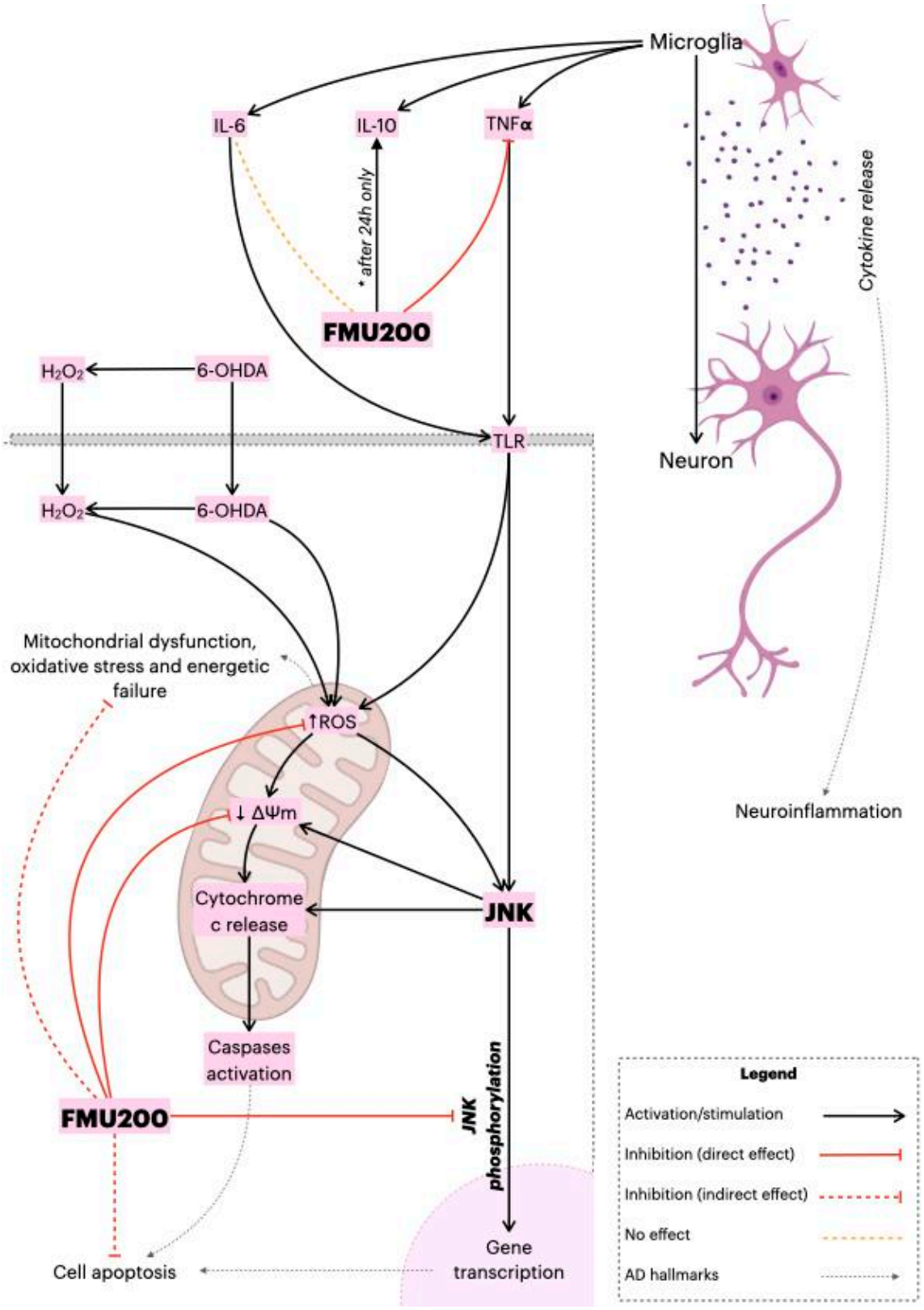

Figure 8. Proposed overall mechanism of action of FMU200. FMU200 blocked the phosphorylation of JNK and, therefore, inhibited apoptosis. Regarding the mitochondria, the direct effect of FMU200 was to reduce ROS production and prevent ΔΨm depolarization. As an indirect result, FMU200 contributed to reduce mitochondrial dysfunction, oxidative stress, and (possibly) to energetic failure. In a microglia model, FMU200 was able to reduce TNF-α production, and induce IL-10 (after 24 h), which contributes to modulate the neuroinflammation.

Supplementary Materials: The following are available online at https://www.mdpi.com/article/10.3390/ijms22073701/s1.

Author Contributions: S.C.H.R. was responsible for data collection, analysis, and draft preparation and writing the article. M.I.G. and S.L. participated in its design and coordination and helped to draft the manuscript. All authors have read and agreed to the published version of the manuscript.

Funding: This study was supported in part by the Coordenação de Aperfeiçoamento de Pessoal de Nível Superior-Brasil (CAPES)-Finance Code 001 and Conselho Nacional de Pesquisa (CNPq) 420381/2018-0 and by Universidade do Vale do Taquari (Univates).

Institutional Review Board Statement: Not applicable.

Informed Consent Statement: Not applicable.

Data Availability Statement: Not applicable.

Acknowledgments: The authors thank Kristine Schmidt for language proofreading.

Conflicts of Interest: The authors declare no conflict of interest.

References

1. Waxman, S. *From Neuroscience to Neurology: Neuroscience, Molecular Medicine, and the Therapeutic Transformation of Neurology*, 1st ed.; Academic Press: Amsterdam, The Netherlands, 2004; p. 552. ISBN 0-12-738903-2.
2. Vajda, F.J.E. Neuroprotection and neurodegenerative disease. *J. Clin. Neurosci.* **2002**, *9*, 4–8. [CrossRef]
3. Drug Safety and Availability | FDA. Available online: https://www.fda.gov/drugs/drug-safety-and-availability (accessed on 8 July 2020).
4. Liu, P.-P.; Xie, Y.; Meng, X.-Y.; Kang, J.-S. History and progress of hypotheses and clinical trials for Alzheimer's disease. *Signal Transduct. Target. Ther.* **2019**, *4*, 29. [CrossRef]
5. Kondoh, K.; Nishida, E. Regulation of MAP kinases by MAP kinase phosphatases. *Biochim. Biophys. Acta* **2007**, *1773*, 1227–1237. [CrossRef]
6. Tournier, C.; Hess, P.; Yang, D.D.; Xu, J.; Turner, T.K.; Nimnual, A.; Bar-Sagi, D.; Jones, S.N.; Flavell, R.A.; Davis, R.J. Requirement of JNK for stress-induced activation of the cytochrome c-mediated death pathway. *Science* **2000**, *288*, 870–874. [CrossRef] [PubMed]
7. Zhu, X.; Castellani, R.J.; Takeda, A.; Nunomura, A.; Atwood, C.S.; Perry, G.; Smith, M.A. Differential activation of neuronal ERK, JNK / SAPK and p38 in Alzheimer disease: The 'two hit' hypothesis. *Mech. Ageing Dev.* **2001**, *123*, 39–46. [CrossRef]
8. Gourmaud, S.; Paquet, C.; Dumurgier, J.; Pace, C.; Bouras, C.; Gray, F.; Laplanche, J.-L.; Meurs, E.F.; Mouton-Liger, F.; Hugon, J. Increased levels of cerebrospinal fluid JNK3 associated with amyloid pathology: Links to cognitive decline. *J. Psychiatry Neurosci.* **2015**, *40*, 151–161. [CrossRef] [PubMed]
9. Takahashi, R.H.; Nagao, T.; Gouras, G.K. Plaque formation and the intraneuronal accumulation of β-amyloid in Alzheimer's disease. *Pathol. Int.* **2017**, *67*, 185–193. [CrossRef] [PubMed]
10. Chambers, J.W.; LoGrasso, P.V. Mitochondrial c-Jun N-terminal kinase (JNK) signaling initiates physiological changes resulting in amplification of reactive oxygen species generation. *J. Biol. Chem.* **2011**, *286*, 16052–16062. [CrossRef] [PubMed]
11. Galluzzi, L.; Vitale, I.; Aaronson, S.A.; Abrams, J.M.; Adam, D.; Agostinis, P.; Alnemri, E.S.; Altucci, L.; Amelio, I.; Andrews, D.W.; et al. Molecular mechanisms of cell death: Recommendations of the Nomenclature Committee on Cell Death 2018. *Cell Death Differ.* **2018**, *25*, 486–541. [CrossRef]
12. Zeke, A.; Misheva, M.; Reményi, A.; Bogoyevitch, M.A. JNK Signaling: Regulation and Functions Based on Complex Protein-Protein Partnerships. *Microbiol. Mol. Biol. Rev.* **2016**, *80*, 793–835. [CrossRef] [PubMed]
13. Roskoski, R. Properties of FDA-approved small molecule protein kinase inhibitors: A 2020 update. *Pharmacol. Res.* **2020**, *152*, 104609. [CrossRef] [PubMed]
14. Ahmed, T.; Zulfiqar, A.; Arguelles, S.; Rasekhian, M.; Nabavi, S.F.; Silva, A.S.; Nabavi, S.M. Map kinase signaling as therapeutic target for neurodegeneration. *Pharmacol. Res.* **2020**, *160*, 105090. [CrossRef] [PubMed]
15. Koch, P.; Gehringer, M.; Laufer, S.A. Inhibitors of c-Jun N-terminal kinases: An update. *J. Med. Chem.* **2015**, *58*, 72–95. [CrossRef] [PubMed]
16. Hepp Rehfeldt, S.C.; Majolo, F.; Goettert, M.I.; Laufer, S. c-Jun N-Terminal Kinase Inhibitors as Potential Leads for New Therapeutics for Alzheimer's Diseases. *Int. J. Mol. Sci.* **2020**, *21*, 9677. [CrossRef]
17. Manning, G.; Whyte, D.B.; Martinez, R.; Hunter, T.; Sudarsanam, S. The protein kinase complement of the human genome. *Science* **2002**, *298*, 1912–1934. [CrossRef]
18. Modi, V.; Dunbrack, R.L. A Structurally-Validated Multiple Sequence Alignment of 497 Human Protein Kinase Domains. *Sci. Rep.* **2019**, *9*, 19790. [CrossRef]
19. Mehan, S.; Meena, H.; Sharma, D.; Sankhla, R. JNK: A stress-activated protein kinase therapeutic strategies and involvement in Alzheimer's and various neurodegenerative abnormalities. *J. Mol. Neurosci.* **2011**, *43*, 376–390. [CrossRef]

20. Zhang, T.; Inesta-Vaquera, F.; Niepel, M.; Zhang, J.; Ficarro, S.B.; Machleidt, T.; Xie, T.; Marto, J.A.; Kim, N.; Sim, T.; et al. Discovery of potent and selective covalent inhibitors of JNK. *Chem. Biol.* **2012**, *19*, 140–154. [CrossRef]
21. Muth, F.; El-Gokha, A.; Ansideri, F.; Eitel, M.; Döring, E.; Sievers-Engler, A.; Lange, A.; Boeckler, F.M.; Lämmerhofer, M.; Koch, P.; et al. Tri- and Tetrasubstituted Pyridinylimidazoles as Covalent Inhibitors of c-Jun N-Terminal Kinase 3. *J. Med. Chem.* **2017**, *60*, 594–607. [CrossRef]
22. Guo, T.; Zhang, D.; Zeng, Y.; Huang, T.Y.; Xu, H.; Zhao, Y. Molecular and cellular mechanisms underlying the pathogenesis of Alzheimer's disease. *Mol. Neurodegener.* **2020**, *15*, 40. [CrossRef]
23. Yarza, R.; Vela, S.; Solas, M.; Ramirez, M.J. c-Jun N-terminal Kinase (JNK) Signaling as a Therapeutic Target for Alzheimer's Disease. *Front. Pharmacol.* **2015**, *6*, 321. [CrossRef] [PubMed]
24. Yoon, S.O.; Park, D.J.; Ryu, J.C.; Ozer, H.G.; Tep, C.; Shin, Y.J.; Lim, T.H.; Pastorino, L.; Kunwar, A.J.; Walton, J.C.; et al. JNK3 perpetuates metabolic stress induced by Aβ peptides. *Neuron* **2012**, *75*, 824–837. [CrossRef] [PubMed]
25. Yue, J.; López, J.M. Understanding MAPK signaling pathways in apoptosis. *Int. J. Mol. Sci.* **2020**, *21*, 2346. [CrossRef]
26. Burkhard, K.; Shapiro, P. Use of inhibitors in the study of MAP kinases. *Methods Mol. Biol.* **2010**, *661*, 107–122. [CrossRef]
27. Cuenda, A.; Rouse, J.; Doza, Y.N.; Meier, R.; Cohen, P.; Gallagher, T.F.; Young, P.R.; Lee, J.C. SB 203580 is a specific inhibitor of a MAP kinase homologue which is stimulated by cellular stresses and interleukin-1. *FEBS Lett.* **1995**, *364*, 229–233. [CrossRef] [PubMed]
28. Bennett, B.L.; Sasaki, D.T.; Murray, B.W.; O'Leary, E.C.; Sakata, S.T.; Xu, W.; Leisten, J.C.; Motiwala, A.; Pierce, S.; Satoh, Y.; et al. SP600125, an anthrapyrazolone inhibitor of Jun N-terminal kinase. *Proc. Natl. Acad. Sci. USA* **2001**, *98*, 13681–13686. [CrossRef]
29. Moon, D.O.; Kim, M.O.; Kang, C.H.; Lee, J.D.; Choi, Y.H.; Kim, G.Y. JNK inhibitor SP600125 promotes the formation of polymerized tubulin, leading to G2/M phase arrest, endoreduplication, and delayed apoptosis. *Exp. Mol. Med.* **2009**, *41*, 665–677. [CrossRef]
30. Inoue, C.; Sobue, S.; Aoyama, Y.; Mizutani, N.; Kawamoto, Y.; Nishizawa, Y.; Ichihara, M.; Abe, A.; Hayakawa, F.; Suzuki, M.; et al. BCL2 inhibitor ABT-199 and JNK inhibitor SP600125 exhibit synergistic cytotoxicity against imatinib-resistant Ph+ ALL cells. *Biochem. Biophys. Rep.* **2018**, *15*, 69–75. [CrossRef]
31. Yang, C.; Pei, W.; Zhao, J.; Cheng, Y.; Zheng, X.; Rong, J. Bornyl caffeate induces apoptosis in human breast cancer MCF-7 cells via the ROS- and JNK-mediated pathways. *Acta Pharmacol. Sin.* **2014**, *35*, 113–123. [CrossRef]
32. Tang, C.; Liang, J.; Qian, J.; Jin, L.; Du, M.; Li, M.; Li, D. Opposing role of JNK-p38 kinase and ERK1/2 in hydrogen peroxide-induced oxidative damage of human trophoblast-like JEG-3 cells. *Int. J. Clin. Exp. Pathol.* **2014**, *7*, 959–968.
33. Xia, M.; Huang, R.; Witt, K.L.; Southall, N.; Fostel, J.; Cho, M.-H.; Jadhav, A.; Smith, C.S.; Inglese, J.; Portier, C.J.; et al. Compound cytotoxicity profiling using quantitative high-throughput screening. *Environ. Health Perspect.* **2008**, *116*, 284–291. [CrossRef] [PubMed]
34. Soto-Otero, R.; Méndez-Alvarez, E.; Hermida-Ameijeiras, A.; Muñoz-Patiño, A.M.; Labandeira-Garcia, J.L. Autoxidation and neurotoxicity of 6-hydroxydopamine in the presence of some antioxidants: Potential implication in relation to the pathogenesis of Parkinson's disease. *J. Neurochem.* **2000**, *74*, 1605–1612. [CrossRef]
35. Halliwell, B.; Whiteman, M. Measuring reactive species and oxidative damage in vivo and in cell culture: How should you do it and what do the results mean? *Br. J. Pharmacol.* **2004**, *142*, 231–255. [CrossRef] [PubMed]
36. Halliwell, B. Oxidative stress in cell culture: An under-appreciated problem? *FEBS Lett.* **2003**, *540*, 3–6. [CrossRef]
37. Goettert, M.; Luik, S.; Graeser, R.; Laufer, S.A. A direct ELISA assay for quantitative determination of the inhibitory potency of small molecules inhibitors for JNK3. *J. Pharm. Biomed. Anal.* **2011**, *55*, 236–240. [CrossRef] [PubMed]
38. Allan, S.M.; Rothwell, N.J. Cytokines and acute neurodegeneration. *Nat. Rev. Neurosci.* **2001**, *2*, 734–744. [CrossRef] [PubMed]
39. Afridi, R.; Lee, W.-H.; Suk, K. Microglia gone awry: Linking immunometabolism to neurodegeneration. *Front. Cell. Neurosci.* **2020**, *14*, 246. [CrossRef] [PubMed]
40. Yu, T.; Li, Y.J.; Bian, A.H.; Zuo, H.B.; Zhu, T.W.; Ji, S.X.; Kong, F.; Yin, D.Q.; Wang, C.B.; Wang, Z.F.; et al. The regulatory role of activating transcription factor 2 in inflammation. *Mediat. Inflamm.* **2014**, *2014*, 950472. [CrossRef]
41. Allan, S.M. The role of pro- and antiinflammatory cytokines in neurodegeneration. *Ann. N. Y. Acad. Sci.* **2000**, *917*, 84–93. [CrossRef]
42. Azam, S.; Haque, M.E.; Kim, I.-S.; Choi, D.-K. Microglial Turnover in Ageing-Related Neurodegeneration: Therapeutic Avenue to Intervene in Disease Progression. *Cells* **2021**, *10*, 150. [CrossRef]
43. Stenvinkel, P.; Ketteler, M.; Johnson, R.J.; Lindholm, B.; Pecoits-Filho, R.; Riella, M.; Heimbürger, O.; Cederholm, T.; Girndt, M. IL-10, IL-6, and TNF-alpha: Central factors in the altered cytokine network of uremia–the good, the bad, and the ugly. *Kidney Int.* **2005**, *67*, 1216–1233. [CrossRef] [PubMed]
44. Påhlman, S.; Ruusala, A.I.; Abrahamsson, L.; Mattsson, M.E.; Esscher, T. Retinoic acid-induced differentiation of cultured human neuroblastoma cells: A comparison with phorbolester-induced differentiation. *Cell Differ.* **1984**, *14*, 135–144. [CrossRef]
45. Xie, H.; Hu, L.; Li, G. SH-SY5Y human neuroblastoma cell line: In vitro cell model of dopaminergic neurons in Parkinson's disease. *Chin. Med. J.* **2010**, *123*, 1086–1092. [PubMed]
46. Lopes, F.M.; Schröder, R.; da Frota, M.L.C.; Zanotto-Filho, A.; Müller, C.B.; Pires, A.S.; Meurer, R.T.; Colpo, G.D.; Gelain, D.P.; Kapczinski, F.; et al. Comparison between proliferative and neuron-like SH-SY5Y cells as an in vitro model for Parkinson disease studies. *Brain Res.* **2010**, *1337*, 85–94. [CrossRef] [PubMed]

47. Glinka, Y.; Gassen, M.; Youdim, M.B. Mechanism of 6-hydroxydopamine neurotoxicity. *J. Neural Transm. Suppl.* **1997**, *50*, 55–66. [CrossRef]
48. Cohen, G.; Heikkila, R.E. The generation of hydrogen peroxide, superoxide radical, and hydroxyl radical by 6-hydroxydopamine, dialuric acid, and related cytotoxic agents. *J. Biol. Chem.* **1974**, *249*, 2447–2452. [CrossRef]
49. Glinka, Y.; Tipton, K.F.; Youdim, M.B. Mechanism of inhibition of mitochondrial respiratory complex I by 6-hydroxydopamine and its prevention by desferrioxamine. *Eur. J. Pharmacol.* **1998**, *351*, 121–129. [CrossRef]
50. Glinka, Y.Y.; Youdim, M.B. Inhibition of mitochondrial complexes I and IV by 6-hydroxydopamine. *Eur. J. Pharmacol.* **1995**, *292*, 329–332. [CrossRef]
51. Glinka, Y.; Tipton, K.F.; Youdim, M.B. Nature of inhibition of mitochondrial respiratory complex I by 6-Hydroxydopamine. *J. Neurochem.* **1996**, *66*, 2004–2010. [CrossRef]
52. Sharma, L.K.; Lu, J.; Bai, Y. Mitochondrial respiratory complex I: Structure, function and implication in human diseases. *Curr. Med. Chem.* **2009**, *16*, 1266–1277. [CrossRef]
53. Tysnes, O.-B.; Storstein, A. Epidemiology of Parkinson's disease. *J. Neural Transm.* **2017**, *124*, 901–905. [CrossRef] [PubMed]
54. Norat, P.; Soldozy, S.; Sokolowski, J.D.; Gorick, C.M.; Kumar, J.S.; Chae, Y.; Yağmurlu, K.; Prada, F.; Walker, M.; Levitt, M.R.; et al. Mitochondrial dysfunction in neurological disorders: Exploring mitochondrial transplantation. *NPJ Regen. Med.* **2020**, *5*, 22. [CrossRef] [PubMed]
55. Manczak, M.; Park, B.S.; Jung, Y.; Reddy, P.H. Differential expression of oxidative phosphorylation genes in patients with Alzheimer's disease: Implications for early mitochondrial dysfunction and oxidative damage. *Neuromol. Med.* **2004**, *5*, 147–162. [CrossRef]
56. Wang, W.; Zhao, F.; Ma, X.; Perry, G.; Zhu, X. Mitochondria dysfunction in the pathogenesis of Alzheimer's disease: Recent advances. *Mol. Neurodegener.* **2020**, *15*, 30. [CrossRef]
57. Du, H.; ShiDu Yan, S. Unlocking the Door to Neuronal Woes in Alzheimer's Disease: Aβ and Mitochondrial Permeability Transition Pore. *Pharmaceuticals* **2010**, *3*, 1936–1948. [CrossRef]
58. Parks, J.K.; Smith, T.S.; Trimmer, P.A.; Bennett, J.P.; Parker, W.D. Neurotoxic Abeta peptides increase oxidative stress in vivo through NMDA-receptor and nitric-oxide-synthase mechanisms, and inhibit complex IV activity and induce a mitochondrial permeability transition in vitro. *J. Neurochem.* **2001**, *76*, 1050–1056. [CrossRef]
59. Hanawa, N.; Shinohara, M.; Saberi, B.; Gaarde, W.A.; Han, D.; Kaplowitz, N. Role of JNK translocation to mitochondria leading to inhibition of mitochondria bioenergetics in acetaminophen-induced liver injury. *J. Biol. Chem.* **2008**, *283*, 13565–13577. [CrossRef]
60. Zorov, D.B.; Juhaszova, M.; Sollott, S.J. Mitochondrial reactive oxygen species (ROS) and ROS-induced ROS release. *Physiol. Rev.* **2014**, *94*, 909–950. [CrossRef]
61. Schroeter, H.; Boyd, C.S.; Ahmed, R.; Spencer, J.P.E.; Duncan, R.F.; Rice-Evans, C.; Cadenas, E. c-Jun N-terminal kinase (JNK)-mediated modulation of brain mitochondria function: New target proteins for JNK signalling in mitochondrion-dependent apoptosis. *Biochem. J.* **2003**, *372*, 359–369. [CrossRef]
62. Melino, G.; Thiele, C.J.; Knight, R.A.; Piacentini, M. Retinoids and the control of growth/death decisions in human neuroblastoma cell lines. *J. Neurooncol.* **1997**, *31*, 65–83. [CrossRef]
63. Cheung, Y.-T.; Lau, W.K.-W.; Yu, M.-S.; Lai, C.S.-W.; Yeung, S.-C.; So, K.-F.; Chang, R.C.-C. Effects of all-trans-retinoic acid on human SH-SY5Y neuroblastoma as in vitro model in neurotoxicity research. *Neurotoxicology* **2009**, *30*, 127–135. [CrossRef] [PubMed]
64. Shipley, M.M.; Mangold, C.A.; Szpara, M.L. Differentiation of the SH-SY5Y Human Neuroblastoma Cell Line. *J. Vis. Exp.* **2016**, 53193. [CrossRef] [PubMed]
65. Presgraves, S.P.; Ahmed, T.; Borwege, S.; Joyce, J.N. Terminally differentiated SH-SY5Y cells provide a model system for studying neuroprotective effects of dopamine agonists. *Neurotox. Res.* **2004**, *5*, 579–598. [CrossRef]
66. Fornari, F.A.; Randolph, J.K.; Yalowich, J.C.; Ritke, M.K.; Gewirtz, D.A. Interference by doxorubicin with DNA unwinding in MCF-7 breast tumor cells. *Mol. Pharmacol.* **1994**, *45*, 649–656. [PubMed]
67. Chen, X.; Ji, Z.L.; Chen, Y.Z. TTD: Therapeutic target database. *Nucleic Acids Res.* **2002**, *30*, 412–415. [CrossRef]
68. López-Carballo, G.; Moreno, L.; Masiá, S.; Pérez, P.; Barettino, D. Activation of the phosphatidylinositol 3-kinase/Akt signaling pathway by retinoic acid is required for neural differentiation of SH-SY5Y human neuroblastoma cells. *J. Biol. Chem.* **2002**, *277*, 25297–25304. [CrossRef]
69. Itano, Y.; Ito, A.; Uehara, T.; Nomura, Y. Regulation of Bcl-2 protein expression in human neuroblastoma SH-SY5Y cells: Positive and negative effects of protein kinases C and A, respectively. *J. Neurochem.* **1996**, *67*, 131–137. [CrossRef]
70. Vroegop, S.M.; Decker, D.E.; Buxser, S.E. Localization of damage induced by reactive oxygen species in cultured cells. *Free Radic. Biol. Med.* **1995**, *18*, 141–151. [CrossRef]
71. Lee, Y.M.; He, W.; Liou, Y.-C. The redox language in neurodegenerative diseases: Oxidative post-translational modifications by hydrogen peroxide. *Cell Death Dis.* **2021**, *12*, 58. [CrossRef]
72. Starkov, A.A. The role of mitochondria in reactive oxygen species metabolism and signaling. *Ann. N. Y. Acad. Sci.* **2008**, *1147*, 37–52. [CrossRef]
73. Hamanaka, R.B.; Chandel, N.S. Mitochondrial reactive oxygen species regulate cellular signaling and dictate biological outcomes. *Trends Biochem. Sci.* **2010**, *35*, 505–513. [CrossRef]

74. Whittemore, E.R.; Loo, D.T.; Watt, J.A.; Cotman, C.W. A detailed analysis of hydrogen peroxide-induced cell death in primary neuronal culture. *Neuroscience* **1995**, *67*, 921–932. [CrossRef]
75. Murphy, M.P. How mitochondria produce reactive oxygen species. *Biochem. J.* **2009**, *417*, 1–13. [CrossRef]
76. Butterfield, D.A.; Castegna, A.; Lauderback, C.M.; Drake, J. Evidence that amyloid beta-peptide-induced lipid peroxidation and its sequelae in Alzheimer's disease brain contribute to neuronal death. *Neurobiol. Aging* **2002**, *23*, 655–664. [CrossRef]
77. Dexter, D.T.; Carter, C.J.; Wells, F.R.; Javoy-Agid, F.; Agid, Y.; Lees, A.; Jenner, P.; Marsden, C.D. Basal lipid peroxidation in substantia nigra is increased in Parkinson's disease. *J. Neurochem.* **1989**, *52*, 381–389. [CrossRef]
78. Pedersen, W.A.; Fu, W.; Keller, J.N.; Markesbery, W.R.; Appel, S.; Smith, R.G.; Kasarskis, E.; Mattson, M.P. Protein modification by the lipid peroxidation product 4-hydroxynonenal in the spinal cords of amyotrophic lateral sclerosis patients. *Ann. Neurol.* **1998**, *44*, 819–824. [CrossRef]
79. Zabel, M.; Nackenoff, A.; Kirsch, W.M.; Harrison, F.E.; Perry, G.; Schrag, M. Markers of oxidative damage to lipids, nucleic acids and proteins and antioxidant enzymes activities in Alzheimer's disease brain: A meta-analysis in human pathological specimens. *Free Radic. Biol. Med.* **2018**, *115*, 351–360. [CrossRef]
80. Andersen, J.K. Oxidative stress in neurodegeneration: Cause or consequence? *Nat. Med.* **2004**, *10*, S18–S25. [CrossRef]
81. Polidori, M.C.; Nelles, G. Antioxidant clinical trials in mild cognitive impairment and Alzheimer's disease—Challenges and perspectives. *Curr. Pharm. Des.* **2014**, *20*, 3083–3092. [CrossRef]
82. Galasko, D.R.; Peskind, E.; Clark, C.M.; Quinn, J.F.; Ringman, J.M.; Jicha, G.A.; Cotman, C.; Cottrell, B.; Montine, T.J.; Thomas, R.G.; et al. Alzheimer's Disease Cooperative Study Antioxidants for Alzheimer disease: A randomized clinical trial with cerebrospinal fluid biomarker measures. *Arch. Neurol.* **2012**, *69*, 836–841. [CrossRef]
83. Kamenecka, T.; Jiang, R.; Song, X.; Duckett, D.; Chen, W.; Ling, Y.Y.; Habel, J.; Laughlin, J.D.; Chambers, J.; Figuera-Losada, M.; et al. Synthesis, biological evaluation, X-ray structure, and pharmacokinetics of aminopyrimidine c-jun-N-terminal kinase (JNK) inhibitors. *J. Med. Chem.* **2010**, *53*, 419–431. [CrossRef]
84. Turrens, J.F. Mitochondrial formation of reactive oxygen species. *J. Physiol.* **2003**, *552*, 335–344. [CrossRef]
85. Korshunov, S.S.; Skulachev, V.P.; Starkov, A.A. High protonic potential actuates a mechanism of production of reactive oxygen species in mitochondria. *FEBS Lett.* **1997**, *416*, 15–18. [CrossRef]
86. Marchi, S.; Giorgi, C.; Suski, J.M.; Agnoletto, C.; Bononi, A.; Bonora, M.; De Marchi, E.; Missiroli, S.; Patergnani, S.; Poletti, F.; et al. Mitochondria-ros crosstalk in the control of cell death and aging. *J. Signal Transduct.* **2012**, *2012*, 329635. [CrossRef]
87. Kim, I.; Rodriguez-Enriquez, S.; Lemasters, J.J. Selective degradation of mitochondria by mitophagy. *Arch. Biochem. Biophys.* **2007**, *462*, 245–253. [CrossRef]
88. Connolly, N.M.C.; Theurey, P.; Adam-Vizi, V.; Bazan, N.G.; Bernardi, P.; Bolaños, J.P.; Culmsee, C.; Dawson, V.L.; Deshmukh, M.; Duchen, M.R.; et al. Guidelines on experimental methods to assess mitochondrial dysfunction in cellular models of neurodegenerative diseases. *Cell Death Differ.* **2018**, *25*, 542–572. [CrossRef]
89. Heslop, K.A.; Rovini, A.; Hunt, E.G.; Fang, D.; Morris, M.E.; Christie, C.F.; Gooz, M.B.; DeHart, D.N.; Dang, Y.; Lemasters, J.J.; et al. JNK activation and translocation to mitochondria mediates mitochondrial dysfunction and cell death induced by VDAC opening and sorafenib in hepatocarcinoma cells. *Biochem. Pharmacol.* **2020**, *171*, 113728. [CrossRef]
90. Lucero, M.; Suarez, A.E.; Chambers, J.W. Phosphoregulation on mitochondria: Integration of cell and organelle responses. *CNS Neurosci. Ther.* **2019**, *25*, 837–858. [CrossRef] [PubMed]
91. Shieh, J.-M.; Huang, T.-F.; Hung, C.-F.; Chou, K.-H.; Tsai, Y.-J.; Wu, W.-B. Activation of c-Jun N-terminal kinase is essential for mitochondrial membrane potential change and apoptosis induced by doxycycline in melanoma cells. *Br. J. Pharmacol.* **2010**, *160*, 1171–1184. [CrossRef] [PubMed]
92. Wang, Y.; Guo, S.-H.; Shang, X.-J.; Yu, L.-S.; Zhu, J.-W.; Zhao, A.; Zhou, Y.-F.; An, G.-H.; Zhang, Q.; Ma, B. Triptolide induces Sertoli cell apoptosis in mice via ROS/JNK-dependent activation of the mitochondrial pathway and inhibition of Nrf2-mediated antioxidant response. *Acta Pharmacol. Sin.* **2018**, *39*, 311–327. [CrossRef]
93. Chauhan, D.; Li, G.; Hideshima, T.; Podar, K.; Mitsiades, C.; Mitsiades, N.; Munshi, N.; Kharbanda, S.; Anderson, K.C. JNK-dependent release of mitochondrial protein, Smac, during apoptosis in multiple myeloma (MM) cells. *J. Biol. Chem.* **2003**, *278*, 17593–17596. [CrossRef]
94. Che, X.-F.; Moriya, S.; Zheng, C.-L.; Abe, A.; Tomoda, A.; Miyazawa, K. 2-Aminophenoxazine-3-one-induced apoptosis via generation of reactive oxygen species followed by c-jun N-terminal kinase activation in the human glioblastoma cell line LN229. *Int. J. Oncol.* **2013**, *43*, 1456–1466. [CrossRef]
95. Fan, P.; Yu, X.-Y.; Xie, X.-H.; Chen, C.-H.; Zhang, P.; Yang, C.; Peng, X.; Wang, Y.-T. Mitophagy is a protective response against oxidative damage in bone marrow mesenchymal stem cells. *Life Sci.* **2019**, *229*, 36–45. [CrossRef]
96. Kilbride, S.M.; Telford, J.E.; Davey, G.P. Complex I controls mitochondrial and plasma membrane potentials in nerve terminals. *Neurochem. Res.* **2021**, *46*, 100–107. [CrossRef]
97. Rhein, V.; Baysang, G.; Rao, S.; Meier, F.; Bonert, A.; Müller-Spahn, F.; Eckert, A. Amyloid-beta leads to impaired cellular respiration, energy production and mitochondrial electron chain complex activities in human neuroblastoma cells. *Cell. Mol. Neurobiol.* **2009**, *29*, 1063–1071. [CrossRef] [PubMed]
98. Wajant, H. The Fas signaling pathway: More than a paradigm. *Science* **2002**, *296*, 1635–1636. [CrossRef]
99. Shi, Y.; Holtzman, D.M. Interplay between innate immunity and Alzheimer disease: APOE and TREM2 in the spotlight. *Nat. Rev. Immunol.* **2018**, *18*, 759–772. [CrossRef]

100. Gupta, S.; Barrett, T.; Whitmarsh, A.J.; Cavanagh, J.; Sluss, H.K.; Dérijard, B.; Davis, R.J. Selective interaction of JNK protein kinase isoforms with transcription factors. *EMBO J.* **1996**, *15*, 2760–2770. [CrossRef]
101. Ventura, J.-J.; Cogswell, P.; Flavell, R.A.; Baldwin, A.S.; Davis, R.J. JNK potentiates TNF-stimulated necrosis by increasing the production of cytotoxic reactive oxygen species. *Genes Dev.* **2004**, *18*, 2905–2915. [CrossRef] [PubMed]
102. Kamata, H.; Honda, S.-I.; Maeda, S.; Chang, L.; Hirata, H.; Karin, M. Reactive oxygen species promote TNFalpha-induced death and sustained JNK activation by inhibiting MAP kinase phosphatases. *Cell* **2005**, *120*, 649–661. [CrossRef] [PubMed]
103. Tong, W.; Chen, X.; Song, X.; Chen, Y.; Jia, R.; Zou, Y.; Li, L.; Yin, L.; He, C.; Liang, X.; et al. Resveratrol inhibits LPS-induced inflammation through suppressing the signaling cascades of TLR4-NF-κB/MAPKs/IRF3. *Exp. Ther. Med.* **2020**, *19*, 1824–1834. [CrossRef] [PubMed]
104. Lai, L.; Song, Y.; Liu, Y.; Chen, Q.; Han, Q.; Chen, W.; Pan, T.; Zhang, Y.; Cao, X.; Wang, Q. MicroRNA-92a negatively regulates Toll-like receptor (TLR)-triggered inflammatory response in macrophages by targeting MKK4 kinase. *J. Biol. Chem.* **2013**, *288*, 7956–7967. [CrossRef] [PubMed]
105. Yim, M.-J.; Lee, J.M.; Choi, G.; Lee, D.-S.; Park, W.S.; Jung, W.-K.; Park, S.; Seo, S.-K.; Park, J.; Choi, I.-W.; et al. Anti-Inflammatory Potential of Carpomitra costata Ethanolic Extracts via Inhibition of NF-κB and AP-1 Activation in LPS-Stimulated RAW264.7 Macrophages. *Evid. Based Complement. Alternat. Med.* **2018**, *2018*, 6914514. [CrossRef] [PubMed]
106. Park, J.-W.; Kwon, O.-K.; Ryu, H.W.; Paik, J.-H.; Paryanto, I.; Yuniato, P.; Choi, S.; Oh, S.-R.; Ahn, K.-S. Anti-inflammatory effects of Passiflora foetida L. in LPS-stimulated RAW264.7 macrophages. *Int. J. Mol. Med.* **2018**, *41*, 3709–3716. [CrossRef]
107. Lim, M.X.; Png, C.W.; Tay, C.Y.B.; Teo, J.D.W.; Jiao, H.; Lehming, N.; Tan, K.S.W.; Zhang, Y. Differential regulation of proinflammatory cytokine expression by mitogen-activated protein kinases in macrophages in response to intestinal parasite infection. *Infect. Immun.* **2014**, *82*, 4789–4801. [CrossRef]
108. Carlson, N.G.; Wieggel, W.A.; Chen, J.; Bacchi, A.; Rogers, S.W.; Gahring, L.C. Inflammatory cytokines IL-1 alpha, IL-1 beta, IL-6, and TNF-alpha impart neuroprotection to an excitotoxin through distinct pathways. *J. Immunol.* **1999**, *163*, 3963–3968.
109. Yasukawa, H.; Ohishi, M.; Mori, H.; Murakami, M.; Chinen, T.; Aki, D.; Hanada, T.; Takeda, K.; Akira, S.; Hoshijima, M.; et al. IL-6 induces an anti-inflammatory response in the absence of SOCS3 in macrophages. *Nat. Immunol.* **2003**, *4*, 551–556. [CrossRef]
110. Walker, D.G.; Whetzel, A.M.; Lue, L.F. Expression of suppressor of cytokine signaling genes in human elderly and Alzheimer's disease brains and human microglia. *Neuroscience* **2015**, *302*, 121–137. [CrossRef]
111. Wichmann, M.A.; Cruickshanks, K.J.; Carlsson, C.M.; Chappell, R.; Fischer, M.E.; Klein, B.E.K.; Klein, R.; Tsai, M.Y.; Schubert, C.R. Long-term systemic inflammation and cognitive impairment in a population-based cohort. *J. Am. Geriatr. Soc.* **2014**, *62*, 1683–1691. [CrossRef]
112. Toulmond, S.; Vige, X.; Fage, D.; Benavides, J. Local infusion of interleukin-6 attenuates the neurotoxic effects of NMDA on rat striatal cholinergic neurons. *Neurosci. Lett.* **1992**, *144*, 49–52. [CrossRef]
113. Yamada, M.; Hatanaka, H. Interleukin-6 protects cultured rat hippocampal neurons against glutamate-induced cell death. *Brain Res.* **1994**, *643*, 173–180. [CrossRef]
114. Pizzi, M.; Sarnico, I.; Boroni, F.; Benarese, M.; Dreano, M.; Garotta, G.; Valerio, A.; Spano, P. Prevention of neuron and oligodendrocyte degeneration by interleukin-6 (IL-6) and IL-6 receptor/IL-6 fusion protein in organotypic hippocampal slices. *Mol. Cell. Neurosci.* **2004**, *25*, 301–311. [CrossRef]
115. Erta, M.; Quintana, A.; Hidalgo, J. Interleukin-6, a major cytokine in the central nervous system. *Int. J. Biol. Sci.* **2012**, *8*, 1254–1266. [CrossRef] [PubMed]
116. Yang, D.D.; Kuan, C.Y.; Whitmarsh, A.J.; Rincón, M.; Zheng, T.S.; Davis, R.J.; Rakic, P.; Flavell, R.A. Absence of excitotoxicity-induced apoptosis in the hippocampus of mice lacking the Jnk3 gene. *Nature* **1997**, *389*, 865–870. [CrossRef] [PubMed]
117. Hoque, A.; Williamson, N.A.; Ameen, S.S.; Ciccotosto, G.D.; Hossain, M.I.; Oakhill, J.S.; Ng, D.C.H.; Ang, C.-S.; Cheng, H.-C. Quantitative proteomic analyses of dynamic signalling events in cortical neurons undergoing excitotoxic cell death. *Cell Death Dis.* **2019**, *10*, 213. [CrossRef] [PubMed]
118. Johnson, J.W.; Kotermanski, S.E. Mechanism of action of memantine. *Curr. Opin. Pharmacol.* **2006**, *6*, 61–67. [CrossRef]
119. Kim, B.-J.; Silverman, S.M.; Liu, Y.; Wordinger, R.J.; Pang, I.-H.; Clark, A.F. In vitro and in vivo neuroprotective effects of cJun N-terminal kinase inhibitors on retinal ganglion cells. *Mol. Neurodegener.* **2016**, *11*, 30. [CrossRef]
120. Centeno, C.; Repici, M.; Chatton, J.Y.; Riederer, B.M.; Bonny, C.; Nicod, P.; Price, M.; Clarke, P.G.H.; Papa, S.; Franzoso, G.; et al. Role of the JNK pathway in NMDA-mediated excitotoxicity of cortical neurons. *Cell Death Differ.* **2007**, *14*, 240–253. [CrossRef]
121. Marcelli, S.; Iannuzzi, F.; Ficulle, E.; Mango, D.; Pieraccini, S.; Pellegrino, S.; Corbo, M.; Sironi, M.; Pittaluga, A.; Nisticò, R.; et al. The selective disruption of presynaptic JNK2/STX1a interaction reduces NMDA receptor-dependent glutamate release. *Sci. Rep.* **2019**, *9*, 7146. [CrossRef]
122. Wang, X.-Q.; Peng, Y.-P.; Lu, J.-H.; Cao, B.-B.; Qiu, Y.-H. Neuroprotection of interleukin-6 against NMDA attack and its signal transduction by JAK and MAPK. *Neurosci. Lett.* **2009**, *450*, 122–126. [CrossRef]
123. Jung, J.E.; Kim, G.S.; Chan, P.H. Neuroprotection by interleukin-6 is mediated by signal transducer and activator of transcription 3 and antioxidative signaling in ischemic stroke. *Stroke* **2011**, *42*, 3574–3579. [CrossRef]
124. Knight, J.M.; Costanzo, E.S.; Singh, S.; Yin, Z.; Szabo, A.; Pawar, D.S.; Hillard, C.J.; Rizzo, J.D.; D'Souza, A.; Pasquini, M.; et al. The IL-6 antagonist tocilizumab is associated with worse depression and related symptoms in the medically ill. *Transl. Psychiatry* **2021**, *11*, 58. [CrossRef]

125. Dafsari, F.S.; Jessen, F. Depression-an underrecognized target for prevention of dementia in Alzheimer's disease. *Transl. Psychiatry* **2020**, *10*, 160. [CrossRef]
126. Lim, G.Y.; Tam, W.W.; Lu, Y.; Ho, C.S.; Zhang, M.W.; Ho, R.C. Prevalence of Depression in the Community from 30 Countries between 1994 and 2014. *Sci. Rep.* **2018**, *8*, 2861. [CrossRef]
127. Snowden, M.B.; Atkins, D.C.; Steinman, L.E.; Bell, J.F.; Bryant, L.L.; Copeland, C.; Fitzpatrick, A.L. Longitudinal association of dementia and depression. *Am. J. Geriatr. Psychiatry* **2015**, *23*, 897–905. [CrossRef]
128. Gao, S.; Howard, S.; LoGrasso, P.V. Pharmacological Inhibition of c-Jun N-terminal Kinase Reduces Food Intake and Sensitizes Leptin's Anorectic Signaling Actions. *Sci. Rep.* **2017**, *7*, 41795. [CrossRef]
129. Ouyang, W.; O'Garra, A. IL-10 Family Cytokines IL-10 and IL-22: From Basic Science to Clinical Translation. *Immunity* **2019**, *50*, 871–891. [CrossRef] [PubMed]
130. Mosser, D.M.; Zhang, X. Interleukin-10: New perspectives on an old cytokine. *Immunol. Rev.* **2008**, *226*, 205–218. [CrossRef] [PubMed]
131. Wang, B.; Rao, Y.-H.; Inoue, M.; Hao, R.; Lai, C.-H.; Chen, D.; McDonald, S.L.; Choi, M.-C.; Wang, Q.; Shinohara, M.L.; et al. Microtubule acetylation amplifies p38 kinase signalling and anti-inflammatory IL-10 production. *Nat. Commun.* **2014**, *5*, 3479. [CrossRef] [PubMed]
132. Guillot-Sestier, M.-V.; Doty, K.R.; Gate, D.; Rodriguez, J.; Leung, B.P.; Rezai-Zadeh, K.; Town, T. Il10 deficiency rebalances innate immunity to mitigate Alzheimer-like pathology. *Neuron* **2015**, *85*, 534–548. [CrossRef] [PubMed]
133. Chakrabarty, P.; Li, A.; Ceballos-Diaz, C.; Eddy, J.A.; Funk, C.C.; Moore, B.; DiNunno, N.; Rosario, A.M.; Cruz, P.E.; Verbeeck, C.; et al. IL-10 alters immunoproteostasis in APP mice, increasing plaque burden and worsening cognitive behavior. *Neuron* **2015**, *85*, 519–533. [CrossRef]
134. Loewenbrueck, K.F.; Tigno-Aranjuez, J.T.; Boehm, B.O.; Lehmann, P.V.; Tary-Lehmann, M. Th1 responses to beta-amyloid in young humans convert to regulatory IL-10 responses in Down syndrome and Alzheimer's disease. *Neurobiol. Aging* **2010**, *31*, 1732–1742. [CrossRef]
135. Lopes, K.O.; Sparks, D.L.; Streit, W.J. Microglial dystrophy in the aged and Alzheimer's disease brain is associated with ferritin immunoreactivity. *Glia* **2008**, *56*, 1048–1060. [CrossRef]
136. Ma, S.L.; Tang, N.L.S.; Lam, L.C.W.; Chiu, H.F.K. The association between promoter polymorphism of the interleukin-10 gene and Alzheimer's disease. *Neurobiol. Aging* **2005**, *26*, 1005–1010. [CrossRef]
137. Zheng, C.; Zhou, X.-W.; Wang, J.-Z. The dual roles of cytokines in Alzheimer's disease: Update on interleukins, TNF-α, TGF-β and IFN-γ. *Transl. Neurodegener.* **2016**, *5*, 7. [CrossRef]
138. Fiebich, B.L.; Batista, C.R.A.; Saliba, S.W.; Yousif, N.M.; de Oliveira, A.C.P. Role of microglia tlrs in neurodegeneration. *Front. Cell. Neurosci.* **2018**, *12*, 329. [CrossRef]
139. Saraiva, M.; Christensen, J.R.; Tsytsykova, A.V.; Goldfeld, A.E.; Ley, S.C.; Kioussis, D.; O'Garra, A. Identification of a macrophage-specific chromatin signature in the IL-10 locus. *J. Immunol.* **2005**, *175*, 1041–1046. [CrossRef] [PubMed]
140. Ma, W.; Lim, W.; Gee, K.; Aucoin, S.; Nandan, D.; Kozlowski, M.; Diaz-Mitoma, F.; Kumar, A. The p38 mitogen-activated kinase pathway regulates the human interleukin-10 promoter via the activation of Sp1 transcription factor in lipopolysaccharide-stimulated human macrophages. *J. Biol. Chem.* **2001**, *276*, 13664–13674. [CrossRef] [PubMed]
141. Kim, C.; Sano, Y.; Todorova, K.; Carlson, B.A.; Arpa, L.; Celada, A.; Lawrence, T.; Otsu, K.; Brissette, J.L.; Arthur, J.S.C.; et al. The kinase p38 alpha serves cell type-specific inflammatory functions in skin injury and coordinates pro- and anti-inflammatory gene expression. *Nat. Immunol.* **2008**, *9*, 1019–1027. [CrossRef]
142. Jarnicki, A.G.; Conroy, H.; Brereton, C.; Donnelly, G.; Toomey, D.; Walsh, K.; Sweeney, C.; Leavy, O.; Fletcher, J.; Lavelle, E.C.; et al. Attenuating regulatory T cell induction by TLR agonists through inhibition of p38 MAPK signaling in dendritic cells enhances their efficacy as vaccine adjuvants and cancer immunotherapeutics. *J. Immunol.* **2008**, *180*, 3797–3806. [CrossRef] [PubMed]
143. Foey, A.D.; Parry, S.L.; Williams, L.M.; Feldmann, M.; Foxwell, B.M.; Brennan, F.M. Regulation of monocyte IL-10 synthesis by endogenous IL-1 and TNF-alpha: Role of the p38 and p42/44 mitogen-activated protein kinases. *J. Immunol.* **1998**, *160*, 920–928. [PubMed]
144. Chanteux, H.; Guisset, A.C.; Pilette, C.; Sibille, Y. LPS induces IL-10 production by human alveolar macrophages via MAPKinases- and Sp1-dependent mechanisms. *Respir. Res.* **2007**, *8*, 71. [CrossRef] [PubMed]
145. Saraiva, M.; O'Garra, A. The regulation of IL-10 production by immune cells. *Nat. Rev. Immunol.* **2010**, *10*, 170–181. [CrossRef]
146. Lowry, O.H.; Rosebrough, N.J.; Farr, A.L.; Randall, R.J. Protein measurement with the Folin phenol reagent. *J. Biol. Chem.* **1951**, *193*, 265–275. [CrossRef]
147. Pukac, L.A.; Carter, J.E.; Morrison, K.S.; Karnovsky, M.J. Enhancement of diaminobenzidine colorimetric signal in immunoblotting. *BioTechniques* **1997**, *23*, 385–388. [CrossRef] [PubMed]
148. Janes, K.A. An analysis of critical factors for quantitative immunoblotting. *Sci. Signal* **2015**, *8*, rs2. [CrossRef] [PubMed]
149. Silva, J.; Alves, C.; Martins, A.; Susano, P.; Simões, M.; Guedes, M.; Rehfeldt, S.; Pinteus, S.; Gaspar, H.; Rodrigues, A.; et al. Loliolide, a New Therapeutic Option for Neurological Diseases? In Vitro Neuroprotective and Anti-Inflammatory Activities of a Monoterpenoid Lactone Isolated from Codium tomentosum. *Int. J. Mol. Sci.* **2021**, *22*, 1888. [CrossRef] [PubMed]

Capítulo V

Artigo científico:

"Neuroprotective effect of Luteolin-7-O-glucoside against 6-OHDA-induced damage in undifferentiated and RA-differentiated SH-SY5Y cells"

Em preparação.

Original article

Neuroprotective effect of Luteolin-7-O-glucoside against 6-OHDA-induced damage in undifferentiated and RA-differentiated SH-SY5Y cells

Stephanie Cristine Hepp Rehfeldt [1], Joana R. Silva [2], Celso Alves [2], Susete Pinteus [2], Rui F. P. Pedrosa [2], Stefan Laufer [3,4], Márcia Inês Goettert[1,*]

[1] Graduate Program in Biotechnology, University of Vale do Taquari (Univates), Lajeado, Rio Grande do Sul, Brazil; srehfeldt@universo.univates.br
[2] Marine and Environmental Sciences Centre (MARE), Polytechnic of Leiria, 2520-630 Peniche, Portugal
[3] Department of Pharmaceutical and Medicinal Chemistry, Institute of Pharmacy, Eberhard Karls Universität Tübingen, Tübingen, Germany.
[4] Tübingen Center for Academic Drug Discovery (TüCAD2), Tübingen, Germany
* Correspondence: marcia.goettert@univates.br and stefan.laufer@uni-tuebingen.de; Graduate Program in Biotechnology, University of Vale do Taquari - Univates, Av. Avelino Talini, 171; 95914-014 – Lajeado, Brazil. Tel.: +555137147000 (ext: 5445) (M. I. G.)

Received: date; Accepted: date; Published: date

Abstract: Luteolin is one of the most common flavonoids present in edible plants and its potential benefits to the central nervous system include decreased microglia activation, neuronal damage and antioxidant properties. The aim of this research was to evaluate the neuroprotective, antioxidant and antiinflammatory effect of luteolin-7-O-glucoside (Lut7). Undifferentiated and retinoic acid (RA)-differentiated SH-SY5Y cells were pretreated with Lut7 and incubated with 6-hydroxydopamine (6-OHDA). Cytotoxic and neuroprotective effects were determined by MTT assay. Antioxidant capacity was determined by DPPH, FRAP, ORAC assays. ROS production, mitochondrial membrane potential ($\Delta\Psi m$), caspase–3 activity and nuclear damage were also determined in SH-SY5Y cells. TNF-α, IL-6 and IL-10 releases were evaluated in LPS-induced RAW264.7 cells by ELISA assay. In undifferentiated SH-SY5Y cells, Lut7 increased cell viability after 24h, while in RA-differentiated SH-SY5Y cells Lut7 increased cell viability after 24 and 48h. Lut7 showed a high antioxidant activity when compared with synthetic antioxidants. In undifferentiated cells Lut7 conferred a preventive effect in mitochondria membrane depolarization induced by 6-OHDA exposition, decreased caspase-3 activity, and inhibited nuclear condensation and fragmentation against 6-OHDA-induced apoptosis. In LPS-stimulated RAW264.7 cells Lut7 reduced TNF-α levels after a 3h treatment and increased IL-10 levels after 24h. In summary, our results show that Lut7 could be a viable alternative to clinical treatment of neurodegenerative diseases.

Keywords: 6-hydroxydopamine; Apoptosis; Mitochondrial membrane Potential; Neurodegenerative diseases; Oxidative stress; Cell Culture Techniques; Neurodegenerative Disorders; Neuroprotective Effect; Biological Products.

1. Introduction

Neurodegenerative diseases (ND) are composed of distinct and heterogeneous disorders characterized by progressive and selective loss of neurons which reflects directly on the major phenotype of the disease. Usually, prevalence and symptom worsening are intimately related to age, and, since the global population is getting older the need for a treatment for ND and better understanding of the entire pathophysiology are urgent. In fact, the World Health Organization (WHO) estimates that by 2040, ND such as Alzheimer's disease (AD) and other types of dementia and conditions that compromises motor function like Parkinson's disease (PD) or amyotrophic lateral sclerosis (ALS) will be the second most prevalent cause of death, after cardiovascular

diseases [1] . However, due to the heterogeneity of NDs, the development of an efficient disease-modifying treatment may be tricky [2] and synthetic drugs frequently evaluated in *in vitro* models and clinical trials provide poor results due to uncountable reasons.

Luteolin, a phytochemical that belongs to the flavone class of polyphenols is one of the most common flavonoids present in edible plants and its potential benefits to the CNS include decreased microglia activation and neuronal damage [3–5]. However, the glycosylated form of luteolin, known as Cyranoside or Luteolin-7-O-glucoside (Lut7) (PubChem ID 5280637) was reported as a selective JNK3 inhibitor, five times more selective for JNK3 than luteolin [6]. The overall importance of JNK signaling in brain development relies on basal functions such as regulating region-specific neuronal death or migration and neuronal polarity, neuronal regeneration, learning and memory for example. In fact, embryonic death occurs in mice lacking either MKK4 or MKK7 genes or JNK1, JNK2 and JNK3 genes [7]. In humans, both JNK1 and JNK2 genes are expressed in all tissues, whereas JNK3 is restricted almost exclusively to the CNS. Further studies have identified that JNK3 is highly expressed and activated in brain tissue and cerebrospinal fluid in patients with AD and was found to be statistically correlated with the level of cognitive decline [8,9], while the JNK3 inhibition led to significant reduction of Aβ plaque burden, cell death markers and the release of pro-inflammatory cytokine in AD in vivo models [10]. Additionally, evidence suggests that patients with neurodegenerative diseases such as AD might benefit with a natural product-based therapy [11].

The effect of herbal extracts containing Lut7 as a majoritary compound was extensively explored in the literature. However, it is not possible to confirm that those reported effects are a result of the Lut7 activity or if other components are mediating the observed effects. Studies evaluating the effect of isolated Lut7 are less common. In this sense, the aim of this research was to evaluate the effects of Lut7 in an in vitro human neuronal stress model induced by 6-hydroxidopamine (6-OHDA) in both undifferentiated and differentiated SH-SY5Y cells.

2. Materials and methods

2.1 Cell lines and reagents

Dulbecco's modified Eagle medium (DMEM) (D5523), F12 (N6760), heat-inactivated fetal bovine serum (FBS) (F4135), 6-hydroxydopamine hydrobromide (6-OHDA) (162957), 3-[4,5-dimethylthiazol-2]-2,5 diphenyltetrazolium bromide (MTT) (M5655), Penicillin (P3032), Streptomycin (S9137), LPS (from *Escherichia coli,* O111:B4, L2630), Trypsin-EDTA (T4049), 2′,7′-Dichlorofluorescin diacetate (DCFDA) (D6883), Caspase-3 Activity Fluorimetric kit (CASP3F), 2,4,6-Tris(2-pyridyl-s-triazine (TPTZ) (T125) were purchased from Sigma-Aldrich™ (St. Louis, MO, USA). DMEM (1200-058) used to culture RAW264.7 cell line and enzyme-linked immunosorbent assay (ELISA) kits for TNF-α, IL-6, and IL-10 were obtained was acquired from Gibco®, Invitrogen Life Science Technologies (Grand Island, NY, USA). All-trans-retinoic acid (ATRA) (SC200898) were purchased from Santa Cruz Biotechnology, (Dallas, TX, USA). PE Annexin V Apoptosis Detection Kit I was purchased from BD Biosciences (USA). Spectrophotometer analysis was performed using SpectraMax® i3 (Molecular Devices, San Jose, CA, USA). 5,5,6,6-tetrachloro-1,1,3,3-tetraethylbenzimidazolylcarbocyanine iodide (JC-1) staining is from Molecular Probes (Eugene, OR, USA) and 4,6-diamidino-2-phenylindole (DAPI) staining was obtained from Applichem (Darmstadt, Germany). Photographs for the DAPI probe were taken with a fluorescence microscope Zeiss, model Axio Vert. A1, (Oberkochen, Germany). SH-SY5Y (ATCC® CRL-2266™) and RAW264.7 cell line (ATCC® TIB-71™) were acquired from American Type Culture Collection (ATCC). Lut7 (26-S) from Extrasynthese (Genay, Cedex, France) was kindly donated by Dr. Stefan Laufer. MAPK inhibitors (SP600125 and SB203580) were synthesized by research of Prof. Dr. Stefan Laufer with a high purity grade (≥95%).

2.2 Cell culture methods

2.2.1 SH-SY5Y cell line.

Undifferentiated human SH-SY5Y neuroblastoma cells were cultured in DMEM mixed with F12 (1:1) and supplemented with 10% (v/v) FBS and 1% streptomycin/penicillin under controlled conditions in a 95% humidified atmosphere, at 37 °C and 5% CO_2. Culture medium was replaced every two days until the cells

reached confluence 4–5 days after the initial seeding. For subculture, SH-SY5Y cells were dissociated with trypsin-EDTA, split into a 1:3 ratio. Cells were grown to 80% confluence before treatment. Culture conditions were performed according to ATCC recommendations.

2.2.2 SH-SY5Y differentiation protocol

To differentiate the SH-SY5Y cells we adapted a protocol previously described and exposed cells to 10 μM of ATRA for 10 days. The medium was changed every 4 days.

2.2.3 RAW264.7 cell line

RAW264.7 cells were cultured in DMEM supplemented with 10% (v/v) of FBS and 1% of streptomycin/penicillin. The medium was replaced every 2 to 3 days. Sub-culturing was carried out with a cell scraper at a 1:4 split ratio. All procedures were in accordance with ATCC recommendations.

2.3 Determination of cell viability and neuroprotection potential by MTT assay

2.3.1 MTT assay and cytotoxicity of Lut7

Cell viability was assessed using the colorimetric MTT assay [12]. SH-SY5Y (differentiated and undifferentiated) and RAW264.7 cells were seeded in 96-well dishes and left overnight in the incubator for proper attachment. Cells were exposed to different concentrations (10 - 0.1μM) of Lut7 for 24 or 48 hours. At the end of the incubation period, MTT reagent was applied to each well at a final concentration of 5 mg/ml and the plate was placed in a humidified incubator at 37 °C with 5% of CO_2 for a further 3 hours period. Formazan salts were dissolved in DMSO and the colorimetric determination of reduction of MTT was determined at 570 nm wavelength using the spectrophotometer SpectraMax® i3. Control cells treated with maintenance media were considered to be 100% viable.

2.3.2 Neuroprotection potential

Neuroprotection effect was assessed using the colorimetric MTT assay with adaptations as previously described [12,13]. To investigate the neuroprotective potential of the compound SH-SY5Y (differentiated and undifferentiated) cells were seeded at a density of $2x10^4$ per well in a 96-well dish and left overnight in the incubator. Next, the media was replaced with different concentrations (1 or 0.1 μM) of Lut7 for 30 minutes before adding 100 μM of 6-OHDA stabilized with 0,02% of ascorbic acid to avoid auto-oxidation of 6-OHDA. After 24 or 48 hours, the treatment was removed, and it was added MTT (5 mg/mL) for 3 hours. Following the MTT removal, DMSO was used to dissolve the formazan salts and the OD was evaluated at 570 nm using a spectrophotometer (SpectraMax®).

2.4 Determination of antioxidant activity

The antioxidant activity determined by using different methodologies as described previously [14]. The analysis included: (a) 2,2-diphenyl-1-picrylhydrazyl (DPPH) radical scavenging ability [15]; (b) oxygen radical absorbance capacity (ORAC) [16]; and (c) ferric reducing antioxidant power (FRAP) assays [17] with few adaptations as described by Silva et al. 2021. [14].

2.5 Mechanisms of cell recovery after 6-OHDA-induced damage induced by Lut7

2.5.1 Mitochondrial Membrane Potential (MMP) assay

Cells were seeded in 96-well plates and left overnight in the incubator. Next, SH-SY5Y cells were treated with 6-OHDA (100 μM) for 6 h, in the absence or presence of Lut7 (0.1 or 1 μM). After the appropriate period of exposure, cells were washed with PBS 1X and incubated with JC-1 at 37°C for 30 min. Then, the reagent was gently removed, and cells were washed with PBS 1X. 100 μL/well of PBS 1X was added and the fluorescence was measured at 540/570 nm (red fluorescence) and 485/535 nm (green fluorescence) using a fluorescence microplate reader SpectraMax® i3. Mitochondrial membrane potential was estimated by measuring the

fluorescence of free JC-1 monomers (green) and JC-1 aggregates in mitochondria (red) and the results were expressed as the ratio of the monomers/aggregates of JC-1 in percentage of control.

2.5.2 ROS production

The levels of reactive oxygen species (ROS) were determined using the oxidations sensitive fluoroprobe 5-(and-6)-carboxy-2′,7′-dichlorodihydrofluorescein diacetate (carboxy-H2DCFDA) as previously described [18] with modifications. In brief, SH-SY5Y cells were treated with Lut7 at different concentrations (0.1 or 1 μM) and 100 μM 6-OHDA for 6 h. Following treatment, cells were washed with PBS (1X). Then, 20 μM carboxyH2DCFDA dissolved in serum-free medium was added to the cells. After 1h at 37 ºC the fluorescence was read at 527 nm, with an excitation wavelength of 495 nm. All experiments were performed at least three times.

2.5.3 Caspase 3 activity

This activity was assessed using the Caspase-3 Activity Fluorometric kit, according to manufacturer's instructions. SH-SY5Y cells were cultured in 6-well plates and treated with 6-OHDA (100 μM) for 6 h in the presence or absence of Lut7 (0.1 or 1 μM). Caspase-3 activity was calculated by the slope of the linear phase of the fluorescence resulting from the rhodamine 110 accumulation and expressed in arbitrary fluorescence units per mg protein per minute (Δ fluorescence (a.u.)/mg protein/min).

2.5.4 DAPI staining

The nucleic condensation was determined by 4,6-diamidino-2-phenylindole (DAPI) staining. SH-SY5Y cells were cultured in 6-well plates and treated with 6-OHDA (100 μM) for 24 h in the presence or absence of Lut7 (0.1 or 1 μM). The cells were fixed in paraformaldehyde (4%) for 30 min. After this time, it was removed, and cells incubated in Triton X-100 (0.1%) for 30 min. Then, Triton X-100 was removed, followed by the addition of DAPI (1 μg/mL) solution. After a 30 min reaction, DAPI was removed, and 1 mL PBS (pH 7.4) was added to each well. Then, the cells were observed through an Axio Vert. A1 fluorescence microscope (Zeiss).

2.6 Cytokine determination in RAW264.7 cell line

RAW264.7 cells were seeded at a density of, $5x10^5$ cells per well in a 24-dish plate. After adherence time, cells were pretreated for 1 hour before LPS (1μg/mL) was added. The supernatant was collected at different times. To evaluate TNF-α release, samples of supernatant were collected after 3 and 24 hours of treatment. For IL-6 analysis, samples were collected after 12 hours of treatment. For IL-10, samples were analyzed after 48 hours of treatment. All samples were frozen at -80ºC until the analysis. The ELISA assay was performed according to the manufacturer's instructions. The absorbances were measured at 450 nm and 570 nm using a spectrophotometer (SpectraMax® i3). Values of 570 nm were subtracted from those of 450 nm to remove background interference. TNF-α, IL-6 and IL-10 standard curves were used to quantify the release from each cytokine by the cells.

2.7 Statistical analysis

The statistical analysis was performed on GraphPad Prism 6.0 software using ANOVA. The results are expressed in mean ± standard deviation mean (SEM). A $p<0.05$ was considered statistically significant.

3. Results

3.1. Cytotoxic and neuroprotective effect of Lut7 *in undifferentiated and RA-differentiated SH-SY5Y cells*

The first set of analyses examined the impact of Lut7 on cell viability. The results, as shown in Figure 1A, indicate that in SH-SY5Y cells, Lut7 at 10 μM reduced cell viability by 33% ($p = 0.002$). At 1 μM and 0.1 μM did not appear to influence cell viability.

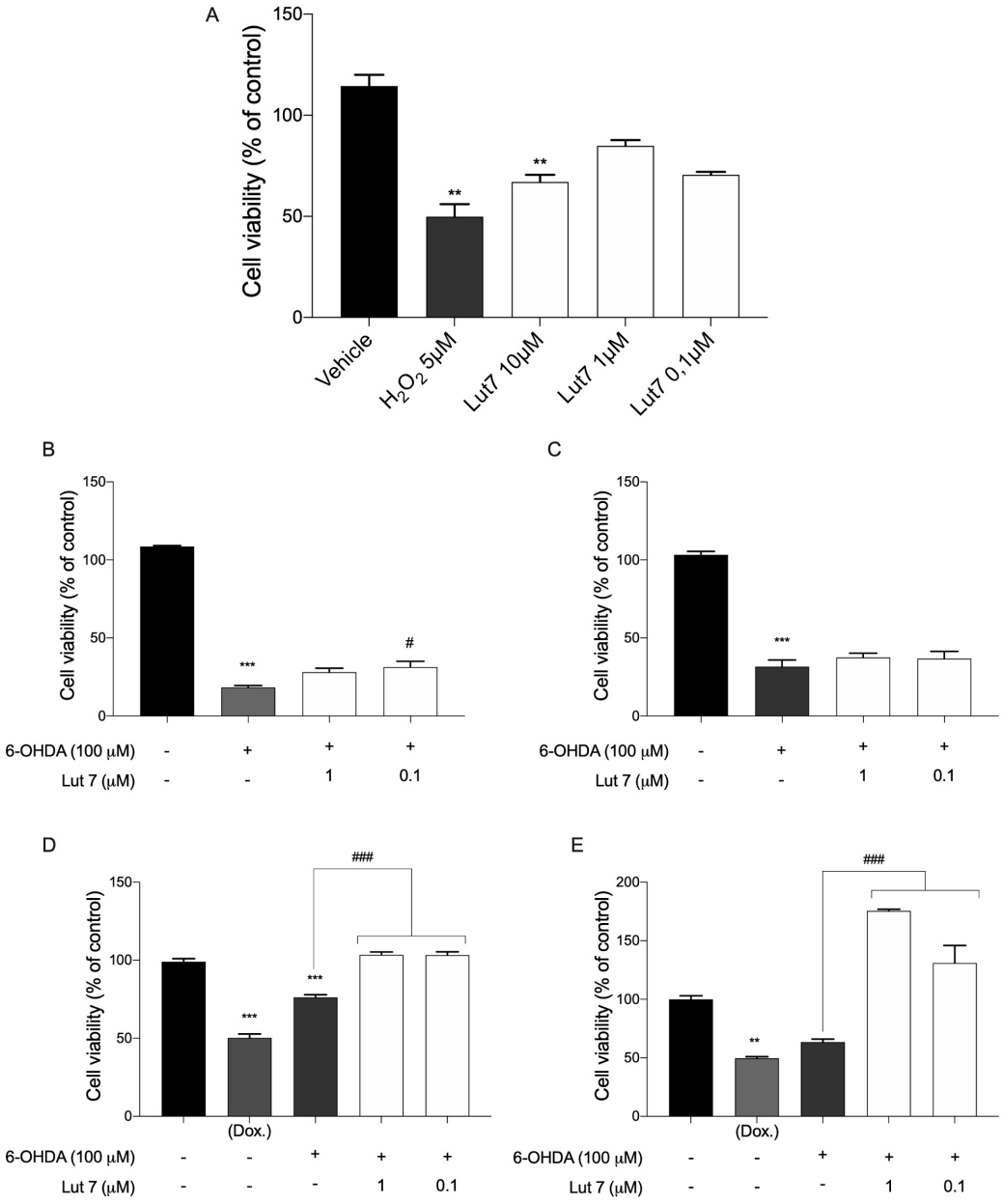

Figure 1. (a) Cytotoxicity induced by Luteolin-7-O-glucoside (Lut7) on SH-SY5Y cell viability after a 24-h incubation period in SH-SY5Y cells; Neuroprotective effect of Lut7 against 6-OHDA (stabilized with 0.02% of ascorbic acid) induced neurotoxicity on undifferentiated SH-SY5Y cells and RA-differentiated SH-SY5Y cells. SH-SY5Y cells were pre-treated with different concentrations Lut7 for 1 hour, prior to 6-OHDA exposure. Undifferentiated cells were incubated for **(b)** 24 hours and **(c)** 48 hours. Cells were differentiated in 10-µM retinoic acid (RA) and the effect was also evaluated in RA-differentiated cells after **(d)** 24 hours and **(e)** 48 hours. The results are the mean ± SEM of at least three experiments in triplicates. Statistical calculations were performed by ANOVA via the Tukey post hoc test. Statistical significance values were *** P<0.001; ** P<0.01; * P<0.05 (vs. control); ### P<0.001; ## P<0.01; # P<0.05 (vs. 6-OHDA). Doxorubicin was used as positive control; DMSO 0.1% was used as vehicle.

After the viability assay, the capacity of undifferentiated SH-SY5Y cells to recover from the 6-OHDA stimuli was evaluated using an MTT assay. For this assay specifically, cells were pretreated with Lut7 for 1h before 6-OHDA treatment. The exposition of SH-SY5Y cells to 6-OHDA (100 μM) led to a reduction of cell viability after 24 hours incubation when compared to negative control. However,

when cells treated with Lut7 at 0.1 μM showed an increase of 13% (p = 0.017) in cell viability when compared to cells treated with 6-OHDA only (Figure 1 B). We also verified if the effect of Lut7 persisted after 48h but the results were not statistically significant (Figure 1C).

After differentiation, cells start to upregulate genes involved with antioxidant defense. This modified profile of gene expression reflects directly in the capacity of cells to recover from the oxidative stress caused by 6-OHDA. To confirm this higher resistance, one positive control of Doxorubicin (10 μM) was included. The mechanism of action of doxorubicin is by specifically blocking the activity of enzyme topoisomerase II, which is involved in DNA replication during mitosis and does not interfere in oxidative stress and, therefore, doesn't impact the damage caused by 6-OHDA. In this sense, we differentiated SH-SY5Y cells for 10 days before the MTT assay. RA-differentiated SH-SY5Y cells pretreated with Lut7 at 1 and 0.1 μM increased cell viability in 27.4 and 27.1%, respectively (p<0.001) (Figure 1D). Surprisingly, after 48 hours of treatment, RA-differentiated SH-SY5Y cells pretreated with Lut7 at 1 μM showed an increase in cell viability of 112% (p<0.001), while a pretreatment with Lut7 at 1 μM increased cell viability in 67.5% (<0.001) (Figure 1E).

3.2 Lut7 presented an important antioxidant activity

To evaluate the antioxidant activity of Lut7, we used three different approaches. We used a) ORAC method to evaluate the presence of antioxidant molecules with the ability to neutralize the peroxyl radicals; b) DPPH assay to determine the capacity of Lut7 to scavenge the radical DPPH and; c) FRAP to determine the Lut7 capacity of reducing ferric ions. The results of antioxidant activities are presented in Table 1 and Figure 2.

Samples	**Assay**		
	DPPH[a]	**FRAP[b]**	**ORAC[c]**
Lut7	6.80 (0.76 – 0.90)	19,570.78 ± 291.48	8,804.19 ± 409.99
BHT	>100	2,821.50 ± 63.03	143.70 ± 23.36

Table 1. Antioxidant activity of Lut7 and BHT (butylated hydroxytoluene) (used as a standard). The values in the table represent the mean ± SEM from 3 independent experiments. a radical scavenging activity (IC50 μg/mL); b The difference between the absorbance of test sample and the blank reading was calculated and expressed as μM of FeSO4 per gram of compound; c ORAC values were expressed as Trolox equivalents by using the standard curve calculated for each assay. Results presented in μM of Trolox equivalent (TE)/g of compound.

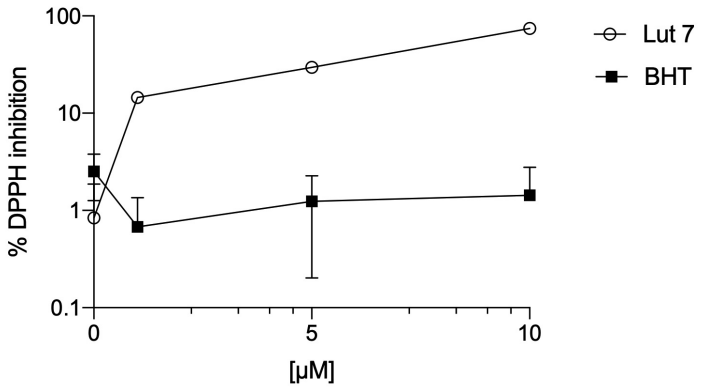

Figure 2. DPPH assay of Lut7.

We observed that Lut7 presented the highest potential of scavenging DPPH radical with an IC_{50} of 6.80 μM (0.76 – 0.90) with a 95% confidence interval when compared to the standard BHT (IC_{50} > 100 μM). In the ORAC method Lut7 showed the highest antioxidant activity, 8,804.19 ± 409.99 μmol of Trolox/ g compound when compared with BTH (143.70 ± 23.36 μmol of Trolox/g compound). Lut7 also revealed to be effective in reducing ferric ions (19,570.78 ± 291.48 μM $FeSO_4$/g of compound) when compared with a synthetic antioxidant.

3.3 Lut7 *protects against cellular hallmarks associated with ND*

Some hallmarks of the apoptotic cell death include the activation of caspases, the disruption of mitochondrial membrane potential and DNA fragmentation. These same events are also present during neurodegenerative diseases. To verify if the neuroprotective effect demonstrated by Lut7 on the viability of SH-SY5Y cells was associated with ND hallmarks, we performed different *in vitro* assays on cells treated with neurotoxin 6-OHDA in the absence or presence of Lut7 (Figure 3).

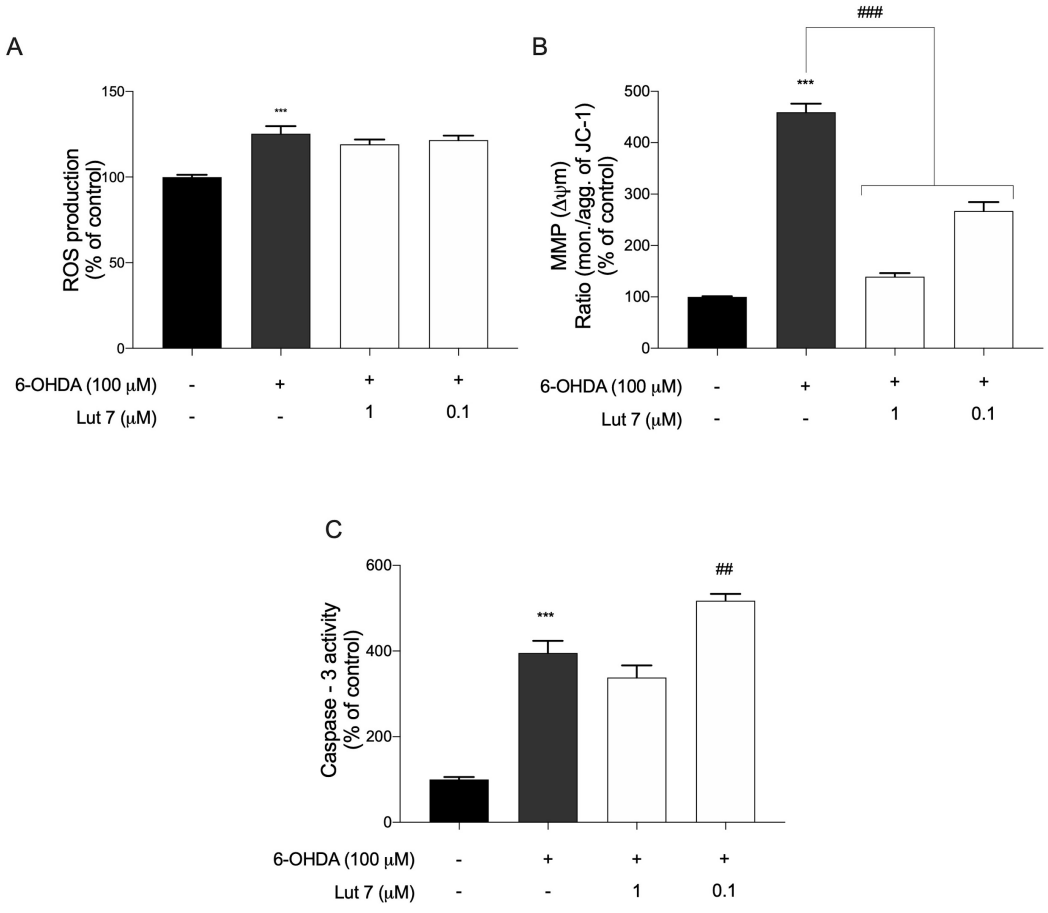

Figure 3. Effect of Luteolin-7-O-glucoside (Lut7) on SH-SY5Y cells after 6-OHDA (100 μM) exposition for 6 hours. **(A)** Effect on ROS production; **(B)** Effect on MMP and; **(C)** caspase-3 activity. The values in each column represent the mean ± standard error of the mean (SEM) from 3 to 4 experiments. Symbols represent statistically significant differences ($p<0.05$, ANOVA, Dunett's test) when compared to: * untreated cells (control). # to 6-OHDA

Firstly, we measured ROS production to evaluate the ability of Lut7 to prevent the condition of oxidative stress induced by the neurotoxin. As expected, after exposing SH-SY5Y cells to 6-OHDA

(100 μM, 6 hours) we observed a two-fold increase in ROS levels when compared to vehicle. However, Lut7 does not appear to influence ROS production after 6-OHDA exposure (Figure 3A).

Secondly, we determined the MMP in order to measure the mitochondrial dysfunction and to understand if the neuroprotective effects of Lut7 were mediated by biological events that usually take place on mitochondria. Treatment with 6-OHDA at 100 μM for 6 hours induced a depolarization of the MMP in SH-SY5Y cells when compared to vehicle. After treating cells with Lut7, on the other hand, we observed a preventive effect against the depolarization of MMP. In this sense, Lut7 at 1 μM reverted the 6-OHDA-induced depolarization in 320% (139.2 ± 7.07% of vehicle, $p<0.001$), while Lut7 at 0.1 μM showed a similar but less intense effect, with 192% decrease in monomers/aggregates ratio of JC-1 (297.2 ± 17.1% of vehicle, $p<0.001$) (Figure 3B).

Thirdly, Caspase-3 activity was measured to understand if the Lut7 had capability to prevent the cell death mediated by apoptosis when exposed to the neurotoxin 6-OHDA. Compared to the 6-OHDA group, Lut7 at 1 promoted a discrete decrease in caspase-3 activity in 57.55% but not statistically significant. Lut7 at 0.1, on the other hand, led to an increase in caspase-3 activity of 121.8% ($p = 0.007$) (Figure 3C).

Finally, to understand if Lut7 had the ability to prevent the DNA fragmentation induced by 6-OHDA treatment, the integrity of SH-SY5Y DNA was evaluated by DAPI staining. Cell death by apoptosis was investigated through fluorescence microscopy as shown in Figure 4.

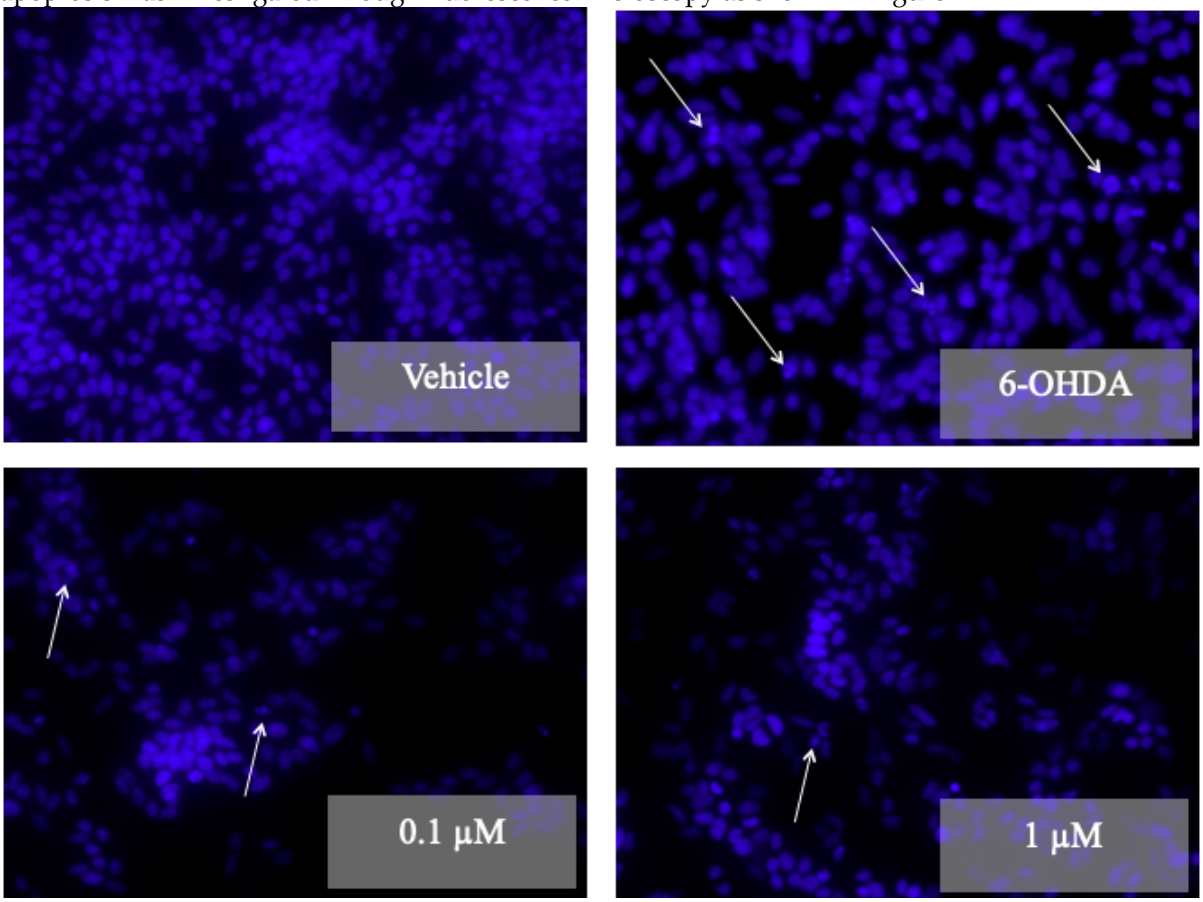

Figure 4. Nuclear morphology of SH-SY5Y cells stained with DAPI probe. SH-SY5Y cell stained with DAPI showing the anti-apoptotic effect of the Lut7 (0.1 or 1 μM) against neurotoxicity mediated by 6-OHDA (100 μM; 24hours). The fragmentation pattern is an indicator of apoptosis. * the images are representative of one experiment.

We exposed SH-SY5Y cells to 100 μM of 6-OHDA for 24 hours and observed nuclear condensation and fragmentation, characteristic features of apoptosis. However, it was possible to verify that Lut7 inhibited apoptosis due to nuclear condensation and fragmentation induced by 6-OHDA.

3.4 Effects of Lut7 on LPS-induced cytokine production

Cytokines play a crucial role in the inflammatory response but before evaluating the effect of Lut7 over cytokine release, we determined its cytotoxic effect over the RAW267.4 cell line. Since Lut7 at 10 μM reduced cell viability in SH-SY5Y, we evaluated the cytotoxic effect of Lut7 at 1 and 0.1 μM in RAW264.7 cells. At both concentrations, no significant reduction in cell viability was found compared with control (Figure 5A). After confirming Lut7 was not cytotoxic, we evaluated proinflammatory cytokines (IL-6 and TNF-α), and an antiinflammatory cytokine (IL-10).

In this sense, RAW264.7 cells were pretreated with Lut7 at 1 μM or 0.1 μM for 1h. Then, 1μg/mL of LPS was added to each well and the supernatant was collected on different times. According to our results, the effect of Lut7 over IL-6 was discrete. Lut7 at 1 μM decreased in 1.56% ($p>0.99$), while Lut7 at 0.1 μM increased in 8.43% ($p>0.99$) (Figure 5B). As illustrated in Figure 5C, after 3 hours, cells pretreated with Lut7 at 1 μM showed a decreased TNF-α levels in 30.97% ($p<0.01$), while treatment with Lut7 at 0.1 μM decreased TNF-α levels in 43.02% ($p<0.001$). Figure 5D shows the TNF-α levels after 24h. Lut7 at 1 μM and 0.1 μM promoted a discrete decrease in TNF-α levels (21.69% and 28.92%, respectively), but the differences between groups did not meet conventional levels of statistical significance ($p = 0.21$ and 0.08, respectively). To investigate the IL-10 release, which is delayed, we collected the supernatant after 24 and 48 hours of treatment. After 24h, Lut7 at 1 μM increased IL-10 in 37.58% ($p = 0.38$), while Lut7 at 0.1 μM increased in 96.9% ($p<0.001$) (Figure 5E). However, these effects were not sustained for a 48h period of time, as Lut7 at 1 μM increased in 7.39% ($p>0.99$) and Lut7 at 0.1 μM increased in 4.3% ($p>0.99$) (Figure 5F).

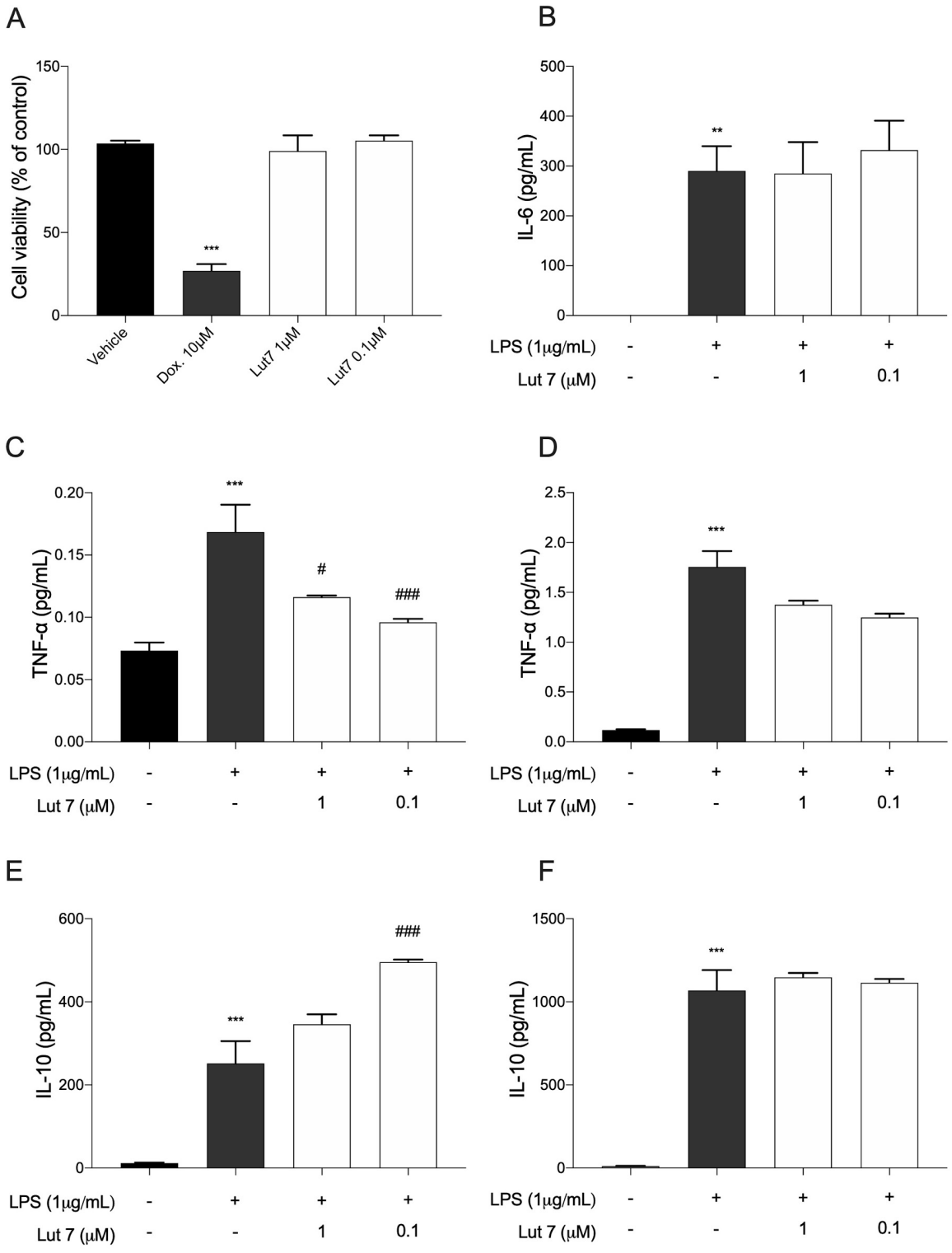

Figure 5. (A) Cytotoxicity induced by Luteolin-7-O-glucoside (Lut7) on RAW264.7 cell viability after a 24-h incubation period; **(B)** IL-6 was determined after 12 hours of treatment; (C) TNF-α levels after 3 hours and (**D**) after 24 hours of treatment. IL-10 was evaluated **(E)** after 24 hours; and after **(F)** 48 hours of treatment. Mean ± SEM of at least three experiments. *** P<0.001; ** P<0.01; * P<0.05 (vs. control); ### P<0.001; ## P<0.01; # P<0.05 (vs. LPS). Doxorubicin was used as positive control; DMSO 0.1% was used as vehicle.

4. Discussion

Pre-clinical studies reported that luteolin, a flavonoid present in many fruits and vegetables, has anti inflammatory and antioxidative properties [19–22]. However, the impact on neuroprotection using the RA-differentiated SH-SY5Y cell line has been poorly explored. Despite both differentiated and undifferentiated SH-SY5Y cells have been used in experiments as suitable in vivo models of NDs, authors suggest that cells should be differentiated since undifferentiated cells are prevenient from a metastatic tumor and continuously undergo division, making it difficult to predict the effect of protective agents against neurotoxins. Indeed, differences in gene expression profiles, antioxidant capacity, synthesis of neurotransmitters and other phenotypic aspects have been observed between differentiated and undifferentiated cells [23–25]. Those findings suggest that SH-SY5Y cell line may respond to the 6-OHDA stimuli differently, depending on whether they are differentiated or not.

In undifferentiated SH-SY5Y cells, our findings do not support a significant neuroprotection effect. These results are similar to a previous study where Lut7 also did not show statistically difference in cell viability when SH-SY5Y cells were incubated with an amyloidogenic molecule [26]. On the other hand, on RA-differentiated cells, Lut7 showed an important protective effect against 6-OHDA-induced damage, probably due to its increased ability of expressing genes related to antioxidant defenses. This is consistent with what has been found in previous study where RA-induced differentiation of SH-SY5Y cells has been related with resistance to oxidants, possibly due to modulation of ROS production and oxidative stress responses [27–30]. This result ties well with previous studies wherein intensified oxidative phosphorylation in differentiated SH-SY5Y was observed [31].

Here, by three separate methodologies, we demonstrate that Lut7 has a high antioxidant capacity. This potential is especially interesting as neuron cells have a high metabolic rate, continuously generating reactive oxygen species (ROS) during aerobic metabolism as a result of electron transport chain (ETC) action during oxidative phosphorylation. As a consequence, brain tissue is particularly susceptible to oxidative stress [32,33]. Several events have been associated with neurodegeneration such as synaptic dysfunction, excitotoxicity, and oxidative stress. Indeed, because of its high metabolic rate combined with a limited capacity of cellular regeneration, the brain is particularly sensitive to oxidative damage.

The neurotoxin 6-OHDA is a potent inhibitor of complex I and causes direct oxidative damage through superoxide and hydrogen peroxide production and indirect damage after suffering auto-oxidation, generating even more ROS [34–37]. In order to evaluate the ROS production and the capacity of Lut7 to promote cell recovery after 6-OHDA-induced damage, we used undifferentiated SH-SY5Y cells due to their less antioxidant scavenging capacity. Our findings revealed that Lut7 did not affect ROS production. Another study reported that Lut7 did not interfere on hepatitis B virus-induced intracellular ROS accumulation in HepG2 cells [38]. However, in contrast to our results, some previous studies reported that Lut7 decreases ROS in many cell lines or in vivo models. Our divergent findings may be a result of the concentration of Lut7 we used in our experiments and/or the cell line used. Palombo et al. (2016) evaluated ROS production in IL-22 or IL-6-stimulated human keratinocytes (HEKn cells). At 20 μM, Lut7 treatment reduced ROS generation [39]. Similarly, in HUVEC cells (human umbilical vein endothelial cells) Lut7 at 20 μM reduced ROS generation and downregulated genes involved in inflammation [40].

A correlation between mitochondrial membrane potential ($\Delta\Psi$m) and reactive oxygen species (ROS) production has been demonstrated [41–43]. Additionally, $\Delta\psi$m depolarisation is usually correlated with neuronal death [44,45] . In this case, our results indicate that Lut7 reverted the 6-OHDA-induced $\Delta\psi$m depolarisation. Similarly, although ROS levels were not affected by Lut7, HepG2 cells normalized ROS-induced MMP damage [38]. The MMP recovery mediated by Lut7 we observed in SH-SY5Y cells after 6-OHDA-induced cell injury was similar to another previous study with cisplatin-induced HK-2 cells (human proximal tubule cell line). According to Nho et al. (2018), Lut7 decreased cell death, promoted a recovery in MMP and abolished caspase-3 activity [46]. Here, we also identified an decrease in caspase-3 activity induced by Lut7 in SH-SY5Y cells exposed to 6-OHDA. In H9c2 cells (rat cardiomyoblast cell line), Lut7 pretreatment reduced apoptosis, intracellular ROS, chromatin condensation and DNA damage, and reverted mitochondrial dysfunction induced by

doxorubicin [47]. Another study reported similar results in H9c2 cells (reduction of apoptosis, ROS generation and mitochondrial dysfunction) but also showed downregulation of caspase-3, p-ERK1/2, p-JNK and p-P38 inhibition, and p-ERK5 activation in angiotensin II-induced cells [48].

It was reported that mitochondrial dysfunction is mediated by JNK activation, while the JNK inhibition by SP600125 prevented both the loss of $\Delta\psi m$ and the increase in apoptosis by inhibiting JNK activation in different cell types [49–52]. One possible explanation for these findings is that JNK plays a significant role in apoptosis via the intrinsic pathway (also known as the 'mitochondrial pathway'), which is activated by extracellular or intracellular perturbations usually found in AD, such as oxidative stress. In response to a deleterious stimulus (such as ROS) JNK phosphorylates 14-3-3 protein and induces the translocation of pro-apoptotic proteins (Bax and Bad) from the cytoplasm to the mitochondria, the major source of ROS in cells. The translocation of these pro-apoptotic proteins induces mitochondrial outer membrane permeabilization (MOMP), allowing the cytosolic release of pro-apoptogenic factors that normally reside in the mitochondrial intermembrane space, such as cytochrome c and Smac/DIABLO [53,54]. Cytochrome c then associates with Apaf-1, pro-caspase 9 (CASP9), (and possibly other proteins) to form an apoptosome, which activates CASP9. When activated, CASP9 catalyzes the proteolytic activation of CASP3 and CASP7 (known as 'executioner caspases'), which handle cell demolition during intrinsic and extrinsic apoptosis pathways. However, DNA damage can also activate JNK. p53 is another JNK substrate that induces expression of pro-apoptotic genes (*puma, fas* and *bax),* leading to apoptosis in a mitochondrial-independent manner. On the other hand, p53 can trigger the MOMP as well in a transcription-independent manner by activating pro-apoptotic Bcl-2 proteins (Bax or Bak) or by inactivating anti-apoptotic Bcl-2 proteins (Bcl-2 and Bcl-X1) [55,56].

Recently, the role of JNK3 in Alzheimer's disease (AD) was reviewed and reported synthetic JNK3 inhibitors explored so far with a promising future as therapeutic proposals for AD [57]. Luteolin-7-O-glucoside, a polyphenol, also showed important JNK3 selectivity. The IC50 for JNK3 was reported to be as low as 2.45 ± 0.1 μM, while the IC_{50} for p38α was 87.1 ± 2.1 μM, indicating a 35-fold increase of selectivity to JNK3 over p38 . Authors hypothesized that the selectivity for JNK3 is a result of the interaction of Lut7 and the residues Asn152, Gln155, Asn 194 and Ser 193 of JNK3 [6]. According to our results, it is possible that the main mechanism of Lut7 in preventing mitochondrial-dependent apoptosis is by inhibiting JNK3.

Both toxic protein accumulation and oxidative stress are main hallmarks of NDs and contribute to neuroinflammation, further worsening the disease. Previously studies had already reported that luteolin suppressed the production of proinflammatory cytokines in macrophages by blocking kappa B (NFkB) and activator protein 1 (AP1) nuclear signaling pathways and inhibited the production of nitric oxide and proinflammatory eicosanoids and also decreased the release of TNF-α and superoxide after LPS induced in microglial cell cultures and reduced the production of LPS-induced IL-6 in cerebral microglia *in vivo* and *in vitro [58,59].* In CNS, it decreased inflammation and axonal damage by preventing monocyte migration through the blood-brain barrier (BBB)[3–5]. Since both microglia cells and RAW264.7 cell line are capable of expressing major histocompatibility complex (MHC) antigens, as well as T and B cell markers and share other phenotypic traits and innate immunological functions with other mononuclear phagocytes, we also demonstrated that Lut7 can reduce TNF-α after 3 hours, as well as IL-10 after 24 hours. In the past two decades, neuroinflammation has been considered an important component of the NDs pathogenesis. It is well established that the CNS is composed of distinct kinds of cells that perform specific roles in brain homeostasis and therefore, may contribute differently to the worsening of symptoms or progression of ND.

A previous study reported that pretreatment with Lut7 suppressed the induction of nitrite, ROS, PGE2, and TNF-α in a dose-dependent manner in IL-1β-stimulated rat primary chondrocytes [60], suggesting that Lut7 has a potent anti-inflammatory effect. Additionally, Lut7 inhibited the IL-1β-induced nuclear accumulation of NF-κB subunit p65 by suppressing phosphorylation and degradation of IκB-α and significantly inhibited the IL-1β-induced phosphorylation of ERK, JNK, and p38 MAPK in a dose-dependent manner [60].

In summary, our results show that Lut7 protected SH-SY5Y cell line against 6-OHDA-induced damage after 24 hours, protected differentiated SH-SY5Y cells against neurotoxicity induced by 6-OHDA after 24 and 48 hours. Although we did not observe a difference in ROS production, Lut7 protected SH-SY5Y cells against 6-OHDA-induced mitochondrial and nuclear damage and reduced caspase-3 activity. In the RAW264.7 cell line, we demonstrated that Lut7 decreases TNF-α and increases IL-10. Together with previous data [6], our results provide support to the hypothesis that the mechanism of action of Lut7 is based on JNK3 inhibition as shown in Figure 6. Several questions remain unanswered and we believe this is an interesting topic for future work.

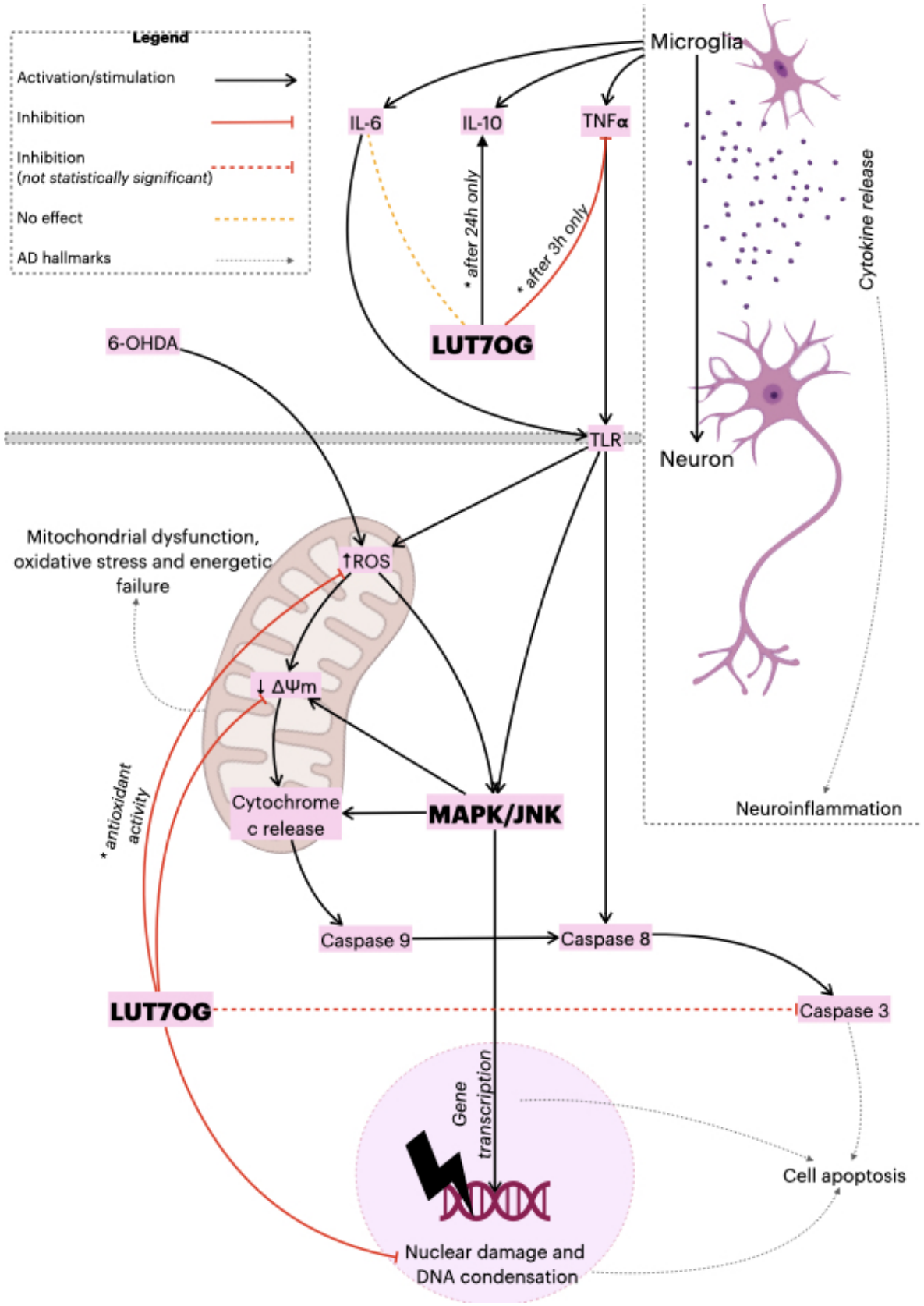

Figure 6. Proposed overall mechanism of action of Lut7.

Author Contributions:. SCHR, JRS, CA and SP did main experiments (antioxidant, cytotoxicity, neuroprotective, signaling pathways mechanisms and anti-inflammatory activity) and wrote the manuscript. MIG, SF and RFPP participated in designing and coordinating the study. All authors read and approved the final manuscript.

Acknowledgments:

Funding: This study was funded in part by the Coordenação de Aperfeiçoamento de Pessoal de Nível Superior – Brasil (CAPES) – Finance Code 001 and Conselho Nacional de Pesquisa (CNPq) 420381/2018-0.

Conflicts of Interest: The authors declare no conflict of interest.

References

1. Gammon, K. Neurodegenerative disease: brain windfall. *Nature* **2014**, *515*, 299–300, doi:10.1038/nj7526-299a.
2. Rezak, M.; de Carvalho, M. Disease modification in neurodegenerative diseases: Not quite there yet. *Neurology* **2020**, *94*, 12–13, doi:10.1212/WNL.0000000000008690.
3. Bakhtiari, M.; Panahi, Y.; Ameli, J.; Darvishi, B. Protective effects of flavonoids against Alzheimer's disease-related neural dysfunctions. *Biomed. Pharmacother.* **2017**, *93*, 218–229, doi:10.1016/j.biopha.2017.06.010.
4. Heim, K. E.; Tagliaferro, A. R.; Bobilya, D. J. Flavonoid antioxidants: chemistry, metabolism and structure-activity relationships. *J. Nutr. Biochem.* **2002**, *13*, 572–584, doi:10.1016/S0955-2863(02)00208-5.
5. Rasool, M.; Malik, A.; Qureshi, M. S.; Manan, A.; Pushparaj, P. N.; Asif, M.; Qazi, M. H.; Qazi, A. M.; Kamal, M. A.; Gan, S. H.; Sheikh, I. A. Recent updates in the treatment of neurodegenerative disorders using natural compounds. *Evid. Based Complement. Alternat. Med.* **2014**, *2014*, 979730, doi:10.1155/2014/979730.
6. Goettert, M.; Schattel, V.; Koch, P.; Merfort, I.; Laufer, S. Biological evaluation and structural determinants of p38α mitogen-activated-protein kinase and c-Jun-N-terminal kinase 3 inhibition by flavonoids. *Chembiochem* **2010**, *11*, 2579–2588, doi:10.1002/cbic.201000487.
7. Haeusgen, W.; Boehm, R.; Zhao, Y.; Herdegen, T.; Waetzig, V. Specific activities of individual c-Jun N-terminal kinases in the brain. *Neuroscience* **2009**, *161*, 951–959, doi:10.1016/j.neuroscience.2009.04.014.
8. Gourmaud, S.; Paquet, C.; Dumurgier, J.; Pace, C.; Bouras, C.; Gray, F.; Laplanche, J.-L.; Meurs, E. F.; Mouton-Liger, F.; Hugon, J. Increased levels of cerebrospinal fluid JNK3 associated with amyloid pathology: links to cognitive decline. *J. Psychiatry Neurosci.* **2015**, *40*, 151–161, doi:10.1503/jpn.140062.
9. Takahashi, R. H.; Nagao, T.; Gouras, G. K. Plaque formation and the intraneuronal accumulation of β-amyloid in Alzheimer's disease. *Pathol. Int.* **2017**, *67*, 185–193, doi:10.1111/pin.12520.
10. Gourmaud, S.; Thomas, P.; Thomasseau, S.; Tible, M.; Abadie, C.; Paquet, C.; Hugon, J. Brimapitide reduced neuronal stress markers and cognitive deficits in 5XFAD transgenic mice. *J Alzheimers Dis* **2018**, *63*, 665–674, doi:10.3233/JAD-171099.
11. Dey, A.; Bhattacharya, R.; Mukherjee, A.; Pandey, D. K. Natural products against Alzheimer's disease: Pharmaco-therapeutics and biotechnological interventions. *Biotechnol. Adv.* **2017**, *35*, 178–216, doi:10.1016/j.biotechadv.2016.12.005.
12. Mosmann, T. Rapid colorimetric assay for cellular growth and survival: application to proliferation and cytotoxicity assays. *J. Immunol. Methods* **1983**, *65*, 55–63, doi:10.1016/0022-1759(83)90303-4.
13. Silva, J.; Alves, C.; Pinteus, S.; Mendes, S.; Pedrosa, R. Neuroprotective effects of seaweeds

against 6-hydroxidopamine-induced cell death on an in vitro human neuroblastoma model. *BMC Complement. Altern. Med.* **2018**, *18*, 58, doi:10.1186/s12906-018-2103-2.
14. Silva, J.; Alves, C.; Martins, A.; Susano, P.; Simões, M.; Guedes, M.; Rehfeldt, S.; Pinteus, S.; Gaspar, H.; Rodrigues, A.; Goettert, M. I.; Alfonso, A.; Pedrosa, R. Loliolide, a New Therapeutic Option for Neurological Diseases? In Vitro Neuroprotective and Anti-Inflammatory Activities of a Monoterpenoid Lactone Isolated from Codium tomentosum. *Int. J. Mol. Sci.* **2021**, *22*, doi:10.3390/ijms22041888.
15. Pinteus, S.; Silva, J.; Alves, C.; Horta, A.; Fino, N.; Rodrigues, A. I.; Mendes, S.; Pedrosa, R. Cytoprotective effect of seaweeds with high antioxidant activity from the Peniche coast (Portugal). *Food Chem.* **2017**, *218*, 591–599, doi:10.1016/j.foodchem.2016.09.067.
16. Dávalos, A.; Gómez-Cordovés, C.; Bartolomé, B. Extending applicability of the oxygen radical absorbance capacity (ORAC-fluorescein) assay. *J. Agric. Food Chem.* **2004**, *52*, 48–54, doi:10.1021/jf0305231.
17. Benzie, I. F.; Strain, J. J. The ferric reducing ability of plasma (FRAP) as a measure of "antioxidant power": the FRAP assay. *Anal. Biochem.* **1996**, *239*, 70–76, doi:10.1006/abio.1996.0292.
18. Ouazia, D.; Levros, L. C.; Rassart, É.; Desrosiers, R. R. The protein l-isoaspartyl (d-aspartyl) methyltransferase protects against dopamine-induced apoptosis in neuroblastoma SH-SY5Y cells. *Neuroscience* **2015**, *295*, 139–150, doi:10.1016/j.neuroscience.2015.03.026.
19. Mansuri, M. L.; Parihar, P.; Solanki, I.; Parihar, M. S. Flavonoids in modulation of cell survival signalling pathways. *Genes Nutr.* **2014**, *9*, 400, doi:10.1007/s12263-014-0400-z.
20. Rahal, A.; Kumar, A.; Singh, V.; Yadav, B.; Tiwari, R.; Chakraborty, S.; Dhama, K. Oxidative stress, prooxidants, and antioxidants: the interplay. *Biomed Res. Int.* **2014**, *2014*, 761264, doi:10.1155/2014/761264.
21. Nabavi, S. F.; Braidy, N.; Gortzi, O.; Sobarzo-Sanchez, E.; Daglia, M.; Skalicka-Woźniak, K.; Nabavi, S. M. Luteolin as an anti-inflammatory and neuroprotective agent: A brief review. *Brain Res. Bull.* **2015**, *119*, 1–11, doi:10.1016/j.brainresbull.2015.09.002.
22. Kim, S.; Chin, Y.; Cho, J. Protection of Cultured Cortical Neurons by Luteolin against Oxidative Damage through Inhibition of Apoptosis and Induction of Heme. *Biol. Pharm. Bull.* **2017**, *40*, 256–265.
23. Luchtman, D. W.; Song, C. Why SH-SY5Y cells should be differentiated. *Neurotoxicology* **2010**, *31*, 164–5; author reply 165, doi:10.1016/j.neuro.2009.10.015.
24. Korecka, J. A.; van Kesteren, R. E.; Blaas, E.; Spitzer, S. O.; Kamstra, J. H.; Smit, A. B.; Swaab, D. F.; Verhaagen, J.; Bossers, K. Phenotypic characterization of retinoic acid differentiated SH-SY5Y cells by transcriptional profiling. *PLoS ONE* **2013**, *8*, e63862, doi:10.1371/journal.pone.0063862.
25. Krishna, A.; Biryukov, M.; Trefois, C.; Antony, P. M. A.; Hussong, R.; Lin, J.; Heinäniemi, M.; Glusman, G.; Köglsberger, S.; Boyd, O.; van den Berg, B. H. J.; Linke, D.; Huang, D.; Wang, K.; Hood, L.; Tholey, A.; Schneider, R.; Galas, D. J.; Balling, R.; May, P. Systems genomics evaluation of the SH-SY5Y neuroblastoma cell line as a model for Parkinson's disease. *BMC Genomics* **2014**, *15*, 1154, doi:10.1186/1471-2164-15-1154.
26. Iakovleva, I.; Begum, A.; Pokrzywa, M.; Walfridsson, M.; Sauer-Eriksson, A. E.; Olofsson, A. The flavonoid luteolin, but not luteolin-7-O-glucoside, prevents a transthyretin mediated toxic response. *PLoS ONE* **2015**, *10*, e0128222, doi:10.1371/journal.pone.0128222.
27. Cheung, Y.-T.; Lau, W. K.-W.; Yu, M.-S.; Lai, C. S.-W.; Yeung, S.-C.; So, K.-F.; Chang, R. C.-C. Effects of all-trans-retinoic acid on human SH-SY5Y neuroblastoma as in vitro model in

neurotoxicity research. *Neurotoxicology* **2009**, *30*, 127–135, doi:10.1016/j.neuro.2008.11.001.
28. Schneider, L.; Giordano, S.; Zelickson, B. R.; S Johnson, M.; A Benavides, G.; Ouyang, X.; Fineberg, N.; Darley-Usmar, V. M.; Zhang, J. Differentiation of SH-SY5Y cells to a neuronal phenotype changes cellular bioenergetics and the response to oxidative stress. *Free Radic. Biol. Med.* **2011**, *51*, 2007–2017, doi:10.1016/j.freeradbiomed.2011.08.030.
29. de Bittencourt Pasquali, M. A.; de Ramos, V. M.; Albanus, R. D. O.; Kunzler, A.; de Souza, L. H. T.; Dalmolin, R. J. S.; Gelain, D. P.; Ribeiro, L.; Carro, L.; Moreira, J. C. F. Gene Expression Profile of NF-κB, Nrf2, Glycolytic, and p53 Pathways During the SH-SY5Y Neuronal Differentiation Mediated by Retinoic Acid. *Mol. Neurobiol.* **2016**, *53*, 423–435, doi:10.1007/s12035-014-8998-9.
30. Kunzler, A.; Zeidán-Chuliá, F.; Gasparotto, J.; Girardi, C. S.; Klafke, K.; Petiz, L. L.; Bortolin, R. C.; Rostirolla, D. C.; Zanotto-Filho, A.; de Bittencourt Pasquali, M. A.; Dickson, P.; Dunkley, P.; Moreira, J. C. F.; Gelain, D. P. Changes in Cell Cycle and Up-Regulation of Neuronal Markers During SH-SY5Y Neurodifferentiation by Retinoic Acid are Mediated by Reactive Species Production and Oxidative Stress. *Mol. Neurobiol.* **2017**, *54*, 6903–6916, doi:10.1007/s12035-016-0189-4.
31. Forster, J. I.; Köglsberger, S.; Trefois, C.; Boyd, O.; Baumuratov, A. S.; Buck, L.; Balling, R.; Antony, P. M. A. Characterization of Differentiated SH-SY5Y as Neuronal Screening Model Reveals Increased Oxidative Vulnerability. *J. Biomol. Screen.* **2016**, *21*, 496–509, doi:10.1177/1087057115625190.
32. Hamanaka, R. B.; Chandel, N. S. Mitochondrial reactive oxygen species regulate cellular signaling and dictate biological outcomes. *Trends Biochem. Sci.* **2010**, *35*, 505–513, doi:10.1016/j.tibs.2010.04.002.
33. Murphy, M. P. How mitochondria produce reactive oxygen species. *Biochem. J.* **2009**, *417*, 1–13, doi:10.1042/BJ20081386.
34. Glinka, Y.; Gassen, M.; Youdim, M. B. Mechanism of 6-hydroxydopamine neurotoxicity. *J. Neural Transm. Suppl.* **1997**, *50*, 55–66, doi:10.1007/978-3-7091-6842-4_7.
35. Glinka, Y.; Tipton, K. F.; Youdim, M. B. Nature of inhibition of mitochondrial respiratory complex I by 6-Hydroxydopamine. *J. Neurochem.* **1996**, *66*, 2004–2010, doi:10.1046/j.1471-4159.1996.66052004.x.
36. Glinka, Y.; Tipton, K. F.; Youdim, M. B. Mechanism of inhibition of mitochondrial respiratory complex I by 6-hydroxydopamine and its prevention by desferrioxamine. *Eur. J. Pharmacol.* **1998**, *351*, 121–129, doi:10.1016/s0014-2999(98)00279-9.
37. Glinka, Y. Y.; Youdim, M. B. Inhibition of mitochondrial complexes I and IV by 6-hydroxydopamine. *Eur. J. Pharmacol.* **1995**, *292*, 329–332, doi:10.1016/0926-6917(95)90040-3.
38. Cui, X.-X.; Yang, X.; Wang, H.-J.; Rong, X.-Y.; Jing, S.; Xie, Y.-H.; Huang, D.-F.; Zhao, C. Luteolin-7-O-Glucoside Present in Lettuce Extracts Inhibits Hepatitis B Surface Antigen Production and Viral Replication by Human Hepatoma Cells in Vitro. *Front. Microbiol.* **2017**, *8*, 2425, doi:10.3389/fmicb.2017.02425.
39. Palombo, R.; Savini, I.; Avigliano, L.; Madonna, S.; Cavani, A.; Albanesi, C.; Mauriello, A.; Melino, G.; Terrinoni, A. Luteolin-7-glucoside inhibits IL-22/STAT3 pathway, reducing proliferation, acanthosis, and inflammation in keratinocytes and in mouse psoriatic model. *Cell Death Dis.* **2016**, *7*, e2344, doi:10.1038/cddis.2016.201.
40. De Stefano, A.; Caporali, S.; Di Daniele, N.; Rovella, V.; Cardillo, C.; Schinzari, F.; Minieri, M.; Pieri, M.; Candi, E.; Bernardini, S.; Tesauro, M.; Terrinoni, A. Anti-Inflammatory and Proliferative Properties of Luteolin-7-O-Glucoside. *Int. J. Mol. Sci.* **2021**, *22*, doi:10.3390/ijms22031321.

41. Zorov, D. B.; Juhaszova, M.; Sollott, S. J. Mitochondrial reactive oxygen species (ROS) and ROS-induced ROS release. *Physiol. Rev.* **2014**, *94*, 909–950, doi:10.1152/physrev.00026.2013.
42. Turrens, J. F. Mitochondrial formation of reactive oxygen species. *J Physiol (Lond)* **2003**, *552*, 335–344, doi:10.1113/jphysiol.2003.049478.
43. Korshunov, S. S.; Skulachev, V. P.; Starkov, A. A. High protonic potential actuates a mechanism of production of reactive oxygen species in mitochondria. *FEBS Lett.* **1997**, *416*, 15–18, doi:10.1016/s0014-5793(97)01159-9.
44. Connolly, N. M. C.; Theurey, P.; Adam-Vizi, V.; Bazan, N. G.; Bernardi, P.; Bolaños, J. P.; Culmsee, C.; Dawson, V. L.; Deshmukh, M.; Duchen, M. R.; Düssmann, H.; Fiskum, G.; Galindo, M. F.; Hardingham, G. E.; Hardwick, J. M.; Jekabsons, M. B.; Jonas, E. A.; Jordán, J.; Lipton, S. A.; Manfredi, G.; Prehn, J. H. M. Guidelines on experimental methods to assess mitochondrial dysfunction in cellular models of neurodegenerative diseases. *Cell Death Differ.* **2018**, *25*, 542–572, doi:10.1038/s41418-017-0020-4.
45. Norat, P.; Soldozy, S.; Sokolowski, J. D.; Gorick, C. M.; Kumar, J. S.; Chae, Y.; Yağmurlu, K.; Prada, F.; Walker, M.; Levitt, M. R.; Price, R. J.; Tvrdik, P.; Kalani, M. Y. S. Mitochondrial dysfunction in neurological disorders: Exploring mitochondrial transplantation. *npj Regen. Med.* **2020**, *5*, 22, doi:10.1038/s41536-020-00107-x.
46. Nho, J.-H.; Jung, H.-K.; Lee, M.-J.; Jang, J.-H.; Sim, M.-O.; Jeong, D.-E.; Cho, H.-W.; Kim, J.-C. Beneficial Effects of Cynaroside on Cisplatin-Induced Kidney Injury In Vitro and In Vivo. *Toxicol. Res.* **2018**, *34*, 133–141, doi:10.5487/TR.2018.34.2.133.
47. Yao, H.; Shang, Z.; Wang, P.; Li, S.; Zhang, Q.; Tian, H.; Ren, D.; Han, X. Protection of Luteolin-7-O-Glucoside Against Doxorubicin-Induced Injury Through PTEN/Akt and ERK Pathway in H9c2 Cells. *Cardiovasc. Toxicol.* **2016**, *16*, 101–110, doi:10.1007/s12012-015-9317-z.
48. Chen, S.; Yang, B.; Xu, Y.; Rong, Y.; Qiu, Y. Protection of Luteolin-7-O-glucoside against apoptosis induced by hypoxia/reoxygenation through the MAPK pathways in H9c2 cells. *Mol. Med. Report.* **2018**, *17*, 7156–7162, doi:10.3892/mmr.2018.8774.
49. Wang, Y.; Guo, S.-H.; Shang, X.-J.; Yu, L.-S.; Zhu, J.-W.; Zhao, A.; Zhou, Y.-F.; An, G.-H.; Zhang, Q.; Ma, B. Triptolide induces Sertoli cell apoptosis in mice via ROS/JNK-dependent activation of the mitochondrial pathway and inhibition of Nrf2-mediated antioxidant response. *Acta Pharmacol. Sin.* **2018**, *39*, 311–327, doi:10.1038/aps.2017.95.
50. Chauhan, D.; Li, G.; Hideshima, T.; Podar, K.; Mitsiades, C.; Mitsiades, N.; Munshi, N.; Kharbanda, S.; Anderson, K. C. JNK-dependent release of mitochondrial protein, Smac, during apoptosis in multiple myeloma (MM) cells. *J. Biol. Chem.* **2003**, *278*, 17593–17596, doi:10.1074/jbc.C300076200.
51. Che, X.-F.; Moriya, S.; Zheng, C.-L.; Abe, A.; Tomoda, A.; Miyazawa, K. 2-Aminophenoxazine-3-one-induced apoptosis via generation of reactive oxygen species followed by c-jun N-terminal kinase activation in the human glioblastoma cell line LN229. *Int. J. Oncol.* **2013**, *43*, 1456–1466, doi:10.3892/ijo.2013.2088.
52. Fan, P.; Yu, X.-Y.; Xie, X.-H.; Chen, C.-H.; Zhang, P.; Yang, C.; Peng, X.; Wang, Y.-T. Mitophagy is a protective response against oxidative damage in bone marrow mesenchymal stem cells. *Life Sci.* **2019**, *229*, 36–45, doi:10.1016/j.lfs.2019.05.027.
53. Schroeter, H.; Boyd, C. S.; Ahmed, R.; Spencer, J. P. E.; Duncan, R. F.; Rice-Evans, C.; Cadenas, E. c-Jun N-terminal kinase (JNK)-mediated modulation of brain mitochondria function: new target proteins for JNK signalling in mitochondrion-dependent apoptosis. *Biochem. J.* **2003**, *372*, 359–369, doi:10.1042/BJ20030201.
54. Hanawa, N.; Shinohara, M.; Saberi, B.; Gaarde, W. A.; Han, D.; Kaplowitz, N. Role of JNK

translocation to mitochondria leading to inhibition of mitochondria bioenergetics in acetaminophen-induced liver injury. *J. Biol. Chem.* **2008**, *283*, 13565–13577, doi:10.1074/jbc.M708916200.
55. Roos, W. P.; Kaina, B. DNA damage-induced cell death by apoptosis. *Trends Mol. Med.* **2006**, *12*, 440–450, doi:10.1016/j.molmed.2006.07.007.
56. Yue, J.; López, J. M. Understanding MAPK signaling pathways in apoptosis. *Int. J. Mol. Sci.* **2020**, *21*, doi:10.3390/ijms21072346.
57. Hepp Rehfeldt, S. C.; Majolo, F.; Goettert, M. I.; Laufer, S. c-Jun N-Terminal Kinase Inhibitors as Potential Leads for New Therapeutics for Alzheimer's Diseases. *Int. J. Mol. Sci.* **2020**, *21*, doi:10.3390/ijms21249677.
58. Jang, S.; Kelley, K. W.; Johnson, R. W. Luteolin reduces IL-6 production in microglia by inhibiting JNK phosphorylation and activation of AP-1. *Proc Natl Acad Sci USA* **2008**, *105*, 7534–7539, doi:10.1073/pnas.0802865105.
59. Zhang, J.-X.; Xing, J.-G.; Wang, L.-L.; Jiang, H.-L.; Guo, S.-L.; Liu, R. Luteolin Inhibits Fibrillary β-Amyloid1-40-Induced Inflammation in a Human Blood-Brain Barrier Model by Suppressing the p38 MAPK-Mediated NF-κB Signaling Pathways. *Molecules* **2017**, *22*, doi:10.3390/molecules22030334.
60. Lee, S. A.; Park, B.-R.; Moon, S.-M.; Hong, J. H.; Kim, D. K.; Kim, C. S. Chondroprotective Effect of Cynaroside in IL-1β-Induced Primary Rat Chondrocytes and Organ Explants via NF-κB and MAPK Signaling Inhibition. *Oxid. Med. Cell. Longev.* **2020**, *2020*, 9358080, doi:10.1155/2020/9358080.

Capítulo VI

Discussão geral

Conclusão geral

5. DISCUSSÃO

Devido ao aumento da prevalência de doenças neurodegenerativas associado a um número muito restrito de terapias farmacológicas, a necessidade de novas alternativas terapêuticas é evidente. Além disso, o papel fundamental de JNK3 no progresso da doença tem sido reforçado por meio de diversos estudos, o que torna JNK3 um alvo terapêutico interessante. Por outro lado, segundo Rehfeldt *et al.*, 2020, o desenvolvimento de moléculas com seletividade para JNK e, mais ainda, para JNK3, é um desafio a ser superado. Além disso, sabe-se que durante a investigação dos efeitos de drogas candidatas sobre *hallmarks* de doenças neurodegenerativas, outro grande desafio é o acesso ao tecido humano viável do SNC, seja por questões práticas ou éticas. Nesse sentido, durante a Convenção sobre Diversidade Biológica, também conhecida como "ECO-92", estabeleceu-se de acordo com o Art. 2º que:

> "Biotecnologia significa qualquer aplicação tecnológica que utilize sistemas biológicos, organismos vivos, ou seus derivados, para fabricar ou modificar produtos ou processos para utilização específica" (BRASIL, 1998).

Nesse sentido, o processo de descoberta e desenvolvimento de medicamentos depende de desenhos experimentais estrategicamente eficientes de ensaios *in silico*, *in vitro* e *in vivo* para discernir quais benefícios podem ser oferecidos por uma nova molécula e quais os efeitos colaterais indesejáveis que poderão ocorrer. Assim, a biotecnologia fornece meios necessários que permitem que uma nova droga seja extensivamente testada e aperfeiçoada antes de entrar em testes clínicos.

Estudos prévios sugeriram que, dentre centenas de quinases, a molécula sintética FMU200 e o flavonoide LUT7OG possuíam uma seletiva atividade inibitória para JNK3 (GOETTERT *et al.*, 2011, 2010; MUTH *et al.*, 2017). No caso do imidazol tetrasubstituído FMU200, autores observaram uma seletividade 120 vezes maior para JNK3 (IC_{50} JNK3: 0,3 ± 0,03 nM), em comparação a p38 (IC_{50} p38: 36 ± 4,38 nM) (MUTH *et al.*, 2017). De forma semelhante, LU7OG também demonstrou uma seletividade 35 vezes maior para JNK3 (IC_{50} JNK3: 2,45 ± 0,1 μM; IC_{50} p38: 87,1 ± 2,1 μM) (GOETTERT *et al.*, 2010). Assim, tendo em vista a significativa contribuição de JNK3 na fisiopatologia das doenças neurodegenerativas conforme apresentado no Capítulo I, ambas as moléculas possuíam suporte teórico que justificasse os ensaios aqui realizados. Nesse sentido, nos Capítulos IV e V deste estudo

objetivamos demonstrar a capacidade neuroprotetora de FMU200 e de LUT7OG, respectivamente, em um modelo experimental *in vitro* de doença neurodegenerativa, utilizando células SH-SY5Y diferenciadas e não-diferenciadas, bem como elucidar o mecanismo de ação das referidas moléculas, além de verificar suas ações frente a alguns *hallmarks* associados a doenças neurodegenerativas.

Após a determinação das concentrações não-tóxicas realizou-se ensaios de neurotoxicidade/neuroproteção. Em nosso modelo *in vitro* de neurodegeneração (em células SH-SY5Y não-diferenciadas), observamos que o pré-tratamento com FMU200 ou LUT7OG protegeu as células contra a apoptose induzida por 6-OHDA. Vários estudos indicaram que 6-OHDA é um inibidor potente do complexo I e IV nas mitocôndrias do cérebro (GLINKA, Y; GASSEN; YOUDIM, 1997; GLINKA, Y; TIPTON; YOUDIM, 1998; GLINKA, Y Y; YOUDIM, 1995), inibindo os complexos da cadeia respiratória mitocondrial. Glinka *et al.* (1997) relataram que a inibição do complexo mitocondrial I induzida por 6-OHDA não é revertida com o uso de antioxidantes. Dessa forma, infere-se que a morte celular (e, portanto, a neurodegeneração) é causada pela depleção de ATP (GLINKA, Y; GASSEN; YOUDIM, 1997; GLINKA, Y; TIPTON; YOUDIM, 1996). Sabe-se que o complexo I é a principal porta de entrada de elétrons na cadeia respiratória e sua inibição resulta no bloqueio da maioria das reações metabólicas oxidativas dentro das mitocôndrias (SHARMA; LU; BAI, 2009), o que fornece suporte para essa teoria. De fato, a deficiência no complexo I da cadeia transportadora de elétrons (ETC) foi descrita em pacientes com DP (NORAT *et al.*, 2020; TYSNES; STORSTEIN, 2017) e com DA (MANCZAK *et al.*, 2004; WANG, Wenzhang *et al.*, 2020), enquanto que em modelos animais de DA foi relatado diminuição da atividade do complexo IV e de produção de ATP (DU; SHIDU YAN, 2010; PARKS *et al.*, 2001). Ou seja, nos neurônios, um dos efeitos da 6-OHDA é a inibição dos complexos I e IV, fazendo com que os níveis de ATP diminuam, levando à apoptose. Em hepatócitos de camundongos, o paracetamol diminuiu os níveis de ATP (de forma semelhante à 6-OHDA nos neurônios), enquanto um pré-tratamento com SP600125 evitou o declínio nos níveis de ATP, sugerindo que JNK se transloca para mitocôndrias e inibe a bioenergética mitocondrial (pelo menos em parte) ao desencadear a transição de permeabilidade mitocondrial (HANAWA *et al.*, 2008; ZOROV; JUHASZOVA; SOLLOTT, 2014). Efeito semelhante foi observado em mitocôndrias cerebrais isoladas, nas quais JNK

induziu diretamente a transição de permeabilidade mitocondrial (SCHROETER *et al.*, 2003).

Embora nossos resultados não possam confirmar ou descartar a possibilidade, é possível que FMU200 e LUT7OG possam prevenir uma diminuição nos níveis de ATP induzida pela inibição dos complexos mitocondriais provocada por 6-OHDA, contribuindo para a diminuição da morte celular que observamos em nossos ensaios de MTT. Sugerimos análises adicionais para confirmar se FMU200 e LU7OG possuem algum efeito sobre os níveis de ATP em células SH-SY5Y.

Após verificarmos a capacidade neuroprotetora dos diferentes compostos, realizamos os ensaios com o objetivo de entender o mecanismo de ação de FMU200 e LUT7OG. Foram avaliados os efeitos de cada composto em diferentes eventos que precedem a apoptose e que estejam envolvidos com a sinalização de JNK, como a formação de ROS e o estresse oxidativo. As células geram constantemente ROS durante o metabolismo aeróbico. Devido à alta taxa metabólica do cérebro, ele consome quase 25% da ingestão total de glicose do corpo e 20% da ingestão total de oxigênio durante a produção de ATP. Durante esse processo, as ROS também são geradas como resultado da atividade da ETC durante a fosforilação oxidativa e, como resultado, o tecido cerebral é particularmente suscetível ao estresse oxidativo (HAMANAKA; CHANDEL, 2010; MURPHY, 2009). Vários eventos têm sido associados à neurodegeneração, como disfunção sináptica, excitotoxicidade e estresse oxidativo. Na verdade, devido a sua alta taxa metabólica associada a uma capacidade limitada de regeneração celular, o cérebro é particularmente suscetível ao dano oxidativo. Os danos causados por ROS em regiões cerebrais específicas foram associados com DA, comprometimento cognitivo leve (MCI), doença de Parkinson (DP) e esclerose lateral amiotrófica (ALS) (ANDERSEN, 2004; BUTTERFIELD *et al.*, 2002; DEXTER *et al.*, 1989; PEDERSEN *et al.*, 1998; ZABEL *et al.*, 2018). De fato, existem evidências que associam ROS e a fisiopatologia de várias doenças neurodegenerativas, no entanto, ensaios clínicos randomizados que avaliaram os efeitos de antioxidantes em pacientes com DA forneceram resultados conflitantes (GALASKO *et al.*, 2012; POLIDORI; NELLES, 2014). Ou seja, níveis mais elevados de ROS ativam processos de morte (LEE; HE; LIOU, 2021) porém, neste caso, a terapia antioxidante parece ser insuficiente para promover melhorias significativas, apoiando a necessidade de explorar novos alvos.

É importante ressaltar que nos ensaios subsequentes nos quais foram avaliados os níveis intracelulares de ROS e o ΔΨm, o modelo experimental utilizado foi o de células SH-SY5Y não diferenciadas estimuladas por H_2O_2. A opção de utilizarmos o modelo experimental com células não diferenciadas ocorreu pelo fato de que o processo de diferenciação promove uma série de modificações com potencial de interferir nos resultados. Foi demonstrado que o tratamento com RA promove a sobrevivência das células SH-SY5Y por meio da ativação da via de sinalização fosfatidilinositol 3-quinase/Akt (PI3K/Akt) e da regulação positiva da proteína Bcl-2 anti-apoptótica (ITANO *et al.*, 1996; LÓPEZ-CARBALLO *et al.*, 2002). Além disso, alguns estudos mostram que as células diferenciadas por RA são menos vulneráveis à morte celular induzida por toxinas como 6-OHDA, 1-metil-4-fenil-1,2,3,6-tetra-hidropiridina (MPTP), ou seu metabólito, íon 1-metil-4-fenil-piridínio (MPP^+) do que as células não-diferenciadas (CHEUNG *et al.*, 2009). Já o uso de H_2O_2 como indutor de lesão celular ocorreu pelos seguintes motivos: (I) H_2O_2 é o ROS mais estável, (II) transita facilmente através das membranas celulares, (III) um dos subprodutos da auto-oxidação de 6-OHDA é H_2O_2 (COHEN; HEIKKILA, 1974; GLINKA, Y; GASSEN; YOUDIM, 1997; SOTO-OTERO *et al.*, 2000), (IV) em células N18, o dano à estrutura celular e função induzida por 6-OHDA e H_2O_2 foi semelhante (VROEGOP; DECKER; BUXSER, 1995), (V) H_2O_2 atua como mensageiro extracelular e intracelular (HAMANAKA; CHANDEL, 2010; LEE; HE; LIOU, 2021; STARKOV, 2008) e; (VI) a via JNK desempenha um papel fundamental na morte celular de vários tipos de células e a ativação de JNK3 parece ser essencial para a fisiopatologia de muitas doenças neurodegenerativas e H_2O_2 é amplamente utilizado como modelo *in vitro* de estresse oxidativo geral de doenças neurodegenerativas (WHITTEMORE *et al.*, 1995).

ROS e JNK estão altamente interligados e estudos anteriores relataram que o tratamento com um inibidor de JNK3 (composto 9l ou SR-3562) mostrou uma inibição potente da geração de ROS após a ativação de JNK em células HeLa (CHAMBERS; LOGRASSO, 2011) e células INS-1 (KAMENECKA *et al.*, 2010). Aqui, demonstramos que FMU200 e LUT7OG também foram capazes de diminuir a produção de ROS, corroborando com estudos publicados anteriormente. Além disso, o SR-3562, assim como o FMU200 e LUT7OG, evitou a formação de ROS de forma semelhante ao NAC, um antioxidante genérico (CHAMBERS; LOGRASSO, 2011).

Nesse caso, parece que a ativação de JNK por H_2O_2 induz a geração de ROS, enquanto que a sua inibição por FMU200 ou por LUT7OG diminui a produção de ROS induzidos por H_2O_2.

Análises realizadas pelo grupo parceiro do MARE (*Marine and Environmental Sciences Centre*) do Instituto Politécnico de Leiria (IPL) o flavonoide LUT7OG demonstrou uma capacidade antioxidante significativa. Estudos pré-clínicos relataram que a luteolina, que é um flavonoide presente em muitas frutas e vegetais, possui propriedades antiinflamatórias e antioxidantes (KIM; CHIN; CHO, 2017; MANSURI *et al.*, 2014; NABAVI *et al.*, 2015; RAHAL *et al.*, 2014). Por outro lado, em células SH-SY5Y não diferenciadas estimuladas com 6-OHDA, LUT7OG não afetou a produção de ROS. Outro estudo relatou que LUT7OG não interferiu no acúmulo de ROS intracelular induzido pelo vírus da hepatite B em células HepG2 (CUI *et al.*, 2017). Em células H9c2, o pré-tratamento com LUT7OG reduziu a apoptose, ROS intracelular, condensação da cromatina e dano ao DNA, e reverteu a disfunção mitocondrial induzidos por doxorrubicina (YAO *et al.*, 2016). Outro estudo relatou resultados semelhantes em células H9c2, nos quais observou-se redução da apoptose, da geração de ROS e na disfunção mitocondrial (CHEN, *et al.*, 2018). Contudo, quando avaliada a despolarização Δψm induzida por 6-OHDA em células tratadas com SH-SY5Y evidenciou-se que LUT7OG restabeleceu o $\Delta\Psi m$. Estudos prévios relatam efeitos semelhantes em outros modelos experimentais *in vitro*. Em células HK-2 induzidas por cisplatina (linhagem celular derivada do túbulo proximal humano) LUT7OG diminuiu a morte celular, promoveu uma recuperação em Δψm e aboliu a atividade da caspase-3 (NHO *et al.*, 2018). A redução na atividade de caspase-3 também foi observada nos ensaios realizados em Portugal.

No presente estudo, entretanto, demonstramos que tanto FMU200 quanto LUT7OG atenuaram a produção de ROS intracelular induzida por H_2O_2 e inibiram a despolarização de $\Delta\Psi m$ induzida por H_2O_2. Esses resultados conectam a via JNK diretamente com a via intrínseca de apoptose, além de sugerir que as mitocôndrias são importantes organelas-alvo para os compostos e que tais organelas podem ser essenciais para sua ação neuroprotetora. Qualquer aumento na produção de ROS mitocondrial depende do estado metabólico desta organela e foi demonstrada uma correlação entre o $\Delta\Psi m$ e a produção de ROS (KORSHUNOV; SKULACHEV; STARKOV, 1997; TURRENS, 2003; ZOROV; JUHASZOVA; SOLLOTT, 2014). Em

doenças mitocondriais, a diminuição do ΔΨm e da atividade da cadeia respiratória são observadas com um aumento simultâneo na produção de ROS (KIM; RODRIGUEZ-ENRIQUEZ; LEMASTERS, 2007; MARCHI *et al.*, 2012). Além disso, a despolarização Δψm está geralmente correlacionada com a morte neuronal (CONNOLLY *et al.*, 2018; NORAT *et al.*, 2020). A despolarização mitocondrial induzida por JNK foi avaliada em células Huh7 e HepG2 (HESLOP *et al.*, 2020). Heslop *et al.* (2020) demonstraram que a disfunção mitocondrial é mediada pela ativação de JNK, enquanto a inibição de JNK pelo *inhibitor VIII* de JNK e SP600125 preveniu a disfunção mitocondrial e bloqueou a translocação de JNK para a mitocôndria. Ao impedir a translocação de JNK para a membrana mitocondrial externa, foi observada uma diminuição na produção de ROS (LUCERO; SUAREZ; CHAMBERS, 2019). Em células de melanoma humano, a ativação de JNK foi necessária para a mudança de ΔΨm e apoptose celular (SHIEH *et al.*, 2010) e o tratamento com SP600125 evitou o dissipamento de Δψm e o aumento da apoptose ao inibir a ativação de JNK em diferentes linhagens de células (CHAUHAN *et al.*, 2003; CHE *et al.*, 2013; FAN *et al.*, 2019; WANG, *et al.*, 2018). Uma possível explicação para esses achados é que JNK desempenha um papel significativo na apoptose por meio da via intrínseca (também conhecida como 'via mitocondrial'), que é ativada por perturbações extracelulares e intracelulares geralmente encontradas na DA, como o estresse oxidativo. Em resposta a um estímulo deletério (como ROS), JNK fosforila a proteína 14-3-3 e induz a translocação de proteínas pró-apoptóticas (Bax e Bad) do citoplasma para a mitocôndria, a principal fonte de ROS nas células. No entanto, foi relatado que JNK pode fosforilar diretamente Bad, Bim e Bid induzindo sua atividade pró-apoptótica enquanto inibe proteínas anti-apoptóticas. Uma vez translocado para a mitocôndria, o JNK aumenta em 80% a formação de ROS, principalmente pelo Complexo I (CHAMBERS; LOGRASSO, 2011). A translocação dessas proteínas pró-apoptóticas induz a permeabilização da membrana externa mitocondrial (MOMP), permitindo a liberação citosólica de fatores pró-apoptogênicos que normalmente residem no espaço intermembranar na mitocôndria, como citocromo c Smac/DIABLO (HANAWA *et al.*, 2008; SCHROETER *et al.*, 2003). O citocromo c então se associa com Apaf-1, pró-caspase 9, (e possivelmente outras proteínas) para formar um apoptossoma, que ativa Caspase-9. Quando ativada, a Caspase-9 catalisa a ativação proteolítica de Caspase-3 e

Caspase-7 (conhecido como 'caspases executoras'), que lidam com a demolição celular durante as vias de apoptose intrínseca e extrínseca. No entanto, o dano ao DNA também pode ativar JNK. O p53 é outro substrato JNK que induz a expressão de genes pró-apoptóticos (*puma, fas e bax*), levando à apoptose de forma independente da mitocôndria. Por outro lado, o p53 também pode desencadear o MOMP de uma maneira independente da transcrição, ativando proteínas Bcl-2 pró-apoptóticas (Bax ou Bak) ou inativando proteínas Bcl-2 anti-apoptóticas (Bcl-2 e Bcl-X1) (ROOS; KAINA, 2006; YUE; LÓPEZ, 2020).

Na via intrínseca de apoptose, JNK fosforila fatores de transcrição que induzem a expressão de proteínas pró-apoptóticas e diminui a expressão de proteínas anti-apoptóticas. O principal alvo de JNK é o fator de transcrição AP-1, que é um complexo formado por membros das famílias de proteínas Jun, Fos, ATF e MAF. Conforme mencionado no início da presente discussão, LUT7OG foi apontado como um inibidor de JNK3 (IC_{50} 2,45 ± 0,1 μM) e inúmeros estudos dão suporte a essa evidência mostrando que LUT7OG inibe p-ERK1/2, p-JNK e p-P38 e ativa p-ERK5 (CHEN, *et al.*, 2018). Entretanto, por se tratar de uma molécula nova, tais dados ainda não haviam sido descritos para o inibidor FMU200. Nesse caso, nossa análise de western blot é consistente com Muth *et al*., 2017, indicando uma regulação negativa em p-JNK. Neste caso, nosso estudo suporta evidências de observações anteriores que apontaram para uma diminuição na atividade de JNK3.

Apesar de sua principal contribuição para a fisiopatologia das doenças neurodegenerativas ser por meio de sinais pró-apoptóticos, o JNK também pode promover efeitos pró-inflamatórios (WAJANT, 2002). Além disso, o estresse oxidativo e a neuroinflamação crônica são dois fatores patológicos-chave intimamente relacionados e que atuam no desenvolvimento e agravamento das doenças neurodegenerativas. Na DA, por exemplo, a neuroinflamação depende de respostas imunes inatas mediadas pela microglia (SHI; HOLTZMAN, 2018). Após um estímulo, a microglia produz vários mediadores inflamatórios, como IL-1β, IL-6, TNF-α, prostaglandina E2 (PGE2), óxido nítrico (NO), fator neurotrófico derivado do cérebro (BDNF), que podem ativar a via de JNK. A principal contribuição de JNK para a neuroinflamação é por meio de seu fator de transcrição, AP-1, que regula genes pró-inflamatórios como *COX2, NOS2, TNF-α, CCL2* e *VCAM-1* (GUPTA *et al.*, 1996) e as

evidências sugerem que a produção de TNF-α induzida ROS é dependente de JNK (KAMATA *et al.*, 2005; VENTURA *et al.*, 2004).

Embora as linhagens celulares microgliais BV2 (derivada de murinos) e HMO6 (derivada de humanos) sejam frequentemente utilizadas em modelos experimentais *in vitro* de doenças neurodegenerativas (TIMMERMAN; BURM; BAJRAMOVIC, 2018), a linhagem de macrófagos murinos RAW264.7 também é capaz de expressar antígenos do complexo principal de histocompatibilidade (MHC), bem como marcadores de células T e B e compartilham outras características fenotípicas e funções imunológicas inatas com as linhagens BV2 e HMO6 (BERGHAUS *et al.*, 2010; SAXENA; VALLYATHAN; LEWIS, 2003; TACIAK *et al.*, 2018; TAYLOR *et al.*, 2005). Além disso, o uso de LPS em modelos experimentais i*n vitro* e *in vivo* de doenças neurodegenerativas é bem estabelecido (BATISTA *et al.*, 2019; HOOGLAND *et al.*, 2015). De fato, a linhagem RAW264.7 estimulada com LPS foi um modelo desenvolvido e implementado com sucesso em nosso laboratório e por grupos parceiros (SILVA *et al.*, 2021).

Estudos anteriores já haviam relatado que a luteolina suprimiu a produção de citocinas pró-inflamatórias em macrófagos, por meio do bloqueio de NFkB e AP1, da inibição da produção de óxido nítrico e eicosanóides pró-inflamatórios, diminuiu a liberação de TNF-α e IL-6 e superóxido em células de microglia cerebral *in vivo* e *in vitro* após indução com LPS (JANG; KELLEY; JOHNSON, 2008; ZHANG *et al.*, 2017). No SNC, a luteolina diminuiu a inflamação e o dano axonal ao impedir a migração de monócitos através BBB (*blood-brain barrier*) (BAKHTIARI *et al.*, 2017; HEIM; TAGLIAFERRO; BOBILYA, 2002; RASOOL *et al.*, 2014). Nesse sentido, avaliamos o potencial anti-inflamatório de FMU200 e LUT7OG por meio da dosagem de duas citocinas pró-inflamatórias (TNF-α e IL-6) e uma citocina anti-inflamatória (IL-10).

Nesse caso, identificamos que FMU200 e LUT7OG diminuíram a liberação de TNF-α em células RAW264.7 após um tratamento de 3 horas, mas não reduziram os níveis TNF-α após 24 horas. Contrariamente ao que identificamos no presente estudo, os autores relatam uma diminuição nas citocinas pró-inflamatórias, juntamente com um aumento de citocinas anti-inflamatórias em células RAW264.7 induzidas por LPS e tratadas com SP600125 (LAI *et al.*, 2013; PARK *et al.*, 2018; TONG *et al.*, 2020; YIM *et al.*, 2018). No entanto, deve-se ressaltar que em nosso

estudo as células foram pré-tratadas com, no máximo, 1 μM de SP600125 e posteriormente exportas a 1μg/mL de LPS. Por outro lado, estudos semelhantes que apontam uma significativa redução na produção de TNF-α após 24 horas trataram as células RAW264.7 com concentrações de SP600125 de 10 a 200 vezes maior (10 a 20 μM) e induziram as células com concentrações de LPS entre 50 e 90% inferiores (0,5 e 0,1μg/mL) (PARK *et al.*, 2018; TONG *et al.*, 2020) (LAI *et al.*, 2013; YIM *et al.*, 2018). Uma vez que não avaliamos o efeito de SP600125 a 10 μM, não podemos fazer uma comparação direta.

A citotoxicidade de diferentes concentrações de LPS foi avaliada em células RAW264.7 por Tong et al. De acordo com seus resultados, LPS a uma concentração máxima de 1,25 μg/mL não foi citotóxico, (o que fornece suporte para a concentração de LPS que usamos) e que a liberação de citocinas (TNF-α e IL-6) foi dose-dependente da concentração de LPS. Outro fator potencialmente interferente é o sorotipo de LPS utilizado em cada estudo. Conforme descrito nos materiais e métodos, no presente estudo utilizou-se LPS do sorotipo O111:B4, o qual demonstrou uma maior e mais potente ativação de AP-1 e, consequentemente, maior estimulação de mRNA de TNF-α e IL-6 e de expressão proteica de IL-1β em animais (MIGALE *et al.*2015). Nesse sentido, é importante considerar alguns vieses relacionados a metodologia utilizada.

Além de TNF-α, a interleucina IL-6, um produto de linfócitos T e B ativados, monócitos e fibroblastos e macrófagos ativados também foi avaliada. Embora entenda-se a IL-6 como uma interleucina pró-inflamatória, esta é uma citocina pleiotrópica com uma infinidade de funções (CARLSON *et al.*, 1999). Inclusive, demonstrou-se que o supressor de sinalização de citocinas 3 (SOCS3) é um regulador chave para a ação pró-inflamatória de IL-6 e anti-inflamatória de IL-10 e que, na ausência de SOCS-3, IL-6 induz uma resposta anti-inflamatória (YASUKAWA *et al.*, 2003). De fato, uma quantidade superior de mRNA de SOCS-3 foi encontrada em análises *post-mortem* de pacientes com DA (WALKER; WHETZEL; LUE, 2015). Ainda, corroborando com os dois estudos mencionados, uma coorte com duração de 20 anos, observou que há uma maior probabilidade de comprometimento cognitivo em indivíduos com níveis elevados ou crescentes de IL-6 ao longo dos anos (WICHMANN *et al.*, 2014).

Por outro lado, a hipótese de que IL-6 atenua efeitos neurotóxicos de NMDA em neurônios colinérgicos já é discutida há quase 30 anos (ERTA; QUINTANA; HIDALGO, 2012; PIZZI *et al.*, 2004; TOULMOND *et al.*, 1992; YAMADA; HATANAKA, 1994). O excesso de estímulo provocado pelo glutamato em receptores NMDA provoca um fenômeno conhecido como "excitotoxicidade" e induz a morte celular por meio da ativação de JNK (HOQUE *et al.*, 2019; YANG, *et al.*, 1997). Destaca-se que a memantina, um dos fármacos disponíveis para o tratamento da DA, é um antagonista de receptores NMDA (JOHNSON; KOTERMANSKI, 2006) e que o tratamento com inibidores de JNK como D-JNKI1, SP600125 ou TAT-JNK-III protegeram contra a excitotoxicidade do glutamato e a morte celular *in vivo* e *in vitro* (CENTENO *et al.*, 2007; KIM, *et al.*, 2016; MARCELLI *et al.*, 2019). Além disso, a exposição crônica à IL-6 exógena evitou a morte neuronal e o aumento da atividade de caspase-3 induzidas por NMDA. Tanto AG490 (inibidor de JAK2) quanto PD98059 (inibidor de ERK) bloquearam a proteção de IL-6 contra a diminuição da vitalidade neuronal induzida por NMDA e o aumento da ativação da caspase-3 (JUNG; KIM; CHAN, 2011; WANG, *et al.*, 2009). Ainda, recentemente, demonstrou-se que a inibição de IL-6 poderia contribuir para o agravamento de transtornos depressivos (KNIGHT *et al.*, 2021) que são mais prevalentes na população idosa e, mais ainda, na população idosa que possui alguma doença neurodegenerativa (DAFSARI; JESSEN, 2020; LIM, *et al.*, 2018; SNOWDEN *et al.*, 2015). Nesse sentido, infere-se que o efeito neuroprotetor da IL-6 depende da concentração de IL-6 e do grau de lesão neuronal. Hipotetiza-se que bloqueio total da produção de IL-6 não seja benéfica no tratamento de doenças neurodegenerativas, sendo preferível uma modulação de IL-6 por meio da inibição de JNK e que tal efeito modulatório poderia ser alcançado por meio do tratamento com FMU200 ou LUT7OG, uma vez que o tratamento com SR3306, um inibidor seletivo de JNK2/3, reduziu a expressão de SOCS-3 em modelos *in vivo* (GAO; HOWARD; LOGRASSO, 2017). Ou seja, o fato de que, no presente estudo, os níveis de IL-6, após 12 horas de tratamento, não foram afetados por FMU200 ou LUT7OG pode ser entendido como um resultado ambíguo.

Ainda, avaliou-se níveis de uma segunda interleucina. Sabe-se que a IL-10 inibe a secreção da secreção de citocinas pró-inflamatórias (IL-1α, IL-1β, IL-6, TNF-α), quimiocinas (IL-8) e fatores de crescimento e desenvolvimento (GM-CSF e G-

CSF) induzida por LPS ou IFN-γ (MOSSER; ZHANG, 2008; OUYANG; O'GARRA, 2019). No presente estudo demonstrou-se que tratamento com FMU200 (1 e 0,1 μM) e LUT7OG (0,1 μM) aumentaram níveis de IL-10 após 24 horas em comparação com o grupo tratado apenas com LPS, enquanto que após 48 horas nenhum efeito nos níveis de IL-10 foi observado.

Entretanto, um aumento na expressão de IL-10 em vários modelos animais de DA reduziu a fagocitose de Aβ pela microglia e exacerbou os depósitos de Aβ, levando a um comprometimento cognitivo. Por outro lado, o bloqueio de *IL10* promove uma redução da sinalização IL-10/STAT3, o que parece aumentar a atividade fagocítica microglial (CHAKRABARTY *et al.*, 2015; GUILLOT-SESTIER *et al.*, 2015). É importante ressaltar os achados são consistentes com um aumento nos níveis de IL-10 encontrados em pacientes com DA (LOEWENBRUECK *et al.*, 2010; LOPES; SPARKS; STREIT, 2008; MA, *et al.*, 2005; ZHENG; ZHOU; WANG, 2016).

Sabe-se que neurônios, células microgliais e macrófagos expressam receptores TLR (especialmente TLR2, 4 e 9) e que estes receptores estão superexpressos em pacientes com DA, PD e em vários modelos experimentais destas doenças (FIEBICH *et al.*, 2018). Além disso, é consenso de que a ativação destes receptores desencadeia a via de JNK. Apesar dos efeitos deletérios da ativação do receptor TLR, sabe-se que a síntese de IL-10 depende, em parte, da ativação de TLR. Evidenciou-se que a estimulação de TLR leva a ativação de MAPK que então modula a produção de IL-10. Por outro lado, a inibição de ERK, p38 ou JNK em macrófagos estimulados por LPS leva a uma significativa redução na produção de IL-10 (CHANTEUX *et al.*, 2007; FIEBICH *et al.*, 2018; FOEY *et al.*, 1998; JARNICKI *et al.*, 2008; KIM, *et al.*, 2008; MA, *et al.*, 2001; SARAIVA *et al.*, 2005). Além disso, fatores de transcrição ativados por JNK como ATF-1, MAF, NF-kβ (p65), JUN, CREB, foram descritos como regulatórios da expressão de IL-10 (SARAIVA; O'GARRA, 2010). Inclusive, LUT7OG inibiu a acumulação nuclear da subunidade p65 de NF-κB e inibiu significativamente a fosforilação induzida por IL-1β de ERK, JNK e p38 MAPK em uma dose forma dependente (LEE, *et al.*, 2020). Tais observações poderiam explicar, em parte, nossos resultados para IL-10 após 48 horas, uma vez que FMU200 e LUT7OG, enquanto inibidores de JNK, podem estar atuando na modulação de IL-10.

É evidente a existência de uma complexidade na regulação das citocinas por meio de ciclos de *feedbacks* positivo e negativo e que o controle rígido é essencial para atingir um equilíbrio entre uma resposta imunológica eficaz e a imunopatologia. Coletivamente, esses resultados sugerem que o reequilíbrio da imunidade inata cerebral e a promoção da "neuroinflamação benéfica" podem ser mais eficazes do que a terapia anti-inflamatória generalizada para a DA. Apesar da classificação de citocinas como "pró" ou "anti-inflamatórias" ser amplamente adotada na literatura e de ser interessante sob um ponto de vista didático, trata-se de uma caracterização reducionista e que deve ser evitada visto que as ações benéficas ou maléficas de IL-10 e IL-6 dependem de um contexto mais abrangente.

De maneira geral, os resultados apresentados nos capítulos IV e V dessa Tese indicam que tanto FMU200 quanto LUT7OG apresentam potencial efeito neuroprotetor, antioxidante e (até certo ponto) antiinflamatório em diferentes modelos de neurodegeneração. Dessa forma, por meio dos dados aqui apresentados, podemos propor que esses efeitos podem ocorrer em resposta a inibição de JNK3.

Além disso, conforme apresentado no Capítulo II desse estudo, todos os protocolos desenvolvidos e validados configuram-se como ferramentas úteis para uma avaliação mais ampla e complexa dos efeitos de diferentes drogas *in vitro*. Destaca-se que tais protocolos podem ser replicados pelos demais alunos e que, mediante adaptações, poderão ser utilizados em outras linhagens celulares. Ainda, além de fornecer ferramentas que possibilitam uma maior diversidade de ensaios realizados nos laboratórios da Univates, contribuiu para explorar um maior número de recursos oferecidos por equipamentos já disponíveis na instituição e diminuir sua ociosidade.

6. CONCLUSÃO

A partir dos dados obtidos no presente estudo, conclui-se que o inibidor sintético de JNK3, FMU200 é uma molécula altamente promissora uma vez que: (I) não apresentou efeito citotóxico nas linhagens celulares SH-SY5Y e RAW264.7 nas concentrações de 1 e 0,1 μM; (II) apresentou um efeito neuroprotetor frente à apoptose induzida por 6-OHDA e H_2O_2 nas concentrações de 1 e 0,1 μM; (III) inibiu a formação de ROS intracelulares após estímulo com H_2O_2; (IV) preveniu uma alterações ΔΨm após dano celular induzido por H_2O_2; (V) inibiu a fosforilação de JNK e reduz a razão entre p-JNK/JNK total e; (VI) reduziu os níveis de TNF-α (após 3 horas) enquanto que induzem a liberação de IL-10 em um tratamento de 24 horas em células RAW264.7 estimuladas por LPS.

Além disso, o presente estudo amplia as informações acerca dos efeitos *in vitro* de LUT7OG uma vez que observamos que essa molécula: (I) não apresentou efeito citotóxico nas linhagens celulares SH-SY5Y e RAW264.7 nas concentrações de 1 e 0,1 μM; (II) apresentou um efeito neuroprotetor frente à apoptose induzida por 6-OHDA em células SH-SY5Y não diferenciadas e, pela primeira vez na literatura, em células SH-SY5Y diferenciadas por RA; (III) desempenhou um efeito neuroprotetor frente à apoptose induzida por H_2O_2 nas concentrações de 1 e 0,1 μM; (IV) inibiu a formação de ROS intracelulares após estímulo com 6-OHDA e H_2O_2; (V) preveniu uma alterações ΔΨm após dano celular induzido por 6-OHDA e H_2O_2; (VI) reduziu os níveis de TNF-α (após 3 horas) enquanto que induzem a liberação de IL-10 em um tratamento de 24 horas em células RAW264.7 estimuladas por LPS; (VII) possui uma elevada capacidade antioxidante; (VIII) preveniu a condensação e fragmentação do DNA após dano celular induzido por 6-OHDA e; (IX) reduziu a atividade de caspase-3 após dano por 6-OHDA.

Finalmente, embora FMU200 e LUT7OG sejam altamente seletivos para JNK3, alguns dos efeitos observados no presente estudo podem ter ocorrido devido à inibição de alvos "*off-target*". Portanto, é imprescindível que tanto FMU200 quanto LUT7OG sejam submetidos ao maior número possível de ensaios de forma que os resultado obtidos *in vitro* correspondam o máximo possível com a realidade. Dessa forma, sugerimos que futuramente seja realizada uma análise mais aprofundada com ambos os compostos a fim de elucidar completamente seus mecanismos de ação. Além disso, ressalta-se que as implicações clínicas dos resultados aqui

relatados não são claras neste momento, mas, com base em nossas observações sugerimos que estudos futuros realizem uma triagem ADME (acrônimo para Absorção, Distribuição, Metabolização e Eliminação) pré-clínica, uma vez que um composto com características farmacocinéticas favoráveis têm maior probabilidade de se mostrar eficaz e seguro em testes *in vivo* e testes clínicos. Nesse sentido, a biotecnologia foi e, continuará sendo uma ferramenta valiosa que permite a eliminação precoce de drogas candidatas não adequadas e a exploração abrangente das potencialidades dos compostos mais promissores contribuindo na prospeção e rastreamento de moléculas promissoras para o tratamento de doenças neurodegenerativas.

7. REFERÊNCIAS

ACCORRONI, A.; GIORGI, F. S.; DONZELLI, R.; LORENZINI, L.; PRONTERA, C.; SABA, A.; VERGALLO, A.; TOGNONI, G.; SICILIANO, G.; BALDACCI, F.; BONUCCELLI, U.; CLERICO, A.; ZUCCHI, R. Thyroid hormone levels in the cerebrospinal fluid correlate with disease severity in euthyroid patients with Alzheimer's disease. **Endocrine**, vol. 55, no. 3, p. 981–984, Mar. 2017. https://doi.org/10.1007/s12020-016-0897-6.

AGEING AND HEALTH. [*s. d.*]. Disponível em: https://www.who.int/news-room/fact-sheets/detail/ageing-and-health. Acesso em: 27 Fev. 2021.

AHMED, T.; ZULFIQAR, A.; ARGUELLES, S.; RASEKHIAN, M.; NABAVI, S. F.; SILVA, A. S.; NABAVI, S. M. Map kinase signaling as therapeutic target for neurodegeneration. **Pharmacological Research**, vol. 160, p. 105090, 21 Jul. 2020. https://doi.org/10.1016/j.phrs.2020.105090.

AKHTER, R.; SANPHUI, P.; DAS, H.; SAHA, P.; BISWAS, S. C. The regulation of p53 up-regulated modulator of apoptosis by JNK/c-Jun pathway in β-amyloid-induced neuron death. **Journal of Neurochemistry**, vol. 134, no. 6, p. 1091–1103, Set. 2015. https://doi.org/10.1111/jnc.13128.

ALBARRACIN, S. L.; STAB, B.; CASAS, Z.; SUTACHAN, J. J.; SAMUDIO, I.; GONZALEZ, J.; GONZALO, L.; CAPANI, F.; MORALES, L.; BARRETO, G. E. Effects of natural antioxidants in neurodegenerative disease. **Nutritional Neuroscience**, vol. 15, no. 1, p. 1–9, Jan. 2012. https://doi.org/10.1179/1476830511Y.0000000028.

ALZHEIMER'S ASSOCIATION. 2017 Alzheimer's disease facts and figures. **Alzheimer's & Dementia**, vol. 13, no. 4, p. 325–373, Abr. 2017. https://doi.org/10.1016/j.jalz.2017.02.001.

ALZHEIMER'S ASSOCIATION. 2019 Alzheimer's disease facts and figures. **Alzheimer's & Dementia**, vol. 15, no. 3, p. 321–387, Mar. 2019. https://doi.org/10.1016/j.jalz.2019.01.010.

ALZHEIMER, A.Über eine eigenartige Erkrankung der Hirnrinde. **Allgemeine Zeitschrift fur Psychiatrie und Psychisch-gerichttliche Medizin** vol. 64, p. 146–148, 1907.

ANDERSEN, J. K. Oxidative stress in neurodegeneration: cause or consequence? **Nature Medicine**, vol. 10 Suppl, p. S18-25, Jul. 2004. https://doi.org/10.1038/nrn1434.

AMERICAN PSYCHIATRIC ASSOCIATION. **DSM-V. Manual Diagnóstico e Estatístico de Transtornos Mentais.** Porto Alegre: Artmed, 2013, 5a. ed.

ATANASOV, A. G.; WALTENBERGER, B.; PFERSCHY-WENZIG, E. Europe PMC Funders Group Discovery and resupply of pharmacologically active plant- derived natural products : A review. vol. 33, no. 8, p. 1582–1614, 2016. .

BAKHTIARI, M.; PANAHI, Y.; AMELI, J.; DARVISHI, B. Protective effects of flavonoids against Alzheimer's disease-related neural dysfunctions. **Biomedicine & Pharmacotherapy (Biomedecine & Pharmacotherapie)**, vol. 93, p. 218–229, Set. 2017. https://doi.org/10.1016/j.biopha.2017.06.010.

BATISTA, C. R. A.; GOMES, G. F.; CANDELARIO-JALIL, E.; FIEBICH, B. L.; DE

OLIVEIRA, A. C. P. Lipopolysaccharide-Induced Neuroinflammation as a Bridge to Understand Neurodegeneration. **International Journal of Molecular Sciences**, vol. 20, no. 9, 9 Mai 2019. https://doi.org/10.3390/ijms20092293.

BENEDICTUS, M. R.; LEEUWIS, A. E.; BINNEWIJZEND, M. A. A.; KUIJER, J. P. A.; SCHELTENS, P.; BARKHOF, F.; VAN DER FLIER, W. M.; PRINS, N. D. Lower cerebral blood flow is associated with faster cognitive decline in Alzheimer's disease. **European Radiology**, vol. 27, no. 3, p. 1169–1175, Mar. 2017. https://doi.org/10.1007/s00330-016-4450-z.

BERGHAUS, L. J.; MOORE, J. N.; HURLEY, D. J.; VANDENPLAS, M. L.; FORTES, B. P.; WOLFERT, M. A.; BOONS, G.-J. Innate immune responses of primary murine macrophage-lineage cells and RAW 264.7 cells to ligands of Toll-like receptors 2, 3, and 4. **Comparative Immunology, Microbiology and Infectious Diseases**, vol. 33, no. 5, p. 443–454, Set. 2010. https://doi.org/10.1016/j.cimid.2009.07.001.

BOGOYEVITCH, M. A.; BOEHM, I.; OAKLEY, A.; KETTERMAN, A. J.; BARR, R. K. Targeting the JNK MAPK cascade for inhibition: basic science and therapeutic potential. **Biochimica et Biophysica Acta**, vol. 1697, no. 1–2, p. 89–101, 11 Mar. 2004. https://doi.org/10.1016/j.bbapap.2003.11.016.

BOGOYEVITCH, M. A.; NGOEI, K. R. W.; ZHAO, T. T.; YEAP, Y. Y. C.; NG, D. C. H. c-Jun N-terminal kinase (JNK) signaling: recent advances and challenges. **Biochimica et Biophysica Acta**, vol. 1804, no. 3, p. 463–475, Mar. 2010. https://doi.org/10.1016/j.bbapap.2009.11.002.

BOWEN, D. M.; SMITH, C. B.; WHITE, P.; DAVISON, A. N. Neurotransmitter-related enzymes and indices of hypoxia in senile dementia and other abiotrophies. **Brain: A Journal of Neurology**, vol. 99, no. 3, p. 459–496, Set. 1976. https://doi.org/10.1093/brain/99.3.459.

BRAAK, H.; BRAAK, E. Diagnostic criteria for neuropathologic assessment of alzheimer's disease. **Neurobiology of Aging**, vol. 18, no. 4, p. S85–S88, Jul. 1997. https://doi.org/10.1016/S0197-4580(97)00062-6.

BURKE, J. F.; LANGA, K. M.; HAYWARD, R. A.; ALBIN, R. L. Modeling test and treatment strategies for presymptomatic Alzheimer disease. **Plos One**, vol. 9, no. 12, p. e114339, 4 Dez. 2014. https://doi.org/10.1371/journal.pone.0114339.

BUTTERFIELD, D. A.; CASTEGNA, A.; LAUDERBACK, C. M.; DRAKE, J. Evidence that amyloid beta-peptide-induced lipid peroxidation and its sequelae in Alzheimer's disease brain contribute to neuronal death. **Neurobiology of Aging**, vol. 23, no. 5, p. 655–664, Out. 2002. https://doi.org/10.1016/s0197-4580(01)00340-2.

BU, X.-L.; RAO, P. P. N.; WANG, Y.-J. Anti-amyloid Aggregation Activity of Natural Compounds: Implications for Alzheimer's Drug Discovery. **Molecular Neurobiology**, vol. 53, no. 6, p. 3565–3575, 2016. https://doi.org/10.1007/s12035-015-9301-4.

CARLSON, N. G.; WIEGGEL, W. A.; CHEN, J.; BACCHI, A.; ROGERS, S. W.; GAHRING, L. C. Inflammatory cytokines IL-1 alpha, IL-1 beta, IL-6, and TNF-alpha impart neuroprotection to an excitotoxin through distinct pathways. **Journal of Immunology**, vol. 163, no. 7, p. 3963–3968, 1 Out. 1999. .

CASTELLO, M. A.; SORIANO, S. On the origin of Alzheimer's disease. Trials and tribulations of the amyloid hypothesis. **Ageing Research Reviews**, vol. 13, p. 10–12, Jan. 2014. https://doi.org/10.1016/j.arr.2013.10.001.

CENTENO, C.; REPICI, M.; CHATTON, J. Y.; RIEDERER, B. M.; BONNY, C.; NICOD, P.; PRICE, M.; CLARKE, P. G. H.; PAPA, S.; FRANZOSO, G.; BORSELLO, T. Role of the JNK pathway in NMDA-mediated excitotoxicity of cortical neurons. **Cell Death and Differentiation**, vol. 14, no. 2, p. 240–253, Fev. 2007. https://doi.org/10.1038/sj.cdd.4401988.

CHAKRABARTY, P.; LI, A.; CEBALLOS-DIAZ, C.; EDDY, J. A.; FUNK, C. C.; MOORE, B.; DINUNNO, N.; ROSARIO, A. M.; CRUZ, P. E.; VERBEECK, C.; SACINO, A.; NIX, S.; JANUS, C.; PRICE, N. D.; DAS, P.; GOLDE, T. E. IL-10 alters immunoproteostasis in APP mice, increasing plaque burden and worsening cognitive behavior. **Neuron**, vol. 85, no. 3, p. 519–533, 4 Fev. 2015. https://doi.org/10.1016/j.neuron.2014.11.020.

CHAMBERS, J. W.; LOGRASSO, P. V. Mitochondrial c-Jun N-terminal kinase (JNK) signaling initiates physiological changes resulting in amplification of reactive oxygen species generation. **The Journal of Biological Chemistry**, vol. 286, no. 18, p. 16052–16062, 6 Mai 2011. https://doi.org/10.1074/jbc.M111.223602.

CHANG, L.; KARIN, M. Mammalian MAP kinase signalling cascades. **Nature**, vol. 410, no. 6824, p. 37–40, 1 Mar. 2001. https://doi.org/10.1038/35065000.

CHANTEUX, H.; GUISSET, A. C.; PILETTE, C.; SIBILLE, Y. LPS induces IL-10 production by human alveolar macrophages via MAPKinases- and Sp1-dependent mechanisms. **Respiratory Research**, vol. 8, p. 71, 4 Out. 2007. https://doi.org/10.1186/1465-9921-8-71.

CHAUHAN, D.; LI, G.; HIDESHIMA, T.; PODAR, K.; MITSIADES, C.; MITSIADES, N.; MUNSHI, N.; KHARBANDA, S.; ANDERSON, K. C. JNK-dependent release of mitochondrial protein, Smac, during apoptosis in multiple myeloma (MM) cells. **The Journal of Biological Chemistry**, vol. 278, no. 20, p. 17593–17596, 16 Mai 2003. https://doi.org/10.1074/jbc.C300076200.

CHE, X.-F.; MORIYA, S.; ZHENG, C.-L.; ABE, A.; TOMODA, A.; MIYAZAWA, K. 2-Aminophenoxazine-3-one-induced apoptosis via generation of reactive oxygen species followed by c-jun N-terminal kinase activation in the human glioblastoma cell line LN229. **International Journal of Oncology**, vol. 43, no. 5, p. 1456–1466, Nov. 2013. https://doi.org/10.3892/ijo.2013.2088.

CHEN, A. Y.; LÜ, J.-M.; YAO, Q.; CHEN, C. Entacapone is an Antioxidant More Potent than Vitamin C and Vitamin E for Scavenging of Hypochlorous Acid and Peroxynitrite, and the Inhibition of Oxidative Stress-Induced Cell Death. **Medical Science Monitor**, vol. 22, p. 687–696, 1 Mar. 2016. https://doi.org/10.12659/msm.896462.

CHEN, G.-F.; XU, T.-H.; YAN, Y.; ZHOU, Y.-R.; JIANG, Y.; MELCHER, K.; XU, H. E. Amyloid beta: structure, biology and structure-based therapeutic development. **Acta Pharmacologica Sinica**, vol. 38, no. 9, p. 1205–1235, Set. 2017. https://doi.org/10.1038/aps.2017.28.

CHEN, S.; YANG, B.; XU, Y.; RONG, Y.; QIU, Y. Protection of Luteolin-7-O-glucoside against apoptosis induced by hypoxia/reoxygenation through the MAPK pathways in H9c2 cells. **Molecular medicine reports**, vol. 17, no. 5, p. 7156–7162, Mai. 2018. https://doi.org/10.3892/mmr.2018.8774.

CHEN, X.; JI, Z. L.; CHEN, Y. Z. TTD: therapeutic target database. **Nucleic Acids**

Research, vol. 30, no. 1, p. 412–415, 1 Jan. 2002. https://doi.org/10.1093/nar/30.1.412.

CHEUNG, Y.-T.; LAU, W. K.-W.; YU, M.-S.; LAI, C. S.-W.; YEUNG, S.-C.; SO, K.-F.; CHANG, R. C.-C. Effects of all-trans-retinoic acid on human SH-SY5Y neuroblastoma as in vitro model in neurotoxicity research. **Neurotoxicology**, vol. 30, no. 1, p. 127–135, Jan. 2009. https://doi.org/10.1016/j.neuro.2008.11.001.

CHILMONCZYK, Z.; BOJARSKI, A. J.; PILC, A.; SYLTE, I. Serotonin transporter and receptor ligands with antidepressant activity as neuroprotective and proapoptotic agents. **Pharmacological Reports**, vol. 69, no. 3, p. 469–478, Mai. 2017. https://doi.org/10.1016/j.pharep.2017.01.011.

CHOI, J. S.; ISLAM, M. N.; ALI, M. Y.; KIM, Y. M.; PARK, H. J.; SOHN, H. S.; JUNG, H. A. The effects of C-glycosylation of luteolin on its antioxidant, anti-Alzheimer's disease, anti-diabetic, and anti-inflammatory activities. **Archives of Pharmacal Research**, vol. 37, no. 10, p. 1354–1363, Out. 2014. https://doi.org/10.1007/s12272-014-0351-3.

CHOI, W.; YOON, S.; OH, T. H.; CHOI, E.; MALLEY, K. L. O. Two distinct mechanisms are involved in 6-hydroxydopamine- and MPP+-induced dopaminergic neuronal cell death: role of caspases, ROS, and JNK. **Journal of Neuroscience Research.** vol. 94, no. 1, p. 86–94, Dez. 1999. https://doi.org/10.1002/(SICI)1097-4547(19990701)57:1<86::AID-JNR9>3.0.CO;2-E.

CLARKE, M.; PENTZ, R.; BOBYN, J.; HAYLEY, S. Stressor-like effects of c-Jun N-terminal kinase (JNK) inhibition. **Plos One**, vol. 7, no. 8, p. e44073, 29 Ago. 2012. https://doi.org/10.1371/journal.pone.0044073.

COFFEY, E. T. Nuclear and cytosolic JNK signalling in neurons. **Nature Reviews. Neuroscience**, vol. 15, no. 5, p. 285–299, Mai. 2014. https://doi.org/10.1038/nrn3729.

COHEN, G.; HEIKKILA, R. E. The generation of hydrogen peroxide, superoxide radical, and hydroxyl radical by 6-hydroxydopamine, dialuric acid, and related cytotoxic agents. **The Journal of Biological Chemistry**, vol. 249, no. 8, p. 2447–2452, 25 Abr. 1974. .

BRASIL. **CONFERÊNCIA DAS NAÇÕES UNIDAS SOBRE MEIO AMBIENTE E DESENVOLVIMENTO**. Rio de Janeiro, 1992.

CONNOLLY, N. M. C.; THEUREY, P.; ADAM-VIZI, V.; BAZAN, N. G.; BERNARDI, P.; BOLAÑOS, J. P.; CULMSEE, C.; DAWSON, V. L.; DESHMUKH, M.; DUCHEN, M. R.; DÜSSMANN, H.; FISKUM, G.; GALINDO, M. F.; HARDINGHAM, G. E.; HARDWICK, J. M.; JEKABSONS, M. B.; JONAS, E. A.; JORDÁN, J.; LIPTON, S. A.; … PREHN, J. H. M. Guidelines on experimental methods to assess mitochondrial dysfunction in cellular models of neurodegenerative diseases. **Cell Death and Differentiation**, vol. 25, no. 3, p. 542–572, 2018. https://doi.org/10.1038/s41418-017-0020-4.

CORDER, E. H.; SAUNDERS, A. M.; STRITTMATTER, W. J.; SCHMECHEL, D. E.; GASKELL, P. C.; SMALL, G. W.; ROSES, A. D.; HAINES, J. L.; PERICAK-VANCE, M. A. Gene dose of apolipoprotein E type 4 allele and the risk of Alzheimer's disease in late onset families. **Science**, vol. 261, no. 5123, p. 921–923, 13 Ago. 1993. https://doi.org/10.1126/science.8346443.

CRAFT, S.; CLAXTON, A.; BAKER, L. D.; HANSON, A. J.; CHOLERTON, B.;

TRITTSCHUH, E. H.; DAHL, D.; CAULDER, E.; NETH, B.; MONTINE, T. J.; JUNG, Y.; MALDJIAN, J.; WHITLOW, C.; FRIEDMAN, S. Effects of Regular and Long-Acting Insulin on Cognition and Alzheimer's Disease Biomarkers: A Pilot Clinical Trial. **Journal of Alzheimer's Disease**, vol. 57, no. 4, p. 1325–1334, 2017. https://doi.org/10.3233/JAD-161256.

CROFT, K. D. The chemistry and biological effects of flavonoids and phenolic acids. **Annals of the New York Academy of Sciences**, vol. 854, p. 435–442, 20 Nov. 1998. https://doi.org/10.1111/j.1749-6632.1998.tb09922.x.

CROSS-DISORDER GROUP OF THE PSYCHIATRIC GENOMICS CONSORTIUM; LEE, S. H.; RIPKE, S.; NEALE, B. M.; FARAONE, S. V.; PURCELL, S. M.; PERLIS, R. H.; MOWRY, B. J.; THAPAR, A.; GODDARD, M. E.; WITTE, J. S.; ABSHER, D.; AGARTZ, I.; AKIL, H.; AMIN, F.; ANDREASSEN, O. A.; ANJORIN, A.; ANNEY, R.; ANTTILA, V.; … ET AL. Genetic relationship between five psychiatric disorders estimated from genome-wide SNPs. **Nature Genetics**, vol. 45, no. 9, p. 984–994, Set. 2013. https://doi.org/10.1038/ng.2711.

CUADRADO, A.; NEBREDA, A. R. Mechanisms and functions of p38 MAPK signalling. **The Biochemical Journal**, vol. 429, no. 3, p. 403–417, 1 Ago. 2010. https://doi.org/10.1042/BJ20100323.

CUI, X.-X.; YANG, X.; WANG, H.-J.; RONG, X.-Y.; JING, S.; XIE, Y.-H.; HUANG, D.-F.; ZHAO, C. Luteolin-7-O-Glucoside Present in Lettuce Extracts Inhibits Hepatitis B Surface Antigen Production and Viral Replication by Human Hepatoma Cells in Vitro. **Frontiers in microbiology**, vol. 8, p. 2425, 6 Dez. 2017. https://doi.org/10.3389/fmicb.2017.02425.

CUMMINGS, J.; LEE, G.; MORTSDORF, T.; RITTER, A.; ZHONG, K. Alzheimer's disease drug development pipeline: 2017. **Alzheimer's & dementia : translational research & clinical interventions**, vol. 3, no. 3, p. 367–384, Set. 2017. https://doi.org/10.1016/j.trci.2017.05.002.

CUYVERS, E.; SLEEGERS, K. Genetic variations underlying Alzheimer's disease: evidence from genome-wide association studies and beyond. **Lancet Neurology**, vol. 15, no. 8, p. 857–868, 2016. https://doi.org/10.1016/S1474-4422(16)00127-7.

DAFSARI, F. S.; JESSEN, F. Depression-an underrecognized target for prevention of dementia in Alzheimer's disease. **Translational psychiatry**, vol. 10, no. 1, p. 160, 20 Mai. 2020. https://doi.org/10.1038/s41398-020-0839-1.

DAVIES, P.; MALONEY, A. J. Selective loss of central cholinergic neurons in Alzheimer's disease. **The Lancet**, vol. 2, no. 8000, p. 1403, 25 Dez. 1976. https://doi.org/10.1016/S0140-6736(76)91936-X.

DAVIS, M. I.; HUNT, J. P.; HERRGARD, S.; CICERI, P.; WODICKA, L. M.; PALLARES, G.; HOCKER, M.; TREIBER, D. K.; ZARRINKAR, P. P. Comprehensive analysis of kinase inhibitor selectivity. **Nature Biotechnology**, vol. 29, no. 11, p. 1046–1051, 30 Out. 2011. https://doi.org/10.1038/nbt.1990.

DEXTER, D. T.; CARTER, C. J.; WELLS, F. R.; JAVOY-AGID, F.; AGID, Y.; LEES, A.; JENNER, P.; MARSDEN, C. D. Basal lipid peroxidation in substantia nigra is increased in Parkinson's disease. **Journal of Neurochemistry**, vol. 52, no. 2, p. 381–389, Fev. 1989. https://doi.org/10.1111/j.1471-4159.1989.tb09133.x.

DEY, A.; BHATTACHARYA, R.; MUKHERJEE, A.; PANDEY, D. K. Natural products

against Alzheimer's disease: Pharmaco-therapeutics and biotechnological interventions. **Biotechnology advances**, vol. 35, no. 2, p. 178–216, 2017. https://doi.org/10.1016/j.biotechadv.2016.12.005.

DE BITTENCOURT PASQUALI, M. A.; DE RAMOS, V. M.; ALBANUS, R. D. O.; KUNZLER, A.; DE SOUZA, L. H. T.; DALMOLIN, R. J. S.; GELAIN, D. P.; RIBEIRO, L.; CARRO, L.; MOREIRA, J. C. F. Gene Expression Profile of NF-κB, Nrf2, Glycolytic, and p53 Pathways During the SH-SY5Y Neuronal Differentiation Mediated by Retinoic Acid. **Molecular Neurobiology**, vol. 53, no. 1, p. 423–435, Jan. 2016. https://doi.org/10.1007/s12035-014-8998-9.

DHANASEKARAN, D. N.; JOHNSON, G. L. MAPKs: function, regulation, role in cancer and therapeutic targeting. **Oncogene**, vol. 26, no. 22, p. 3097–3099, 14 Mai. 2007. https://doi.org/10.1038/sj.onc.1210395.

DIRSCHERL, K.; KARLSTETTER, M.; EBERT, S.; KRAUS, D.; HLAWATSCH, J.; WALCZAK, Y.; MOEHLE, C.; FUCHSHOFER, R.; LANGMANN, T. Luteolin triggers global changes in the microglial transcriptome leading to a unique anti-inflammatory and neuroprotective phenotype. **Journal of Neuroinflammation**, vol. 7, p. 3, 14 Jan. 2010. https://doi.org/10.1186/1742-2094-7-3.

DRACHMAN, D. A.; LEAVITT, J. Human memory and the cholinergic system. A relationship to aging? **Archives of Neurology**, vol. 30, no. 2, p. 113–121, Fev. 1974. https://doi.org/10.1001/archneur.1974.00490320001001.

DRUG SAFETY AND AVAILABILITY | FDA. [*s. d.*]. Disponível em: https://www.fda.gov/drugs/drug-safety-and-availability. Acesso em: 8 Jul. 2020.

DUONG, M. T. H.; LEE, J.-H.; AHN, H.-C. C-Jun N-terminal kinase inhibitors: Structural insight into kinase-inhibitor complexes. **Computational and structural biotechnology journal**, vol. 18, p. 1440–1457, 12 Jun. 2020. https://doi.org/10.1016/j.csbj.2020.06.013.

DUTHIE, A.; CHEW, D.; SOIZA, R. L. Non-psychiatric comorbidity associated with Alzheimer's disease. **QJM: Monthly Journal of the Association of Physicians**, vol. 104, no. 11, p. 913–920, Nov. 2011. https://doi.org/10.1093/qjmed/hcr118.

DU, H.; SHIDU YAN, S. Unlocking the Door to Neuronal Woes in Alzheimer's Disease: Aβ and Mitochondrial Permeability Transition Pore. **Pharmaceuticals (Basel, Switzerland)**, vol. 3, no. 6, p. 1936–1948, 14 Jun. 2010. https://doi.org/10.3390/ph3061936.

ERTA, M.; QUINTANA, A.; HIDALGO, J. Interleukin-6, a major cytokine in the central nervous system. **International Journal of Biological Sciences**, vol. 8, no. 9, p. 1254–1266, 25 Out. 2012. https://doi.org/10.7150/ijbs.4679.

FAN, P.; YU, X.-Y.; XIE, X.-H.; CHEN, C.-H.; ZHANG, P.; YANG, C.; PENG, X.; WANG, Y.-T. Mitophagy is a protective response against oxidative damage in bone marrow mesenchymal stem cells. **Life Sciences**, vol. 229, p. 36–45, 15 Jul. 2019. https://doi.org/10.1016/j.lfs.2019.05.027.

FERNÁNDEZ-PACHÓN, M. S.; BERNÁ, G.; OTAOLAURRUCHI, E.; TRONCOSO, A. M.; MARTÍN, F.; GARCÍA-PARRILLA, M. C. Changes in antioxidant endogenous enzymes (activity and gene expression levels) after repeated red wine intake. **Journal of Agricultural and Food Chemistry**, vol. 57, no. 15, p. 6578–6583, 12 Ago. 2009. https://doi.org/10.1021/jf901863w.

FERRI, C. P.; PRINCE, M.; BRAYNE, C.; BRODATY, H.; FRATIGLIONI, L.; GANGULI, M.; HALL, K.; HASEGAWA, K.; HENDRIE, H.; HUANG, Y.; JORM, A.; MATHERS, C.; MENEZES, P. R.; RIMMER, E.; SCAZUFCA, M.; ALZHEIMER'S DISEASE INTERNATIONAL. Global prevalence of dementia: a Delphi consensus study. **The Lancet**, vol. 366, no. 9503, p. 2112–2117, 17 Dez. 2005. https://doi.org/10.1016/S0140-6736(05)67889-0.

FIEBICH, B. L.; BATISTA, C. R. A.; SALIBA, S. W.; YOUSIF, N. M.; DE OLIVEIRA, A. C. P. Role of microglia tlrs in neurodegeneration. **Frontiers in Cellular Neuroscience**, vol. 12, p. 329, 2 Out. 2018. https://doi.org/10.3389/fncel.2018.00329.

FOEY, A. D.; PARRY, S. L.; WILLIAMS, L. M.; FELDMANN, M.; FOXWELL, B. M.; BRENNAN, F. M. Regulation of monocyte IL-10 synthesis by endogenous IL-1 and TNF-alpha: role of the p38 and p42/44 mitogen-activated protein kinases. **Journal of Immunology**, vol. 160, no. 2, p. 920–928, 15 Jan. 1998. .

FORNARI, F. A.; RANDOLPH, J. K.; YALOWICH, J. C.; RITKE, M. K.; GEWIRTZ, D. A. Interference by doxorubicin with DNA unwinding in MCF-7 breast tumor cells. **Molecular Pharmacology**, vol. 45, no. 4, p. 649–656, Abr. 1994. .

FORSTER, J. I.; KÖGLSBERGER, S.; TREFOIS, C.; BOYD, O.; BAUMURATOV, A. S.; BUCK, L.; BALLING, R.; ANTONY, P. M. A. Characterization of Differentiated SH-SY5Y as Neuronal Screening Model Reveals Increased Oxidative Vulnerability. **Journal of Biomolecular Screening**, vol. 21, no. 5, p. 496–509, Jun. 2016. https://doi.org/10.1177/1087057115625190.

FRIEDLANDER, R. M. Apoptosis and caspases in neurodegenerative diseases. **The New England Journal of Medicine**, vol. 348, no. 14, p. 1365–1375, 3 Abr. 2003. https://doi.org/10.1056/NEJMra022366.

FUSTER-MATANZO, A.; LLORENS-MARTÍN, M.; HERNÁNDEZ, F.; AVILA, J. Role of neuroinflammation in adult neurogenesis and Alzheimer disease: therapeutic approaches. **Mediators of Inflammation**, vol. 2013, p. 260925, 3 Abr. 2013. https://doi.org/10.1155/2013/260925.

GALASKO, D. R.; PESKIND, E.; CLARK, C. M.; QUINN, J. F.; RINGMAN, J. M.; JICHA, G. A.; COTMAN, C.; COTTRELL, B.; MONTINE, T. J.; THOMAS, R. G.; AISEN, P.; ALZHEIMER'S DISEASE COOPERATIVE STUDY. Antioxidants for Alzheimer disease: a randomized clinical trial with cerebrospinal fluid biomarker measures. **Archives of Neurology**, vol. 69, no. 7, p. 836–841, Jul. 2012. https://doi.org/10.1001/archneurol.2012.85.

GALEOTTI, N.; GHELARDINI, C. Regionally selective activation and differential regulation of ERK, JNK and p38 MAP kinase signalling pathway by protein kinase C in mood modulation. **The International Journal of Neuropsychopharmacology**, vol. 15, no. 6, p. 781–793, Jul. 2012. https://doi.org/10.1017/S1461145711000897.

GAO, S.; HOWARD, S.; LOGRASSO, P. V. Pharmacological Inhibition of c-Jun N-terminal Kinase Reduces Food Intake and Sensitizes Leptin's Anorectic Signaling Actions. **Scientific Reports**, vol. 7, p. 41795, 6 Fev. 2017. https://doi.org/10.1038/srep41795.

GBD 2016 DEMENTIA COLLABORATORS. Global, regional, and national burden of Alzheimer's disease and other dementias, 1990-2016: a systematic analysis for the

Global Burden of Disease Study 2016. **Lancet Neurology**, vol. 18, no. 1, p. 88–106, 2019. https://doi.org/10.1016/S1474-4422(18)30403-4.

GBD 2016 NEUROLOGY COLLABORATORS. Global, regional, and national burden of neurological disorders, 1990-2016: a systematic analysis for the Global Burden of Disease Study 2016. **Lancet Neurology**, vol. 18, no. 5, p. 459–480, 14 Mar. 2019. https://doi.org/10.1016/S1474-4422(18)30499-X.

GLINKA, Y.; GASSEN, M.; YOUDIM, M. B. Mechanism of 6-hydroxydopamine neurotoxicity. **Journal of Neural Transmission. Supplementum**, vol. 50, p. 55–66, 1997. https://doi.org/10.1007/978-3-7091-6842-4_7.

GLINKA, Y.; TIPTON, K. F.; YOUDIM, M. B. Mechanism of inhibition of mitochondrial respiratory complex I by 6-hydroxydopamine and its prevention by desferrioxamine. **European Journal of Pharmacology**, vol. 351, no. 1, p. 121–129, 12 Jun. 1998. https://doi.org/10.1016/s0014-2999(98)00279-9.

GLINKA, Y.; TIPTON, K. F.; YOUDIM, M. B. Nature of inhibition of mitochondrial respiratory complex I by 6-Hydroxydopamine. **Journal of Neurochemistry**, vol. 66, no. 5, p. 2004–2010, Mai. 1996. https://doi.org/10.1046/j.1471-4159.1996.66052004.x.

GLINKA, Y. Y.; YOUDIM, M. B. Inhibition of mitochondrial complexes I and IV by 6-hydroxydopamine. **European Journal of Pharmacology**, vol. 292, no. 3–4, p. 329–332, 16 Mar. 1995. https://doi.org/10.1016/0926-6917(95)90040-3.

GOETTERT, M.; LUIK, S.; GRAESER, R.; LAUFER, S. A. A direct ELISA assay for quantitative determination of the inhibitory potency of small molecules inhibitors for JNK3. **Journal of Pharmaceutical and Biomedical Analysis**, vol. 55, no. 1, p. 236–240, 28 Abr. 2011. https://doi.org/10.1016/j.jpba.2011.01.014.

GOETTERT, M.; SCHATTEL, V.; KOCH, P.; MERFORT, I.; LAUFER, S. Biological evaluation and structural determinants of p38α mitogen-activated-protein kinase and c-Jun-N-terminal kinase 3 inhibition by flavonoids. **Chembiochem**, vol. 11, no. 18, p. 2579–2588, 10 Dez. 2010. https://doi.org/10.1002/cbic.201000487.

GOLDMAN, J. S.; HAHN, S. E.; CATANIA, J. W.; LARUSSE-ECKERT, S.; BUTSON, M. B.; RUMBAAUGH, M.; STRECKER, M. N.; ROBERTS, J. S.; BURKE, W.; MAYEUX, R.; BIRD, T.; AMERICAN COLLEGE OF MEDICAL GENETICS AND THE NATIONAL SOCIETY OF GENETIC COUNSELORS. Genetic counseling and testing for Alzheimer disease: joint practice guidelines of the American College of Medical Genetics and the National Society of Genetic Counselors. **Genetics in Medicine**, vol. 13, no. 6, p. 597–605, Jun. 2011. https://doi.org/10.1097/GIM.0b013e31821d69b8.

GOURMAUD, S.; PAQUET, C.; DUMURGIER, J.; PACE, C.; BOURAS, C.; GRAY, F.; LAPLANCHE, J.-L.; MEURS, E. F.; MOUTON-LIGER, F.; HUGON, J. Increased levels of cerebrospinal fluid JNK3 associated with amyloid pathology: links to cognitive decline. **Journal of Psychiatry & Neuroscience**, vol. 40, no. 3, p. 151–161, Mai. 2015. https://doi.org/10.1503/jpn.140062.

GRIMMIG, B.; KIM, S.-H.; NASH, K.; BICKFORD, P. C.; DOUGLAS SHYTLE, R. Neuroprotective mechanisms of astaxanthin: a potential therapeutic role in preserving cognitive function in age and neurodegeneration. **GeroScience**, vol. 39, no. 1, p. 19–32, 13 Fev. 2017. https://doi.org/10.1007/s11357-017-9958-x.

GUILLOT-SESTIER, M.-V.; DOTY, K. R.; GATE, D.; RODRIGUEZ, J.; LEUNG, B. P.; REZAI-ZADEH, K.; TOWN, T. Il10 deficiency rebalances innate immunity to mitigate Alzheimer-like pathology. **Neuron**, vol. 85, no. 3, p. 534–548, 4 Fev. 2015. https://doi.org/10.1016/j.neuron.2014.12.068.

GUPTA, S.; BARRETT, T.; WHITMARSH, A. J.; CAVANAGH, J.; SLUSS, H. K.; DÉRIJARD, B.; DAVIS, R. J. Selective interaction of JNK protein kinase isoforms with transcription factors. **The EMBO Journal**, vol. 15, no. 11, p. 2760–2770, 3 Jun. 1996. https://doi.org/10.1002/j.1460-2075.1996.tb00636.x.

GUZZI, C.; COLOMBO, L.; LUIGI, A. D.; SALMONA, M.; NICOTRA, F.; AIROLDI, C. Flavonoids and Their Glycosides as Anti-amyloidogenic Compounds: Aβ1-42 Interaction Studies to Gain New Insights into Their Potential for Alzheimer's Disease Prevention and Therapy. **Chemistry, An Asian Journal**, vol. 12, no. 1, p. 67–75, 3 Jan. 2017. https://doi.org/10.1002/asia.201601291.

HAAKSMA, M. L.; VILELA, L. R.; MARENGONI, A.; CALDERÓN-LARRAÑAGA, A.; LEOUTSAKOS, J.-M. S.; OLDE RIKKERT, M. G. M.; MELIS, R. J. F. Comorbidity and progression of late onset Alzheimer's disease: A systematic review. **Plos One**, vol. 12, no. 5, p. e0177044, 4 Mai. 2017. https://doi.org/10.1371/journal.pone.0177044.

HAEUSGEN, W.; BOEHM, R.; ZHAO, Y.; HERDEGEN, T.; WAETZIG, V. Specific activities of individual c-Jun N-terminal kinases in the brain. **Neuroscience**, vol. 161, no. 4, p. 951–959, 21 Jul. 2009. https://doi.org/10.1016/j.neuroscience.2009.04.014.

HAMANAKA, R. B.; CHANDEL, N. S. Mitochondrial reactive oxygen species regulate cellular signaling and dictate biological outcomes. **Trends in Biochemical Sciences**, vol. 35, no. 9, p. 505–513, Set. 2010. https://doi.org/10.1016/j.tibs.2010.04.002.

HANAWA, N.; SHINOHARA, M.; SABERI, B.; GAARDE, W. A.; HAN, D.; KAPLOWITZ, N. Role of JNK translocation to mitochondria leading to inhibition of mitochondria bioenergetics in acetaminophen-induced liver injury. **The Journal of Biological Chemistry**, vol. 283, no. 20, p. 13565–13577, 16 Mai. 2008. https://doi.org/10.1074/jbc.M708916200.

HEIM, K. E.; TAGLIAFERRO, A. R.; BOBILYA, D. J. Flavonoid antioxidants: chemistry, metabolism and structure-activity relationships. **The Journal of Nutritional Biochemistry**, vol. 13, no. 10, p. 572–584, Out. 2002. https://doi.org/10.1016/S0955-2863(02)00208-5.

HENSLEY, K.; FLOYD, R. A.; ZHENG, N. Y.; NAEL, R.; ROBINSON, K. A.; NGUYEN, X.; PYE, Q. N.; STEWART, C. A.; GEDDES, J.; MARKESBERY, W. R.; PATEL, E.; JOHNSON, G. V.; BING, G. p38 kinase is activated in the Alzheimer's disease brain. **Journal of Neurochemistry**, vol. 72, no. 5, p. 2053–2058, Mai. 1999. https://doi.org/10.1046/j.1471-4159.1999.0722053.x.

HEPP REHFELDT, S. C.; MAJOLO, F.; GOETTERT, M. I.; LAUFER, S. c-Jun N-Terminal Kinase Inhibitors as Potential Leads for New Therapeutics for Alzheimer's Diseases. **International Journal of Molecular Sciences**, vol. 21, no. 24, 18 Dez. 2020. https://doi.org/10.3390/ijms21249677.

HERLAAR, E.; BROWN, Z. p38 MAPK signalling cascades in inflammatory disease. **Molecular medicine today**, vol. 5, no. 10, p. 439–447, Out. 1999. https://doi.org/10.1016/S1357-4310(99)01544-0.

HESLOP, K. A.; ROVINI, A.; HUNT, E. G.; FANG, D.; MORRIS, M. E.; CHRISTIE, C.

F.; GOOZ, M. B.; DEHART, D. N.; DANG, Y.; LEMASTERS, J. J.; MALDONADO, E. N. JNK activation and translocation to mitochondria mediates mitochondrial dysfunction and cell death induced by VDAC opening and sorafenib in hepatocarcinoma cells. **Biochemical Pharmacology**, vol. 171, p. 113728, 2020. https://doi.org/10.1016/j.bcp.2019.113728.

HOOGLAND, I. C. M.; HOUBOLT, C.; VAN WESTERLOO, D. J.; VAN GOOL, W. A.; VAN DE BEEK, D. Systemic inflammation and microglial activation: systematic review of animal experiments. **Journal of Neuroinflammation**, vol. 12, p. 114, 6 Jun. 2015. https://doi.org/10.1186/s12974-015-0332-6.

HOQUE, A.; WILLIAMSON, N. A.; AMEEN, S. S.; CICCOTOSTO, G. D.; HOSSAIN, M. I.; OAKHILL, J. S.; NG, D. C. H.; ANG, C.-S.; CHENG, H.-C. Quantitative proteomic analyses of dynamic signalling events in cortical neurons undergoing excitotoxic cell death. **Cell death & disease**, vol. 10, no. 3, p. 213, 1 Mar. 2019. https://doi.org/10.1038/s41419-019-1445-0.

IAKOVLEVA, I.; BEGUM, A.; POKRZYWA, M.; WALFRIDSSON, M.; SAUER-ERIKSSON, A. E.; OLOFSSON, A. The flavonoid luteolin, but not luteolin-7-O-glucoside, prevents a transthyretin mediated toxic response. **Plos One**, vol. 10, no. 5, p. e0128222, 28 Mai. 2015. https://doi.org/10.1371/journal.pone.0128222.

IMBIMBO, B. P.; LOMBARD, J.; POMARA, N. Pathophysiology of Alzheimer's disease. **Neuroimaging clinics of North America**, vol. 15, no. 4, p. 727–53, ix, Nov. 2005. https://doi.org/10.1016/j.nic.2005.09.009.

ITANO, Y.; ITO, A.; UEHARA, T.; NOMURA, Y. Regulation of Bcl-2 protein expression in human neuroblastoma SH-SY5Y cells: positive and negative effects of protein kinases C and A, respectively. **Journal of Neurochemistry**, vol. 67, no. 1, p. 131–137, Jul. 1996. https://doi.org/10.1046/j.1471-4159.1996.67010131.x.

JANG, S.; KELLEY, K. W.; JOHNSON, R. W. Luteolin reduces IL-6 production in microglia by inhibiting JNK phosphorylation and activation of AP-1. **Proceedings of the National Academy of Sciences of the United States of America**, vol. 105, no. 21, p. 7534–7539, 27 Mai. 2008. https://doi.org/10.1073/pnas.0802865105.

JARNICKI, A. G.; CONROY, H.; BRERETON, C.; DONNELLY, G.; TOOMEY, D.; WALSH, K.; SWEENEY, C.; LEAVY, O.; FLETCHER, J.; LAVELLE, E. C.; DUNNE, P.; MILLS, K. H. G. Attenuating regulatory T cell induction by TLR agonists through inhibition of p38 MAPK signaling in dendritic cells enhances their efficacy as vaccine adjuvants and cancer immunotherapeutics. **Journal of Immunology**, vol. 180, no. 6, p. 3797–3806, 15 Mar. 2008. https://doi.org/10.4049/jimmunol.180.6.3797.

JAYASENA, T.; POLJAK, A.; SMYTHE, G.; BRAIDY, N.; MÜNCH, G.; SACHDEV, P. The role of polyphenols in the modulation of sirtuins and other pathways involved in Alzheimer's disease. **Ageing Research Reviews**, vol. 12, no. 4, p. 867–883, Set. 2013. https://doi.org/10.1016/j.arr.2013.06.003.

JOHNSON, J. W.; KOTERMANSKI, S. E. Mechanism of action of memantine. **Current Opinion in Pharmacology**, vol. 6, no. 1, p. 61–67, Fev. 2006. https://doi.org/10.1016/j.coph.2005.09.007.

JOVICIC, M. J.; LUKIC, I.; RADOJCIC, M.; ADZIC, M.; MARIC, N. P. Modulation of c-Jun N-terminal kinase signaling and specific glucocorticoid receptor phosphorylation in the treatment of major depression. **Medical Hypotheses**, vol. 85, no. 3, p. 291–

294, Set. 2015. https://doi.org/10.1016/j.mehy.2015.05.015.

JUNG, J. E.; KIM, G. S.; CHAN, P. H. Neuroprotection by interleukin-6 is mediated by signal transducer and activator of transcription 3 and antioxidative signaling in ischemic stroke. **Stroke**, vol. 42, no. 12, p. 3574–3579, Dez. 2011. https://doi.org/10.1161/STROKEAHA.111.626648.

KAMATA, H.; HONDA, S.-I.; MAEDA, S.; CHANG, L.; HIRATA, H.; KARIN, M. Reactive oxygen species promote TNFalpha-induced death and sustained JNK activation by inhibiting MAP kinase phosphatases. **Cell**, vol. 120, no. 5, p. 649–661, 11 Mar. 2005. https://doi.org/10.1016/j.cell.2004.12.041.

KAMENECKA, T.; JIANG, R.; SONG, X.; DUCKETT, D.; CHEN, W.; LING, Y. Y.; HABEL, J.; LAUGHLIN, J. D.; CHAMBERS, J.; FIGUERA-LOSADA, M.; CAMERON, M. D.; LIN, L.; RUIZ, C. H.; LOGRASSO, P. V. Synthesis, biological evaluation, X-ray structure, and pharmacokinetics of aminopyrimidine c-jun-N-terminal kinase (JNK) inhibitors. **Journal of Medicinal Chemistry**, vol. 53, no. 1, p. 419–431, 14 Jan. 2010. https://doi.org/10.1021/jm901351f.

KANDEL, E. R.; DUDAI, Y.; MAYFORD, M. R. The molecular and systems biology of memory. **Cell**, vol. 157, no. 1, p. 163–186, 27 Mar. 2014. https://doi.org/10.1016/j.cell.2014.03.001.

KANG, S. S.; LEE, J. Y.; CHOI, Y. K.; KIM, G. S.; HAN, B. H. Neuroprotective effects of flavones on hydrogen peroxide-induced apoptosis in SH-SY5Y neuroblostoma cells. **Bioorganic & Medicinal Chemistry Letters**, vol. 14, no. 9, p. 2261–2264, 3 Mai. 2004. https://doi.org/10.1016/j.bmcl.2004.02.003.

KANUNGO, J. DNA-PK and P38 MAPK: A Kinase Collusion in Alzheimer's Disease? **Brain disorders & therapy**, vol. 6, no. 2, 1 Mai. 2017. https://doi.org/10.4172/2168-975X.1000232.

KEREN-SHAUL, H.; SPINRAD, A.; WEINER, A.; MATCOVITCH-NATAN, O.; DVIR-SZTERNFELD, R.; ULLAND, T. K.; DAVID, E.; BARUCH, K.; LARA-ASTAISO, D.; TOTH, B.; ITZKOVITZ, S.; COLONNA, M.; SCHWARTZ, M.; AMIT, I. A Unique Microglia Type Associated with Restricting Development of Alzheimer's Disease. **Cell**, vol. 169, no. 7, p. 1276-1290.e17, 15 Jun. 2017. https://doi.org/10.1016/j.cell.2017.05.018.

KERIMI, A.; WILLIAMSON, G. Differential impact of flavonoids on redox modulation, bioenergetics, and cell signaling in normal and tumor cells: A comprehensive review. **Antioxidants & Redox Signaling**, vol. 29, no. 16, p. 1633–1659, 1 Dez. 2018. https://doi.org/10.1089/ars.2017.7086.

KHEIRI, G.; DOLATSHAHI, M.; RAHMANI, F.; REZAEI, N. Role of p38/MAPKs in Alzheimer's disease: implications for amyloid beta toxicity targeted therapy. **Reviews in the neurosciences**, vol. 30, no. 1, p. 9–30, 19 Dez. 2018. https://doi.org/10.1515/revneuro-2018-0008.

KHOLODENKO, B. N.; BIRTWISTLE, M. R. Four-dimensional dynamics of MAPK information processing systems. **Wiley interdisciplinary reviews. Systems biology and medicine**, vol. 1, no. 1, p. 28–44, Ago. 2009. https://doi.org/10.1002/wsbm.16.

KILLICK, R.; RIBE, E. M.; AL-SHAWI, R.; MALIK, B.; HOOPER, C.; FERNANDES, C.; DOBSON, R.; NOLAN, P. M.; LOURDUSAMY, A.; FURNEY, S.; LIN, K.; BREEN, G.; WROE, R.; TO, A. W. M.; LEROY, K.; CAUSEVIC, M.; USARDI, A.; ROBINSON,

M.; NOBLE, W.; … LOVESTONE, S. Clusterin regulates β-amyloid toxicity via Dickkopf-1-driven induction of the wnt-PCP-JNK pathway. **Molecular Psychiatry**, vol. 19, no. 1, p. 88–98, Jan. 2014. https://doi.org/10.1038/mp.2012.163.

KIM, B.-J.; SILVERMAN, S. M.; LIU, Y.; WORDINGER, R. J.; PANG, I.-H.; CLARK, A. F. In vitro and in vivo neuroprotective effects of cJun N-terminal kinase inhibitors on retinal ganglion cells. **Molecular Neurodegeneration**, vol. 11, p. 30, 21 Abr. 2016. https://doi.org/10.1186/s13024-016-0093-4.

KIM, C.; SANO, Y.; TODOROVA, K.; CARLSON, B. A.; ARPA, L.; CELADA, A.; LAWRENCE, T.; OTSU, K.; BRISSETTE, J. L.; ARTHUR, J. S. C.; PARK, J. M. The kinase p38 alpha serves cell type-specific inflammatory functions in skin injury and coordinates pro- and anti-inflammatory gene expression. **Nature Immunology**, vol. 9, no. 9, p. 1019–1027, Set. 2008. https://doi.org/10.1038/ni.1640.

KIM, E. K.; CHOI, E.-J. Pathological roles of MAPK signaling pathways in human diseases. **Biochimica et Biophysica Acta**, vol. 1802, no. 4, p. 396–405, Abr. 2010. https://doi.org/10.1016/j.bbadis.2009.12.009.

KIM, I.; RODRIGUEZ-ENRIQUEZ, S.; LEMASTERS, J. J. Selective degradation of mitochondria by mitophagy. **Archives of Biochemistry and Biophysics**, vol. 462, no. 2, p. 245–253, 15 Jun. 2007. https://doi.org/10.1016/j.abb.2007.03.034.

KIM, S.; CHIN, Y.; CHO, J. Protection of Cultured Cortical Neurons by Luteolin against Oxidative Damage through Inhibition of Apoptosis and Induction of Heme. **Biol. Pharm. Bull.**, vol. 40, no. 3, p. 256–265, 2017. .

KNIGHT, J. M.; COSTANZO, E. S.; SINGH, S.; YIN, Z.; SZABO, A.; PAWAR, D. S.; HILLARD, C. J.; RIZZO, J. D.; D'SOUZA, A.; PASQUINI, M.; COE, C. L.; IRWIN, M. R.; RAISON, C. L.; DROBYSKI, W. R. The IL-6 antagonist tocilizumab is associated with worse depression and related symptoms in the medically ill. **Translational psychiatry**, vol. 11, no. 1, p. 58, 18 Jan. 2021. https://doi.org/10.1038/s41398-020-01164-y.

KONDOH, K.; NISHIDA, E. Regulation of MAP kinases by MAP kinase phosphatases. **Biochimica et Biophysica Acta**, vol. 1773, no. 8, p. 1227–1237, Ago. 2007. https://doi.org/10.1016/j.bbamcr.2006.12.002.

KORECKA, J. A.; VAN KESTEREN, R. E.; BLAAS, E.; SPITZER, S. O.; KAMSTRA, J. H.; SMIT, A. B.; SWAAB, D. F.; VERHAAGEN, J.; BOSSERS, K. Phenotypic characterization of retinoic acid differentiated SH-SY5Y cells by transcriptional profiling. **Plos One**, vol. 8, no. 5, p. e63862, 28 Mai. 2013. https://doi.org/10.1371/journal.pone.0063862.

KORSHUNOV, S. S.; SKULACHEV, V. P.; STARKOV, A. A. High protonic potential actuates a mechanism of production of reactive oxygen species in mitochondria. **FEBS Letters**, vol. 416, no. 1, p. 15–18, 13 Out. 1997. https://doi.org/10.1016/s0014-5793(97)01159-9.

KRISHNA, A.; BIRYUKOV, M.; TREFOIS, C.; ANTONY, P. M. A.; HUSSONG, R.; LIN, J.; HEINÄNIEMI, M.; GLUSMAN, G.; KÖGLSBERGER, S.; BOYD, O.; VAN DEN BERG, B. H. J.; LINKE, D.; HUANG, D.; WANG, K.; HOOD, L.; THOLEY, A.; SCHNEIDER, R.; GALAS, D. J.; BALLING, R.; Mai., P. Systems genomics evaluation of the SH-SY5Y neuroblastoma cell line as a model for Parkinson's disease. **BMC Genomics**, vol. 15, p. 1154, 20 Dez. 2014. https://doi.org/

10.1186/1471-2164-15-1154.

KUNZLER, A.; ZEIDÁN-CHULIÁ, F.; GASPAROTTO, J.; GIRARDI, C. S.; KLAFKE, K.; PETIZ, L. L.; BORTOLIN, R. C.; ROSTIROLLA, D. C.; ZANOTTO-FILHO, A.; DE BITTENCOURT PASQUALI, M. A.; DICKSON, P.; DUNKLEY, P.; MOREIRA, J. C. F.; GELAIN, D. P. Changes in Cell Cycle and Up-Regulation of Neuronal Markers During SH-SY5Y Neurodifferentiation by Retinoic Acid are Mediated by Reactive Species Production and Oxidative Stress. **Molecular Neurobiology**, vol. 54, no. 9, p. 6903–6916, 2017. https://doi.org/10.1007/s12035-016-0189-4.

LAI, L.; SONG, Y.; LIU, Y.; CHEN, Q.; HAN, Q.; CHEN, W.; PAN, T.; ZHANG, Y.; CAO, X.; WANG, Q. MicroRNA-92a negatively regulates Toll-like receptor (TLR)-triggered inflammatory response in macrophages by targeting MKK4 kinase. **The Journal of Biological Chemistry**, vol. 288, no. 11, p. 7956–7967, 15 Mar. 2013. https://doi.org/10.1074/jbc.M112.445429.

LEE, S. A.; PARK, B.-R.; MOON, S.-M.; HONG, J. H.; KIM, D. K.; KIM, C. S. Chondroprotective Effect of Cynaroside in IL-1β-Induced Primary Rat Chondrocytes and Organ Explants via NF-κB and MAPK Signaling Inhibition. **Oxidative medicine and cellular longevity**, vol. 2020, p. 9358080, 24 Jan. 2020. https://doi.org/10.1155/2020/9358080.

LEE, Y. M.; HE, W.; LIOU, Y.-C. The redox language in neurodegenerative diseases: oxidative post-translational modifications by hydrogen peroxide. **Cell death & disease**, vol. 12, no. 1, p. 58, 11 Jan. 2021. https://doi.org/10.1038/s41419-020-03355-3.

LEHMENSIEK, V.; TAN, E.-M.; LIEBAU, S.; LENK, T.; ZETTLMEISL, H.; SCHWARZ, J.; STORCH, A. Dopamine transporter-mediated cytotoxicity of 6-hydroxydopamine in vitro depends on expression of mutant alpha-synucleins related to Parkinson's disease. **Neurochemistry International**, vol. 48, no. 5, p. 329–340, Abr. 2006. https://doi.org/10.1016/j.neuint.2005.11.008.

LEVITES, Y.; AMIT, T.; YOUDIM, M. B. H.; MANDEL, S. Involvement of protein kinase C activation and cell survival/ cell cycle genes in green tea polyphenol (-)-epigallocatechin 3-gallate neuroprotective action. **The Journal of Biological Chemistry**, vol. 277, no. 34, p. 30574–30580, 23 Ago. 2002. https://doi.org/10.1074/jbc.M202832200.

LIM, G. Y.; TAM, W. W.; LU, Y.; HO, C. S.; ZHANG, M. W.; HO, R. C. Prevalence of Depression in the Community from 30 Countries between 1994 and 2014. **Scientific Reports**, vol. 8, no. 1, p. 2861, 12 Fev. 2018. https://doi.org/10.1038/s41598-018-21243-x.

LIM, M. X.; PNG, C. W.; TAY, C. Y. B.; TEO, J. D. W.; JIAO, H.; LEHMING, N.; TAN, K. S. W.; ZHANG, Y. Differential regulation of proinflammatory cytokine expression by mitogen-activated protein kinases in macrophages in response to intestinal parasite infection. **Infection and Immunity**, vol. 82, no. 11, p. 4789–4801, Nov. 2014. https://doi.org/10.1128/IAI.02279-14.

LIU, P.-P.; XIE, Y.; MENG, X.-Y.; KANG, J.-S. History and progress of hypotheses and clinical trials for Alzheimer's disease. **Signal transduction and targeted therapy**, vol. 4, p. 29, 23 Ago. 2019. https://doi.org/10.1038/s41392-019-0063-8.

LIU, Z.; LI, T.; LI, P.; WEI, N.; ZHAO, Z.; LIANG, H.; JI, X.; CHEN, W.; XUE, M.; WEI,

J. The ambiguous relationship of oxidative stress, tau hyperphosphorylation, and autophagy dysfunction in alzheimer's disease. **Oxidative medicine and cellular longevity**, vol. 2015, p. 352723, 15 Jun. 2015. https://doi.org/10.1155/2015/352723.

LOEWENBRUECK, K. F.; TIGNO-ARANJUEZ, J. T.; BOEHM, B. O.; LEHMANN, P. V.; TARY-LEHMANN, M. Th1 responses to beta-amyloid in young humans convert to regulatory IL-10 responses in Down syndrome and Alzheimer's disease. **Neurobiology of Aging**, vol. 31, no. 10, p. 1732–1742, Out. 2010. https://doi.org/10.1016/j.neurobiolaging.2008.09.007.

LOPES, F. M.; SCHRÖDER, R.; DA FROTA, M. L. C.; ZANOTTO-FILHO, A.; MÜLLER, C. B.; PIRES, A. S.; MEURER, R. T.; COLPO, G. D.; GELAIN, D. P.; KAPCZINSKI, F.; MOREIRA, J. C. F.; FERNANDES, M. da C.; KLAMT, F. Comparison between proliferative and neuron-like SH-SY5Y cells as an in vitro model for Parkinson disease studies. **Brain Research**, vol. 1337, p. 85–94, 14 Jun. 2010. https://doi.org/10.1016/j.brainres.2010.03.102.

LOPES, K. O.; SPARKS, D. L.; STREIT, W. J. Microglial dystrophy in the aged and Alzheimer's disease brain is associated with ferritin immunoreactivity. **Glia**, vol. 56, no. 10, p. 1048–1060, 1 Ago. 2008. https://doi.org/10.1002/glia.20678.

LÓPEZ-CARBALLO, G.; MORENO, L.; MASIÁ, S.; PÉREZ, P.; BARETTINO, D. Activation of the phosphatidylinositol 3-kinase/Akt signaling pathway by retinoic acid is required for neural differentiation of SH-SY5Y human neuroblastoma cells. **The Journal of Biological Chemistry**, vol. 277, no. 28, p. 25297–25304, 12 Jul. 2002. https://doi.org/10.1074/jbc.M201869200.

LÓPEZ-OTÍN, C.; BLASCO, M. A.; PARTRIDGE, L.; SERRANO, M.; KROEMER, G. The hallmarks of aging. **Cell**, vol. 153, no. 6, p. 1194–1217, 6 Jun. 2013. https://doi.org/10.1016/j.cell.2013.05.039.

LUCERO, M.; SUAREZ, A. E.; CHAMBERS, J. W. Phosphoregulation on mitochondria: Integration of cell and organelle responses. **CNS Neuroscience & Therapeutics**, vol. 25, no. 7, p. 837–858, 25 Abr. 2019. https://doi.org/10.1111/cns.13141.

LUCHTMAN, D. W.; SONG, C. Why SH-SY5Y cells should be differentiated. **Neurotoxicology**, vol. 31, no. 1, p. 164–5; author reply 165, Jan. 2010. https://doi.org/10.1016/j.neuro.2009.10.015.

MAEZAWA, I.; ZIMIN, P. I.; WULFF, H.; JIN, L.-W. Amyloid-beta protein oligomer at low nanomolar concentrations activates microglia and induces microglial neurotoxicity. **The Journal of Biological Chemistry**, vol. 286, no. 5, p. 3693–3706, 4 Fev. 2011. https://doi.org/10.1074/jbc.M110.135244.

MANCZAK, M.; PARK, B. S.; JUNG, Y.; REDDY, P. H. Differential expression of oxidative phosphorylation genes in patients with Alzheimer's disease: implications for early mitochondrial dysfunction and oxidative damage. **Neuromolecular Medicine**, vol. 5, no. 2, p. 147–162, 2004. https://doi.org/10.1385/NMM:5:2:147.

MANSURI, M. L.; PARIHAR, P.; SOLANKI, I.; PARIHAR, M. S. Flavonoids in modulation of cell survival signalling pathways. **Genes & Nutrition**, vol. 9, no. 3, p. 400, Mai. 2014. https://doi.org/10.1007/s12263-014-0400-z.

MARCELLI, S.; IANNUZZI, F.; FICULLE, E.; MANGO, D.; PIERACCINI, S.; PELLEGRINO, S.; CORBO, M.; SIRONI, M.; PITTALUGA, A.; NISTICÒ, R.;

FELIGIONI, M. The selective disruption of presynaptic JNK2/STX1a interaction reduces NMDA receptor-dependent glutamate release. **Scientific Reports**, vol. 9, no. 1, p. 7146, 9 Mai. 2019. https://doi.org/10.1038/s41598-019-43709-2.

MARCHI, S.; GIORGI, C.; SUSKI, J. M.; AGNOLETTO, C.; BONONI, A.; BONORA, M.; DE MARCHI, E.; MISSIROLI, S.; PATERGNANI, S.; POLETTI, F.; RIMESSI, A.; DUSZYNSKI, J.; WIECKOWSKI, M. R.; PINTON, P. Mitochondria-ros crosstalk in the control of cell death and aging. **Journal of signal transduction**, vol. 2012, p. 329635, 2012. https://doi.org/10.1155/2012/329635.

MAYEUX, R. Genetic epidemiology of Alzheimer disease. **Alzheimer Disease and Associated Disorders**, vol. 20, no. 3 Suppl 2, p. S58-62, Set. 2006. https://doi.org/10.1097/00002093-200607001-00008.

MA, S. L.; TANG, N. L. S.; LAM, L. C. W.; CHIU, H. F. K. The association between promoter polymorphism of the interleukin-10 gene and Alzheimer's disease. **Neurobiology of Aging**, vol. 26, no. 7, p. 1005–1010, Jul. 2005. https://doi.org/10.1016/j.neurobiolaging.2004.08.010.

MA, W.; LIM, W.; GEE, K.; AUCOIN, S.; NANDAN, D.; KOZLOWSKI, M.; DIAZ-MITOMA, F.; KUMAR, A. The p38 mitogen-activated kinase pathway regulates the human interleukin-10 promoter via the activation of Sp1 transcription factor in lipopolysaccharide-stimulated human macrophages. **The Journal of Biological Chemistry**, vol. 276, no. 17, p. 13664–13674, 27 Abr. 2001. https://doi.org/10.1074/jbc.M011157200.

MCCORMICK, W. C.; KUKULL, W. A.; VAN BELLE, G.; BOWEN, J. D.; TERI, L.; LARSON, E. B. Symptom patterns and comorbidity in the early stages of Alzheimer's disease. **Journal of the American Geriatrics Society**, vol. 42, no. 5, p. 517–521, Mai. 1994. https://doi.org/10.1111/j.1532-5415.1994.tb04974.x.

MCKEEVER, P. M.; KIM, T.; HESKETH, A. R.; MACNAIR, L.; MILETIC, D.; FAVRIN, G.; OLIVER, S. G.; ZHANG, Z.; ST GEORGE-HYSLOP, P.; ROBERTSON, J. Cholinergic neuron gene expression differences captured by translational profiling in a mouse model of Alzheimer's disease. **Neurobiology of Aging**, vol. 57, p. 104–119, 25 Mai. 2017. https://doi.org/10.1016/j.neurobiolaging.2017.05.014.

MCKHANN, G.; DRACHMAN, D.; FOLSTEIN, M.; KATZMAN, R.; PRICE, D.; STADLAN, E. M. Clinical diagnosis of Alzheimer's disease: report of the NINCDS-ADRDA Work Group under the auspices of Department of Health and Human Services Task Force on Alzheimer's Disease. **Neurology**, vol. 34, no. 7, p. 939–944, Jul. 1984. https://doi.org/10.1212/wnl.34.7.939.

MCKHANN, G. M.; KNOPMAN, D. S.; CHERTKOW, H.; HYMAN, B. T.; JACK, C. R.; KAWAS, C. H.; KLUNK, W. E.; KOROSHETZ, W. J.; MANLY, J. J.; MAYEUX, R.; MOHS, R. C.; MORRIS, J. C.; ROSSOR, M. N.; SCHELTENS, P.; CARRILLO, M. C.; THIES, B.; WEINTRAUB, S.; PHELPS, C. H. The diagnosis of dementia due to Alzheimer's disease: recommendations from the National Institute on Aging-Alzheimer's Association workgroups on diagnostic guidelines for Alzheimer's disease. **Alzheimer's & Dementia**, vol. 7, no. 3, p. 263–269, Mai. 2011. https://doi.org/10.1016/j.jalz.2011.03.005.

MELINO, G.; THIELE, C. J.; KNIGHT, R. A.; PIACENTINI, M. Retinoids and the control of growth/death decisions in human neuroblastoma cell lines. **Journal of Neuro-Oncology**, vol. 31, no. 1–2, p. 65–83, Jan. 1997. https://doi.org/10.1023/

a:1005733430435.

MELZER, D.; PILLING, L. C.; FERRUCCI, L. The genetics of human ageing. **Nature Reviews. Genetics**, vol. 21, no. 2, p. 88–101, 2020. https://doi.org/10.1038/s41576-019-0183-6.

MIGALE, R.; HERBERT, B. R.; LEE, Y. S.; SYKES, L.; WADDINGTON, S. N.; PEEBLES, D.; HAGBERG, H.; JOHNSON, M. R.; BENNETT, P. R.; MACINTYRE, D. A. Specific lipopolysaccharide serotypes induce differential maternal and neonatal inflammatory responses in a murine model of preterm labor. **The American Journal of Pathology**, vol. 185, no. 9, p. 2390–2401, Set. 2015. https://doi.org/10.1016/j.ajpath.2015.05.015.

MITTAL, M.; SIDDIQUI, M. R.; TRAN, K.; REDDY, S. P.; MALIK, A. B. Reactive oxygen species in inflammation and tissue injury. **Antioxidants & Redox Signaling**, vol. 20, no. 7, p. 1126–1167, 1 Mar. 2014. https://doi.org/10.1089/ars.2012.5149.

MOHANDAS, E.; RAJMOHAN, V.; RAGHUNATH, B. Neurobiology of Alzheimer's disease. **Indian journal of psychiatry**, vol. 51, no. 1, p. 55–61, Jan. 2009. https://doi.org/10.4103/0019-5545.44908.

MOSSER, D. M.; ZHANG, X. Interleukin-10: new perspectives on an old cytokine. **Immunological Reviews**, vol. 226, p. 205–218, Dez. 2008. https://doi.org/10.1111/j.1600-065X.2008.00706.x.

MULLER, F. L.; LUSTGARTEN, M. S.; JANG, Y.; RICHARDSON, A.; VAN REMMEN, H. Trends in oxidative aging theories. **Free Radical Biology & Medicine**, vol. 43, no. 4, p. 477–503, 15 Ago. 2007. https://doi.org/10.1016/j.freeradbiomed.2007.03.034.

MUNOZ, L.; AMMIT, A. J. Targeting p38 MAPK pathway for the treatment of Alzheimer's disease. **Neuropharmacology**, vol. 58, no. 3, p. 561–568, Mar. 2010. https://doi.org/10.1016/j.neuropharm.2009.11.010.

MURPHY, M. P. How mitochondria produce reactive oxygen species. **The Biochemical Journal**, vol. 417, no. 1, p. 1–13, 1 Jan. 2009. https://doi.org/10.1042/BJ20081386.

MUTH, F.; EL-GOKHA, A.; ANSIDERI, F.; EITEL, M.; DOERING, E.; SIEVERS-, A.; LANGE, A.; BOECKLER, F. M.; LÄMMERHOFER, M.; KOCH, P.; LAUFER, S. A. Tri- and Tetra-substituted Pyridinylimidazoles as Covalent Inhibitors of c-Jun N-Terminal Kinase 3. **Journal of medicinal chemistry**. vol. 60, no. 2, p. 594-607, 26 Jan 2017. https://doi.org/10.1021/acs.jmedchem.6b01180.

NABAVI, S. F.; BRAIDY, N.; GORTZI, O.; SOBARZO-SANCHEZ, E.; DAGLIA, M.; SKALICKA-WOŹNIAK, K.; NABAVI, S. M. Luteolin as an anti-inflammatory and neuroprotective agent: A brief review. **Brain Research Bulletin**, vol. 119, no. Pt A, p. 1–11, Out. 2015. https://doi.org/10.1016/j.brainresbull.2015.09.002.

NEWMAN, D. J.; CRAGG, G. M. Natural Products as Sources of New Drugs from 1981 to 2014. **Journal of Natural Products**, vol. 79, no. 3, p. 629–661, 25 Mar. 2016. https://doi.org/10.1021/acs.jnatprod.5b01055.

NHO, J.-H.; JUNG, H.-K.; LEE, M.-J.; JANG, J.-H.; SIM, M.-O.; JEONG, D.-E.; CHO, H.-W.; KIM, J.-C. Beneficial Effects of Cynaroside on Cisplatin-Induced Kidney Injury In Vitro and In Vivo. **Toxicological research**, vol. 34, no. 2, p. 133–141, 15 Abr. 2018. https://doi.org/10.5487/TR.2018.34.2.133.

NORAT, P.; SOLDOZY, S.; SOKOLOWSKI, J. D.; GORICK, C. M.; KUMAR, J. S.; CHAE, Y.; YAĞMURLU, K.; PRADA, F.; WALKER, M.; LEVITT, M. R.; PRICE, R. J.; TVRDIK, P.; KALANI, M. Y. S. Mitochondrial dysfunction in neurological disorders: Exploring mitochondrial transplantation. **npj Regenerative medicine**, vol. 5, no. 1, p. 22, 23 Nov. 2020. https://doi.org/10.1038/s41536-020-00107-x.

OKAZAWA, H.; ESTUS, S. The JNK/c-Jun cascade and Alzheimer's disease. **American Journal of Alzheimer's Disease & Other Dementias**. vol. 17, no. 2, p. 79–88, 2002. https://doi.org/10.1177/153331750201700209.

OUYANG, W.; O'GARRA, A. IL-10 Family Cytokines IL-10 and IL-22: from Basic Science to Clinical Translation. **Immunity**, vol. 50, no. 4, p. 871–891, 16 Abr. 2019. https://doi.org/10.1016/j.immuni.2019.03.020.

PÅHLMAN, S.; RUUSALA, A. I.; ABRAHAMSSON, L.; MATTSSON, M. E.; ESSCHER, T. Retinoic acid-induced differentiation of cultured human neuroblastoma cells: a comparison with phorbolester-induced differentiation. **Cell differentiation**, vol. 14, no. 2, p. 135–144, Jun. 1984. https://doi.org/10.1016/0045-6039(84)90038-1.

PARKS, J. K.; SMITH, T. S.; TRIMMER, P. A.; BENNETT, J. P.; PARKER, W. D. Neurotoxic Abeta peptides increase oxidative stress in vivo through NMDA-receptor and nitric-oxide-synthase mechanisms, and inhibit complex IV activity and induce a mitochondrial permeability transition in vitro. **Journal of Neurochemistry**, vol. 76, no. 4, p. 1050–1056, Fev. 2001. https://doi.org/10.1046/j.1471-4159.2001.00112.x.

PARK, J.-W.; KWON, O.-K.; RYU, H. W.; PAIK, J.-H.; PARYANTO, I.; YUNIATO, P.; CHOI, S.; OH, S.-R.; AHN, K.-S. Anti-inflammatory effects of Passiflora foetida L. in LPS-stimulated RAW264.7 macrophages. **International Journal of Molecular Medicine**, vol. 41, no. 6, p. 3709–3716, Jun. 2018. https://doi.org/10.3892/ijmm.2018.3559.

PEDERSEN, W. A.; FU, W.; KELLER, J. N.; MARKESBERY, W. R.; APPEL, S.; SMITH, R. G.; KASARSKIS, E.; MATTSON, M. P. Protein modification by the lipid peroxidation product 4-hydroxynonenal in the spinal cords of amyotrophic lateral sclerosis patients. **Annals of Neurology**, vol. 44, no. 5, p. 819–824, Nov. 1998. https://doi.org/10.1002/ana.410440518.

PILLAI, J. A.; BENA, J.; BEBEK, G.; BEKRIS, L. M.; BONNER-JACKSON, A.; KOU, L.; PAI, A.; SØRENSEN, L.; NEILSEN, M.; RAO, S. M.; CHANCE, M.; LAMB, B. T.; LEVERENZ, J. B.; ALZHEIMER'S DISEASE NEUROIMAGING INITIATIVE. Inflammatory pathway analytes predicting rapid cognitive decline in MCI stage of Alzheimer's disease. **Annals of clinical and translational neurology**, vol. 7, no. 7, p. 1225–1239, 7 Jul. 2020. https://doi.org/10.1002/acn3.51109.

PIZZI, M.; SARNICO, I.; BORONI, F.; BENARESE, M.; DREANO, M.; GAROTTA, G.; VALERIO, A.; SPANO, P. Prevention of neuron and oligodendrocyte degeneration by interleukin-6 (IL-6) and IL-6 receptor/IL-6 fusion protein in organotypic hippocampal slices. **Molecular and Cellular Neurosciences**, vol. 25, no. 2, p. 301–311, Fev. 2004. https://doi.org/10.1016/j.mcn.2003.10.022.

POLIDORI, M. C.; NELLES, G. Antioxidant clinical trials in mild cognitive impairment and Alzheimer's disease - challenges and perspectives. **Current Pharmaceutical Design**, vol. 20, no. 18, p. 3083–3092, 2014. https://doi.org/10.2174/13816128113196660706.

POOLER, A. M.; NOBLE, W.; HANGER, D. P. A role for tau at the synapse in Alzheimer's disease pathogenesis. **Neuropharmacology**, vol. 76 Pt A, p. 1–8, Jan. 2014. https://doi.org/10.1016/j.neuropharm.2013.09.018.

PRAUSE, M.; BERCHTOLD, L. A.; URIZAR, A. I.; HYLDGAARD TRAUELSEN, M.; BILLESTRUP, N.; MANDRUP-POULSEN, T.; STØRLING, J. TRAF2 mediates JNK and STAT3 activation in response to IL-1β and IFNγ and facilitates apoptotic death of insulin-producing β-cells. **Molecular and Cellular Endocrinology**, vol. 420, p. 24–36, 15 Jan. 2016. https://doi.org/10.1016/j.mce.2015.11.021.

PRESGRAVES, S. P.; AHMED, T.; BORWEGE, S.; JOYCE, J. N. Terminally differentiated SH-SY5Y cells provide a model system for studying neuroprotective effects of dopamine agonists. **Neurotoxicity Research**, vol. 5, no. 8, p. 579–598, 2004. https://doi.org/10.1007/BF03033178.

RAHAL, A.; KUMAR, A.; SINGH, V.; YADAV, B.; TIWARI, R.; CHAKRABORTY, S.; DHAMA, K. Oxidative stress, prooxidants, and antioxidants: the interplay. **BioMed research international**, vol. 2014, p. 761264, 23 Jan. 2014. https://doi.org/10.1155/2014/761264.

RAMAN, M.; CHEN, W.; COBB, M. H. Differential regulation and properties of MAPKs. **Oncogene**, vol. 26, no. 22, p. 3100–3112, 14 Mai. 2007. https://doi.org/10.1038/sj.onc.1210392.

RAMASSAMY, C. Emerging role of polyphenolic compounds in the treatment of neurodegenerative diseases: a review of their intracellular targets. **European Journal of Pharmacology**, vol. 545, no. 1, p. 51–64, 1 Set. 2006. https://doi.org/10.1016/j.ejphar.2006.06.025.

RASOOL, M.; MALIK, A.; QURESHI, M. S.; MANAN, A.; PUSHPARAJ, P. N.; ASIF, M.; QAZI, M. H.; QAZI, A. M.; KAMAL, M. A.; GAN, S. H.; SHEIKH, I. A. Recent updates in the treatment of neurodegenerative disorders using natural compounds. **Evidence-Based Complementary and Alternative Medicine**, vol. 2014, p. 979730, 23 Abr. 2014. https://doi.org/10.1155/2014/979730.

RAW 264.7 ATCC® TIB-71™. [*s. d.*]. Disponível em: https://www.atcc.org/products/all/TIB-71.aspx. Acesso em: 4 Mar. 2021.

REVETT, T. J.; BAKER, G. B.; JHAMANDAS, J.; KAR, S. Glutamate system, amyloid ß peptides and tau protein: functional interrelationships and relevance to Alzheimer disease pathology. **Journal of Psychiatry & Neuroscience**, vol. 38, no. 1, p. 6–23, Jan. 2013. https://doi.org/10.1503/jpn.110190.

ROOS, W. P.; KAINA, B. DNA damage-induced cell death by apoptosis. **Trends in Molecular Medicine**, vol. 12, no. 9, p. 440–450, Set. 2006. https://doi.org/10.1016/j.molmed.2006.07.007.

ROSKOSKI, R. A historical overview of protein kinases and their targeted small molecule inhibitors. **Pharmacological Research**, vol. 100, p. 1–23, Out. 2015. https://doi.org/10.1016/j.phrs.2015.07.010.

ROSKOSKI, R. Classification of small molecule protein kinase inhibitors based upon the structures of their drug-enzyme complexes. **Pharmacological Research**, vol. 103, p. 26–48, Jan. 2016. https://doi.org/10.1016/j.phrs.2015.10.021.

RUDZIŃSKA, M.; PARODI, A.; BALAKIREVA, A. V.; CHEPIKOVA, O. E.; VENANZI,

F. M.; ZAMYATNIN, A. A. Cellular Aging Characteristics and Their Association with Age-Related Disorders. **Antioxidants (Basel, Switzerland)**, vol. 9, no. 2, 22 Jan. 2020. https://doi.org/10.3390/antiox9020094.

SARAIVA, M.; CHRISTENSEN, J. R.; TSYTSYKOVA, A. V.; GOLDFELD, A. E.; LEY, S. C.; KIOUSSIS, D.; O'GARRA, A. Identification of a macrophage-specific chromatin signature in the IL-10 locus. **Journal of Immunology**, vol. 175, no. 2, p. 1041–1046, 15 Jul. 2005. https://doi.org/10.4049/jimmunol.175.2.1041.

SARAIVA, M.; O'GARRA, A. The regulation of IL-10 production by immune cells. **Nature Reviews. Immunology**, vol. 10, no. 3, p. 170–181, Mar. 2010. https://doi.org/10.1038/nri2711.

SAUNDERS, A. M.; SCHMADER, K.; BREITNER, J. C.; BENSON, M. D.; BROWN, W. T.; GOLDFARB, L.; GOLDGABER, D.; MANWARING, M. G.; SZYMANSKI, M. H.; MCCOWN, N. Apolipoprotein E epsilon 4 allele distributions in late-onset Alzheimer's disease and in other amyloid-forming diseases. **The Lancet**, vol. 342, no. 8873, p. 710–711, 18 Set. 1993. https://doi.org/10.1016/0140-6736(93)91709-u.

SAVAGE, M. J.; LIN, Y.-G.; CIALLELLA, J. R.; FLOOD, D. G.; SCOTT, R. W. Activation of c-Jun N-terminal kinase and p38 in an Alzheimer's disease model is associated with amyloid deposition. **The Journal of Neuroscience**, vol. 22, no. 9, p. 3376–3385, 1 Mai. 2002. https://doi.org/20026352.

SAXENA, R. K.; VALLYATHAN, V.; LEWIS, D. M. Evidence for lipopolysaccharide-induced differentiation of RAW264.7 murine macrophage cell line into dendritic like cells. **Journal of Biosciences**, vol. 28, no. 1, p. 129–134, Fev. 2003. https://doi.org/10.1007/BF02970143.

SCHNEIDER, L.; GIORDANO, S.; ZELICKSON, B. R.; S JOHNSON, M.; A BENAVIDES, G.; OUYANG, X.; FINEBERG, N.; DARLEY-USMAR, V. M.; ZHANG, J. Differentiation of SH-SY5Y cells to a neuronal phenotype changes cellular bioenergetics and the response to oxidative stress. **Free Radical Biology & Medicine**, vol. 51, no. 11, p. 2007–2017, 1 Dez. 2011. https://doi.org/10.1016/j.freeradbiomed.2011.08.030.

SCHNEIDER, L. S.; MANGIALASCHE, F.; ANDREASEN, N.; FELDMAN, H.; GIACOBINI, E.; JONES, R.; MANTUA, V.; MECOCCI, P.; PANI, L. Clinical trials and late-stage drug development for Alzheimer's disease: an appraisal from 1984 to 2014. **Journal of Internal Medicine**. vol. 275, no. 3, p. 251–283, 2015. https://doi.org/10.1111/joim.12191.

SCHROETER, H.; BOYD, C. S.; AHMED, R.; SPENCER, J. P. E.; DUNCAN, R. F.; RICE-EVANS, C.; CADENAS, E. c-Jun N-terminal kinase (JNK)-mediated modulation of brain mitochondria function: new target proteins for JNK signalling in mitochondrion-dependent apoptosis. **The Biochemical Journal**, vol. 372, no. Pt 2, p. 359–369, 1 Jun. 2003. https://doi.org/10.1042/BJ20030201.

SCHULZ, E.; WENZEL, P.; MÜNZEL, T.; DAIBER, A. Mitochondrial redox signaling: Interaction of mitochondrial reactive oxygen species with other sources of oxidative stress. **Antioxidants & Redox Signaling**, vol. 20, no. 2, p. 308–324, 10 Jan. 2014. https://doi.org/10.1089/ars.2012.4609.

SERRANO-POZO, A.; BETENSKY, R. A.; FROSCH, M. P.; HYMAN, B. T. Plaque-Associated Local Toxicity Increases over the Clinical Course of Alzheimer Disease.

The American Journal of Pathology, vol. 186, no. 2, p. 375–384, Fev. 2016. https://doi.org/10.1016/j.ajpath.2015.10.010.

SERRANO-POZO, A.; FROSCH, M. P.; MASLIAH, E.; HYMAN, B. T. Neuropathological alterations in Alzheimer disease. **Cold Spring Harbor perspectives in medicine**, vol. 1, no. 1, p. a006189, Set. 2011. https://doi.org/10.1101/cshperspect.a006189.

SERRANO-POZO, A.; QIAN, J.; MONSELL, S. E.; FROSCH, M. P.; BETENSKY, R. A.; HYMAN, B. T. Examination of the clinicopathologic continuum of Alzheimer disease in the autopsy cohort of the National Alzheimer Coordinating Center. **Journal of Neuropathology and Experimental Neurology**, vol. 72, no. 12, p. 1182–1192, Dez. 2013. https://doi.org/10.1097/NEN.0000000000000016.

SH-SY5Y ATCC ® CRL-2266™ HOMO SAPIENS BONE MARROW NEUROBLAST. [*s. d.*]. Disponível em: https://www.atcc.org/products/all/CRL-2266.aspx. Acesso em: 4 Mar. 2021.

SHARMA, L. K.; LU, J.; BAI, Y. Mitochondrial respiratory complex I: structure, function and implication in human diseases. **Current Medicinal Chemistry**, vol. 16, no. 10, p. 1266–1277, 2009. https://doi.org/10.2174/092986709787846578.

SHASHANK, K.; ABHAY, K. P. Review Article Chemistry and Biological Activities of Flavonoids: An Overview. **The Scientif World J**, vol. 4, no. 2, p. 32–48, 2013. .

SHIEH, J.-M.; HUANG, T.-F.; HUNG, C.-F.; CHOU, K.-H.; TSAI, Y.-J.; WU, W.-B. Activation of c-Jun N-terminal kinase is essential for mitochondrial membrane potential change and apoptosis induced by doxycycline in melanoma cells. **British Journal of Pharmacology**, vol. 160, no. 5, p. 1171–1184, Jul. 2010. https://doi.org/10.1111/j.1476-5381.2010.00746.x.

SHIPLEY, M. M.; MANGOLD, C. A.; SZPARA, M. L. Differentiation of the SH-SY5Y Human Neuroblastoma Cell Line. **Journal of Visualized Experiments**, no. 108, p. 53193, 17 Fev. 2016. https://doi.org/10.3791/53193.

SHI, Y.; HOLTZMAN, D. M. Interplay between innate immunity and Alzheimer disease: APOE and TREM2 in the spotlight. **Nature Reviews. Immunology**, vol. 18, no. 12, p. 759–772, 2018. https://doi.org/10.1038/s41577-018-0051-1.

SHUAIB, A.; HARTWELL, A.; KISS-TOTH, E.; HOLCOMBE, M. Multi-Compartmentalisation in the MAPK Signalling Pathway Contributes to the Emergence of Oscillatory Behaviour and to Ultrasensitivity. **Plos One**, vol. 11, no. 5, p. e0156139, 31 Mai. 2016. https://doi.org/10.1371/journal.pone.0156139.

SILVA, J.; ALVES, C.; FREITAS, R.; MARTINS, A.; PINTEUS, S.; RIBEIRO, J.; GASPAR, H.; ALFONSO, A.; PEDROSA, R. Antioxidant and Neuroprotective Potential of the Brown Seaweed Bifurcaria bifurcata in an in vitro Parkinson's Disease Model. **Marine Drugs**, vol. 17, no. 2, 1 Fev. 2019. https://doi.org/10.3390/md17020085.

SILVA, J.; ALVES, C.; MARTINS, A.; SUSANO, P.; SIMÕES, M.; GUEDES, M.; REHFELDT, S.; PINTEUS, S.; GASPAR, H.; RODRIGUES, A.; GOETTERT, M. I.; ALFONSO, A.; PEDROSA, R. Loliolide, a New Therapeutic Option for Neurological Diseases? In Vitro Neuroprotective and Anti-Inflammatory Activities of a Monoterpenoid Lactone Isolated from Codium tomentosum. **International Journal of Marine Science**, vol. 22, no. 4, p. 1888, 14 Fev. 2021. https://doi.org/10.3390/

ijms22041888.

SILVA, J.; ALVES, C.; PINTEUS, S.; MENDES, S.; PEDROSA, R. Neuroprotective effects of seaweeds against 6-hydroxidopamine-induced cell death on an in vitro human neuroblastoma model. **BMC complementary and alternative medicine**, vol. 18, no. 1, p. 58, 14 Fev. 2018. https://doi.org/10.1186/s12906-018-2103-2.

SILVERS, A. L.; BACHELOR, M. A.; BOWDEN, G. T. The role of JNK and p38 MAPK activities in UVA-induced signaling pathways leading to AP-1 activation and c-Fos expression. **Neoplasia**, vol. 5, no. 4, p. 319–329, Ago. 2003. https://doi.org/10.1016/S1476-5586(03)80025-8.

SMALL, D. H.; CAPPAI, R. Alois Alzheimer and Alzheimer's disease: a centennial perspective. **Journal of Neurochemistry**, vol. 99, no. 3, p. 708–710, Nov. 2006. https://doi.org/10.1111/j.1471-4159.2006.04212.x.

SNOWDEN, M. B.; ATKINS, D. C.; STEINMAN, L. E.; BELL, J. F.; BRYANT, L. L.; COPELAND, C.; FITZPATRICK, A. L. Longitudinal association of dementia and depression. **The American Journal of Geriatric Psychiatry**, vol. 23, no. 9, p. 897–905, Set. 2015. https://doi.org/10.1016/j.jagp.2014.09.002.

SOTO-OTERO, R.; MÉNDEZ-ALVAREZ, E.; HERMIDA-AMEIJEIRAS, A.; MUÑOZ-PATIÑO, A. M.; LABANDEIRA-GARCIA, J. L. Autoxidation and neurotoxicity of 6-hydroxydopamine in the presence of some antioxidants: potential implication in relation to the pathogenesis of Parkinson's disease. **Journal of Neurochemistry**, vol. 74, no. 4, p. 1605–1612, Abr. 2000. https://doi.org/10.1046/j.1471-4159.2000.0741605.x.

STARKOV, A. A. The role of mitochondria in reactive oxygen species metabolism and signaling. **Annals of the New York Academy of Sciences**, vol. 1147, p. 37–52, Dez. 2008. https://doi.org/10.1196/annals.1427.015.

SWERDLOW, R. H. Pathogenesis of Alzheimer ' s disease. **Clinical Interventions in aging.** vol. 2, no. 3, p. 347–359, 2007. .

TACIAK, B.; BIAŁASEK, M.; BRANIEWSKA, A.; SAS, Z.; SAWICKA, P.; KIRAGA, Ł.; RYGIEL, T.; KRÓL, M. Evaluation of phenotypic and functional stability of RAW 264.7 cell line through serial passages. **Plos One**, vol. 13, no. 6, p. e0198943, 11 Jun. 2018. https://doi.org/10.1371/journal.pone.0198943.

TACRINE - DRUGBANK. [*s. d.*]. Disponível em: https://www.drugbank.ca/drugs/DB00382. Acesso em: 8 Jul. 2020.

TAKAHASHI, R. H.; NAGAO, T.; GOURAS, G. K. Plaque formation and the intraneuronal accumulation of β-amyloid in Alzheimer's disease. **Pathology International**, vol. 67, no. 4, p. 185–193, Abr. 2017. https://doi.org/10.1111/pin.12520.

TAKASHIMA, A. Mechanism of neurodegeneration through tau and therapy for Alzheimer's disease. **Journal of sport and health science**, vol. 5, no. 4, p. 391–392, Dez. 2016. https://doi.org/10.1016/j.jshs.2016.08.009.

TAN, Y.; DOURDIN, N.; WU, C.; DE VEYRA, T.; ELCE, J. S.; GREER, P. A. Ubiquitous calpains promote caspase-12 and JNK activation during endoplasmic reticulum stress-induced apoptosis. **The Journal of Biological Chemistry**, vol. 281, no. 23, p. 16016–16024, 9 Jun. 2006. https://doi.org/10.1074/jbc.M601299200.

TARAGANO, F. E.; LYKETSOS, C. G.; MANGONE, C. A.; ALLEGRI, R. F.; COMESAÑA-DIAZ, E. A double-blind, randomized, fixed-dose trial of fluoxetine vs. amitriptyline in the treatment of major depression complicating Alzheimer's disease. **Psychosomatics**, vol. 38, no. 3, p. 246–252, Jun. 1997. https://doi.org/10.1016/S0033-3182(97)71461-0.

TAYLOR, P. R.; MARTINEZ-POMARES, L.; STACEY, M.; LIN, H. H.; BROWN, G. D.; GORDON, S. Macrophage receptors and immune recognition. **Annual Review of Immunology**, vol. 23, p. 901–944, 2005. https://doi.org/10.1146/annurev.immunol.23.021704.115816.

TIMMERMAN, R.; BURM, S. M.; BAJRAMOVIC, J. J. An Overview of in vitro Methods to Study Microglia. **Frontiers in Cellular Neuroscience**, vol. 12, p. 242, 6 Ago. 2018. https://doi.org/10.3389/fncel.2018.00242.

TONG, W.; CHEN, X.; SONG, X.; CHEN, Y.; JIA, R.; ZOU, Y.; LI, L.; YIN, L.; HE, C.; LIANG, X.; YE, G.; LV, C.; LIN, J.; YIN, Z. Resveratrol inhibits LPS-induced inflammation through suppressing the signaling cascades of TLR4-NF-κB/MAPKs/IRF3. **Experimental and therapeutic medicine**, vol. 19, no. 3, p. 1824–1834, Mar. 2020. https://doi.org/10.3892/etm.2019.8396.

TOULMOND, S.; VIGE, X.; FAGE, D.; BENAVIDES, J. Local infusion of interleukin-6 attenuates the neurotoxic effects of NMDA on rat striatal cholinergic neurons. **Neuroscience Letters**, vol. 144, no. 1–2, p. 49–52, 14 Set. 1992. https://doi.org/10.1016/0304-3940(92)90713-h.

TOURNIER, C.; HESS, P.; YANG, D. D.; XU, J.; TURNER, T. K.; NIMNUAL, A.; BAR-SAGI, D.; JONES, S. N.; FLAVELL, R. A.; DAVIS, R. J. Requirement of JNK for stress-induced activation of the cytochrome c-mediated death pathway. **Science**, vol. 288, no. 5467, p. 870–874, 5 Mai. 2000. https://doi.org/10.1126/science.288.5467.870.

TREUTTER, D. Significance of flavonoids in plant resistance and enhancement of their biosynthesis. **Plant Biology**, vol. 7, no. 6, p. 581–591, Nov. 2005. https://doi.org/10.1055/s-2005-873009.

TURRENS, J. F. Mitochondrial formation of reactive oxygen species. **The Journal of Physiology**, vol. 552, no. Pt 2, p. 335–344, 15 Out. 2003. https://doi.org/10.1113/jphysiol.2003.049478.

TYSNES, O.-B.; STORSTEIN, A. Epidemiology of Parkinson's disease. **Journal of Neural Transmission**, vol. 124, no. 8, p. 901–905, 1 Fev. 2017. https://doi.org/10.1007/s00702-017-1686-y.

VENTURA, J.-J.; COGSWELL, P.; FLAVELL, R. A.; BALDWIN, A. S.; DAVIS, R. J. JNK potentiates TNF-stimulated necrosis by increasing the production of cytotoxic reactive oxygen species. **Genes & Development**, vol. 18, no. 23, p. 2905–2915, 1 Dez. 2004. https://doi.org/10.1101/gad.1223004.

VROEGOP, S. M.; DECKER, D. E.; BUXSER, S. E. Localization of damage induced by reactive oxygen species in cultured cells. **Free Radical Biology & Medicine**, vol. 18, no. 2, p. 141–151, Fev. 1995. https://doi.org/10.1016/0891-5849(94)00107-u.

WAJANT, H. The Fas signaling pathway: more than a paradigm. **Science**, vol. 296, no. 5573, p. 1635–1636, 31 Mai. 2002. https://doi.org/10.1126/science.1071553.

WALKER, D. G.; WHETZEL, A. M.; LUE, L. F. Expression of suppressor of cytokine signaling genes in human elderly and Alzheimer's disease brains and human microglia. **Neuroscience**, vol. 302, p. 121–137, 27 Ago. 2015. https://doi.org/10.1016/j.neuroscience.2014.09.052.

WANG, B.; RAO, Y.-H.; INOUE, M.; HAO, R.; LAI, C.-H.; CHEN, D.; MCDONALD, S. L.; CHOI, M.-C.; WANG, Q.; SHINOHARA, M. L.; YAO, T.-P. Microtubule acetylation amplifies p38 kinase signalling and anti-inflammatory IL-10 production. **Nature Communications**, vol. 5, p. 3479, 17 Mar. 2014. https://doi.org/10.1038/ncomms4479.

WANG, W.; ZHAO, F.; MA, X.; PERRY, G.; ZHU, X. Mitochondria dysfunction in the pathogenesis of Alzheimer's disease: recent advances. **Molecular Neurodegeneration**, vol. 15, no. 1, p. 30, 29 Mai. 2020. https://doi.org/10.1186/s13024-020-00376-6.

WANG, X.-Q.; PENG, Y.-P.; LU, J.-H.; CAO, B.-B.; QIU, Y.-H. Neuroprotection of interleukin-6 against NMDA attack and its signal transduction by JAK and MAPK. **Neuroscience Letters**, vol. 450, no. 2, p. 122–126, 30 Jan. 2009. https://doi.org/10.1016/j.neulet.2008.11.051.

WANG, Y.; GUO, S.-H.; SHANG, X.-J.; YU, L.-S.; ZHU, J.-W.; ZHAO, A.; ZHOU, Y.-F.; AN, G.-H.; ZHANG, Q.; MA, B. Triptolide induces Sertoli cell apoptosis in mice via ROS/JNK-dependent activation of the mitochondrial pathway and inhibition of Nrf2-mediated antioxidant response. **Acta Pharmacologica Sinica**, vol. 39, no. 2, p. 311–327, Fev. 2018. https://doi.org/10.1038/aps.2017.95.

WHITMARSH, A. J. The JIP family of MAPK scaffold proteins. **Biochemical Society Transactions**, vol. 34, no. Pt 5, p. 828–832, Nov. 2006. https://doi.org/10.1042/BST0340828.

WHITTEMORE, E. R.; LOO, D. T.; WATT, J. A.; COTMAN, C. W. A detailed analysis of hydrogen peroxide-induced cell death in primary neuronal culture. **Neuroscience**, vol. 67, no. 4, p. 921–932, Ago. 1995. https://doi.org/10.1016/0306-4522(95)00108-u.

WICHMANN, M. A.; CRUICKSHANKS, K. J.; CARLSSON, C. M.; CHAPPELL, R.; FISCHER, M. E.; KLEIN, B. E. K.; KLEIN, R.; TSAI, M. Y.; SCHUBERT, C. R. Long-term systemic inflammation and cognitive impairment in a population-based cohort. **Journal of the American Geriatrics Society**, vol. 62, no. 9, p. 1683–1691, Set. 2014. https://doi.org/10.1111/jgs.12994.

WILLIAMSON, J.; GOLDMAN, J.; MARDER, K. S. Genetic aspects of Alzheimer disease. **The Neurologist**, vol. 15, no. 2, p. 80–86, Mar. 2009. https://doi.org/10.1097/NRL.0b013e318187e76b.

WILLIAMS, R. J.; SPENCER, J. P. E. Flavonoids, cognition, and dementia: actions, mechanisms, and potential therapeutic utility for Alzheimer disease. **Free Radical Biology & Medicine**, vol. 52, no. 1, p. 35–45, 1 Jan. 2012. https://doi.org/10.1016/j.freeradbiomed.2011.09.010.

WU, Q.; WU, W.; JACEVIC, V.; FRANCA, T. C. C.; WANG, X.; KUCA, K. Selective inhibitors for JNK signalling: a potential targeted therapy in cancer. **Journal of Enzyme Inhibition and Medicinal Chemistry**, vol. 35, no. 1, p. 574–583, Dez. 2020. https://doi.org/10.1080/14756366.2020.1720013.

XIE, H.; HU, L.; LI, G. SH-SY5Y human neuroblastoma cell line: in vitro cell model of

dopaminergic neurons in Parkinson's disease. **Chinese Medical Journal**, vol. 123, no. 8, p. 1086–1092, 20 Abr. 2010. .

YAMADA, M.; HATANAKA, H. Interleukin-6 protects cultured rat hippocampal neurons against glutamate-induced cell death. **Brain Research**, vol. 643, no. 1–2, p. 173–180, 18 Abr. 1994. https://doi.org/10.1016/0006-8993(94)90023-x.

YANG, D. D.; KUAN, C. Y.; WHITMARSH, A. J.; RINCÓN, M.; ZHENG, T. S.; DAVIS, R. J.; RAKIC, P.; FLAVELL, R. A. Absence of excitotoxicity-induced apoptosis in the hippocampus of mice lacking the Jnk3 gene. **Nature**, vol. 389, no. 6653, p. 865–870, 23 Out. 1997. https://doi.org/10.1038/39899.

YANG, Q.; SONG, D.; QING, H. Neural changes in Alzheimer's disease from circuit to molecule: Perspective of optogenetics. **Neuroscience and Biobehavioral Reviews**, vol. 79, p. 110–118, Ago. 2017. https://doi.org/10.1016/j.neubiorev.2017.05.015.

YAO, H.; SHANG, Z.; WANG, P.; LI, S.; ZHANG, Q.; TIAN, H.; REN, D.; HAN, X. Protection of Luteolin-7-O-Glucoside Against Doxorubicin-Induced Injury Through PTEN/Akt and ERK Pathway in H9c2 Cells. **Cardiovascular Toxicology**, vol. 16, no. 2, p. 101–110, Abr. 2016. https://doi.org/10.1007/s12012-015-9317-z.

YARZA, R.; VELA, S.; SOLAS, M.; RAMIREZ, M. J. c-Jun N-terminal Kinase (JNK) Signaling as a Therapeutic Target for Alzheimer's Disease. **Frontiers in pharmacology**, vol. 6, p. 321, 2015. https://doi.org/10.3389/fphar.2015.00321.

YASUKAWA, H.; OHISHI, M.; MORI, H.; MURAKAMI, M.; CHINEN, T.; AKI, D.; HANADA, T.; TAKEDA, K.; AKIRA, S.; HOSHIJIMA, M.; HIRANO, T.; CHIEN, K. R.; YOSHIMURA, A. IL-6 induces an anti-inflammatory response in the absence of SOCS3 in macrophages. **Nature Immunology**, vol. 4, no. 6, p. 551–556, Jun. 2003. https://doi.org/10.1038/ni938.

YIM, M.-J.; LEE, J. M.; CHOI, G.; LEE, D.-S.; PARK, W. S.; JUNG, W.-K.; PARK, S.; SEO, S.-K.; PARK, J.; CHOI, I.-W.; MA, S. Y. Anti-Inflammatory Potential of Carpomitra costata Ethanolic Extracts via Inhibition of NF-κB and AP-1 Activation in LPS-Stimulated RAW264.7 Macrophages. **Evidence-Based Complementary and Alternative Medicine**, vol. 2018, p. 6914514, 26 Fev. 2018. https://doi.org/10.1155/2018/6914514.

YOON, S. O.; PARK, D. J.; RYU, J. C.; OZER, H. G.; TEP, C.; SHIN, Y. J.; LIM, T. H.; PASTORINO, L.; KUNWAR, A. J.; WALTON, J. C.; NAGAHARA, A. H.; LU, K. P.; NELSON, R. J.; TUSZYNSKI, M. H.; HUANG, K. JNK3 perpetuates metabolic stress induced by Aβ peptides. **Neuron**, vol. 75, no. 5, p. 824–837, 6 Set. 2012. https://doi.org/10.1016/j.neuron.2012.06.024.

YUE, J.; LÓPEZ, J. M. Understanding MAPK signaling pathways in apoptosis. **International Journal of Molecular Sciences**, vol. 21, no. 7, 28 Mar. 2020. https://doi.org/10.3390/ijms21072346.

ZABEL, M.; NACKENOFF, A.; KIRSCH, W. M.; HARRISON, F. E.; PERRY, G.; SCHRAG, M. Markers of oxidative damage to lipids, nucleic acids and proteins and antioxidant enzymes activities in Alzheimer's disease brain: A meta-analysis in human pathological specimens. **Free Radical Biology & Medicine**, vol. 115, p. 351–360, 1 Fev. 2018. https://doi.org/10.1016/j.freeradbiomed.2017.12.016.

ZARUBIN, T.; HAN, J. Activation and signaling of the p38 MAP kinase pathway. **Cell**

Research, vol. 15, no. 1, p. 11–18, Jan. 2005. https://doi.org/10.1038/sj.cr.7290257.

ZEKE, A.; MISHEVA, M.; REMÉNYI, A.; BOGOYEVITCH, M. A. JNK Signaling: Regulation and Functions Based on Complex Protein-Protein Partnerships. **Microbiology and Molecular Biology Reviews**, vol. 80, no. 3, p. 793–835, 27 Jul. 2016. https://doi.org/10.1128/MMBR.00043-14.

ZHANG, J.-X.; XING, J.-G.; WANG, L.-L.; JIANG, H.-L.; GUO, S.-L.; LIU, R. Luteolin Inhibits Fibrillary β-Amyloid1-40-Induced Inflammation in a Human Blood-Brain Barrier Model by Suppressing the p38 MAPK-Mediated NF-κB Signaling Pathways. **Molecules (Basel, Switzerland)**, vol. 22, no. 3, 24 Fev. 2017. https://doi.org/10.3390/molecules22030334.

ZHENG, C.; ZHOU, X.-W.; WANG, J.-Z. The dual roles of cytokines in Alzheimer's disease: update on interleukins, TNF-α, TGF-β and IFN-γ. **Translational neurodegeneration**, vol. 5, p. 7, 5 Abr. 2016. https://doi.org/10.1186/s40035-016-0054-4.

ZHOU, Q.; WANG, M.; DU, Y.; ZHANG, W.; BAI, M.; ZHANG, Z.; LI, Z.; MIAO, J. Inhibition of c-Jun N-terminal kinase activation reverses Alzheimer disease phenotypes in APPswe/PS1dE9 mice. **Annals of Neurology**, vol. 77, no. 4, p. 637–654, Abr. 2015. https://doi.org/10.1002/ana.24361.

ZHOU, X.; LI, Y.; SHI, X.; MA, C. An overview on therapeutics attenuating amyloid β level in Alzheimer's disease: targeting neurotransmission, inflammation, oxidative stress and enhanced cholesterol levels. **American journal of translational research**, vol. 8, no. 2, p. 246–269, 15 Fev. 2016. .

ZHU, Xiongwei; CASTELLANI, R. J.; TAKEDA, A.; NUNOMURA, A.; ATWOOD, C. S.; PERRY, G.; SMITH, M. A. Differential activation of neuronal ERK , JNK / SAPK and p38 in Alzheimer disease : the ' two hit ' hypothesis. vol. 123, p. 39–46, 2001. .

ZHU, X; RAINA, A. K.; ROTTKAMP, C. A.; ALIEV, G.; PERRY, G.; BOUX, H.; SMITH, M. A. Activation and redistribution of c-jun N-terminal kinase/stress activated protein kinase in degenerating neurons in Alzheimer's disease. **Journal of Neurochemistry**, vol. 76, no. 2, p. 435–441, Jan. 2001. https://doi.org/10.1046/j.1471-4159.2001.00046.x.

ZHU, X; ROTTKAMP, C. A.; BOUX, H.; TAKEDA, A.; PERRY, G.; SMITH, M. A. Activation of p38 kinase links tau phosphorylation, oxidative stress, and cell cycle-related events in Alzheimer disease. **Journal of Neuropathology and Experimental Neurology**, vol. 59, no. 10, p. 880–888, Out. 2000. https://doi.org/10.1093/jnen/59.10.880.

ZOROV, D. B.; JUHASZOVA, M.; SOLLOTT, S. J. Mitochondrial reactive oxygen species (ROS) and ROS-induced ROS release. **Physiological Reviews**, vol. 94, no. 3, p. 909–950, Jul. 2014. https://doi.org/10.1152/physrev.00026.2013.

ANEXOS E APÊNDICES

Anexo 1 - Instructions for Authors

Disponível em: <https://www.mdpi.com/journal/ijms/instructions>.

Acesso em: 9 de março de 2021.

Apêndice 1 - Protocolo de Diferenciação celular (SH-SY5Y)

Laboratório de Cultura de Células – Área de Farmacologia de Produtos Naturais	
Programa de Pós-Graduação em Biotecnologia	
PROTOCOLO: DIFERENCIAÇÃO CELULAR SH-SY5Y (ATRA) Versão 2019/B	Feito por: Stephanie Rehfeldt

1. PREPARO DE ATRA:

Obs. 1: *procurar realizar a pesagem o mais rápido possível evitando que o frasco fique muito tempo aberto* → ***ATRA oxida-se facilmente em contato com*** O_2.

Obs 2.: *sempre que possível, manipular ATRA com luzes apagadas e/ou barrar a entrada de luz externa com cortinas* → ***ATRA é fotossensível:***

1.1. Materiais: ATRA (*All-trans-retinoic Acid*), papel alumínio, balança de precisão, espátula, eppendorf estéril, DMSO, vórtex/agitador de tubos, álcool, papel, parafilme, luvas, máscara, jaleco.

1.2. Procedimento:

1.2.1. Vestir jaleco, colocar máscara e calçar luvas;

1.2.2. Com um pedaço de papel embebido em álcool, realizar uma limpeza rápida da balança de precisão;

1.2.3. Colocar o eppendorf estéril na balança, apertar botão TARA;

1.2.4. Com a espátula proceder com a pesagem de ATRA (quantidade para uma solução estoque);

1.2.5. Após a pesagem envolver o eppendorf em papel alumínio.

1.2.6. Após a pesagem, já no Laboratório de Cultura de Células, espirrar álcool 70% no eppendorf contendo ATRA (não retirar o papel alumínio) e no frasco de DMSO FILTRADO e inseri-los na capela de fluxo;

1.2.7. Ressuspender o conteúdo pesado de ATRA em quantidade adequada de DMSO FILTRADO.

1.2.8. Homogeneizar bem utilizando o vórtex/agitador de tubs;

1.2.9. Lacrar o eppendorf em parafilme, envolver em papel alumínio, identificar e armazenar a -20°C por até 6 semanas.

1.2.9.1. ***Dica:*** *é preferível fazer alíquotas com volumes menores em uma quantidade maior de eppendorf, assim evita-se o contato frequente com O_2 e luz.*

1.3. Cálculo de molaridade

$$M = m \div (MM \; x \; V)$$

M = Molaridade ou Concentração Molar (mol/L)
m = massa (g)
MM = Massa ou Peso Molecular (g/mol)
V = volume (L)

Exemplo 1. Qual o volume de DMSO necessário para uma solução estoque de 10 mM a partir de 5 mg de ATRA?

$$0,01\ M = 0,005\ g \div (300,43\ g/mol \times volume)$$

volume =

Exemplo 2. Para uma solução estoque de 10 mM com volume final de 1 mL, qual a massa de ATRA a ser pesada?

$$0,01\ M = m \div (300,43\ g/mol \times 0,0001\ L)$$

IMPORTANTE:
10 mM = 0,01 M
5 mg = 0,005 g
1 mL = 0,001 L

2. MANIPULAÇÃO E DIFERENCIAÇÃO SH-SY5Y

Obs.: *processos iniciais estão descritos de forma resumida. Para maiores detalhes consultar protocolos específicos de Descongelamento de Células e Repique/Passagem.*

2.1.Materiais: solução estoque de ATRA (*All-trans-retinoic Acid*) a 10 mM, papel alumínio, meio de cultura DMEM LOW GLUCOSE + F12, soro bovino fetal (SBF), solução de NaCl 0.9% estéril., descarte, álcool 70%, pipetas e ponteiras, placa de Petri e tubos falcon.

2.2.Descongelamento SH-SY5Y e passagens iniciais:

2.2.1. Ligar o fluxo;

2.2.2. Limpar as paredes internas e a superfície da área de trabalho com álcool 70% em sentido único;

2.2.3. Após a limpeza, ligar a lâmpada germicida por 15 a 30 minutos;

2.2.4. Em uma placa de Petri, preparar **meio para descongelamento**;

2.2.5. Após 24 horas, realizar troca de meio. Dessa vez, utilizar **meio de manutenção**.

2.2.6. Assim que atingir confluência, realizar primeira passagem (P1) com meio de manutenção

2.2.7. Quando células em P1 atingirem 90% de confluência, dividir as células em pelo menos duas placas de Petri. Em uma das placas poderá ser iniciado o processo de diferenciação e a outra deverá ser mantida até o final dos experimentos conforme esquema abaixo:

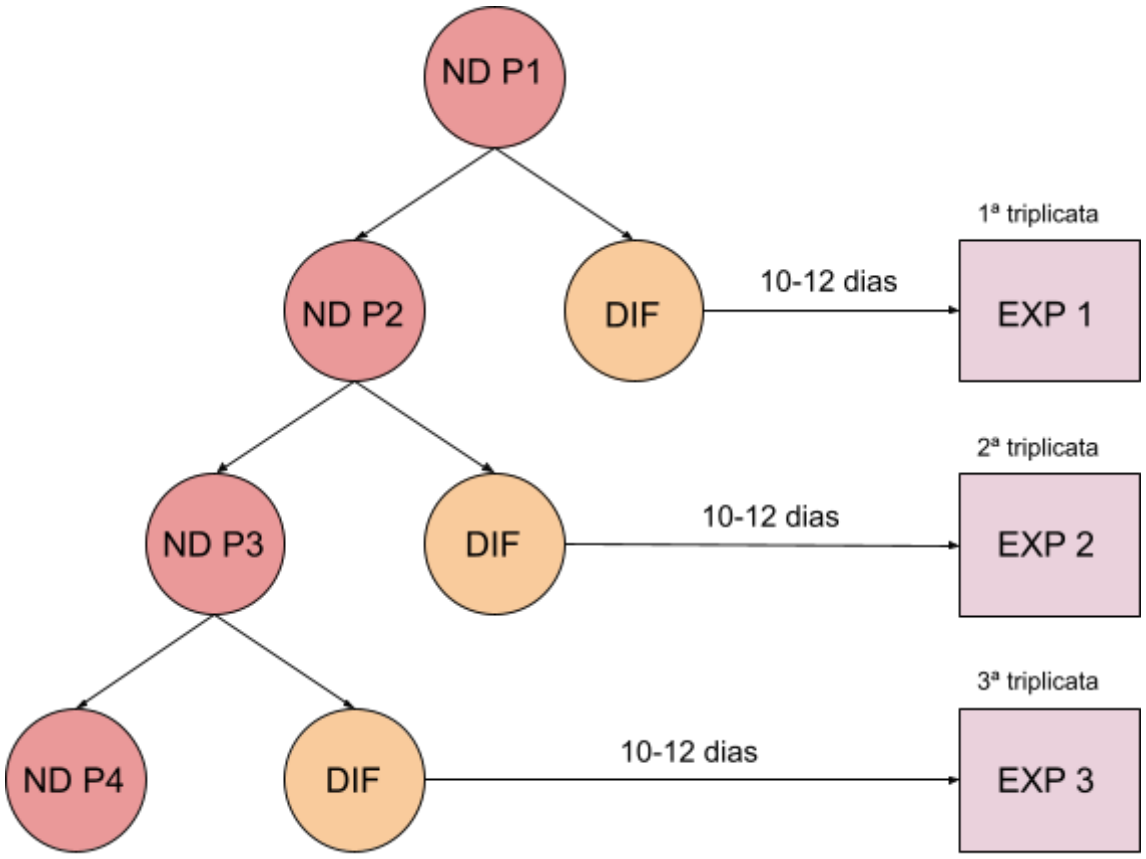

2.2.8. Assim que uma das placas atingir mais de 90% de confluência em Placa de Petri inicia-se a diferenciação (DIA 0).

2.3. Cronograma para diferenciação

DIA 0 (início):

- Retirar meio antigo;
- Lavar **2x** com solução fisiológica;
- Adicionar meio para diferenciação (qsp 10 mL)

* envolver placa em papel alumínio (deixar espaço para "respirar") e colocar na estufa.

DIA 6 (troca de meio):

- Retirar meio antigo;
- Lavar **DELICADAMENTE** com solução fisiológica **1x**;
- Adicionar meio para diferenciação (10 mL)

* envolver a placa novamente em papel alumínio e devolver para estufa.

DIA 10-12 (células diferenciadas):

- Retirar meio antigo;
- **NÃO LAVAR COM SOLUÇÃO FISIOLÓGICA**;
- Prosseguir com tripsinização (monitorar o desprendimento das células), inativação de tripsina com SFB, centrifugação e plaqueamento para MTT, por exemplo.

2.4. Utilização de células diferenciadas em experimentos

2.4.1. Relação Número de células x Placa

Tipo de placa	Número de células para confluência (aprox.)	Área útil	Volume de trabalho
96 poços	$3x10^4$	0,32 cm^2	300 µL
24 poços	$2,5x10^5$	1,9 cm^2	0,5-1 mL
12 poços	$5x10^5$	3,8 cm^2	1-2 mL
6 poços	$1,2x10^6$	9,5 cm^2	1-3 mL
Placa de Petri (100 mm Petri dish)	$7,5x10^6$	60 cm^2	10 ml
"Garrafinha" (T-25 flask)	$3x10^6$	25 cm^2	5-7 mL
"Garrafão" (T-75 flask)	$9x10^6$	75 cm^2	10-15 mL

2.4.2. Ensaios em placas de 96 poços:

- Cultivar e diferenciar células em placa de Petri. Para transferir as células para a placa de 96 poços deve-se usar tripsina (CUIDADO).
- **Para MTT:** $2x10^4$ células/poço;

2.4.3. Ensaios em placas de 6 poços:

- Cultivar as células em placa de Petri e transferir células não diferenciadas para a placa do ensaio
- Iniciar a diferenciação na própria placa após confluência >90%
- Após 10-12 dias de diferenciação as células estarão aptas a experimentação.
- **Para WB/Citocinas:** Plaquear aprox. $1x10^5$ células/poço e aguardar confluência.

Obs. 1: *o protocolo poderá ser iniciado com células a partir de P2 e deverá ser realizado nas células até P8. Após P8, deverá ser descongelada uma nova alíquota.*

Obs 2.: *uma vez diferenciadas, as células não retornarão ao estado "não-diferenciado". Ou seja, uma vez diferenciadas deverão ser utilizadas em experimento imediatamente e, caso "sobrem" células diferenciadas, essas deverão ser descartadas.*

3. MEIOS DE CULTURA

3.1. PREPARO DE DMEM LOW GLUCOSE + F12 (qsp 250 ml):

- DMEM Low glucose (Sigma) - 2,16g
- F12 (Sigma) - 1,225g
- NaHCO3 (Sigma) - 0,925g
- HEPES (Sigma) - 0,925g
- Streptomycin (Sigma) - 0,025g
- Penicilin (Sigma) - 0,015g

DICA 1:
Fazer meio em pequenas quantidades e com maior frequência;
De preferência utilizar meio de cultura em até 2 semanas após preparado.

DICA 2:
pH entre 7,35 - 7,45 (após filtrado)

3.2. MEIO PARA DESCONGELAMENTO

- 20% SFB
- DMEM Low Glucose + F12

3.3.MEIO DE MANUTENÇÃO

- 10% SFB
- DMEM Low Glucose + F12

3.4.MEIO DE DIFERENCIAÇÃO

- 1% SFB
- DMEM Low Glucose + F12
- 10 µM ATRA

Anexo 2 - “Loliolide, a New Therapeutic Option for Neurological Diseases? In Vitro Neuroprotective and Anti-Inflammatory Activities of a Monoterpenoid Lactone Isolated from Codium tomentosum"

Trabalho em colaboração com o MARE do Instituto Politécnico de Leiria (Portugal): Publicado em 2021 no periódico *International Journal of Molecular Sciences* (Fator de Impacto: 4,556).

International Journal of
Molecular Sciences

MDPI

Article

Loliolide, a New Therapeutic Option for Neurological Diseases? In Vitro Neuroprotective and Anti-Inflammatory Activities of a Monoterpenoid Lactone Isolated from *Codium tomentosum*

Joana Silva [1,2,*], Celso Alves [1], Alice Martins [1], Patrícia Susano [1], Marco Simões [1], Miguel Guedes [1], Stephanie Rehfeldt [3], Susete Pinteus [1], Helena Gaspar [4], Américo Rodrigues [1], Márcia Ines Goettert [3], Amparo Alfonso [2] and Rui Pedrosa [5,*]

1 MARE—Marine and Environmental Sciences Centre, Polytechnic of Leiria, 2520-630 Peniche, Portugal; celso.alves@ipleiria.pt (C.A.); alice.martins@ipleiria.pt (A.M.); patricia_susano94@hotmail.com (P.S.); marco.a.simoes@ipleiria.pt (M.S.); mg.cross@hotmail.com (M.G.); susete.pinteus@ipleiria.pt (S.P.); arodrigues@ipleiria.pt (A.R.)
2 Department of Pharmacology, Faculty of Veterinary, University of Santiago de Compostela, 27002 Lugo, Spain; amparo.alfonso@usc.es
3 Cell Culture Laboratory, Graduate Program in Biotechnology, University of Vale do Taquari (Univates), Lajeado, RS 95914-014, Brazil; rehfeldt.stephanie@gmail.com (S.R.); marcia.goettert@univates.br (M.I.G.)
4 BioISI—Biosystems and Integrative Sciences Institute, Faculty of Sciences, University of Lisbon, 1749-016 Lisboa, Portugal; hmgaspar@fc.ul.pt
5 MARE—Marine and Environmental Sciences Centre, ESTM, Polytechnic of Leiria, 2520-614 Peniche, Portugal
* Correspondence: joana.m.silva@ipleiria.pt (J.S.); rui.pedrosa@ipleiria.pt (R.P.); Tel.: +351-262-783-607 (J.S. & R.P.); Fax: +351-262-783-088 (J.S. & R.P.)

Citation: Silva, J.; Alves, C.; Martins, A.; Susano, P.; Simões, M.; Guedes, M.; Rehfeldt, S.; Pinteus, S.; Gaspar, H.; Rodrigues, A.; et al. Loliolide, a New Therapeutic Option for Neurological Diseases? In Vitro Neuroprotective and Anti-Inflammatory Activities of a Monoterpenoid Lactone Isolated from *Codium tomentosum*. *Int. J. Mol. Sci.* **2021**, *22*, 1888. https://doi.org/10.3390/ijms22041888

Academic Editor: Luigi Casella

Received: 14 January 2021
Accepted: 10 February 2021
Published: 14 February 2021

Abstract: Parkinsons Disease (PD) is the second most common neurodegenerative disease worldwide, and is characterized by a progressive degeneration of dopaminergic neurons. Without an effective treatment, it is crucial to find new therapeutic options to fight the neurodegenerative process, which may arise from marine resources. Accordingly, the goal of the present work was to evaluate the ability of the monoterpenoid lactone Loliolide, isolated from the green seaweed *Codium tomentosum*, to prevent neurological cell death mediated by the neurotoxin 6-hydroxydopamine (6-OHDA) on SH-SY5Y cells and their anti-inflammatory effects in RAW 264.7 macrophages. Loliolide was obtained from the diethyl ether extract, purified through column chromatography and identified by NMR spectroscopy. The neuroprotective effects were evaluated by the MTT method. Cells' exposure to 6-OHDA in the presence of Loliolide led to an increase of cells' viability in 40%, and this effect was mediated by mitochondrial protection, reduction of oxidative stress condition and apoptosis, and inhibition of the NF-κB pathway. Additionally, Loliolide also suppressed nitric oxide production and inhibited the production of TNF-α and IL-6 pro-inflammatory cytokines. The results suggest that Loliolide can inspire the development of new neuroprotective therapeutic agents and thus, more detailed studies should be considered to validate its pharmacological potential.

Keywords: antioxidant activity; inflammation; marine natural products; neuroprotection; NF-κB pathway; oxidative stress; Parkinson's disease; seaweeds

1. Introduction

Parkinson´s Disease (PD) is a chronic and progressive disorder of the central nervous system that affects about 6 million people worldwide. It is the most common neurodegenerative disease in aged people [1]. To date, the existent therapies only succeeded in relieving the clinical symptoms, but do not havecapacity to effectively deter the disease progression. Therefore, it is important to find new therapeutic agents that act not only to relieve symptoms, but also to slow down/block the disease progression [2]. Although the etiology of PD remains unclear, the death of dopaminergic (DA) neurons during PD

progression is known to be associated with oxidative stress, mitochondrial dysfunction, and neuroinflammation [3,4]. Oxidative stress is the resulting condition of an imbalance between antioxidant defenses and the generation of oxidative species. Although numerous factors contribute for an increase of oxidative species production, the generation of reactive oxygen species (ROS) due to mitochondrial dysfunction is thought to be a main trigger of oxidative stress. If ROS production is not managed, these reactive species lead to a cascade of events resulting in neuronal cell death [4–7]. On the other hand, in PD is also observed an increase of the dopamine (DA) and nitric oxide (NO) metabolism, which, allied to reduced levels of endogenous antioxidant enzymes such as Catalase (CAT), glutathione peroxidase (GPx) and superoxide dismutase (SOD), also result in neuronal cell death [8,9]. Dopamine is an unstable molecule that undergoes auto-oxidation originating dopamine quinones and free radicals. These are metabolized by both A and B forms of monoamine oxidase (MAO), regulated through the oxidative metabolism of MAO-A that, with aging and neurological disorders increases MAO-B levels, becoming the predominant enzyme involved in dopamine metabolization [10]. One of the products of dopamine -MAO-B mediated metabolism is H_2O_2 that reacts with Fe(II) originating hydroxyl radicals ($^{\bullet}OH$), which target nigral dopaminergic neurons, promoting their loss [4]. Other sources of free radicals include the NO metabolism, which, when overexpressed, dysregulate the complexes I and IV of the mitochondrial electron transport chain, prompting ROS generation [11].

In an attempt to manage oxidative stress damage, several secondary defensive pathways are activated, including the release of inflammatory mediators such as the cytokines TNF-α, IL-1β, IL-6, resulting in inflammation [12,13]. Although inflammation is a protective strategy to promote tissue repair, chronical inflammation results in cellular damage, and when in the brain, neuronal cell loss, being also considered one of the main triggers of PD development [14,15]. On the other hand, there also occurs the release of the anti-inflammatory cytokine IL-10, which plays a critical role in the balance of immune responses, and thus can be a valuable biomarker in PD investigation [16]. In fact, a previous study reported the ability if IL-10 to decrease the number of activated microglia mediating a protective effect against the loss of dopaminergic neurons in the brains of a LPS-induced PD mouse model [17]. The increase of peripheral concentrations of IL-6, IL-1β, TNF-α, IL-2 and IL-10 cytokines was already observed PD patients [18].

The nuclear factor NF-κB is a protein complex that regulates cytokines production, playing a crucial role in the regulation of inflammation and apoptosis involved in the brain programming of systemic aging, as well as in the pathogenesis of several neurodegenerative diseases, including PD [19]. In an oxidative condition, NF-κB initiates the transcription of proinflammatory genes coding cytokines and proteolytic enzymes. However, NF-κB factor is composed by different dimers that can have either protective or noxious effects. For example, p50/RelA dimers induce pro-apoptotic and c-Rel-containing dimers exert neuroprotective actions [19]. Studies in another PD model also reported dopaminergic neuron loss in a 1-methyl-4-phenyl-1,2,3,6-tetrahydropyridine (MPTP)-mouse model suggesting that RelA upregulation may play a role in dopaminergic neuron degeneration when RelA is subexpressed [20]. On the other hand, studies in deficient mice for c-Rel subunit verified that this subunit can exert pro-survival effects, suggesting that a reduction in the protective function of c-Rel may render dopaminergic neurons more vulnerable to aging [19]. As a result, current research has been focused in finding substances that act to prevent mitochondrial dysfunction, oxidative stress, and inflammation for the development of more efficient therapies.

With increasing evidence of marine-derived molecules' pharmacological effects, it is extremely relevant to understand their potential to be explored as novel PD therapeutics. Twenty-nine compounds isolated from marine organisms such as bacteria, fungi, seaweeds, sponges, corals, mollusks, sea cucumber and conus already demonstrated potential for PD therapeutics; however, only five compounds have entered in clinical trials [3]. Among marine organisms, seaweeds have shown to be relevant producers of bioactive

compounds with neuroprotective potential [21–23] on several in vitro and in vivo PD models, including α-synuclein-, MPTP-, and 6-OHDA, revealing capacity to inhibit apoptosis, mitochondrial abnormalities and ROS production [24–26].

Codium tomentosum Stackhouse (Chlorophyta) is a green seaweed belonging to the Codiaceae family. This seaweed is native from the North East Atlantic Ocean, from British Isles southwards to Azores and Cape Verde and can be found on exposed rocks, and in deep rock pools on the lower shore [27]. Although it is a common seaweed on several coastlines all over the world, the existing studies with *C. tomentosum* metabolites are limited to fatty acids, organic acids, phenolics, and volatiles composition [28], and its bioactive potential mainly screened on crude extracts, including antioxidant, antigenotoxic, antimicrobial, antitumorigenic, neuroprotective, and hypoglycemic studies [22,29–32]. Recently, we studied the neuroprotective effect of the *C. tomentosum* fractions, which revealed capacity to recover the 6-OHDA-induced neurotoxicity, decreasing ROS production, mitochondrial dysfunction, and Caspase-3 activity [22]. Accordingly, the study presented here aims to isolate the compounds responsible for the activities mediated by *C. tomentosum* fractions. In the genus *Codium* sp. were already identified several sterols namely, decortinol, sodecortinol, decortinone, clerosterol and 3-*O*-β-D-galacto- pyranosyl clerosterol [33]. However, according to our knowledge, this study reveals for the first time the presence of Loliolide in *C. tomentosum* species.

Loliolide is an ubiquitous monoterpenoid lactone, firstly described in 1974, and isolated from plants and animals [34]. It was also found in marine ecosystems in different brown seaweeds, such as *Sargassum horneri* [35], *Sargassum ringgoldianum* subsp. *coreanum* [36], and *Undaria pinnatifida* [37], revealing antioxidant, anti-fungal, antibacterial and anti-cancer properties [34–36].

The present work is focused on the neuroprotective and anti-inflammatory potential of Loliolide obtained from *C. tomentosum*, and its underlying mechanisms of action, opening alternative research possibilities for the development of new PD therapeutic agents.

2. Results

2.1. Bioguided Fractionation of Codium tomentosum Extracts

2.1.1. Extraction and Fractionation of *Codium tomentosum* Seaweed

Codium tomentosum was subjected to several fractionation steps resulting in three fractions (S1–S3) as illustrated in Figure 1.

2.1.2. Antioxidant Activity of *Codium tomentosum* Fractions

The extraction yields, as well as the antioxidant capacity of each fraction (S1–S3) assessed through 2,2-diphenyl-1-picrylhydrazyl radical (DPPH) scavenging activity and ferric reducing antioxidant power (FRAP) assays, are summarized in Table 1.

Table 1. Extraction yields and antioxidant activity of *Codium tomentosum* fractions.

Fraction	Yield	DPPH [a]	FRAP [b]
S1	0.31%	>200	82.01 ± 0.97
S2	0.03%	>200	8.54 ± 2.66
S3	28.98%	>200	6.07 ± 0.16
BHT	-	143.70 ± 23.26	2821.50 ± 63.03

[a] radical scavenging activity (EC_{50} μg/mL); [b] μM $FeSO_4$/g extract; EC_{50} values were determined for a 95% confidence interval.

As shown in Table 1, the highest extraction yields were achieved with water (S3—28.98%), while lower yields were obtained with ethyl acetate (S2—0.03%).

Concerning the antioxidant activities, none of the fractions demonstrated potential to reduce the DPPH radical. In the FRAP assay, S1 fraction revealed the highest efficiency

to reduce ferric ions (82.01 ± 0.97 μM $FeSO_4$/g extract), while the lowest activity was displayed by fractions S2 and S3 (8.54 ± 2.66 and 6.07 ± 0.16 μM $FeSO_4$/g extract, respectively). However, when compared with synthetic antioxidant butylated hydroxytoluene (BHT), fraction S1 did not show a relevant antioxidant activity.

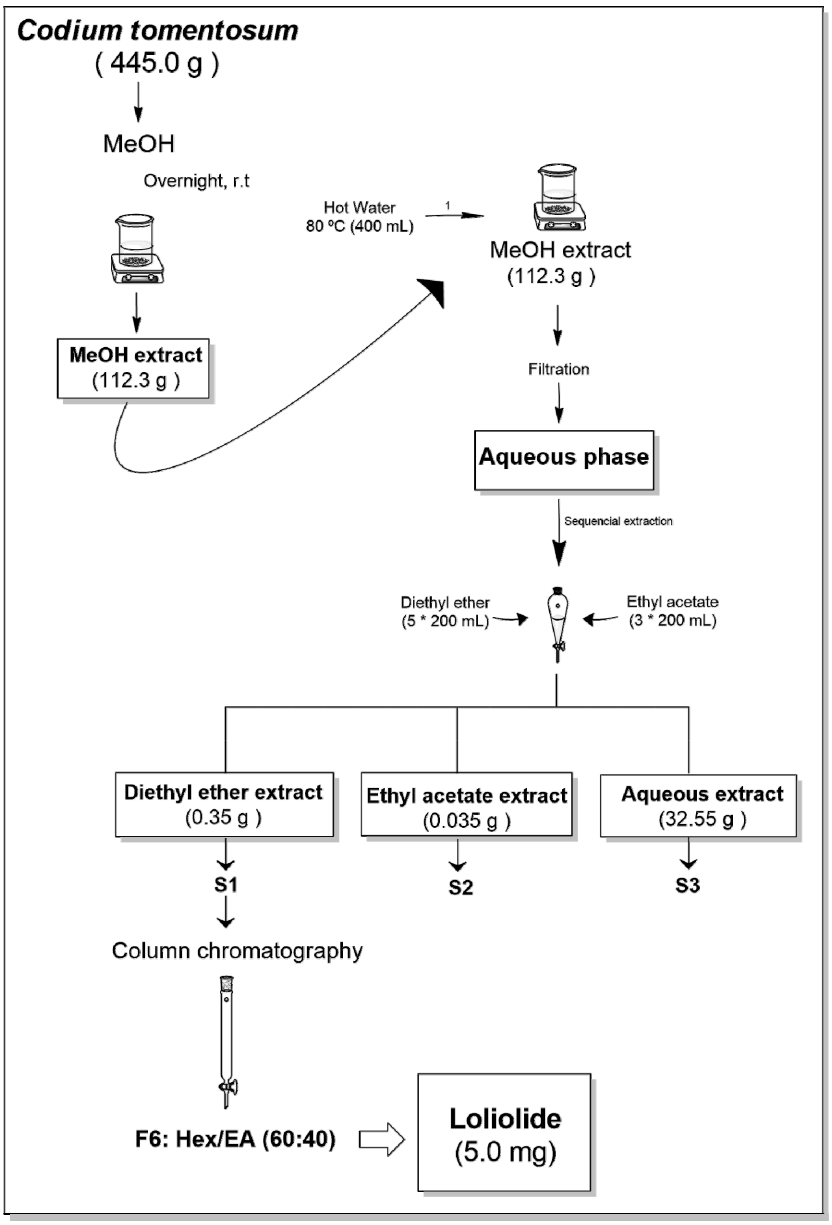

Figure 1. Extraction and fractionation flowchart of the green seaweed *Codium tomentosum*.

2.1.3. Neuroprotective Potential of *Codium tomentosum* Fractions

The neuroprotective effects of *C. tomentosum* fractions (100 μg/mL; 24 h) were evaluated on neuroblastoma cell line (SH-SY5Y) exposed to the neurotoxin 6-OHDA (100 μM). Cell viability was estimated by the 3-(4,5-dimethyl-2-thiazolyl)-2,5-diphenyl-2H-tetrazolium bromide (MTT) assay, and the results are presented in Figure 2.

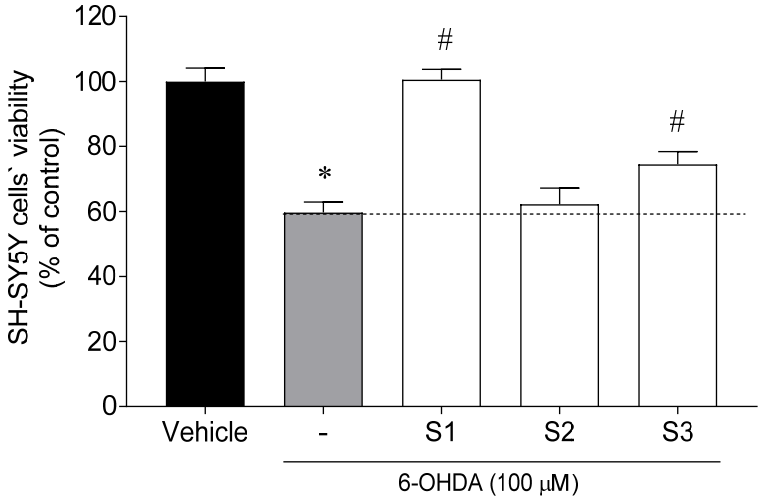

Figure 2. Neuroprotective effects of *Codium tomentosum* fractions (S1–S3 at 100 μg/mL, 24 h) in the presence of 6-OHDA (100 μM) on SH-SY5Y cells. (−) 6-OHDA. The values in each column represent the mean ± standard error of the mean (SEM) of 3 or 4 independent experiments. Symbols represent significant differences (ANOVA, Dunnett's test, $p < 0.05$) when compared to: * vehicle and # 6-OHDA.

The exposure of SH-SY5Y cells to 6-OHDA (100 μM) for 24 h led to a reduction of cell viability of about 41% (59.69 ± 3.23% of viable cells) when compared to vehicle (100.00 ± 4.15% of viable cells). However, when SH-SY5Y cells were treated with 6-OHDA in the presence of *C. tomentosum* fractions (100 μg/mL), two samples exhibited capacity to prevent cell death in 15% and 40%, namely S3 and S1. The latter was selected for further purification processes.

2.2. Isolation and Structural Elucidation of Codium tomentosum Bioactive Compounds

Since fraction S1 attenuated the neurotoxicity induced by 6-OHDA, it was sub-fractionated by column chromatography aiming the isolation of the bioactive compound(s) having attained 10 sub-fractions (Figure 1). Sub-fraction F6 afforded the monoterpene lactone Loliolide, the structure of which was established by nuclear magnetic resonance (NMR) spectroscopy. The obtained ^{13}C and ^{1}H chemical shifts and structural assignments (Table 2) are in accordance with the literature [38].

Table 2. Nuclear magnetic resonance (NMR) data (400 MHz, $CDCl_3$) of Loliolide isolated from *Codium tomentosum*.

Position	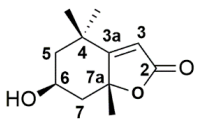 Loliolide (1)	
	δ C	**δH, m, *J*(Hz)**
2	172.07	-
3	112.88	5.69 s
3a	182.60	-
4	35.91	-
5	47.26	1.52 dd, 14.5, 3.2, α-H_{ax} 1.98 brd, 14.5, β-H_{eq}
6	66.79	4.33 m, α-H_{eq}
7	45.57	1.79 m, α-H_{ax} 2.46 brd, 14.2 β-H_{eq}
7a	86.83	-
4α-Me	30.67	1.27 s, Me_{eq}
4β-Me	26.48	1.46 s, Me_{ax}
7a-Me	26.96	1.78 s, β-Me_{ax}

2.3. Antioxidant Capacity of Loliolide

The antioxidant activity of Loliolide was evaluated by three different approaches, namely, DPPH radical scavenging ability, oxygen radical absorbance capacity (ORAC), and ferric reducing antioxidant power (FRAP) methods. It was found that Loliolide did not present a noticeable DPPH radical scavenging ability (EC_{50} > 100 μM). Additionally, in the ORAC (24.22 ± 3.45 μmol TE/g) and FRAP (13.81 ± 1.36 μM $FeSO_4$/g) assays, this compound also has not shown capacity for reducing peroxyl radicals and ferric ions, when compared with BHT (143.70 ± 23.36 μmol TE/g and 2821.50 ± 63.03 μM $FeSO_4$/g, respectively).

2.4. Bioactivity Evaluation of Loliolide on In Vitro Cellular Models

2.4.1. Cell Viability and Neuroprotective Effects of Loliolide on SH-SY5Y Cells

In a first approach, the possibility of Loliolide to induce cytotoxic effects on SH-SY5Y cells was considered (Figure 3A). Subsequently, the neuroprotective effects of Loliolide (1, 5, 10, 50, 100 μM; 24 h) were evaluated in the presence of the 6-OHDA neurotoxin (Figure 3B).

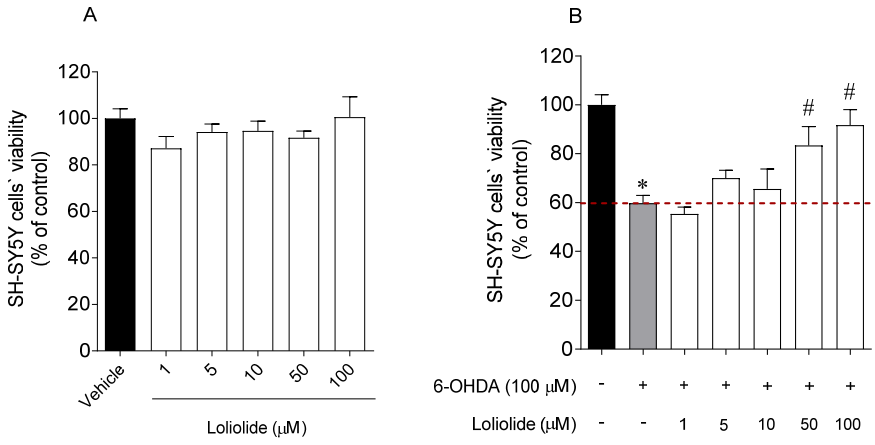

Figure 3. (**A**) SH-SY5Y cells' viability when exposed 24 h to Loliolide (1–100 μM). (**B**) Neuroprotective effects of Loliolide (1–100 μM) on SH-SY5Y cells exposed to 6-OHDA after 24 h of incubation. (+) With 6-OHDA and (−) without 6-OHDA.The values in each column represent the mean ± standard error of the mean (SEM) of 3 or 4 independent experiments. Symbols represent significant differences (ANOVA, Dunnett's test, $p < 0.05$) when compared to: * vehicle and # 6-OHDA.

The results suggest that Loliolide did not present cytotoxicity and exhibited high neuroprotective effects against the 6-OHDA neurotoxin, leading to an increase of cell viability of 23.70 ± 7.77% and 41.06 ± 6.31%, at 50 μM and 100 μM, respectively.

2.4.2. Effects of Loliolide on PD-Hallmarks

Several PD hallmarks associated with Loliolide neuroprotective effects on SH-SY5Y cells were evaluated, namely ROS production, Catalase activity, mitochondrial membrane potential (MMP), adenosine triphosphate (ATP) levels and Caspase-3 activity. These hallmarks were evaluated on SH-SY5Y cells treated with 6-OHDA in the presence and absence of Loliolide (50–100 μM), and results are presented in Figure 4.

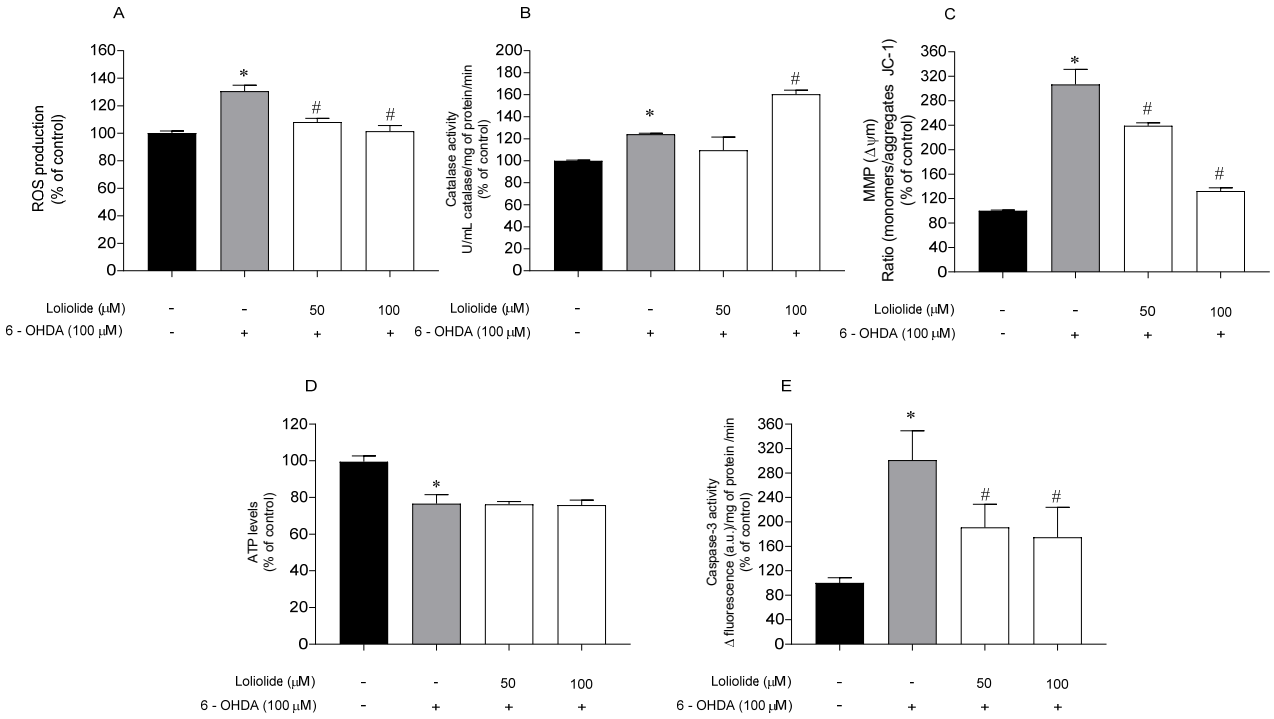

Figure 4. Parkinson's disease hallmarks associated with neuroprotective effects of Loliolide (50–100 μM, 6 h) determined on SH-SY5Y cells. (**A**) ROS production; (**B**) Catalase activity; (**C**) Mitochondrial membrane potential; (**D**) ATP levels; (**E**) Caspase–3 activity. (+) with 6-OHDA and (−) without 6-OHDA. The values in each column represent the mean ± standard error of the mean (SEM) of 3 or 4 independent experiments. Symbols represent significant differences (ANOVA, Dunnett's test, $p < 0.05$) when compared to: * vehicle and # 6-OHDA.

In all biomarkers, the effect of Loliolide in the absence of 6-OHDA was also evaluated, and no significant differences were observed when compared to vehicle.

The exposure of cells to 6-OHDA (100 μM) lead to a marked increase of ROS levels when compared to vehicle (Figure 4A). In the presence of Loliolide, both concentrations induced a significant decrease of ROS levels. The Catalase activity, a stress condition biomarker, was also evaluated representing a stequiometry of 1:1 with H_2O_2 levels. The exposure to 6-OHDA led to an increase of Catalase activity of 24.00 ± 1.03%, when compared with vehicle (Figure 4B). When in the presence of Loliolide, Catalase activity increased to 60.40 ± 3.72% at 100 μM. To understand if the neuroprotective effects of Loliolide were mediated by mitochondrial events, the MMP and ATP levels were evaluated. In the cells exposed to 6-OHDA it was verified a depolarization of the MMP of 206.80 ± 24.55%, accompanied by a 23.36 ± 1.49% decrease of ATP levels, when compared with vehicle (Figure 4C,D). The treatment with Loliolide prevented MMP distress; however, it did not stabilize the ATP levels disrupted by 6-OHDA. Caspase–3 activity was determined to understand if the neuroprotective potential of Loliolide was mediated by apoptotic pathway. Figure 4E shows that when SH-SY5Y cells are exposed to 6-OHDA, Caspase–3 activity is increased by about 200% when compared with the vehicle. On the other hand, the treatment with Loliolide promoted a decrease of Caspase–3 activity of 110.1 ± 37.82% and 126.1 ± 48.95% at 50 μM and 100 μM, respectively.

2.4.3. DNA Fragmentation and Nuclear Condensation

To understand if Loliolide had the ability to prevent the DNA damage and nuclear condensation induced by 6-OHDA treatment, the integrity of SH-SY5Y cells DNA was evaluated through the staining with DAPI probe, and the results are presented in Figure 5.

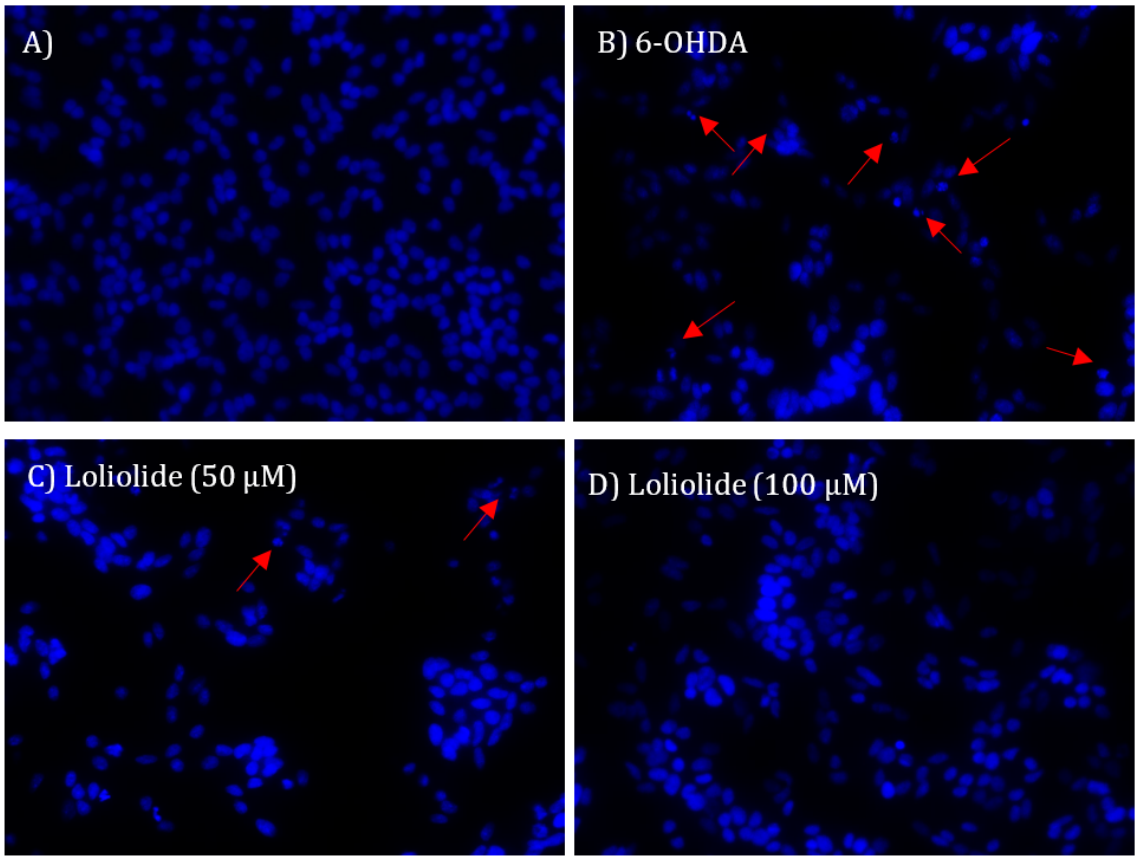

Figure 5. Nuclear morphology of SH-SY5Y cells stained with DAPI probe. (**A**) No treatment; (**B**) Cells exposed to 6-OHDA (100 μM; 24 h); (**C**) Cells exposed concomitantly to Loliolide (50 μM) and 6-OHDA (100 μM) for 24 h; (**D**) cells exposed concomitantly to Loliolide (100 μM) and 6-OHDA (100 μM) for 24 h. The DNA fragmentation pattern is an indicator of apoptosis. Arrows point to nuclear fragmentation. The images are representative of one well of each situation tested.

Figure 5 shows nuclear fragmentation and condensation of SH-SY5Y cells resulting from the exposure to 6-OHDA. The treatment with Loliolide (50 and 100 μM; 24 h) inhibited nuclear condensation and DNA fragmentation.

2.4.4. Loliolide Effects on NF-κB p65 Translocation

Nuclear transcription factor-κB (NF-κB) is an apoptosis/inflammation regulator present in human tissues, including brain. Thus, we tested if Loliolide affected the translocation of this protein to the nucleus of neuronal cells. The expression levels of NF-κB p65 in cytosol and nucleus were studied by Western blot (Figure 6).

As shown in Figure 6A, the neurotoxicity induced by 6-OHDA led to an increase of NF-κB p65 expression in the nucleus accompanied by a decrease in the cytoplasm, when compared with the vehicle (1.39 ± 0.19 and 1.53 ± 0.25, respectively). However, when cells were treated with 6-OHDA in the presence of Loliolide, the nuclear NF-κB p65 levels were downregulated and cytoplasmic NF-κB p65 levels were upregulated. However, at 100 μM, Loliolide exhibited significant ability to block the translocation of NF-κB p65 factor from the cytoplasm to the nucleus, being also possible to observe an increased expression levels of NF-κB p65 factor, when compared with the nucleus levels. On the other hand, in the treatment performed only with 6-OHDA an opposite effect was observed, suggesting that NF-κB p65 factor translocation inhibition may be associated with protective effects of Loliolide against neuronal cell death mediated by 6-OHDA.

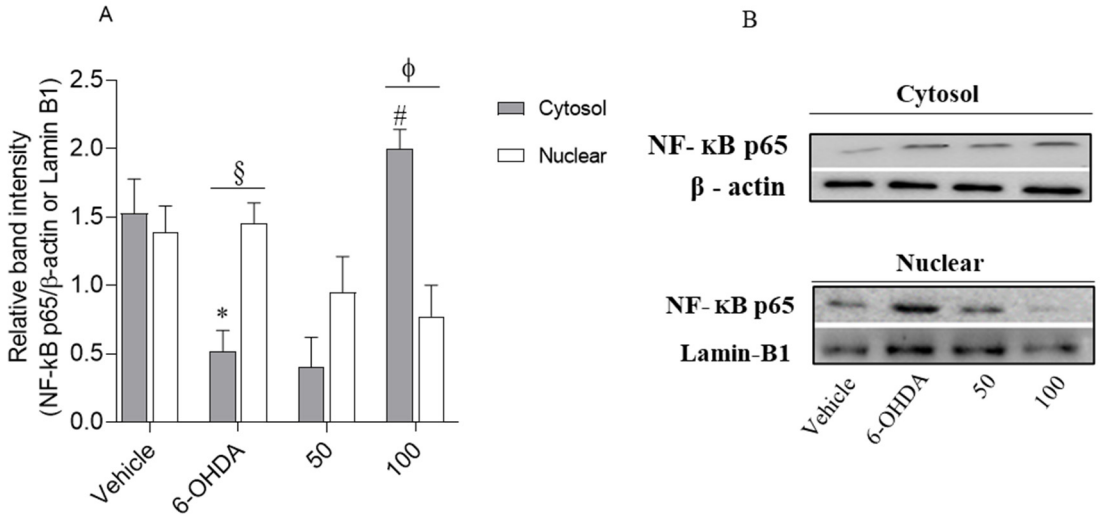

Figure 6. Comparison of the NF-κB p65 expression levels in the cytosol and nucleus in response to 6-OHDA (100 μM), in the absence and presence of Loliolide (50–100 μM). (**A**) The values in each column represent the mean ± standard error of the mean (SEM) of 3 or 4 independent experiments. Symbols represent significant differences (ANOVA, Dunnett's test, $p < 0.05$) when compared to: * vehicle, and $^{\#}$ 6-OHDA, § situation of nucleus and $^{\Phi}$ situation of 50 μM. (**B**) Relative protein expression levels based on Western-blot band intensity; protein levels were normalized with β-actin and Lamin-B1 in the cytosol and nucleus, respectively.

2.5. Anti-Inflammatory Activity of Loliolide on RAW 264.7 Cells

In a first approach, Loliolide was tested for possible cytotoxic and inflammatory effects on murine macrophages (RAW 264.7 cells). The anti-inflammatory potential of Loliolide (50–100 μM; 24 h) was then determined on RAW 264.7 cells, in an inflammatory condition mediated by lipopolysaccharides (LPS). The results are presented in Figure 7.

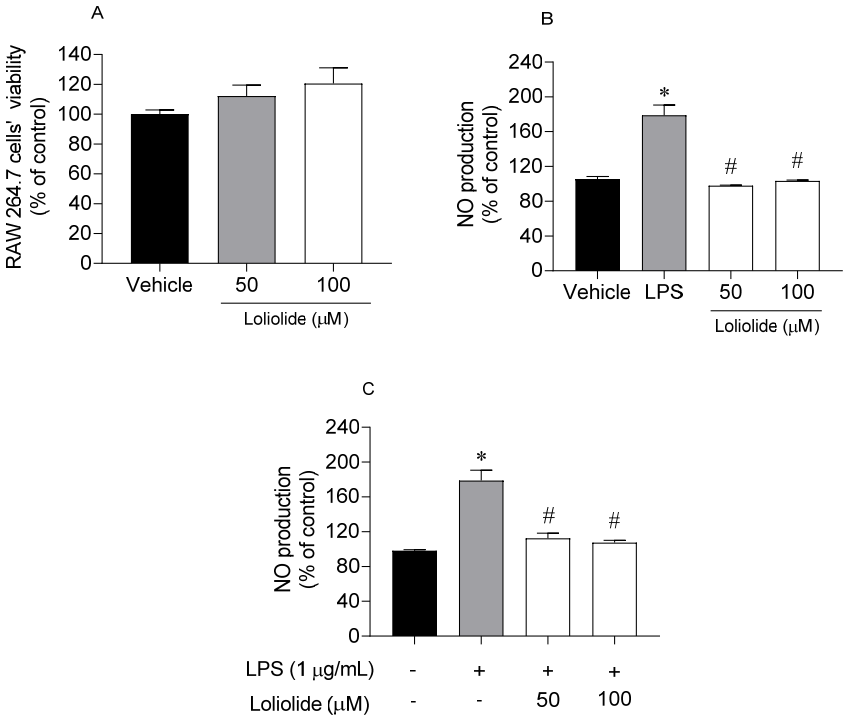

Figure 7. Evaluation of cells' viability and inflammation on RAW 264.7 cells for 24 h. (**A**) RAW 264.7 cells' viability exposed to Loliolide (50–10 μM); (**B**) nitric oxide (NO) production by RAW 264.7 cells exposed to Loliolide (50–10 μM); (**C**) NO production by RAW 264.7 cells exposed to lipopolysaccharide (LPS) (1 μg/mL) and Loliolide (50–10 μM). (+) with LPS and (−) without LPS. The values in each column represent the mean ± standard error of the mean (SEM) of 3 or 4 independent experiments. Symbols represent significant differences (ANOVA, Dunnett's test, $p < 0.05$) when compared to: * vehicle and $^{\#}$ LPS.

In Figure 7, it is possible to observe that Loliolide did not induce cytotoxicity on RAW 264.7 cells at 50 and 100 μM (Figure 7A). Furthermore, the treatment of RAW 264.7 cells with Loliolide at 50 μM and 100 μM did not stimulate the NO production (Figure 7B) when compared with the vehicle. On the other hand, the exposure to LPS stimulated the NO production. However, when LPS-stimulated RAW 264.7 cells were treated with Loliolide at 50 μM and 100 μM the NO production decreased significantly (Figure 7C) when compared with LPS situation.

2.6. Effects of Loliolide on the Pro-Inflammatory and Anti-Inflammatory Cytokines Levels

RAW 264.7 cells were exposed to LPS and Loliolide, and the levels of the pro-inflammatory cytokines TNF-α, IL-6, and anti-inflammatory IL-10 were determined by ELISA. The results are depicted in Figure 8.

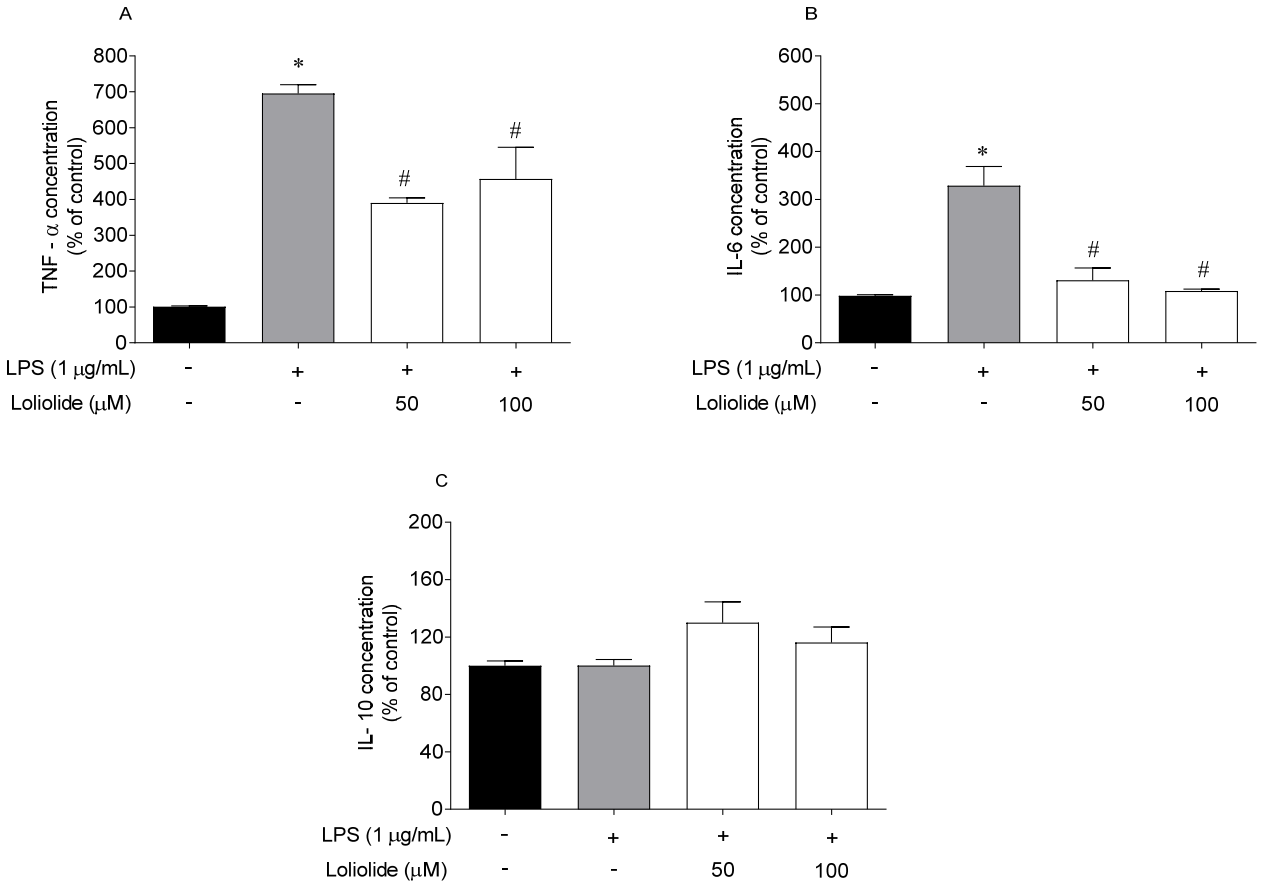

Figure 8. Levels of pro-inflammatory cytokines on RAW 264.7 cells after exposure to Loliolide (50–100 μM) and to LPS (1 μg/mL) for 18 h. (**A**) TNF-α; (**B**) IL-6; (**C**) IL-10. (+) with LPS and (−) without LPS. The values in each column represent the mean ± standard error of the mean (SEM) of 3 or 4 independent experiments. Symbols represent significant differences (ANOVA, Dunnett's test, $p < 0.05$) when compared to: * vehicle and # LPS.

In response to LPS stimulation, the production of cytokines was significantly upregulated compared to the control, except IL-10. The treatment with Loliolide significantly reduced the production of TNF-α by up to 305% and 238% at 50 μM and 100 μM, respectively (Figure 8A). The treatment with Loliolide also significantly reduced the production of IL-6 by up to 197% and 220% at 50 μM and 100 μM, respectively (Figure 8B). However, it did not promote significant effects on the IL-10 levels (Figure 8C).

3. Discussion

PD is the second most common neurodegenerative disease worldwide being characterized by a progressive degeneration of nigrostriatal dopaminergic neurons [39,40]. Currently, the molecular mechanisms underlying the loss of these neurons still remain vague; however, mitochondrial dysfunction, apoptosis, and neuroinflammation are thought to play an important role in dopaminergic neurotoxicity in PD [4]. In all these biological events, oxidative stress is the common underlying mechanism that leads to cellular dysfunction and cell death. Despite the efforts, PD treatment continues to be a major clinical challenge, without an effective cure. Therefore, more studies are needed to understand the pathomechanisms of PD to find effective neuroprotective agent(s).

In the present study, the antioxidant, neuroprotective and anti-inflammatory activity of Loliolide isolated from *C. tomentosum* was evaluated. Regarding its antioxidant capacity, three methods (DPPH, FRAP and ORAC) were assayed but in none Loliolide showed significant antioxidant potential, which is in agreement with a previous work [41]. However, despite the weak antioxidant activity observed in chemical assays, when tested on an in vitro cellular model exposed to UVA-B radiation, this compound inhibited the ROS production and apoptosis [42].

The antioxidant activity of a compound should not be determined based on a unique in vitro test since those have the limitation of targeting a specific oxidative species (e.g., alkoxy and peroxyl radicals, reactive nitrogen species, ROS) [43,44], disregarding all cellular oxidative pathways players, and thus, may not reflect the antioxidant ability in more complex models or in vivo. Since several studies have associated dopaminergic cell death prevention with antioxidative mechanisms [45,46], in this work, the antioxidant potential of Loliolide was screened in a PD cellular model. Neurotoxicity was induced by 6-OHDA, a neurotoxic compound that selectively destroys dopaminergic and noradrenergic neurons in the brain by instigating ROS production [47].

Marine-derived compounds have been previously reported to exhibit neuroprotective effects against 6-OHDA neurotoxicity [23,48]. In this study, Loliolide revealed capacity to promote SH-SY5Y cells recover from the damage induced by 6-OHDA. The results presented herein are consistent with previous studies. For instance, 11-dehydrosinulariolide, a soft coral-derived compound, and Kappa-carrageenan, isolated from *Hypnea musciformis* seaweed, had capacity to protect SH-SY5Y cells against the neurotoxic effects of 6-OHDA [23,48]. Also, Yurchenko et al. (2018) [49] showed that metabolites isolated from the marine fungi *Penicillium* sp., *Aspergillus* sp. and *Aspergillus flocculosus* protected Neuro2a cells against the damaging effects of 6-OHDA. The death of dopaminergic neurons occurs in the central nervous system (CNS), where the neurotransmitter dopamine is synthesized and released into the substantia nigra [50]. Currently, it is known that 70% of those dopaminergic neurons in CNS die along PD development; however, the symptoms are not noticed due to compensatory mechanisms of the striatum body [51]. Although the mechanisms responsible for inducing cell death in PD are not completely clarified, it is known that the dopamine metabolism, oxidative stress, mitochondrial dysfunction and neuroinflammation are involved in the death of dopaminergic neurons in CNS [4,52]. Iron (Fe(II)) plays an important role in oxidative changes in PD, being present in several regions of the brain, mainly in dopaminergic neurons of the substantia nigra [53]. As a result, dopaminergic neurons are highly susceptible to Fenton's reaction, in which H_2O_2 is converted to hydroxyl radicals promoting oxidative stress, leading to apoptosis, DNA damage and cellular death.

There many enzymes are able to decompose H_2O_2, including Catalase, glutathione peroxidase and other peroxidases [54]. Catalase is a key detoxifying enzyme that uses H_2O_2 as substrate, decomposing it into water and oxygen, maintaining an optimum level of this molecule in the cells [55]. Based on the results obtained in the present work, it was observed that Loliolide was able to decrease the ROS production induced by 6-OHDA treatment and stimulate Catalase activity. These results are in agreement with those previously reported by Magalingam and co-workers [56] that also observed a significant increase of Catalase

activity in PC-12 cells exposed to 6-OHDA in the presence of antioxidants, namely rutin and isoquercitrin, when compared with 6-OHDA situation. Regarding 6-OHDA, it was observed a slight increase of Catalase activity that can be explained by the cellular metabolism response to the increase of ROS levels, such as H_2O_2, mediated by 6-OHDA treatment, leading to a stimulation of enzyme activity in order to detoxify H_2O_2. On the other hand, the weak antioxidant capacity of Loliolide and its ability to improve Catalase activity suggest that its activity may not be directly related with the neutralization of ROS but with the stimulation of the antioxidant defense machinery. This point of view is reinforced by the results attained with Loliolide when tested at 100 μM, and it is possible to observe that the highest increase of Catalase activity was accompanied by the highest decrease of ROS levels.

Oxidative stress has been intimately linked to mitochondrial dysfunction. Mitochondria are vitally important organelles involved in energy metabolism, generating over 90% of our cellular energy in the form of ATP, through oxidative phosphorylation, and they are involved in various other processes, including the regulation of calcium homeostasis, and stress response [57]. As a consequence of these processes, mitochondria are also responsible for more than 90% of cellular ROS production [42], and are completely dependent of an efficient antioxidant machinery to prevent oxidative stress. In clinical pathologies such as PD, mitochondrial dysfunction is a characteristic abnormality. An increase of ROS levels is detected, against which antioxidative defenses are overwhelmed [58]. Based on the results presented here, it was verified that Loliolide prevented mitochondrial dysfunction, decreased Caspase-3 activity and inhibited DNA fragmentation/condensation (apoptosis morphological trait) disrupted by 6-OHDA. However, it did not exhibit capacity to recover the ATP levels decreased by 6-OHDA treatment. Since Loliolide was able to decrease the mitochondrial depolarization induced by 6-OHDA exposure, we hypothesize that it would be necessary to increase the incubation time in order to be possible to observe a potential increase of ATP levels. Nevertheless, further studies should be considered to verify this hypothesis.

Several pieces of evidence show that the activation of the transcription factor NF-κB is associated with oxidative stress-induced apoptosis and some researchers verified that this transcription factor can play a role in PD when translocated from the cytoplasm to the nucleus [59]. Under normal conditions, NF-κB is bounded in the cytoplasm to the inhibitor protein, IκBα, which sequesters NF-κB in the cytosol, inactivating its transcription factor by masking the nuclear localization signals of NF-κB proteins. The activation of NF-κB involves its dissociation from IκBα followed by its translocation to nucleus, where it directly binds to DNA sequences, inducing damage [60]. The present results showed that Loliolide had capacity to inhibit NF-κB translocation from the cytoplasm to nucleus, thus preventing DNA damage and apoptosis. Our results are in agreement with Alvariño et al. [61], who reported that gracilin A, a marine-derivates have capacity to downregulate the NF-κB factor, prompted by H_2O_2 in microglia cells. Furthermore, due to the key role of NF-κB factor in the response to oxidative stress and inflammation, the effects mediated by Loliolide in the other biomarkers may be triggered through the translocation of this factor.

Chronic inflammation is characteristic of neurodegenerative diseases such as PD, in which cytotoxic levels of NO and pro-inflammatory cytokines initiate neuronal cell death pathways. Several studies reported that microglia activation could have a protective role in neurodegenerative diseases [13,14]. Therefore, promoting anti-inflammatory cytokines or limiting pro-inflammatory cytokines and NO production by macrophages/microglia activation, can be beneficial for preventing inflammation [13]. The macrophages are known to cross the leaky blood-brain barrier in PD to interact with microglia and stimulate the secretion of inflammatory cytokines causing brain damage via neuroinflammation. Thus, the uncontrolled release of inflammatory cytokines, such as TNF-α and IL-6, is a key event for neurodegenerative diseases progression [62,63]. As a result, the proximity of microglia with macrophages attracted increasing attention in relation to the onset and PD progression. In this study, macrophages were exposed to LPS to induce inflammation [64] in the presence

of Loliolide. It was verified that Loliolide prevented inflammation by decreasing NO production and reducing TNF-α and IL-6 levels. The interleukin-10 (IL-10) is a potent anti-inflammatory cytokine that plays a vital role in immunologic system, acting in acute and chronic inflammation. Both up or downregulation of IL-10 cytokine will result in serious immunologic disorders, including neurodegenerative diseases. Studies performed with the brains of a PD mouse model induced with LPS evidenced that IL-10 cytokine mediated a decrease of the number of activated microglia promoting a protective effect regarding the loss of dopaminergic neurons [16]. In the present work, the treatment of RAW 264.7 cells with LPS, in the presence/absence of Loliolide, did not induced significant changes on IL-10 levels. Although the IL-10 generally mediated effects are able to oppose the actions mediated by the pro-inflammatory cytokines, its activity is highly complex in the immunoregulation that refines IL-10 production to a later stage when compared to pro-inflammatory cytokines. Thus, it is possible that it would be necessary to prolong cell exposure to both the inducer (LPS) and the protective agent (Loliolide) to detect this protein production [65]. Accordingly, with the above-mentioned facts, and knowing that p38 MAPK pathway plays a central role in the inflammation process, stimulating the release of pro-inflammatory cytokines and activating NF-κB transcription factor, it is possible that Loliolide effects may be also linked to p38 activity inhibition. However, additional studies need to be accomplished to prove this hypothesis.

More recently, there are studies indicating that the development of chronic neuroinflammatory diseases can be influenced by intestinal inflammation. Gut bacteria can release factors and metabolites into the blood that can readily cross blood–brain barrier (BBB) or otherwise interact with barrier cells, changing its integrity, and transport rates, thus affecting CNS regulation and functions [66]. Furthermore, metabolic products synthesized by the microbiota when crossing the BBB trigger the inflammatory cascade, including microglial activation and neuronal dysfunction leading to the death of neurons. More recently, previous studies conducted with PD patients have shown evidence of an altered intestinal microbiota, systemically releasing endotoxins such as lipopolysaccharides and metabolic products facilitating their entry into the CNS promoting the activation of the microglia inducing inflammatory responses, such as the release of pro-inflammatory cytokines (IL1-α, IL-β, IL-6 and TNF-α), leading to the degeneration of dopaminergic neurons [66,67]. Therefore, due to the anti-inflammatory properties exhibited by Loliolide, as well as its ability to cross the BBB as described by Ahmed et al. [68], its application as a dietary anti-inflammatory molecule can represent an excellent strategy to contribute for PD therapeutics.

Loliolide showed capacity to protect neuronal cells from the damaging effects of 6-OHDA, neutralizing its cytotoxicity, preventing mitochondrial dysfunction, apoptosis and also showing high anti-inflammatory effects, inhibiting the NF-κB pathway, decreasing the levels of TNF-α and IL-6, thus blocking the inflammatory cascade.

Due to promising activities exhibited by Loliolide in the present work, further studies should be considered in order to fully depict the intracellular signaling pathways underlying its neuroprotective and anti-inflammatory activities, including the study of protein expression levels of other endogenous antioxidant enzymes (e.g., SOD, GSH-Px), other apoptosis biomarkers (e.g., Caspases -9 and -8, Bax, cytochrome C) as well as the study of others factors/proteins related with antioxidant, neuroprotective and anti-inflammatory biological processes (e.g., COX, iNOS, PGE2, JAK, JNK, Nrf2/HO-1, α-synuclein expression). Furthermore, the establishment of more complex in vitro cellular models, such as co-cultures and 3D cell models, as well as the development of smart delivery systems such as nanoparticles for brain drug delivery will be essential to understand the really therapeutic potential of Loliolide on PD.

In conclusion, the monoterpene lactone Loliolide, isolated from the green algae *C. tomentosum*, presented capacity to protect neuronal cells from the damaging effects of 6-OHDA, neutralizing its cytotoxicity. Additionally, the studies here performed suggest that this compound acts in several PD hallmarks, reducing oxidative stress, preventing mito-

chondrial dysfunction, and blocking inflammatory pathways, thus preventing neuronal cell death (Figure 9). This work highlights Loliolide as a promising compound for PD therapeutics and, therefore, should be considered for additional detailed studies in more complex models, aiming at further considerations for pre-clinical trials.

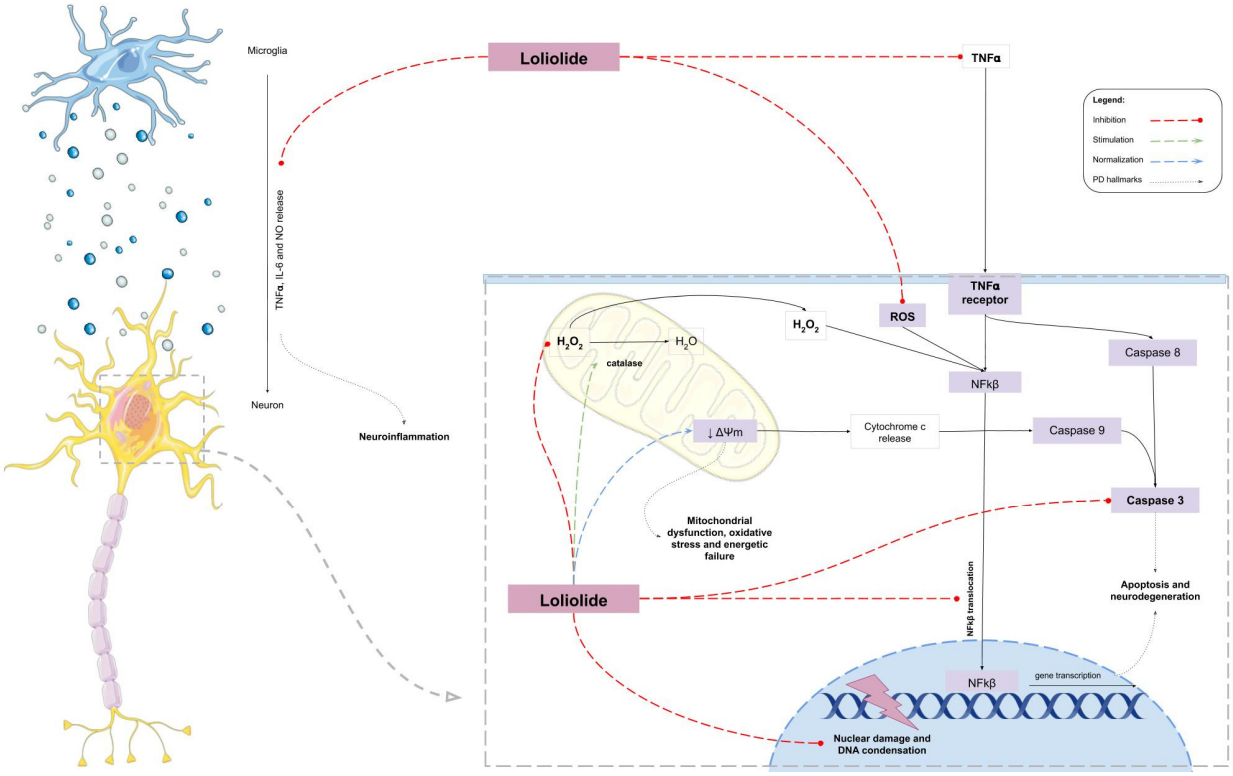

Figure 9. Hypothetical mechanism of action of Loliolide in 6-OHDA-induced cell death and in LPS-induced inflammation.

4. Materials and Methods

4.1. Collection and Preparation of Codium tomentosum Samples

The green seaweed *C. tomentum* Stackouse, (1797) was collected in October 2016 at Peniche coast, Portugal (39°37′05″ N, −9°38′58″ O) and transported to MARE-Polytechnic of Leiria lab facilities. The seaweed was rinsed carefully with seawater and distilled water to remove epiphytes, sand, and debris. Then, it was freeze-dried (Scanvac Cool Safe, LaboGene, Lynge, Denmark), grinded, and stored in a cool place protected from light, until further use.

4.2. Seaweed Extraction and Fractionation

The freeze-dried biomass of *C. tomentosum* (445.0 g) was extracted with methanol (VWR-BDH Chemicals, Fontenay-sous-Bois, France) (in a biomass/solvent ratio of 1:40) overnight, under constant stirring at room temperature. The methanol extract was concentrated until dryness under vacuum, at low temperature (30 °C) in a rotary evaporator (IKA HB10, Staufen, Germany) and in a speed vacuum equipment (Concentrator Plus, Eppendorf, Spain), affording the MeOH crude extract (112.3 g). Afterwards, it was suspended in hot (80 °C) water (400 mL) and filtered (filter paper no. 4, VWR International, Alfragide, Portugal). After cooling to room temperature, the aqueous phase was partitioned, firstly with diethyl ether (5 × 200 mL), and then with ethyl acetate (3 × 200 mL). Organic phases were dried with anhydrous Na_2SO_4, filtered (filter paper no. 4), and concentrated to dryness, resulting in three fractions (S1–S3) (Figure 1).

The dried diethyl ether extract (346.0 mg) (S1) was fractionated by preparative column chromatography on silica gel 60 (0.06–0.2 mm, VWR, Leuven, Belgium) eluted with

mixtures of *n*-hexane, ethyl acetate, and methanol (Fisher Scientific, Loughborough, UK) of increasing polarity, affording a total of 10 fractions. Fractions were screened by thin layer chromatography in TLC-plates ALUGRAM® Xtra Sil G/UV254, pre-coated with silica gel 60 (Merck, Lisbon, Portugal), and those exhibiting the same chemical profile were pooled. Fraction 6 (Hex: EA, 60:40, *v/v*) yielded the bioactive compound **1** (5.0 mg) (Figure 1), the structure of which was attained by NMR spectroscopy.

4.3. Structural Elucidation of the Bioactive Compound

NMR spectra of 1D (^{1}H, ^{13}C APT) and 2D (COSY, HMBC, HSQC and NOESY) experiments were acquired on a Bruker Advance 400 spectrometer with a frequency of 400 MHz for ^{1}H, and 100 MHz for ^{13}C. Compound **1** was dissolved in 500 µL of $CDCl_3$ (Sigma-Aldrich, St. Louis, MO, USA). Chemical shifts are expressed in ppm and reported to the residual solvent signals. Coupling constants (*J*) are expressed in Hertz (Hz).

4.4. Bioactivity Assays

Fractions S1–S3 and compound **1**, from *C. tomentosum*, were subjected to a series of in vitro biological assays, to evaluate their antioxidant, neuroprotective, and anti-inflammatory potential.

4.4.1. Antioxidant Capacity

The antioxidant activity was evaluated according to Silva et al. [21] using different approaches, namely, 2,2-diphenyl-1-picrylhydrazyl (DPPH) radical scavenging ability, oxygen radical absorbance capacity (ORAC), and ferric reducing antioxidant power (FRAP) assays.

4.4.2. Cell Culture Maintenance

Neuroblastoma cell line (SH-SY5Y) was obtained from the German Collection of Microorganisms and Cell Cultures GmbH (DSMZ) Bank (ACC 209). Cells were cultivated at 37 °C and 5% CO_2 with DMEM:F12 medium containing 1% antibiotic/antimycotic (Amphotericin B, Penicillin and Streptomycin) (Biowest, Nuaillé, France) and 10% (*v/v*) Fetal Bovine Serum (FBS) (Biowest, Riverside, MO, USA). Cells were seeded as follows: 4×10^4 cells/well, in 96-well microplates for cell viability and neuroprotection assays; 2×10^5 cells in 12-well culture plates for Catalase assay; 5×10^5 cells in 6-well culture plates for Caspase–3 activity, nuclear morphological damage assessment, and NF-κB p65 translocation analysis.

4.4.3. Cell Viability and Neuroprotective Capacity on a PD Cellular Model

Effects on cell viability and neuroprotection assays were estimated using the MTT (VWR, Solon, Ohio, USA) method, as described by Silva et al. [22]. SH-SY5Y cells were exposed 24 h to 6-OHDA (100 µM) in absence (Vehicle) or presence of compound **1** at concentrations of 1–100 µM. Then, 100 µL MTT (1.2 mM) were added to wells and cells were incubated for 1 h at 37 °C. After this time, MTT was removed and 100 µL DMSO was added. The resulting absorbance was read in a microplate reader (Bioteck, Epoch/2 microplate reader, Winooski, VT, USA) at 570 nm. The results were expressed in percentage of control.

4.4.4. Parkinson's Disease Hallmarks

ROS production: ROS levels were evaluated using the 5(6)-carboxy-2′, 7′-dichlorofluorescein diacetate (carboxy-H2DCFDA) probe (Invitrogen, Bleiswijk, Netherlands) according to Alvariño et al. [69] with slight modifications. After incubation with compound **1,** cells were washed with ice-cold Phosphate-Buffer Saline (PBS) and C-H2DCFDA (100 µL, 20 µM) was added, and incubated for 1 h at 37 °C. The resulting fluorescence was read at 527 nm excitation and 590 nm emission wavelengths, and ROS levels presented in percentage of control (non-treated cells).

Catalase activity: This assay was assessed using the "Amplex ™ Red Catalase assay" kit (Invitrogen, Renfrew, UK). In this assay, catalase first reacts with 40 μM H_2O_2 to produce water and oxygen (O_2). Next, the Amplex Red reagent reacts (1:1 stoichiometry) with any unreacted H_2O_2 in the presence of horseradish peroxidase (HRP), producing a highly fluorescent oxidation product, resorufin. Therefore, the signal from resorufin decreases as catalase activity increases.

SH-SY5Y cells were cultured in 12 -well plates and exposed 6 h to 6-OHDA (100 μM) in the absence (vehicle) and presence of compound **1** (50 and 100 μM). Cells were then rinsed with ice-cold PBS, followed by the addition of 100 μL of lysis buffer (20 mM Tris-HCl pH 7.4, 10 mM NaCl and 3 mM $MgCl_2$), containing a protease inhibitor' cocktail (Roche, Mannheim, Germany). Following, cells were scrapped, incubated on ice for 15 min and centrifuged at 1200× *g*, 4 °C for 10 min. Cells lysates were processed according to manufacturer's instructions. H_2O_2 levels were determined in real time for 30 min at 37 °C. The fluorescence was read at 530 nm, with an excitation wavelength of 590 nm. Catalase activity was calculated by the slope of the linear phase of the fluorescence resulting from the resorufin oxidation, and the results were expressed in percentage of control.

Mitochondrial membrane potential (ΔΨm): MMP was evaluated according to Silva et al. [21] using JC-1 probe (Molecular Probes, Eugene, OR, USA). SH-SY5Y cells were exposed 6 h to 6-OHDA (100 μM) in the presence or absence of compound **1**. Cells were washed with ice-cold PBS, and then, 200 μL of JC-1 (3 μM) were added prior to 15 min at 37 °C. Afterward, JC-1 was removed, and PBS was added. The monomers/aggregates formation were determined by fluorescence extrapolation at 530 nm emission (monomers)/590 nm (aggregates) and 490 nm excitation wavelengths, for 30 min at 37 °C. MMP was calculated through the ratio between monomers/aggregates formation and presented as percentage of control.

Adenosine triphosphate (ATP) levels: The ATP levels were assessed using the "Luminescent ATP detection assay" kit (ABCAM, Cambridge, UK), according to the manufacturer's instructions, and is based on the production of light derived from the reaction of ATP with luciferase and luciferin. The emitted light is proportional to the ATP concentration inside the cells.

SH-SY5Y cells were cultured in 96 -well plates and exposed 6 h to 6-OHDA (100 μM) in the presence or absence of compound **1** (50–100 μM). Later, a detergent solution (50 μL) was added and incubated for 5 min at room temperature, prior to the addition of 50 μL of a substrate solution. After 5 min incubation at room temperature, the ATP levels were measured by luminescence with a luminometer (BioTeck, Synergy H1 microplate reader, Winooski, VT, USA). Results were expressed as percentage of control.

Caspase-3 activity: Caspase-3 activity was evaluated according to Silva et al. [21]. The cells were rinsed with ice-cold PBS, scrapped, and centrifuged at 3300× *g*, for 5 min. After, SH-SY5Y cells were incubated on ice for 20 min with lysis buffer and finally centrifuged at 22,500× *g*, 4 °C, for 20 min. Cells lysates were processed following the manufacturer's protocol "Caspase-3 fluorometric assay" (Sigma, St. Louis, MO, USA) and fluorescence was read at 360 nm excitation and 460 nm emission wavelengths. Caspase–3 activity was calculated through the curve slope and presented as percentage of control.

Nuclear morphological changes: 4′,6-diamidino-2-phenylindole (DAPI) (Applichem, Darmstadt, Germany) assay was conducted according to Lee et al. [70] with minor modifications [21] to determine nuclear morphological changes promoted by 6-OHDA. SH-SY5Y cells were cultured in 6-well plates and exposed 24 h to 6-OHDA (100 μM) in the presence or absence of compound **1** (50–100 μM). The cells were washed twice with ice-cold PBS and fixed with 4% paraformaldehyde (Fisher Scientific, Loughborough, UK) in PBS for 30 min. Fixed cells were washed with PBS and permeabilized with 0.1% Triton X-100 (Sigma, St. Louis, MO, USA) in PBS for 30 min. After washing again with PBS, the cells were stained with DAPI staining solution for 30 min at room temperature. The stained cells were observed under a fluorescence microscope (Zeiss, Axio Vert. A1, Oberkochen, Ger-

many) to confirm the presence of apoptotic signs, such as size-reduced nuclei, chromatin condensation, intense fluorescence, and nuclear fragmentation.

Cytosolic and nuclear protein determination: SH-SY5Y cells were exposed to 6-OHDA (100 μM) in the presence or absence of compound **1** (50–100 μM) for 6 h. The protein content was determined according to Alvariño et al. [61], with slight modifications. Cells were rinsed with ice-cold PBS and a hypotonic buffer was added: 20 mM Tris-HCl pH 7.4 (Biorad, Hercules, CA, USA), 10 mM NaCl (Merck, Darmstadt, Germany) and 3 mM $MgCl_2$ (Sigma, Buchs, Stwitzerland), containing a phosphatase and protease inhibitor cocktail. After the addition of the hypotonic buffer, the cells were incubated for 15 min on ice and centrifuged at 1200× *g*, for 15 min at 4 °C. The supernatant was collected (cytosolic fraction) and the pellet was resuspended in a nuclear extraction solution: 100 mM Tris pH 7.4, 2 mM Na_3VO_4 (Sigma, Karnataka, India), 100 mM NaCl, 1% Triton X-100 (Sigma, St. Louis, MO, USA), 1 mM EDTA (Sigma, Taufkirchen, Germany), 10% glycerol (Fisher Chemical, Geel, Belgium), 1 mM EGTA (Sigma, Buchs, Stwitzerland), 0.1% SDS (Biorad, Higashi-shinagawa Shinagawa-ku, Tokyo, Japan), 1 mM NaF (Fischer Chemical, Loughborough, UK), 0.5% deoxycholate (Sigma, Auckland, New Zealand), containing 1 mM phenylmethylsulfonyl fluoride (PMSF) (Sigma, Taufkirchen, Germany) and a protease inhibitor' cocktail (Roche, Mannheim, Germany). Lysates were incubated for 30 min on ice, with vortexing intervals of 10 min. Then, samples were centrifuged at 14,000× *g*, at 4 °C for 30 min, and the nuclear fraction was obtained. Cytosolic and nuclear protein concentration was determined by the Lowry method according to Waterborg and Matthews [71] with some modifications.

NF-κB p65 translocation analysis: NF-κB p65 translocation analysis was conducted by Western blot as follows: electrophoresis was carried out in 10% sodium dodecyl sulfate polyacrylamide gels (Biorad, Hercules, CA, USA) with 20 or 10 μg of cytosolic or nuclear protein, respectively. After transferring the protein bands to polyvinylidene difluoride (PVDF) membranes (Biorad, Hercules, CA, USA) using the Trans-Blot Turbo transfer system (Biorad, Hercules, CA, USA), blocking was carried out with 5% skim milk (Panreac-Applichem, Darmstadt, Germany), tris-buffered saline (TBS) containing Tween-20 (Biorad, Hercules, CA, USA) for 1 h. Primary antibodies were added to the membranes and incubated overnight at 4 °C with continuous agitation. After this time, the membranes were washed with a mixture of tris-buffered saline with 0.1% Tween-20 (TBST), at room temperature, and the membranes incubated with their respective enzyme-linked secondary antibodies for 2 h at room temperature. The antibodies anti-NF-κB p65 (1:1000) (Santa Cruz Biotechnology, Dallas, TX, USA) were used for the evaluation of protein expression and the signal was normalized using anti-Lamin B1 (1:5000) (Santa Cruz Biotechnology, Dallas, TX, USA) and anti-β-actin (1:5000) (Santa Cruz Biotechnology, Dallas, TX, USA) for nuclear and cytosolic fractions, respectively. Protein bands were detected with "SuperSignal ™ West Pico Plus Chemiluminescent Substrate" (Thermo Scientific Inc., Rockford, IL, USA) on a Chemidoc ™ MP imaging System (Biorad, Hercules, CA, USA).

4.5. Anti-Inflammatory Proprieties on RAW 264.7 Cells

Cell culture maintenance: Murine macrophage cells (RAW 264.7) were obtained from ATCC Bank (TIB-71). Cells were cultured at 37 °C with 5% CO_2 on DMEM medium without phenol red (Sigma, St. Louis, MO, USA), containing 1% antimycotic, 10% (*v/v*) fetal bovine serum and 1% pyruvate sodium. The cells were seeded with 5×10^4 cells/well in 96-well microplates for cell viability and NO production determination, and with 5×10^5 cells/well in 12-well plates for interleukins levels determination.

4.5.1. Cell Viability and Nitric Oxide Production on Lipopolysaccharide (LPS) Inflammation Model

In this assay, RAW 264.7 cells were subjected to an inflammatory condition mediated by lipopolysaccharides (LPS) [72]. The inflammation status was estimated by the quantification of NO levels, which are directly proportional to inflammation. RAW 264.7 cells were pretreated with compound **1** (50–100 μM) for 1 h, and stimulated with 1 μg/mL LPS for 24 h. Cells' viability was then determined by the MTT assay as previously described [73]

and NO production determined using the Griess reagent (1% sulphanilamide (Alfa Aesar, Karlsruhe, Germany) in phosphoric acid (2.5%) (Merck, Darmstadt, Germany) with 0.1% naphtylethylenediamine dihydrochloride (Alfa Aesar, Ward Hill, MA, USA). The results are expressed in percentage of control.

4.5.2. Measurement of Proinflammatory and Anti-inflammatory Cytokines Production

RAW 264.7 cells (5×10^5 cells/mL) were pre-incubated for 1 h with compound **1** (50–100 μM) prior to incubation with LPS (1 μg/mL) at 37 °C for 18 h. The concentration of TNF-α, IL-6 and IL-10 cytokines (Thermoscientific, Vienna, Austria) were assayed using enzyme-linked immunosorbent assay (ELISA) kits according to the manufacturer's instructions.

4.6. Data and Statistical Analysis

The results are presented as mean ± standard error of the mean (SEM). The determination of EC_{50} was attained from sigmoidal dose–response variable-slope curves using the GraphPad Prism V.8 software (GraphPad Software Inc., San Diego, CA, USA). One-way analysis of variance (ANOVA) with Dunnett's multiple comparison of group means was employed to determine significant differences relatively to the control treatment. All data were checked for normality (Shapiro-Wilk test) and homoscedasticity (Levene's test). Comparisons concerning variables, which did not meet variance or distributional assumptions, were carried out with Kruskal–Wallis non-parametric tests. At least three independent experiments were carried out in triplicate for each assay.

Author Contributions: J.S., C.A. and S.P. were involved in the collection and extraction procedures. J.S. and C.A. did main experiments (antioxidant, cytotoxicity, neuroprotective, signaling pathways mechanisms). J.S., P.S., S.R. were involved in the evaluation of anti-inflammatory activity. J.S., M.S., M.G. and A.R. were involved in the evaluation of NF-κB pathway. A.M. and H.G. were involved in the isolation and chemical characterization procedures. J.S., C.A, A.M., S.P., H.G. and R.P conceived the research topic, design the study, and drafted the document. R.P., A.A. and M.I.G. coordinated the study. All authors have read and agreed to the published version of the manuscript, and are accountable for the integrity of this manuscript.

Funding: This work was supported by the Portuguese Foundation for Science and Technology (FCT) through the strategic project UID/04292/2020 granted to MARE—Marine and Environmental Sciences Centre, and UIDP/04046/2020 and UIDB/04046/2020 granted to BioISI—BioSystems and Integrative Sciences Institute, through POINT4PAC project (Oncologia de Precisão: Terapias e Tecnologias Inovadoras, SAICTPAC/0019/2015-LISBOA- 01-0145-FEDER-016405), through CROSS-ATLANTIC project (PTDC/BIA-OUT/29250/2017), co-financed by COMPETE (POCI-01-0145-FEDER-029250) and through Molecules for Health project (PTDC/BIA-BQM/28355/2017). This work was also funded by the Integrated Programme of SR&TD Smart Valorization of Endogenous Marine Biological Resources Under a Changing Climate (Centro-01-0145-FEDER-000018), co-funded by Centro 2020 Programme, Portugal 2020, European Union, through the European Regional Development Fund.

Institutional Review Board Statement: Not applicable.

Informed Consent Statement: Not applicable.

Data Availability Statement: The data presented in this study are available on request from the corresponding author.

Acknowledgments: The authors are very grateful for the financial support of the Projects and Programmes described in the funding section. FCT is also acknowledged for the grants attributed to J.S. (SFRH/BD/103255/2014).

Conflicts of Interest: The authors declare no conflict of interest.

References

1. Chandrasekhar, Y.; Phani Kumar, G.; Ramya, E.M.; Anilakumar, K.R. Gallic acid protects 6-OHDA induced neurotoxicity by attenuating oxidative stress in human dopaminergic cell line. *Neurochem. Res.* **2018**, *43*, 1150–1160. [CrossRef]

2. Feng, C.W.; Chen, N.F.; Wen, Z.H.; Yang, W.Y.; Kuo, H.M.; Sung, P.J.; Su, J.H.; Cheng, S.Y.; Chen, W.F. In Vitro and in vivo neuroprotective e-ects of stellettin b through anti-apoptosis and the nrf2/ho-1 pathway. *Mar. Drugs* **2019**, *17*, 315. [CrossRef] [PubMed]
3. Huang, C.; Zhang, Z.; Cui, W. Marine-Derived Natural Compounds for the Treatment of Parkinson's Disease. *Mar. Drugs* **2019**, *17*, 221. [CrossRef]
4. Dias, V.; Junn, E.; Mouradian, M.M. The Role of Oxidative Stress in Parkinson's Disease. *J. Parkinson Dis.* **2013**, *3*, 461–491. [CrossRef] [PubMed]
5. Juárez Olguín, H.; Calderón Guzmán, D.; Hernández García, E.; Barragán Mejía, G. The role of dopamine and its dysfunction as a consequence of oxidative stress. *Oxid. Med. Cell. Longev.* **2016**, *2016*. [CrossRef]
6. Keane, P.C.; Kurzawa, M.; Blain, P.G.; Morris, C.M. Mitochondrial dysfunction in Parkinson's disease. *Parkinson's Dis.* **2011**, *2011*, 103–116. [CrossRef]
7. Md, S.; Alhakamy, N.A.; Aldawsari, H.M.; Asfour, H.Z. Neuroprotective and Antioxidant Effect of Naringenin-Loaded Nanoparticles for Nose-to-Brain Delivery. *Brain Sci.* **2019**, *9*, 275. [CrossRef]
8. Lee, K.H.; Cha, M.; Lee, B.H. Neuroprotective effect of antioxidants in the brain. *Int. J. Mol. Sci.* **2020**, *21*, 7152. [CrossRef]
9. Cobb, C.A.; Cole, M.P. Oxidative and Nitrative Stress in Neurodegeneration Catherine. *Neurobiol. Dis.* **2015**, *84*, 4–21. [CrossRef] [PubMed]
10. Nagatsu, T.; Sawada, M. Molecular mechanism of the relation of monoamine oxidase B and its inhibitors to Parkinson's disease: Possible implications of glial cells. *J. Neural Transm. Suppl.* **2006**, *71*, 53–65. [CrossRef]
11. Cadenas, E.; Davies, K.J. Mitochondrial free radical generation, oxidative stress, and aging. *Free Radic. Biol. Med.* **2000**, *29*, 3–4.
12. Lee, Y.; Lee, S.; Chang, S.C.; Lee, J. Significant roles of neuroinflammation in Parkinson's disease: Therapeutic targets for PD prevention. *Arch. Pharmacal Res.* **2019**, *42*, 416–425. [CrossRef] [PubMed]
13. Wang, W.Y.; Tan, M.S.; Yu, J.T.; Tan, L. Role of pro-inflammatory cytokines released from microglia in Alzheimer's disease. *Ann. Transl. Med.* **2015**, *3*, 136. [CrossRef]
14. Glass, C.K.; Saijo, K.; Winner, B.; Marchetto, M.C.; Gage, F.H. Mechanisms Underlying Inflammation in Neurodegeneration. *Cell* **2010**, *140*, 918–934. [CrossRef]
15. Tansey, M.G.; Goldberg, M.S. Neuroinflammation in Parkinson's disease: Its role in neuronal death and implications for therapeutic intervention. *Neurobiol. Dis.* **2010**, *37*, 510–518. [CrossRef] [PubMed]
16. Porro, C.; Cianciulli, A.; Panaro, M.A. The regulatory role of IL-10 in neurodegenerative diseases. *Biomolecules* **2020**, *10*, 1017. [CrossRef] [PubMed]
17. Kwilasz, A.J.; Grace, P.M.; Serbedzija, P.; Maier, S.F.; Watkins, L.R. The therapeutic potential of interleukin-10 in neuroimmune diseases. *Neuropharmacology* **2015**, *96*, 55–69. [CrossRef] [PubMed]
18. Qin, X.Y.; Zhang, S.P.; Cao, C.; Loh, Y.P.; Cheng, Y. Aberrations in peripheral inflammatory cytokine levels in Parkinson disease: A systematic review and meta-analysis. *JAMA Neurol.* **2016**, *73*, 1316–1324. [CrossRef]
19. Bellucci, A.; Bubacco, L.; Longhena, F.; Parrella, E.; Faustini, G.; Porrini, V.; Bono, F.; Missale, C.; Pizzi, M. Nuclear Factor-κB Dysregulation and α-Synuclein Pathology: Critical Interplay in the Pathogenesis of Parkinson's Disease. *Front. Aging Neurosci.* **2020**, *12*, 68. [CrossRef]
20. Ghosh, A.; Roy, A.; Liu, X.; Kordower, J.H.; Mufson, E.J.; Hartley, D.M.; Ghosh, S.; Mosley, R.L.; Gendelman, H.E.; Pahan, K. Selective inhibition of NF-κB activation prevents dopaminergic neuronal loss in a mouse model of Parkinson's disease. *Proc. Natl. Acad. Sci. USA* **2007**, *104*, 18754–18759. [CrossRef]
21. Silva, J.; Alves, C.; Freitas, R.; Martins, A.; Pinteus, S.; Ribeiro, J.; Gaspar, H.; Alfonso, A.; Pedrosa, R. Antioxidant and neuroprotective potential of the brown seaweed *Bifurcaria bifurcata* in an in vitro Parkinson's disease model. *Mar. Drugs* **2019**, *17*, 85. [CrossRef]
22. Silva, J.; Martins, A.; Alves, C.; Pinteus, S.; Gaspar, H.; Alfonso, A.; Pedrosa, R. Natural Approaches for Neurological Disorders-The Neuroprotective Potential of *Codium tomentosum*. *Molecules* **2020**, *25*, 5478. [CrossRef]
23. Souza, R.B.; Frota, A.F.; Silva, J.; Alves, C.; Neugebauer, A.Z.; Pinteus, S.; Rodrigues, J.A.G.; Cordeiro, E.M.S.; de Almeida, R.R.; Pedrosa, R.; et al. In vitro activities of kappa-carrageenan isolated from red marine alga *Hypnea musciformis*: Antimicrobial, anticancer and neuroprotective potential. *Int. J. Biol. Macromol.* **2018**, *112*, 1248–1256. [CrossRef] [PubMed]
24. Pabon, M.M.; Jernberg, J.N.; Morganti, J.; Contreras, J.; Hudson, C.E.; Klein, R.L.; Bickford, P.C. A Spirulina-Enhanced Diet Provides Neuroprotection in an α-Synuclein Model of Parkinson's Disease. *PLoS ONE* **2012**, *7*, e45256. [CrossRef] [PubMed]
25. Zhang, F.; Lu, J.; Zhang, J.; Xie, J. Protective effects of a polysaccharide from *Spirulina platensis* on dopaminergic neurons in an MPTP-induced Parkinson's disease model in C57BL/6J mice. *Neural Regen. Res.* **2015**, *10*, 308–313. [CrossRef] [PubMed]
26. Lima, F.A.V.; Joventino, I.P.; Joventino, F.P.; de Almeida, A.C.; Neves, K.R.T.; do Carmo, M.R.; Leal, L.K.A.M.; de Andrade, G.M.; de Barros Viana, G.S. Neuroprotective Activities of *Spirulina platensis* in the 6-OHDA Model of Parkinson's Disease Are Related to Its Anti-Inflammatory Effects. *Neurochem. Res.* **2017**, *42*, 3390–3400. [CrossRef]
27. Jerković, I.; Kranjac, M.; Marijanović, Z.; Šarkanj, B.; Cikoš, A.M.; Aladić, K.; Pedisić, S. Chemical Diversity of *Codium bursa* (Olivi) C. Agardh Headspace Compounds, Volatiles, Fatty Acids and Insight into Its Antifungal Activity. *Molecules* **2019**, *24*, 842. [CrossRef]
28. Valentão, P.; Trindade, P.; Gomes, D.; Guedes de Pinho, P.; Mouga, T.; Andrade, P.B. *Codium tomentosum* and *Plocamium cartilagineum*: Chemistry and antioxidant potential. *Food Chem.* **2010**, *119*, 1359–1368. [CrossRef]

29. Silva, J.; Alves, C.; Pinteus, S.; Mendes, S.; Pedrosa, R. Neuroprotective effects of seaweeds against 6-hydroxidopamine-induced cell death on an in vitro human neuroblastoma model. *BMC Complementary Altern. Med.* **2018**, *18*, 4–13. [CrossRef]
30. Celikler, S.; Vatan, O.; Yildiz, G.; Bilaloglu, R. Evaluation of anti-oxidative, genotoxic and antigenotoxic potency of *Codium tomentosum* Stackhouse ethanolic extract in human lymphocytes in vitro. *Food Chem. Toxicol.* **2009**, *47*, 796–801. [CrossRef]
31. El-Masry, M.H.; Mostafa, M.H.; Ibrahim, A.M.; El-Naggar, M.M.A. Marine algae that display anti-tumorigenic activity against *Agrobacterium tumefaciens*. *FEMS Microbiol. Lett.* **1995**, *128*, 151–155. [CrossRef] [PubMed]
32. Lamela, M.; Anca, J.; Villar, R.; Otero, J.; Calleja, J.M. Hypoglycemic activity of several seaweed extracts. *J. Ethnopharmacol.* **1989**, *27*, 35–43. [CrossRef]
33. Ahmad, V.U.; Aliya, R.; Perveen, S.; Shameel, M. Sterols from marine green alga *Codium decorticatum*. *Phytochemistry* **1993**, *33*, 1189–1192. [CrossRef]
34. Grabarczyk, M.; Wińska, K.; Mączka, W.; Potaniec, B.; Anioł, M. Loliolide—The most ubiquitous lactone. *Folia Biol. Oecologica* **2015**, *11*, 1–8. [CrossRef]
35. Dias, M.K.H.M.; Madusanka, D.M.D.; Han, E.J.; Kim, M.J.; Jeon, Y.J.; Kim, H.S.; Fernando, I.P.S.; Ahn, G. (−)-Loliolide Isolated from *Sargassum Horneri* Protects Against Fine Dust-Induced Oxidative Stress in Human Keratinocytes. *Antioxidants* **2020**, *9*, 474. [CrossRef] [PubMed]
36. Li, L.-L.; Zhao, H.-H.; Kong, C.-H. (−)-Loliolide, the most ubiquitous lactone, is involved in barnyardgrass-induced rice allelopathy. *J. Exp. Bot.* **2020**, *71*, 1540–1550. [CrossRef]
37. Kimura, J.; Maki, N. New loliolide derivatives from the brown alga *Undaria pinnatifida*. *J. Nat. Prod.* **2002**, *65*, 57–58. [CrossRef]
38. Gangadhar, K.N.; Rodrigues, M.J.; Pereira, H.; Gaspar, H.; Malcata, F.X.; Barreira, L.; Varela, J. Anti-Hepatocellular Carcinoma (HepG2) Activities of Monoterpene Hydroxy Lactones Isolated from the Marine Microalga *Tisochrysis Lutea*. *Mar. Drugs* **2020**, *18*, 567. [CrossRef]
39. Salamon, A.; Zádori, D.; Szpisjak, L.; Klivényi, P.; Vécsei, L. Neuroprotection in Parkinson's disease: Facts and hopes. *J. Neural Transm.* **2020**, *127*, 821–829. [CrossRef]
40. Malar, D.S.; Prasanth, M.I.; Brimson, J.M.; Sharika, R.; Sivamaruthi, B.S.; Chaiyasut, C.; Tencomnao, T. Neuroprotective Properties of Green Tea (*Camellia sinensis*) in Parkinson's Disease: A Review. *Molecules* **2020**, *25*, 3926. [CrossRef]
41. Yang, X.; Kang, M.-C.; Lee, K.-W.; Kang, S.-M.; Lee, W.-W.; Jeon, Y.-J. Antioxidant activity and cell protective effect of loliolide isolated from Sargassum ringgoldianum subsp. coreanum. *Algae* **2011**, *26*, 201–208. [CrossRef]
42. Park, J.S.; Davis, R.L.; Sue, C.M. Mitochondrial Dysfunction in Parkinson's Disease: New Mechanistic Insights and Therapeutic Perspectives. *Curr. Neurol. Neurosci. Rep.* **2018**, *18*, 21. [CrossRef]
43. Alam, M.N.; Bristi, N.J.; Rafiquzzaman, M. Review on in vivo and in vitro methods evaluation of antioxidant activity. *Saudi Pharm. J.* **2013**, *21*, 143–152. [CrossRef] [PubMed]
44. Shahidi, F.; Zhong, Y. Measurement of antioxidant activity. *J. Funct. Foods* **2015**, *18*, 757–781. [CrossRef]
45. Duan, W.; Ladenheim, B.; Cutler, R.G.; Kruman, I.I.; Cadet, J.L.; Mattson, M.P. Dietary folate deficiency and elevated homocysteine levels endanger dopaminergic neurons in models of Parkinson's disease. *J. Neurochem.* **2002**, *80*, 101–110. [CrossRef] [PubMed]
46. Shults, C.W. Effects of Coenzyme Q10 in Early Parkinson Disease. *Arch. Neurol.* **2002**, *59*, 1541. [CrossRef] [PubMed]
47. Drechsel, D.A.; Patel, M. Role of Reactive Oxygen Species in the Neurotoxicity of Environmental Agents Implicated in Parkinson's disease. *Free Radic. Biol. Med.* **2008**, *44*, 11873–11886. [CrossRef]
48. Chen, W.F.; Chakraborty, C.; Sung, C.S.; Feng, C.W.; Jean, Y.H.; Lin, Y.Y.; Hung, H.C.; Huang, T.Y.; Huang, S.Y.; Su, T.M.; et al. Neuroprotection by marine-derived compound, 11-dehydrosinulariolide, in an in vitro Parkinson's model: A promising candidate for the treatment of Parkinson's disease. *Naunyn-Schmiedeberg's Arch. Pharmacol.* **2012**, *385*, 265–275. [CrossRef] [PubMed]
49. Yurchenko, E.A.; Menchinskaya, E.S.; Pislyagin, E.A.; Trinh, P.T.H.; Ivanets, E.V.; Smetanina, O.F.; Yurchenko, A.N. Neuroprotective activity of some marine fungal metabolites in the 6-hydroxydopamin- and paraquat-induced Parkinson's disease models. *Mar. Drugs* **2018**, *16*, 457. [CrossRef]
50. Trist, B.G.; Hare, D.J.; Double, K.L. Oxidative stress in the aging substantia nigra and the etiology of Parkinson's disease. *Aging Cell* **2019**, *18*, e13031. [CrossRef] [PubMed]
51. Zeng, X.S.; Geng, W.S.; Jia, J.J.; Chen, L.; Zhang, P.P. Cellular and molecular basis of neurodegeneration in Parkinson disease. *Front. Aging Neurosci.* **2018**, *10*, 109. [CrossRef]
52. Percário, S.; Da Silva Barbosa, A.; Varela, E.L.P.; Gomes, A.R.Q.; Ferreira, M.E.S.; De Nazaré Araújo Moreira, T.; Dolabela, M.F. Oxidative Stress in Parkinson's Disease: Potential Benefits of Antioxidant Supplementation. *Oxid. Med. Cell. Longev.* **2020**. [CrossRef] [PubMed]
53. Ward, R.J.; Zucca, F.A.; Duyn, J.H.; Crichton, R.R.; Zecca, L. The role of iron in brain ageing and neurodegenerative disorders. *Lancet Neurol.* **2017**, *176*, 139–148. [CrossRef]
54. Ighodaro, O.M.; Akinloye, O.A. First line defence antioxidants-superoxide dismutase (SOD), Catalase (CAT) and glutathione peroxidase (GPX): Their fundamental role in the entire antioxidant defence grid. *Alex. J. Med.* **2018**, *54*, 287–293. [CrossRef]
55. Nandi, A.; Yan, L.J.; Jana, C.K.; Das, N. Role of Catalase in Oxidative Stress- and Age-Associated Degenerative Diseases. *Oxid. Med. Cell. Longev.* **2019**, *2019*, 9613090. [CrossRef]
56. Magalingam, K.B.; Radhakrishnan, A.; Haleagrahara, N. Rutin, a bioflavonoid antioxidant protects rat pheochromocytoma (PC-12) cells against 6-hydroxydopamine (6-OHDA)-induced neurotoxicity. *Int. J. Mol. Med.* **2013**, *32*, 235–240. [CrossRef]

57. Yu, S.B.; Pekkurnaz, G. Mechanisms Orchestrating Mitochondrial Dynamics for Energy Homeostasis. *J. Mol. Biol.* **2018**, *430*, 3922–3941. [CrossRef]
58. Cenini, G.; Lloret, A.; Cascella, R. Oxidative stress in neurodegenerative diseases: From a mitochondrial point of view. *Oxid. Med. Cell. Longev.* **2019**, *2019*, 2105607. [CrossRef]
59. Hunot, S.; Brugg, B.; Ricard, D.; Michel, P.P.; Muriel, M.P.; Ruberg, M.; Faucheux, B.A.; Agid, Y.; Hirsch, E.C. Nuclear translocation of NF-κB is increased in dopaminergic neurons of patients with Parkinson disease. *Proc. Natl. Acad. Sci. USA* **1997**, *94*, 7531–7536. [CrossRef]
60. Oeckinghaus, A.; Ghosh, S. The NF-kappaB family of transcription factors and its regulation. *Cold Spring Harb. Perspect. Biol.* **2009**, *1*, a000034. [CrossRef] [PubMed]
61. Alvariño, R.; Alonso, E.; Abbasov, M.E.; Chaheine, C.M.; Conner, M.L.; Romo, D.; Alfonso, A.; Botana, L.M. Gracilin A Derivatives Target Early Events in Alzheimer's Disease: In Vitro Effects on Neuroinflammation and Oxidative Stress. *ACS Chem. Neurosci.* **2019**, *10*, 4102–4111. [CrossRef]
62. Da Fonseca, A.C.C.; Matias, D.; Garcia, C.; Amaral, R.; Geraldo, L.H.; Freitas, C.; Lima, F.R.S. The impact of microglial activation on blood-brain barrier in brain diseases. *Front. Cell. Neurosci.* **2014**, *8*, 362. [CrossRef]
63. Haruwaka, K.; Ikegami, A.; Tachibana, Y.; Ohno, N.; Konishi, H.; Hashimoto, A.; Matsumoto, M.; Kato, D.; Ono, R.; Kiyama, H.; et al. Dual microglia effects on blood brain barrier permeability induced by systemic inflammation. *Nat. Commun.* **2019**, *10*, 5816. [CrossRef]
64. Blaylock, R. Parkinson's disease: Microglial/macrophage-induced immunoexcitotoxicity as a central mechanism of neurodegeneration. *Surg. Neurol. Int.* **2017**, *8*, 65. [CrossRef]
65. Lyer, S.S.; Cheng, G. Role of Interleukin 10 Transcriptional Regulation in Inflammation and Autoimmune Disease. *Crit. Rev. Immunol.* **2012**, *32*, 23–63.
66. Chen, Q.Q.; Haikal, C.; Li, W.; Li, J.Y. Gut Inflammation in Association with Pathogenesis of Parkinson's Disease. *Front. Mol. Neurosci.* **2019**, *12*, 218. [CrossRef]
67. Baizabal-Carvallo, J.F.; Alonso-Juarez, M. The Link between Gut Dysbiosis and Neuroinflammation in Parkinson's Disease. *Neuroscience* **2020**, *432*, 160–173. [CrossRef]
68. Ahmed, S.A.; Rahman, A.A.; Elsayed, K.N.M.; Abd El-Mageed, H.R.; Mohamed, H.S.; Ahmed, S.A. Cytotoxic activity, molecular docking, pharmacokinetic properties and quantum mechanics calculations of the brown macroalga *Cystoseira trinodis* compounds. *J. Biomol. Struct. Dyn.* **2020**, 1102. [CrossRef]
69. Alvariño, R.; Alonso, E.; Tribalat, M.A.; Gegunde, S.; Thomas, O.P.; Botana, L.M. Evaluation of the Protective Effects of Sarains on H_2O_2-Induced Mitochondrial Dysfunction and Oxidative Stress in SH-SY5Y Neuroblastoma Cells. *Neurotox. Res.* **2017**, *32*, 368–380. [CrossRef]
70. Kwon, K.R.; Alam, M.B.; Park, J.H.; Kim, T.H.; Lee, S.H. Attenuation of UVB-induced photo-aging by polyphenolic-rich *Spatholobus suberectus* stem extract via modulation of MAPK/AP-1/MMPs signaling in human keratinocytes. *Nutrients* **2019**, *11*, 1341. [CrossRef]
71. Waterborg, J.H.; Matthews, H.R. The lowry method for protein quantidication. *Methods Mol. Biol.* **1984**, *1*, 1–3.
72. Freitas, R.; Martins, A.; Silva, J.; Alves, C.; Pinteus, S.; Alves, J.; Teodoro, F.; Ribeiro, H.M.; Gonçalves, L.; Petrovski, Ž.; et al. Highlighting the biological potential of the brown seaweed *Fucus spiralis* for skin applications. *Antioxidants* **2020**, *9*, 611. [CrossRef]
73. Marmitt, D.J.; Alves, C.; Silva, J.; Pinteus, S.; Schneider, T.; Christ Vianna Santos, R.; de Freitas, E.M.; Pedrosa, R.; Laufer, S.; Goettert, M.I. Neuroprotective potential of *Myrciaria plinioides* D. Legrand extract in an in vitro human neuroblastoma model. *Inflammopharmacology* **2020**, *28*, 737–748. [CrossRef]

UNIVATES

R. Avelino Talini, 171 | Bairro Universitário | Lajeado | RS | Brasil
CEP 95914.014 | Cx. Postal 155 | Fone: (51) 3714.7000
www.univates.br | 0800 7 07 08 09